UNIVERSITY OF SOUTHAMPTON

FACULTY OF PHYSICAL SCIENCES AND ENGINEERING

ELECTRONICS AND COMPUTER SCIENCE

Volume 1 of 1

Control of Upper-limb Functional Neuromuscular Electrical Stimulation

by

Rodney Paul Lane C.Eng. MPhil. MIET

Thesis for the degree of Doctor of Philosophy

November 2016

UNIVERSITY OF SOUTHAMPTON

ABSTRACT

FACULTY OF PHYSICAL SCIENCES AND ENGINEERING

Electronics & Computer Science

Thesis for the degree of Doctor of Philosophy

CONTROL OF UPPER-LIMB FUNCTIONAL ELECTRICAL STIMULATION

Rodney Paul Lane

Functional electrical stimulation (FES) is the name given for the use of neuromuscular electrical stimulation to achieve patterns of induced movement which are of functional benefit to the user. System are available that use FES to aid persons who have suffered an insult to the motor control region of the brain and been left with movement impairment.

The aim of this research was to investigate methods of providing an FES system that could have a beneficial effect in restoring arm function. The techniques for applying upper-limb stimulation are well established, however the methods of controlling it to provide functional use remain lacking. This is because upper-limb movement can be difficult to measure and quantify as the starting point for any movement may not be well defined. Moreover the movements needed to complete a useful function such as reaching and grasping requires the coordinated control of a number of muscle groups, and that relies on being able to track the position of the limb. Effective control of FES for the arm requires reliable feedback about the position and state of the limb.

Electromyograms (EMG) are a measure of the very small electrical signals that are emitted whenever a muscle is 'fired' to move. EMG can be used to detect muscle activity and so can be a useful feedback control input. It does however have a number of drawbacks that this research sought to address by combining the method with external motion sensors. The intension had been to use the motion sensors to track the position of the limb and then use the EMG measurements to detect the wearer's movements. FES could then be used to assist the wearer in making a desired movement.

Initial studies were done to separately investigate the motion sensing and the EMG measurement components of the system. However before these could be combined a more interesting observation was made relating to bioimpedance.

A study of bioimpedance measurements found a relationship between tissue impedance changes and muscle activity. Different methods for measuring bioimpedance where investigated and the results compared, before a practical technique for capturing measurements was developed and demonstrated. A new set of test equipment was made using these finding. Subsequent results using this equipment were able to demonstrate that bioimpedance measurement could be taken from a limb while FES was being used, and that these measurement could be used as a feedback signal to control the FES to maintain a target limb position.

This work forms the basis of a novel approach to the control of FES that uses feedback from the user's limb to determine the position of the limb in free space without need for additional sensors.

Contents

List of figures

List of tables

DECLARATION OF AUTHORSHIP

I, Rodney Paul Lane

declare that the thesis entitled

Control of Upper-limb Functional Neuromuscular Electrical Stimulation

and the work presented in the thesis are both my own, and have been generated by me as the result of my own original research. I confirm that:

- this work was done wholly or mainly while in candidature for a research degree at this University;
- where any part of this thesis has previously been submitted for a degree or any other qualification at this University or any other institution, this has been clearly stated;
- where I have consulted the published work of others, this is always clearly attributed;
- where I have quoted from the work of others, the source is always given. With the exception of such quotations, this thesis is entirely my own work;
- I have acknowledged all main sources of help;
- where the thesis is based on work done by myself jointly with others, I have made clear exactly what was done by others and what I have contributed myself;
- none of this work has been published before submission, or [delete as appropriate] parts of this work have been published as: [please list references]

Signed: ……..

Date:…….

Acknowledgements

Acknowledgements must first go to the forbearance of my family and especially Linda for enabling me to pursue my goals. Very many thanks also go to Paul for acting as both a sounding board and an inspiration during his long years of persistent and patient supervision and support.

Definitions and abbreviations

BB - Biceps Brachii

The large elbow flexor muscle in the arm

BR - Brachioradialis

The main supinator and flexor muscle of the forearm

CAD - Computer aided design

ECRB - Extensor carpi radialis brevis

The shorter of the two wrist extensor muscles in the forearm

ECRL - Extensor carpi radialis longus

The longer of the two wrist extensor muscles in the forearm

EMG - Electromyography

A method of detecting and measuring muscle movement from the small electrical signal given off from a contracting muscle

FES - Functional electrical stimulation

The functional application of neuromuscular stimulation (NMES) used to produce or develop useful muscle movement; an example of FES is correcting dropped foot.

FSC - Finite State Controller

A type of system control where events are determined by individual or 'finite states' dependent upon the prevailing conditions. The controller will pass control from state to state as required.

MEMS - Micro-Electro-Mechanical Systems

Also known as; micro machines, and micro systems technology (MST). Here MEMS relates to microscopic electronic/electromechanical mechanical structures formed from silicon and packaged to provide discrete fully contained sensors.

NMES - Neuromuscular electrical stimulation

A method of using a successively switched electrical field to evoke action potentials within the motor nerves that control skeletal muscle.

MOSFET - Metal oxide semiconductor field effect transistor

PI - Posterior interosseous

A nerve that emanates from the deep branch of the radial nerve in the forearm to innervate the wrist and hand extensor muscles

PWM - Pulse width modulation

SDK - Software development kit

TB - Triceps Brachii

The large triple headed elbow extensor muscle

UART - Universal Asynchronous Receiver / Transmitter

An electronic communication protocol between devices

USB - Universal Serial Bus

An electronic communication protocol between devices

Chapter 1: Introduction

The work described within this thesis begins by giving an understanding any assumptions made at the outset, before going on to detail the discoveries made during the research. The implication and meaning of these discoveries are explored at each stage before progressing towards the overall objective of determining a clinically useful method for provisioning and controlling functional electrical stimulation for the upper-limb.

1.1 Neuromuscular electrical stimulation

Neuromuscular electrical stimulation (NMES) is a method of using a successively switched electrical field set up through body tissue, to evoke action potentials within the motor nerves that innervate skeletal muscles. As the muscle contracts in response to this stimulation a force is developed capable of causing movement. By modulating the intensity and switching frequency of the stimulation the level of force developed by the contraction can be controlled. NMES can therefore be used as a method to produce controlled movement of limbs. A detailed description and explanation of electrical stimulation is given in Appendix A.

Electrode pairs are required to deliver the stimulation pulses. A circuit is made between these electrodes through the tissue to which they are applied. With the onset of each stimulation pulse the electrical field is established and will collapse when the pulse ends. Accurate positioning of the electrode pairs is required to ensure that the electrical field occurs appositely to the motor nerve. Stimulating electrodes can be categorised into three types; fully implanted, percutaneous, and transcutaneous.

Fully implanted electrodes are placed adjacent to the nerve requiring to be stimulated. Placement of this type of electrode requires a surgical procedure. By implanting so close to the nerve this type of electrodes can achieve an optimal positioning that will remain for many years. Implanted electrodes can be one of several types. Epimysial electrodes (Uhlir, et al., 2004) are placed next to a nerve. Epineural electrodes (Holsheimer, et al., 2000) are positioned within the epineurium, the outer covering of the nerve bundle. A further type is placed around the nerve bundle and contains an array of multiple electrodes, one such type being ‘book’ electrodes (Vanhoest & Donaldson, 2003) and another ‘cuff’ electrode (Schuettler, et al., 1999).

Percutaneous electrodes are inserted through the skin so that the conductive tip resides adjacent to the nerve. Placement of this type of electrode is temporary and used for clinical measurement

of laboratory observations. They can achieve similar levels of positioning accuracy as the fully implanted electrodes.

Transcutaneous electrodes are applied to the surface of the skin to stimulate the nerve from the surface. This type of electrode offers certain benefits and disadvantages when compared to the other two methods. The first drawback is a considerably increased power requirement. The propagation losses of conducting through the skin and additional body tissue requires approximately ten times the power of either the fully implanted or percutaneous electrodes (Lyons, et al., 2002). The second drawback is positioning difficulty. The relatively poor proximity of the electrodes to the nerve can make accurate positioning difficult. It can be time consuming to find a position for the electrodes that will produce an effective conductive path for the electrical field to reach the nerve. This problem can be compounded when the nerve moves relative to the skin surface during movement of the limb. A final drawback can be skin irritation when used on limbs with poor blood circulation. The benefits however of transcutaneous electrodes are that they are non-invasive requiring no surgery and unlike percutaneous electrodes they can be used outside of the clinic or laboratory. The research presented in this thesis is focused on an improvement for the use and control of stimulation using surface electrodes. For the reasons outlined above, surface electrical stimulation has a wider appeal to patients and has therefore been chosen for investigation as the preferred method.

1.2 Neuromuscular electrical stimulation for treatment and functional use

NMES is used to treat the effects of paralysis caused by stroke, spinal cord injury (SCI), head trauma, and a range of neurological diseases. The technique provides rehabilitation while the patient is recovering movement following a stroke, head trauma or non-permanent SCI. The stimulation is used to perform programmes of exercises that have been prescribed by a clinician. Sequences of NMES are timed to produce exercise movements of the limb and the patient is instructed to practice making the movement along with the stimulation. The range of volitional movement of the limb may then improve as a result of the repetition. Where the paralysis is lasting with little recovery following rehabilitation NMES provides an assistive technology that restores useful movements for the activities of daily living. This is referred to as functional neuromuscular electrical stimulation which has become shortened to functional electrical stimulation of more simply FES.

When FES has been applied to restore or improve movement the benefits to the user may continue even after the FES device has been removed. This is known as the 'carry-over effect' (Waters, 1984) and may last for anything from a few of minutes to a number of days.

Long term use of FES can result in neuroplastic reorganisation of the cortex (Kimberley, et al., 2004) with the result that the user will no longer require the FES device and the benefits will have become permanent.

The functional use of NMES relies on timing the stimulation of complimenting muscles to produce useful patterns of movement. Good examples are the FES walking stimulators used by those with a condition known as dropped-foot. Dropped-foot is an inability to achieve dorsiflexion of the foot about the ankle and so raise the toes clear of the ground while swinging the leg forward during walking. Sufferers will often limit their attempts to walk because of the increased likelihood of tripping and falling. FES walking stimulators detect when the heel is about to leave the ground and apply stimulation to the common peroneal nerve just below the knee. This activates the tibialis anterior and peroneus muscles to raise and turn out the foot so that the toes will clear the ground as the leg is swung forward. Once the foot has been planted back onto the ground, following the step, the stimulation is switched off ready to be turned on again in time with the next step.

1.3 Controlling FES

The effective use of FES requires accurate control of the timing and intensity of the stimulation as it is being applied. This has tended to limit the practical application of the technology. In general the more complex a control system an application requires, the less likely it is that it will be found outside of a clinical laboratory setting. Systems that are available for people to use at home and at work like the FES walking stimulators generally make use of simple timing based open-loop controllers. The stimulation parameters are defined by clinical personnel during a routine visit to a clinic by a patient. The electronics then respond to these predefined parameters and easily detectable events during walking when a patient is outside the hospital environment. The control for these systems can be simple because of the regularity inherent in walking and the assumption that a foot once lifted off the ground will usually be placed back down again.

For other movements such as those of the upper-limb the events become less easily detectable with no regular starting condition like a foot on the ground. This has resulted in the development of ever more complex control strategies to detect the starting condition and then monitor movement during the stimulation sequence. The additional cost and difficulties in simplifying the

clinical set-up for these more complicated systems has contributed to a slower development and uptake (Burridge & Ladouceur, 2008).

1.4 Electromyography

Electromyography (EMG) is a method of measuring skeletal muscle activity from the small electrical signals produced by a contracting muscle. The early part of the research presented in this thesis involved a study of the methods for combining the measurement of EMG with relative positional information determined from micro-electromechanical systems (MEMS) accelerometers.

The work of the research led to development of electronic circuits that were robust enough to withstand the effects of NMES stimulation interference, yet sensitive enough to capture the EMG signals between the NMES pulses. The design went through a number of iterations before an optimised arrangement of passive and active analogue filtering combined with digital filtering was arrived at. From using this, EMG signals were captured that were shown to be between five and seven orders of magnitude smaller than the amplitude of NMES pulses. Typical EMG voltages are 10µV compared to 100V for the electrical stimulation.

1.5 Accelerometer signal processing

The development of processing algorithms for use with two-axis MEMS accelerometers led to the ability to detecting forearm orientation and gesture recognition from the wearer's volitional movement. The algorithm tracked gravity referenced changes relating to the orientation of the limb while registering differential changes for the gesture recognition.

1.6 The research acquires a new focus

As work progressed using the robust EMG amplifier a previously unseen artefact on the signal was observed. With understanding of this artefact came the realisation of its potential to reveal dynamic limb position. The research moved in a new direction with the original aims of finding a better control method for FES remaining, but now focussing the way to achieve this upon the use of bioimpedance to track limb movement.

1.7 Electrical Bioimpedance

Electrical bioimpedance sometimes referred to as EBI or just BI is a technique that was developed for measuring the impedance of body tissue. The technique has been used as a way of charting disease progression for neuromuscular diseases (Rutkove, et al., 2002) (Tarulli, et al., 2005). When the composition of muscles is changed by disease and impedance changes can be used to track this change. The method is known as impedance myography. An early problems identified with the method was an artefact on the signal caused by movement of the limb during measuring. It was essentially this same movement artefact that was observed in the EMG measurements using the robust amplifier during stimulation

1.8 Research aims and objectives

The aim of the research was to investigate ways to obtain reliable methods for controlling FES. From the use of control signals derived from captured and suitably conditioned bio-signal coming from the user, and from external movement sensors on the upper-limb of the body. These methods would be investigated in isolation before potentially integrating them.

The outcome objectives for the work were defined as;

1. Investigate potentially useful methods of sensing limb movement using external sensors.
2. Investigate the availabity of functionally useful bio-signals.
3. Investigate the viability of measuring bio-signals while delivering neuromuscular electrical stimulation, and making these measurements through the same electrodes as those used to deliver the stimulation.
4. Determine the extent of any correlation between the measured bioimpedance and the position of the limb.
5. Then if a correlation can be shown to investigate the viability of using the bioimpedance measurement as a feedback signal to control the electrical stimulation to attain and maintain a desired limb position.
6. Consider the benefits of combining bio-signal derived control with control derived from external sensors.

The overall objective being to arrive at a practical and intuitive method to initiate and control FES assisted upper-limb movement, for a patient group who find difficulty in straightening their hand and opening the fingers and thumb to be able to reach and grasp an object.

1.9 Outcomes and achievements

Investigations of upper-limb movement measurement and tracking led to the development of a three axis accelerometer based system that was able to determine voluntary gestures made by the wearers while simultaneously determining the angle of the limb. The method was trialled as a way to control sequenced patterns of FES to improve function. Functional benefits from using the system were demonstrated.

The development of a robust EMG amplifier able to be used within the presence of FES led to the discovery of a movement artefact imposed onto the signal. This was subsequently identified as being due to impedance changes within the body tissue as the limb moved in response to the FES. These changes were predominately caused by an increase in the cross-sectional area of muscles as they contracted. It was realised that this related to the position of the limb about the joint on which the muscles acted.

From returning to the literature at this stage, an understanding was gained that these changes in bioimpedance with respect to limb movement were already understood. Indeed work had been underway by others within the timeframe of this research project to demonstrate bioimpedance control to regulate an FES drop-foot stimulator. The system described in the literature used a separate bioimpedance and FES system with a feed-forward control method whereby measurement of the previous step informed the required stimulation for the next.

The research in this thesis was able to demonstrate the effective use of an integrated bioimpedance and FES system capable of affecting modulated control of the stimulation in real-time in response to tracked measurements of the bioimpedance. The system described in this thesis is less complex to use and offers significant benefits in a number of ways to the one described in the literature. It therefore represents a more appropriate development for clinically useful applications.

1.10 Contribution arising from the research

The work that covered the development of an FES system that used accelerometer feedback control was presented in Japan as a poster at the International Functional Electrical Stimulation Society (IFESS) conference (Lane, et al., 2006). The system went on to be trialled as part of a pilot study, which was presented two year later at the IFESS conference (Mann, et al., 2008). This was followed by a full research trial using the equipment that was written up as a journal publication (Mann, et al., 2011).

The work to investigate a better method for identifying the onset of bursts of EMG led to a patent being granted (Lane & Nolan, 2009).

Much of the work done to improve the design of the FES stimulator used in the research was included into a further patent application (Lane, et al., 2011).

The understanding of the issues surrounding the use of feedback control sensors for ambulatory equipment that was derived from the research was published as a journal article (Lane, 2012).

The bio-impedance method described in the thesis was filed for patent protection by the University of Southampton (Lane & Chappell, 2013). This has subsequently gone on to be protected in a number of territories worldwide. The technology covered by the patent has also since been licenced for commercial exploitation.

Chapter 2: Literature Review

2.1 A background to Neuromuscular Electrical Stimulation and the practical application as Functional Electrical Stimulation

This first section of the chapter reviews the use of neuromuscular electrical stimulation (NMES) for clinical rehabilitation and its use in assistive technologies in the form of neuro-prosthetic or neuro-orthotic devices designed to restore and assist useful functional movement. The functional uses of NMES covered, are the basic activities necessary for daily living of standing, walking, and upper-limb ability. NMES requires the peripheral nervous system (PNS) to be intact, where paralysed or partially paralysed muscles result from injury to the brain or central nervous system (CNS).

NMES excites motor nerves in the PNS to produce evoked action potentials which cause the muscle to 'fire' and so contract. The original understanding of this process comes from the pioneering work done during the nineteenth and early twentieth century (Galvani, 1842) (Lapicque, 1907) It was Galvani who discovered that the dismembered leg from a frog could be made to twitch upon application of an electrical spark. This type of stimulation subsequently became known as galvanism. Lapicque developed the integrate-and-fire model to explain CNS action potential propagation that is still relevant today (Abbot, 1999). The synaptic connection is modelled as a leaky integrator circuit with an output comparator tied to a firing threshold. When sufficient potential has built up in the integrator to reach the threshold the output will fire. This system effectively behaves as a low-pass filter for the presynaptic spikes emanating from the CNS.

Further explanation was provided later in the century (Hodgkin & Huxley, 1952) (McNeal, 1976). Hodgkin and Huxley developed mathematical modelling of the electro-chemical depolarisation and repolarisation processes. McNeal created a model for nerve excitation which allowed computation of the threshold for myelinated nerve fibres for stimulation pulses from electrodes not in direct contact with the fibre. Further discussion on the work defining this size principle was provided by Mendell (Mendell, 2005). The recruitment of nerve fibres and resultant muscle contraction torque profiles are influenced by the tissue physiology and the stimulation being applied.

It was postulated that differences in nerve fibre diameter with associated membrane capacitance affected recruitment patterns (Rushton, 1951) (Hodgkin, 1954). These early studies used stimulating electrodes sited close to the nerve bundles and concluded that the recruitment order

of nerve conduction by NMES is opposite to that for volitional recruitment. In that the larger nerve fibres that innervate larger motor units are recruited before the smaller nerve fibres, whereas volitionally the nerve fibres are recruited upwards from the smallest first.

Grill and Mortimer were able to expand on this by showing that changes to the pulse width related to the distance of the electrodes from the nerve bundles could be used to preferentially select small nerve fibres (Grill & Mortimer, 1996). Shorter pulse widths recruit larger nerve fibres; their explanation was that this is a function of the increased distance between the polarising nodes on the axons. The shorter pulse widths were also shown to produce greater muscle torque which has the effect of making the stimulation more controllable. Szlavik & de Bruin confirmed these findings and also showed that for surface stimulation the effect due to changing the pulse width reaches a plateau (Szlavik & de Bruin, 1999).

Studies investigating transcutaneous stimulation did not support the original findings of reverse recruitment order by NMES (Knaflitz, et al., 1990) (Feiereisen & Duchateau, 1997) (Gregory & Bickel, 2005) (Chou & Binder-Macleod, 2007). Demonstrating that muscle fibre recruitment was not consistent with the previously reported results because both the location of the motor neuron with respect to the electrodes and the motor axonal diameter are major factors in determining motor unit recruitment order. Transcutaneous electrodes were shown to increase recruitment uncertainty because of the distance from the motor neuron and the dynamic variability of current paths.

Studies reported in the literature do however all agree that patterns of muscle recruitment evoked by NMES do not match those that result from normal volitional contraction. Studies of volitional muscle firing patterns have shown there to be a progressive decline in the motor unit discharge rate over the duration of prolonged contractions (Bigland-Ritchie, et al., 1983). Commonly referred to ‘muscle wisdom’ it is supposed that the body modulates muscle firing in this way to combat fatigue. Attempts had been made to replicate this with NMES by using stimulation frequencies that reduced over the duration of evoked contractions although there has been disagreement about whether this is effective. Jones et al. (Jones, et al., 1979) demonstrated good results from using this strategy, however Fugelevand & Keen (Fugelvand & Keen, 2003) later questioned the level of stimulation that had been used and found that at ‘clinical’ levels no benefit was seen. Work around the same time (Kebaetse & Binder-Macleod, 2004) concluded that when comparing patterns of stimulation of high frequency followed by low frequency, constant frequency, and low frequency followed by higher frequency, the later was the most effective against fatigue. Chou & Binder-Macleod (Chou & Binder-Macleod, 2007) confirmed these findings when they investigated the muscle force stimulation intensity

relationship with respect to increasing stimulation and found that this addressed the effects of fatigue. Song et al. (Song, et al., 2005) looked at stimulation pulse types with respect to fatigue, and found that monophasic pulses generated higher torques with greater fatigue resistance when compared with biphasic waveforms. A monophasic pulse is one where the charge is introduced either positively or negatively for the entire duration. A biphasic pulse with have both positive and negative going components (Figure 1).

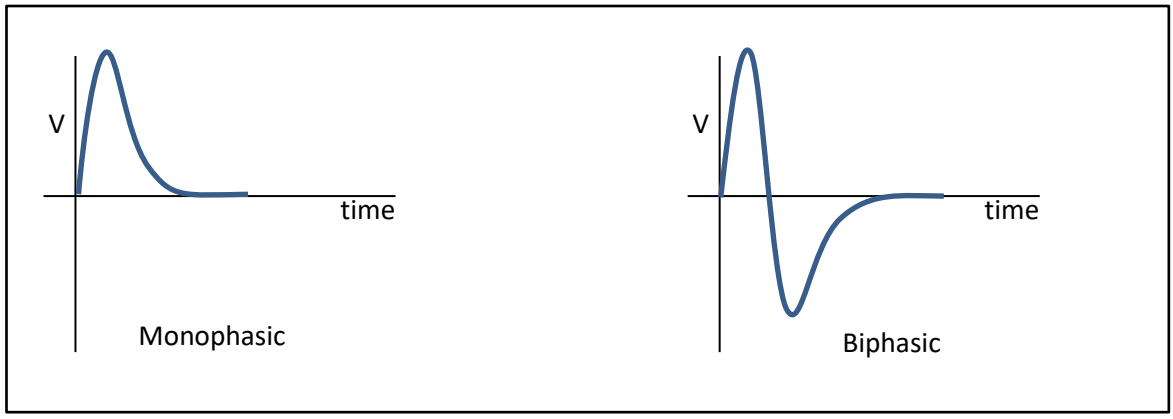

Figure 1 shows a typical representation of monophasic and biphasic pulse waveforms

Clinical benefits have been seen from NMES through aiding the rehabilitation of movement to promote neuroplasticity and motor relearning (Lee & Donkelaar, 1995; Chen, et al., 2002). Lee and Donkelaar were able to show three major mechanisms for this plastic reorganisation; unmasking of existing but functionally inactive pathways, sprouting of fibres from surviving neurons with formation of new synapses, and redundancy of CNS circuitry allowing alternative pathways to take over functions. The findings of Chen et al. suggest that plasticity is normal for a healthy nervous system and that successful rehabilitation will make use of this innate ability of the body to adapt to change. The clinical practice of NMES is described well in the publication *Neuromuscular Electrical Stimulation a Practical Guide* (Baker, et al., 2000). Practical teaching videos based upon this publication and narrated by Lucinda Baker has since been made available (Axelgaard manufacturing company, 2015)

Physical changes can occur in muscles due to poor innervation that can affect rehabilitation. Li et al. (Li, et al., 2008) used ultrasound to demonstrate muscle tissue changes to pennation angles and fascicle lengths in response to voluntary movement following stroke (Figure 2). The pennation angle is a measure of the angle formed by the muscle fibres relative to the line of action of the muscle and indicates the degree of 'bellying'. The range of fascicle length over a contraction is a measure of a muscle fibre bundle's ability to function.

The fibres of pinnate muscle run obliquely. The pennation angle is formed between the direction of the fibres and the line of action of the muscle, as the muscle contracts the pennation angle increases.

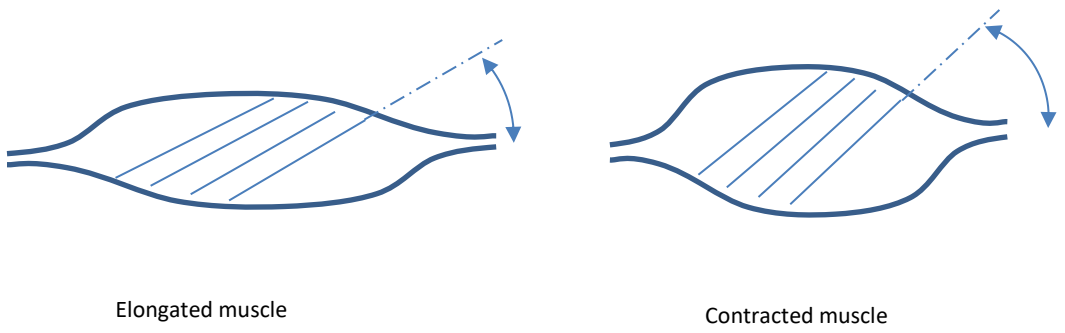

Elongated muscle

Contracted muscle

Figure 2 illustrates how the fibres of pinnate muscle run obliquely. The angle formed between these fibres and a line of action running through the middle of the muscle is known as the pennation angle, when the muscles contracts this angle increases.

The practicing of repetitive movement such as can be produced by NMES has been shown to be instrumental in recovering movement (Donaldson, et al., 2000) (Krakauer, 2005) (Nudo, 2006) (Barker, et al., 2007).

One of the earliest functional uses of NMES was with dropped foot caused by hemiplegia (Lieberson, et al., 1961) (Lyons, et al., 2002). Dropped foot results in an inability to hinge the foot about the ankle and so raise the toes clear of the ground while taking a step. This limits the sufferer's ability to walk and increases the incidence of tripping and falling. Lieberson reported that patients with the condition were able to walk faster and with less effort when using NMES. The system was timed with the swing phase of gait to stimulate the peroneal nerve to innervate the tibialis anterior and peroneus muscles which raises and turns out the foot so that the toes will clear the ground as the leg is swung forward. Lieberson called this assistive application for NMES, functional electrotherapy. However the term functional electrical stimulation or more simply FES was later coined (Moe & Post, 1962) and has since entered common usage.

The clinical use of FES has been compromised by the nonlinearity of muscle response to the electrical stimulation and the variability of the response over time (Riener & Quintern, 1997). The force generation is also influenced by a number of mechanical factors other than the applied stimulation parameters. As a limb moves about a joint the muscle lengths, recruitment pattern, tendon tensions, and muscle bulk will all change. This variability of the muscle tissue beneath the stimulation electrode sites on the skin surface can cause problems maintaining the accuracy of the desired stimulation. The combination of nonlinear muscle response and mechanical changes

to the limb introduce complex variables for the control of FES. It is common for clinically available FES systems to use an open-loop controller to deliver pre-set timed patterns of NMES in response to sensory stimulus (Lyons, et al., 2002) (Mann, et al., 2011) (Lane, et al., 2011). These devices offer a low complexity solution for applications where the functional movement is repetitive and the variability predictable as is the case with walking.

The use of closed-loop-control has been shown as a way to overcome the variability associated with more complex movements. Closed-loop-control enables continuous modification of the delivered stimulation in real-time response to sensory feedback. Crago et al. (Crago, et al., 1980) suggested that the control of contractions elicited by electrical stimulation of muscle could be improved if there was a linear repeatable input output relationship. In these open-loop systems the input is the command to the stimulator and the output is the evoked contraction. He Investigated systems employing closed-loop force feedback to provide regulation of contractions by defining a linear relationship. Allin and Inbar (Allin & Inbar, 1986) investigated the problems of control associated with the application of functional neuromuscular stimulation of the upper limb, concentrating on elbow flexion/extension and wrist pronation/supination. They concluded that closed-loop control was needed in order to overcome the gain nonlinearities and plant dynamic parameter variations. Bajzek and Jaeger (Bajzek & Jaeger, 1987) showed that the mechanical force created from muscle by NMES developed an S-shaped curve as the pulse width of the delivered stimulation increased. The force is initially slow to build, then increases relatively linearly before plateauing as maximal force is reached. They were able to demonstrate how closed-loop-control could be used to linearize the response over the range similar to the earlier work of Crago et al (Crago, et al., 1980).

To successfully deploy closed-loop-control for FES requires appropriate and effective sensory feedback. An ideal control system would enable consistent and predictable response to input perturbation from variations due to; underlying anatomical structures moving relative to the surface electrodes during movement, changes to the mechanical loading of muscles across a movement, and fatigue in the muscle fibres. Closed-loop control can realistically be achieved for an ambulatory system using one of two methods either by; use of a finite-state machine using information from sensors to determine when to switch between states, or by adjusting stimulation in accordance with the continuous monitoring of sensors using some form of proportional-integral-derivative (PID) control (Prochazka, 1993) (Quintern, et al., 1997).

2.1.1 **Lower-limb**

Systems are described here for the lower limb, as sensors and other technologies have been used more extensively for this application than for the upper-limb to date. Some of the techniques described have also formed the foundation for application to the upper limb and therefore are relevant to the research presented in the thesis.

Dai et al. (Dai, et al., 1996) used inertial tilt sensors with finite state FES control to improve the gait of persons who had a stroke or incomplete spinal cord injury (SCI). Different types of tilt sensors were studied for their characteristics and their performance measuring the angular displacement of leg segments during gait. Signal patterns of the lower leg with inertial tilt sensors were identified with control subjects and subjects with drop foot who were being stimulated during level walking. A finite state approach allowed the sensor fixed on the shank to effectively detect the step intention in a population of stroke and incomplete SCI subjects enabling control of the FES. This system featured important advantages over stimulators controlled by foot switches. Initial trials with stroke and SCI subjects demonstrated substantial gait improvement for some subjects, while most liked the good cosmesis and ease of using the device with a tilt sensor. Dai judged the system to be effective but suggested the need for machine learning. Sweeney et al. (Sweeney, et al., 2000) reviewed the use of finite-state control and concluded that it is an established technique for the implementation of intention detection and activity co-ordination levels of hierarchical control in neural prostheses. The first finite state controllers used for functional electrical stimulation of gait were customised to the individual, based on observations of events as they occurred during the gait cycle. Subsequent systems used machine learning to automatically learn finite state control behaviour directly from human experts. Fuzzy control has been utilised as an extension of finite state control, resulting in improved state detection over standard finite state control systems in some instances. Clinical experience has been positive, and has shown finite state control to be an effective and intuitive method for the control of FES in neural prostheses. However at that time although finite state controlled neural prostheses are of interest in the research community the lack of suitable small low-powered sensors meant that they were not widely used outside of this setting.

Chen et al. (Chen, et al., 2001) combined in-shoe footswitches and magneto-resistive tilt sensors to develop a closed-loop control FES system to provide hemiplegic patients with a real-time stimulation to their muscles to prevent drop-foot and the quadriceps weakness from happening during gait training. The FES was triggered by footswitches with real-time feedback from the tilt sensors being used to automatically optimise stimulation parameters. It is uncertain from the

literature whether this approach was any more or less successful than the approaches adopted by either Dai or Sweeney.

The introduction of micro-electro-mechanical systems (MEMS) sensors enabled development of versatile ambulatory systems. These were initially used for laboratory FES research. With O'Keeffe & Lyons (O'Keeffe & Lyons, 2002) able to demonstrate a portable microcontroller based drop foot stimulator developed with a very flexible architecture able to investigation a variety of gait-correction strategies.

Mansfield and Lyons (Mansfield & Lyons, 2003) compared the outputs from accelerometers placed on the torso to conventional pressure switches placed under the foot for detecting heel events in walking. They found that overall the accelerometers produced more reliable results.

Veltink et al. (Veltink, et al., 2003) tested a three dimensional inertial sensing system for measuring foot movements during gait as the basis for an automated tuning system for a two-channel implantable drop-foot stimulator. The foot orientation and position during the swing phase of gait could be reconstructed from the three-dimensional measurement of acceleration and angular velocity. This inertial sensor method was useful for the clinical evaluation of foot movements during gait assisted by a two-channel drop-foot stimulator.

Processed data signals obtained from instrumenting limb segment with MEMS accelerometers and rate angle gyroscopes were analysed using a six camera motion capture system with good correlation of results (Simcox, et al., 2005) (Abdul malik, et al., 2010).

Methods of capturing and conditioning electromyogram (EMG) bio-signals have been developed to enable volitional control of powered prosthetics (Parker & Scott, 1986) (Bagwell & Chappell, 1995). This knowledge into the use of EMG does not directly translate to similar use with FES systems because of the artefacts imposed on the EMG signals by the electrical stimulation pulses. Methods for suppressing the stimulation artefact from the EMG signal have been developed (Thorsen, 1999) along with understanding of changes in signal gain resulting from FES (Taylor & Chappell, 2004).

Chen et al. (Chen, et al., 2010) developed an FES system that used pulse-width-modulation to dynamically control stimulation outputs based on normalised electromyogram (EMG) measurements from the tibialis anterior muscle responsible for raising the foot in walking. A standard EMG signal filtering and normalising technique was used (Konrad, 2005) to interpret movement. EMG bio-feedback control has become available in surface electrical stimulation

rehabilitation systems for drop-foot (Saebo Inc., 2012). Patient involvement in making best use of the system is said to promote motor relearning.

2.1.2 Upper-limb

Research into FES as an assistive technology for tetraplegics opened up the benefits of FES beyond spinal cord injury to include other upper-limb neurological conditions including those caused by cerebral damage such as stroke. (Billian & Gorman, 1992) (Hart, et al., 1998) (Alon, et al., 1998) (Chae, et al., 1998).

2.1.2.1 Instrumentation and Sensors

A multi-channel upper-limb FES system was demonstrated by Ferrari de Castro and Cliquet (Ferrari de Castro & Cliquet, 2000). The system used 8 channel of FES that ran fixed parameter sequences of surface stimulation in response to threshold signals derived from MEMS based sensors. The system enabled paralysed users to perform palmer and lateral prehension and power gripping, that permitted activities such as drinking eating writing and typing.

Hyper-tone in the antagonist muscles is a primary cause for impaired movement patterns following neurological trauma. To counteract these problems therapists will often use splinting of the forearm to hold the limb in a functional position. This type of passive intervention can be augmented with MEMS sensor controlled FES to assist grip and release with benefits to both function and reductions in spasticity (Hendricks, et al., 2001)(Alon, et al., 2002).

In separate research an alternative approach was being taken to the question of restoring reaching and grasping (Popovic, et al., 2002). The hypothesis was that the movements driven by FES are most likely to advance the recovery of functioning if they follow patterns of lifelike motion. To do this this it was important to analyse normal movement for functional tasks for gaining understanding of the influence of the location of the target object, the type of grasp required to acquire the object and the variability of the muscle loading across the pattern of movement. The study went on to identify coordinated synergistic patterns of movement in functional tasks. Then further investigate the differences and similarities between these synergies related to different grasp types, and analysed the impact of direction, distance and load to the synergies. The results were a minimum set of movement mappings necessary for the design of neuro-prosthesis with life-like control. These findings were later applied to an FES system that integrated with goal oriented movement (Popovic, 2003). The study demonstrated significant improvements in function using FES with pre-programmed stimulation parameters. Two problems were highlighted; the difficulty of integrating the user's volitional control within a

simple control strategy, and the complexity of the donning and doffing procedure for such highly instrumented system making it impractical for daily use. The clinical benefits of the system were developed into Functional Electrical Therapy (FET) (Popovic, et al., 2004), involving a programme of intensive exercise that integrates voluntary maximized manipulation and augmented grasping by electrical stimulation of forearm and hand muscles. Later systems introduced bio-feedback for the rehabilitation of chronic stroke (Popovic, et al., 2005).

Research into the use of miniaturised sensors (Tong, et al., 2003) looked for practical control of FES using MEMS accelerometers and rate angle gyroscopes to detect linear acceleration and angular velocity from the upper-limb. An innovation of this work was to use differential signals to generate distinguishable commands allowing the user to give volitional instructions to the system that could be detected over and above the motion tracking function. This meant that event driven finite state control could be directed either by sensor input or user instruction or a mixture of both. One of the drawbacks at that time was the relatively high power consumption of the gyroscopes when used for battery powered ambulatory devices.

A problem with the use of rate angle gyroscopes for practical ambulatory battery powered systems has been the relatively high power consumption. The construction and method of operation of gyros makes them consume tens time more power than that required for accelerometers. Although power requirements have improved with every successive new generation of devices any solution using accelerometers alone will have a substantially reduced power requirement with consequential benefits of battery and device size.

2.1.2.2 **Bio-signal Electromyograms**

Kraft and Hammond (Kraft & Hammond, 1992) evaluated functional improvement in the upper limb of chronic stroke using EMG-initiated electrical stimulation of wrist extensors. There were improvements in grip strength that were shown to have been maintained at long-term follow up after treatment had ended, and suggesting that volitional input from the user reinforces the effectiveness of rehabilitation, a finding supported by later work (Popovic, et al., 2002) (Mann, et al., 2008) (Mann, et al., 2011).

A two-channel, portable, battery operated FES system with surface electrodes to enhance grasping in tetraplegics was developed by Saxena et al (Saxena, et al., 1995). The system was for tetraplegics capable of grasping by using a tenodesis grip. Integrated EMG measurements from surface electrodes positioned over the wrist extensors were used to detect voluntary intention to open the hand to release the grasp. Detection of intent was used to trigger stimulation of the extension muscles. The system proved to work reliably enough for daily home use.

A more complex FES system followed with two-channels of EMG recording and two-channels of FES (Rakos, et al., 1999). The system used one of the EMG channels to switch between functions and the second could be configured to provide proportional control of the stimulation output.

Following his work to develop an EMG detection amplifier with filtering to remove any artefact caused by NMES pulses (Thorsen, 1999), Thorsen developed a system for the control of FES by means of myoelectrical activity detected from voluntarily activated paretic muscles (Thorsen, et al., 2001). He went on to trial this on spinal-cord-injured and stroke patients using residual myoelectric signals from the paretic wrist extensor muscle extensor carpi radialis (ECR), controlling stimulation of either the wrist extension or thumb flexion. Output and tracking accuracy was found to be dependent upon the size of the initial residual force available from the patient.

Sinkjaer et al. (Sinkjaer, et al., 2003) reviewed the use of EMG, ENG and EEG as control strategies. EMG showed potential for reaching and grasping systems but would require significant post processing to cope with stimulation artefact; it was judged to be not viable at that stage outside of the laboratory.

The author (Lane & Taylor, 2004) developed a wearable microcontroller based FES stimulator capable of reading an EMG control signal from the muscle while under electrical stimulation. A software filtering system was developed for this device that reduced the complexity over previous systems and employed a method of windowing the time between stimulation pulses when the EMG signal was measured. This method avoided the problems of stimulation artefact encountered by SinkJaer. Closed-loop control of the output was possible for finite state control.

Naito (Naito, 2004) used a study of electromyography of upper-limb function to quantify muscle firing patterns of synergistic movement underlying the work of earlier studies (Popovic, et al., 2002). Naito used these to develop an application for FES capable of flexing and supinating the forearm in tetraplegics by simultaneous stimulation of the Biceps Brachii and the Brachioradialis muscles. In a further subtlety, by positioning one of the electrodes above the point at which the posterior interosseous nerve emerges he was able to stimulate hand opening at the same time. The method offered an elegant simplicity with effective results, but required high levels of control.

2.2 Bioimpedance

During the course of the research while developing a robust EMG amplifier capable of withstanding NMES voltages, a previously unseen and interesting artefact was observed. The artefact was seen to change with respect to the lengthening and shortening of the muscle over which the EMG amplifier pick-up electrodes where applied. An investigation of the literature led to understanding that this artefact could be explained by an area of electrophysiological measurement relating to bioimpedance.

Shiffman et al. (Shiffman, et al., 1999) described a system for non-invasive impedance measurements as a function of position along body segments such as the thigh. The principal conclusion was that the phase of the impedance falls monotonically with increasing distance from the knee, with average values substantially above what is found using standard, whole-body bioelectrical impedance analysis. This finding was later confirmed (Kyle, et al., 2004) when the relationship was shown to hold for the distance between sensing electrode placement along a muscle.

Tarulli et al. (Tarulli, et al., 2005) called the technique Electrical impedance myography (EIM) and proposed it as a non-invasive bedside assessment of myopathy. They found that the major EIM parameter to be spatially averaged phase difference, and observed that EIM could be used to track muscle change over time. Changes to the bioimpedance were noticed with respect to movement of the limb under test, these were regarded as an unwanted artefact.

Conventional EIM machines perform bioimpedance readings using a 50 kHz injected measurement signal (Rutkove, et al., 2008). Shiffman et al. (Shiffmann, et al., 2008) looked at frequencies beyond this up to 2 MHz and found that other than when using distally placed electrode the impedance of the body matched an accepted three-element resistor capacitor model.

Nahrstaedt et al (Nahrstaedt, et al., 2008) demonstrated a method of using conventional bioimpedance measurement methods to determine the position of the foot. This was combined with a dropped-foot stimulator to determine dorsiflexion and plantar flexion, circumduction, eversion and inversion, and toe movements. Nahrstaedt did however identify that the system was impractical for use outside of a laboratory setting because of the large number of electrodes that needed to be attached.

2.2.1 Electrical properties of biological tissue

In 1925 Fricke and Morse (Preedy, 2012) developed what has come to be the accepted model for electrical properties of cellular biological tissue. The three element model describes the extracellular space as a simple resistance and the intracellular space as a combination of a resistance with the cell membrane represented by a capacitance. This is portrayed in Figure 4.

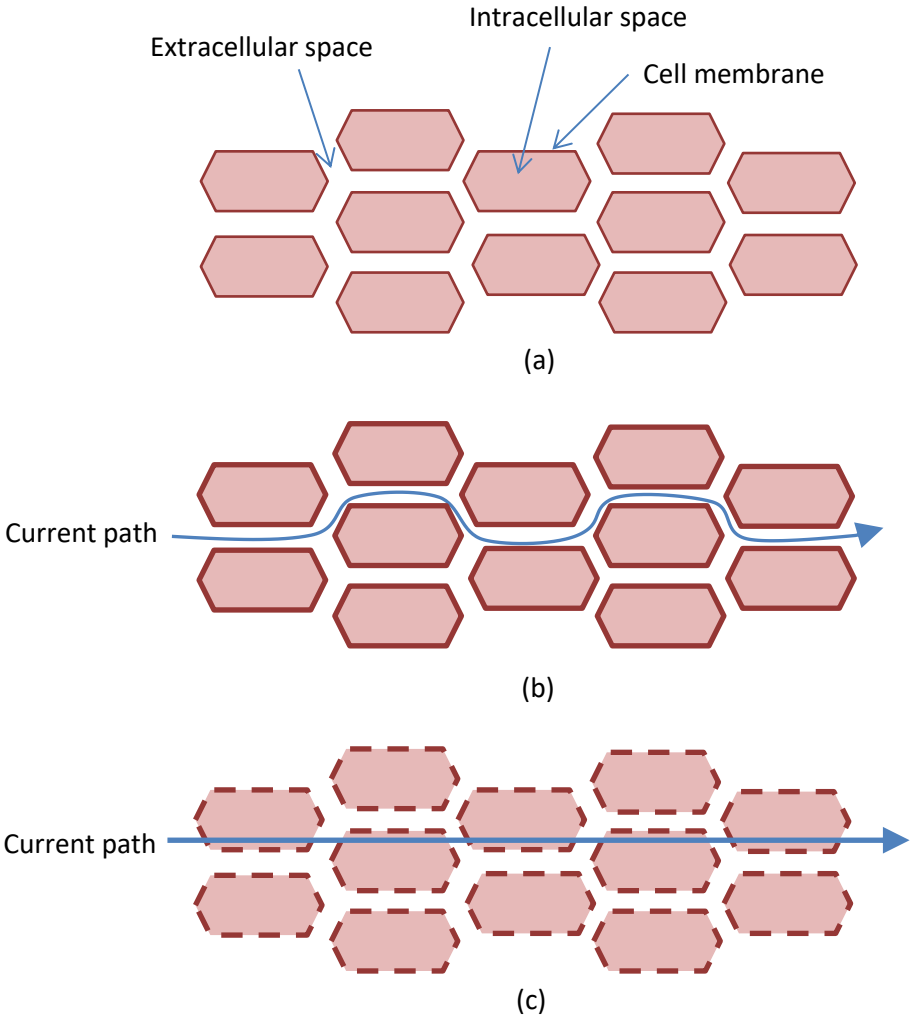

Figure 3 with the equivalent circuit shown in Figure 4.

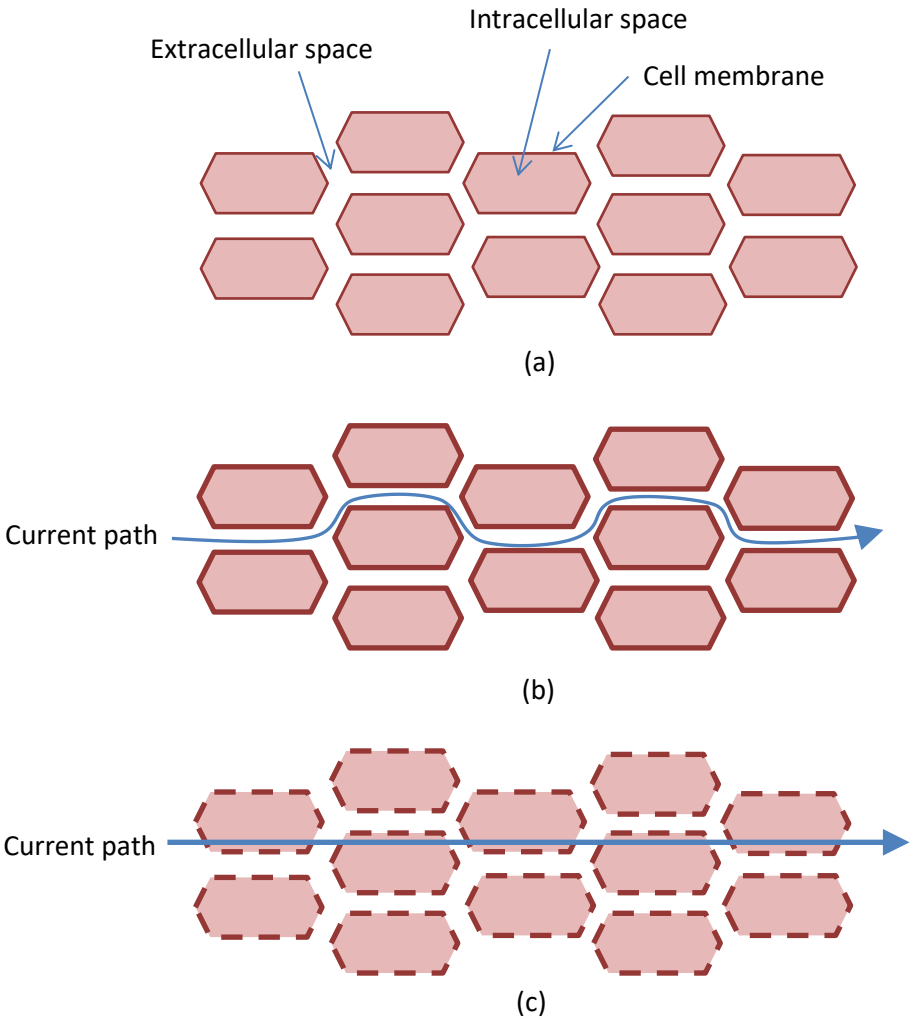

Figure 3 illustrates the Fricke model for electrical properties of cellular biological tissue.

(a) The elements identified by Fricke were the extracellular resistance, the intracellular resistance and the cell membrane capacitance.

(b) At low frequencies the cell membrane capacitance blocks conduction of the current through the cells so conduction is only through the extracellular space.

(c) At higher frequencies the current can cross the cell membrane capacitance

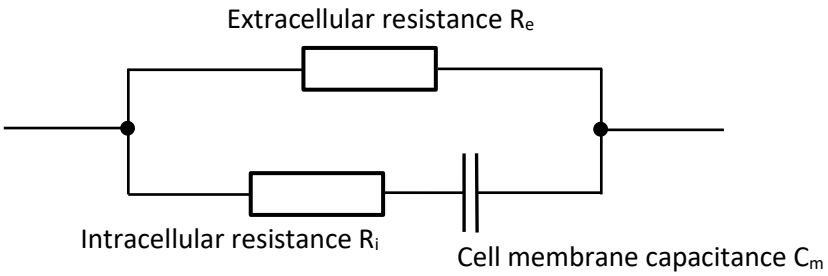

Figure 4 illustrates the equivalent circuit for the Fricke model shown in Figure 3.

R_e represents the resistance of the extracellular space between the cells.

R_i represents the resistance of the intracellular space within the cells.

C_m represents the capacitance due the cell membranes

The extracellular and intracellular spaces contain salt ions making them both highly conductive, whereas the cell membranes are made up from lipids that form an insulation layer. This insulation layer means that low frequency current is unable to flow through the cells.

At low frequencies the current path is restricted to the extracellular space which represents about 20% of the total volume (Figure 3b). Consequently the impedance is relatively high under these conditions.

At higher frequencies the current is able to cross the capacitance of the cell membranes and flow through the intracellular space as well as the extracellular space (Figure 3c). Consequently the impedance is relatively low under these conditions.

Almost needless to say this somewhat over simplifies the real situation as there are a numerous types of tissue within the body, each of which behave in a differing manner. The reactance of the cell membranes is a function of the frequency of the applied signal used for making the impedance measurement. As already stated at low frequencies the current path is through the extracellular space and so the impedance is entirely resistive with no current able to breach the insulation of the cell membranes. When the frequencies is progressively increased the reactance resulting from the cell membranes reaches a maximum before reducing again as very high frequencies are reached.

At very high frequency the membrane capacitance is negligible. The increase in reactance is accompanied by an associated change in the phase angle. This can be represented by an idealised

Cole-Cole plot (Figure 5), where the reactance is plotted against the resistance across a frequency range.

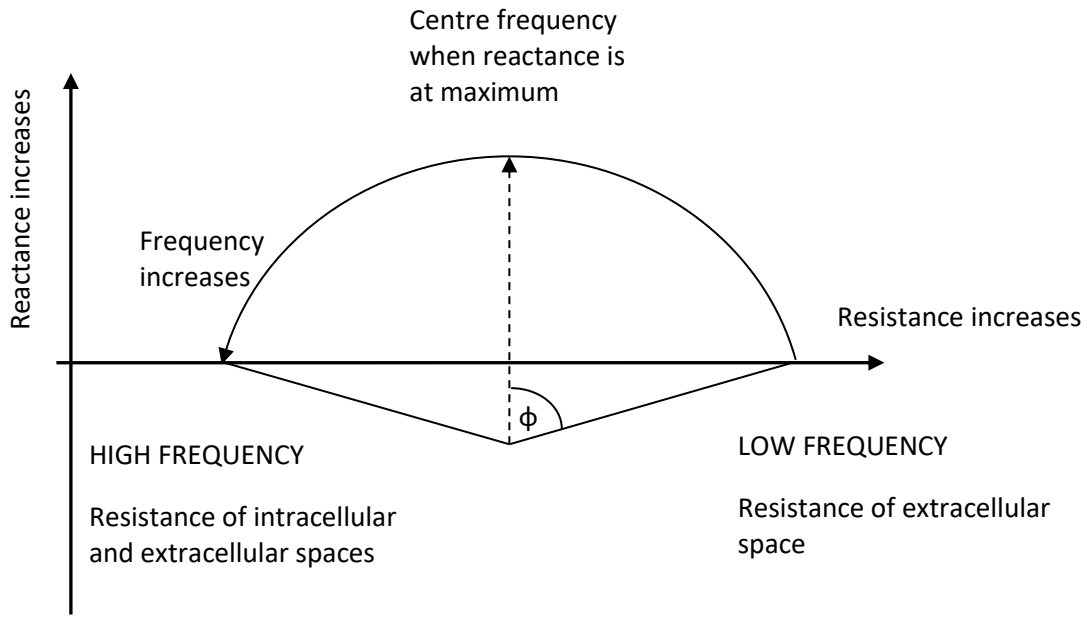

Figure 5 shows an idealised Cole-Cole plot or the resistance and reactance response of human tissue to varying frequency.

The idealised Cole-Cole plot shows the tissue response to frequencies of the range 100Hz to 10GHz. There are two regions of particular interests known as the alpha and beta dispersions. The alpha dispersion occurs at around 100Hz at this frequency the outer cell membranes are able to fully charge and discharge within the period of the applied sinewave. As the frequency increases beyond the alpha dispersion frequency only partial charging of the membrane can occur so the current begins to charge the intracellular spaces which now behave as capacitors. Current can now flow across the cell lipid membrane which produces a structural relaxation of the membrane. This effect reaches a peak at around 100 kHz and is termed the beta dispersion. A third dispersion known as the gamma dispersion occurs at frequencies around 10GHz when dipolar reorganisation of the cell structure occurs along with the relaxation of water molecules but this is not of direct interest as the impedance changes of most relevance fall between the alpha and beta dispersion points. Typically for Bioimpedance tomography used to look for changes in muscle pathology a frequency of 20 - 50 kHz is used.

2.2.2 Application of Bioimpedance for kinematic analysis

Twenty-five years ago Nakamura et al (Nakamura, et al., 1992) used a four electrode bioimpedance measurement system to classify the impedance changes in the upper-limbs of experienced and novice tennis players. The results were able to show that the bioimpedance changes measured across the range of a limb movement were due to changes in the cross-sectional area of the muscle. Nakamura was able to relate the change in impedance to the position of the limb and the rate of change of the impedance to the angular velocity of the limb. An interesting observation was that differences in the torque developed by varying muscle loading had little influence upon the impedance measured. The current electrodes were placed proximally and distally on the tennis player's racket arm. Three sites were compared for the measuring electrode pair before choosing a site on the forearm approximately midway between the elbow and the wrist. From this location Nakamura was able to make measurements of the bioimpedance that could be used to identify the elbow flexion and wrist flexion phases of the racket swing. The results showed the differences between the swings of experienced and novice players.

It was a full decade before any further work on upper-limb bioimpedance of any significance was reported upon. Kim et al (Kim, et al., 2003) sought to locate optimum electrode positions for detecting movement of the limb. As was the case with Nakamura's study a four electrode bioimpedance measurement method was used with the current electrodes placed proximally and distally as before. Eight measuring electrodes were placed on the arm and a further six on the forearm. By making impedance measurements between the various combinations of electrode pairs using this arrangement Kim was able to identify the best electrode position for detecting the individual movement components associated with elbow, wrist and finger extension. Kim was also able to confirm Nakamura's finding that torque changes made little difference to the measured impedance, and was also able to show that this held true for isometric contraction when little cross-sectional area change was present. Kim defined the optimum electrode position as the one that gave the largest bioimpedance change correlated to joint angle changes. This was combined with the highest signal to noise ratio where noise was defined as unwanted involvement from other joints. Kim did not consider the bioimpedance across the elbow joint concentrating only on the muscle groups either side of the joint.

The following year a different team in Korea (Kim, et al., 2004) carried out a very similar study this time on the lower-limb. The findings were substantially similar albeit for the leg this time, the team did however go on to show how with post processing determination of patterns of movement was possible. They were able to show that this could be done with relatively low

levels of computational power. Unlike the upper-limb study (Kim, et al., 2003) where impedance measurements were not made across the elbow joint, in this study measurement were made across the joint, in this case the knee. It was these measurement that proved to be the most useful when determining the joint angle.

Work done by a team in Japan (Ohta, et al., 2005) focussed on the use of bioimpedance as a way to deduce tendon elongation during isometric contraction of the biceps muscles about the elbow. A four electrode bioimpedance measurement method was used with the current electrodes placed distally on the limb being measured and on the other arm. The measuring electrodes were placed at either end of the biceps. The forearm was constrained in a position approximately halfway toward fully flexed from the straight out position. Subjects were asked to go from no effort to 80% of maximum voluntary contraction over a period of 8 seconds. Measurement were made of the force applied, the bioimpedance and tendon length change determined by ultrasound measurements. The results showed that as the effort of the voluntary isometric contraction increased against the restraint there was elongation of the tendon. This was accounted for by contraction of the muscle resulting in a reduction of the bioimpedance.

In Europe a German team (Nahrstaedt, et al., 2008) were the first to combine measurement of lower-limb bioimpedance to determine joint ankle position for control of a drop-foot stimulator. They used a four electrode measuring method with current electrodes placed just below the patella and just above the angle. The measuring electrodes were placed almost as far apart with one below the current electrode at the top of the tibialis anterior muscle and the other on the back of the leg at the base of the calf muscle. A second set of electrodes were used to deliver the FES from the drop-foot stimulator. These were placed on the front of the leg over the tibialis anterior muscle. The bioimpedance measurements obtained were able to characterise dorsiflexion, eversion and circumduction of the foot. These are all important for the proper correction of drop-foot. Conventional FES was used to correct the foot position in gait, with the bioimpedance measurement system protected by suitable circuitry when the stimulation pulses were delivered. Measurements of the bioimpedance were made during the period between the stimulation pulses. An iterative learning feed-forward control strategy was used so that any misalignment detected during a step was corrected for the next. This meant that the system would start to self-tune after the first step. Within these constraints the system demonstrated adaptive control.

Coutinho et al (Coutinho, et al., 2012) revisited isometric contraction of Biceps Brachii, this time at differing elbow angles. The team raised reservations about the use of four electrode measuring systems citing low sensitivity as a recognised problem (Seward & Rutkove, 2009) (Shiffmann, et

al., 2008). Using a two electrode system they were able to obtain results that supported previous findings. The bioimpedance of the biceps muscles was measured under isometric contraction at five angles ranging from 45^0 to 135^0 with the angles selected in random order. The contraction was against a 2.2kg load weight. The measured parameter was shown to be highly correlated to muscle contraction.

2.3 Conclusions

NMES is an established treatment modality for the rehabilitation of patient following the effects of neurological disease that results in partial paralysis. It can be applied functionally as FES to assist with the activities of daily living.

FES for the lower limb is well established for the correction of dropped-foot. These systems are in regular daily use. There are however less options available for FES for the upper-limb outside of the clinical laboratory setting.

Further investigation is needed into understanding how changes in the stimulation parameters affect the recruitment of muscle, particularly the effect upon fatiguing.

Recruitment uncertainty is increased by transcutaneous surface electrodes; and is further complicated by the non-linear response of muscles to the stimulation. These two things are the major contributing factors that compromise open-loop control of FES.

Closed-loop control strategies have addressed the non-linearity issues. The feedback for these systems has been either; external sensors, or measured bio-signals.

MEMS sensors have proved effective; however the complexity of these systems has meant that they remain predominantly laboratory based. The sensors are able to give fixed reference relative to gravity and magnetic compass movement tracking and gesture recognition.

Bio-signals in the form of EMG have been shown to be effective. They are difficult to use but can enable selection from a choice of FES assisted movement and proportional control. EMG holds information about volitional intent as well as a dynamic component. It does not readily provide information about limb position or the starting orientation prior to movement.

Further investigation should be focussed on combining the intentional and dynamic feedback of EMG with the positional tracking and gesture recognition capabilities of external sensors. Bioimpedance measurement has been shown to be a method of directly detecting limb movement. This should be investigated as a method of positional feedback.

Measurements of bioimpedance have been shown to be a reliable and repeatable method to determine the extent of muscle contraction. The muscles contraction can be related to the angle of the joint it acts about. Post processing of the bioimpedance measurements has been shown to enable tracking of patterns of limb movement. This tracking of the movement can be used to control the output parameters of an FES system used to correct impaired movement.

Chapter 3: Description of the Research and Methods

3.1 Introduction

At the outset, the purpose of this research was to investigate the techniques and technologies required for each part of an effective FES system capable of sensing and controlling upper-limb movement in chronic stroke patients. A further aim was to demonstrate how these parts could be integrated for use in a wearable system that could be both user-friendly and functional outside of a laboratory setting.

Research that predates the work covered by this thesis had indicated that a combination of sensing EMG bio-signals combined with real-time movement tracking from MEMS sensors (Lane & Taylor, 2004) would provide the input information from which a practical functional system could be developed.

A set of design criteria was developed when considering the FES system that would be needed for the study. These are summarised below and then subsequently described in greater detail afterwards.

- Two patterns of functional movement would be included, these being derived from previous clinical experience of effective restorative therapy;
    - **Wrist extension with hand opening and thumb abduction**. This movement is especially useful for overcoming high tone in the flexor muscles that result in a hand that is clenched closed with a tightly flexed wrist. The movement restores the ability to open the hand wide enough to form a grip for grasping objects. Care is needed to avoid hyper-extension of the joint which would compromise the function.
    - **Elbow extension with wrist extension and hand opening**. This movement has been shown to be effective with tetraplegics who have little or no adverse muscle tone. The method promotes a reach-and-grasp movement by rotating the forearm to a neutral position while extending the elbow and wrist. However the method becomes difficult to control when adverse muscle tone is encountered due to the complex compound movement it produces.
- Multiple axis MEMS accelerometers would be used to detect movement. The output signals would be conditioned in two discrete ways to derive information about spatial positioning of the limb and volitional movements made by the user.

- EMG bio-signals would be measured from the muscles groups that have been subjected to electrical stimulation. Using a suitable method of collection and conditioning such that it is possible to derive information about the intensity of muscle activity and movement of the limb. Due both to the electrical stimulation and volitional movement.
- A programmable microcontroller based MNES hardware would be needed to deliver controlled patterns of electrical stimulation.

3.2 Patterns of functional movement

3.2.1 **Wrist extension with hand opening and thumb abduction**

The principle activists in producing this movement are the wrist extensor muscles extensor carpi radialis longus and brevis (ECRL & ECRB) along with a correctly stimulated portion of the posterior interosseous nerve (Figure 6).

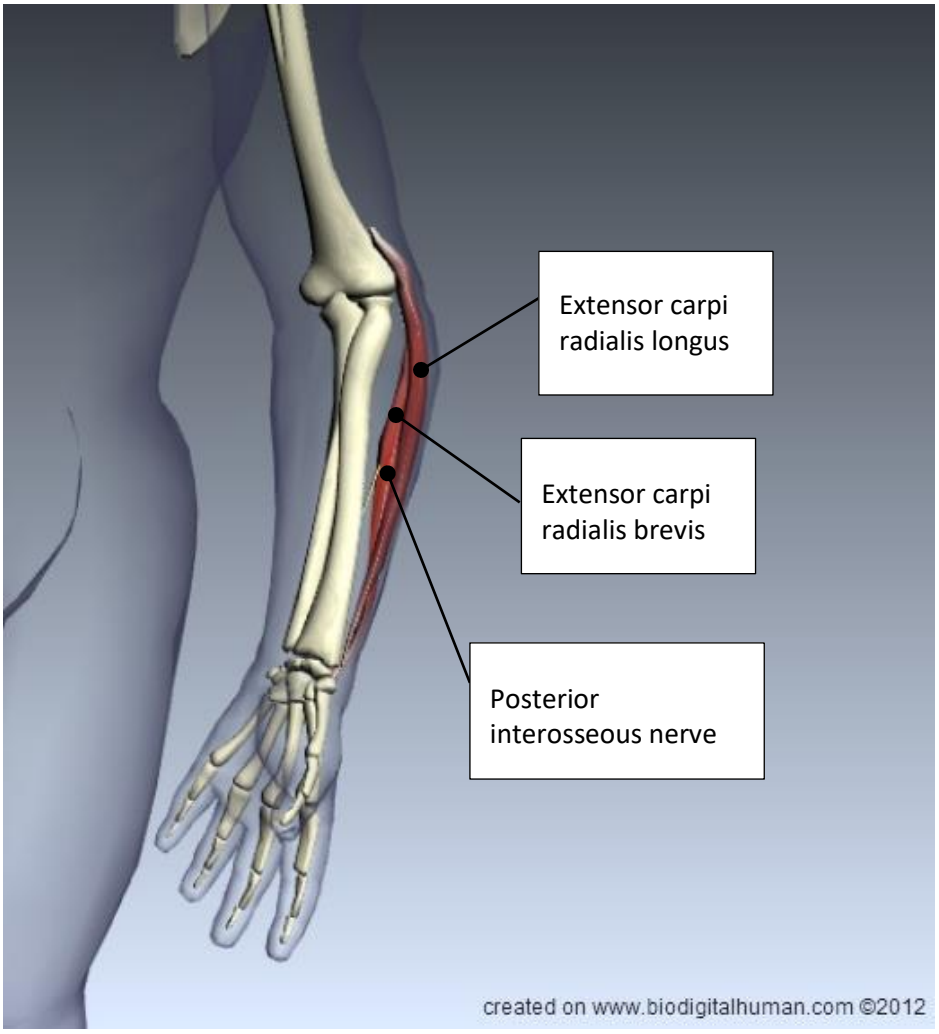

Figure 6 shows the location of skeletal muscles extensor carpi radialis longus and brevis (ECRL & ECRB), and the posterior interosseous nerve.

ECRL, as the name suggests, is the longer of the two wrist extensor muscles attached at the outside edge of the humerus with its base attached to the second metacarpal bone of the index finger. Its function is to extend the wrist and abduct the hand open. ECRB is attached to the humerus at the elbow and ends midway down the forearm onto a tendon that pulls on the wrist. Its function is to extend and abduct the wrist. These two muscles work together with the shorter fatter ECRB muscle providing more of the power while the longer more slender ECRL provides finer control of the movement.

The Posterior Interosseous nerve is a continuation of the deep branch of the Radial nerve that emerges close to the surface of the skin about a third of the way down the forearm. It innervates most of the extensor muscles in the forearm as well as abductor pollicis longus which abducts the thumb (Figure 7).

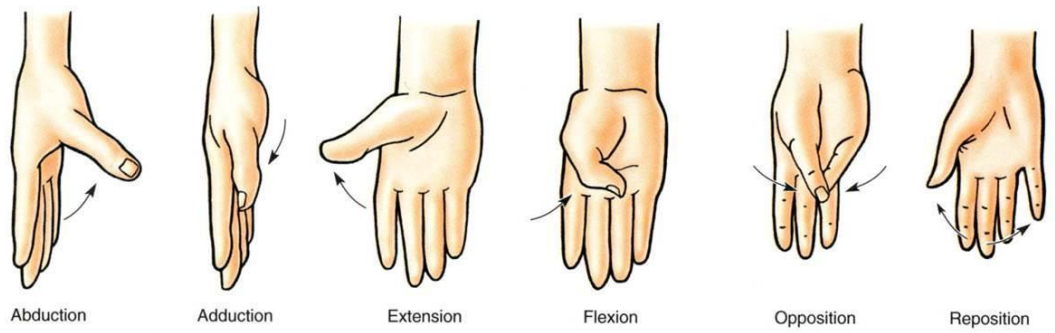

Figure 7 illustrates the range of movement possible for the thumb. A digit is abducted when it is moved away from the palm.

Neuromuscular electrical stimulation can be delivered either as a series of single charged pulse requiring a refractory period for charge balance to be restored, or as a charge balanced pulse where a charge is delivered and then immediately taken back. These are often loosely referred to as monophasic and biphasic waveforms (Figure 1 page 43). Monophasic waveforms have the advantage that the seat of the muscular response is more concentrated under the negative electrode also known as the active electrode. This enhanced effect is under the control of the operator and usually makes setting up the system more straightforward. A fuller explanation of the physiological effects and the functional application of NMES as FES are shown in Appendix A.

When a stimulation pulse flows between a pair of electrode the one that the charge enters the body from is said to be the active electrode, and one that completes the circuit allowing the charge the leave the body is the indifferent electrode. When the active electrode is placed over the ECRL & ECRB muscles it concentrates the majority of the electrical stimulation into these wrist

extensor muscles. Completing the electrical path with the indifferent electrode placed close to the Posterior Interosseous nerve ensures that there is also the stimulation to a lesser extent of the extensor and abductor muscles for the hand (Figure 8). The result is that following the onset of stimulation, as the intensity builds the wrist will extend first followed by the hand opening. Were this to happen in the opposite order and the hand commenced to open before the wrist had begun to move, the fingers would go into hyper-extension while the wrist remained flexed. This movement is both non-functional and potentially quite painful (Figure 9).

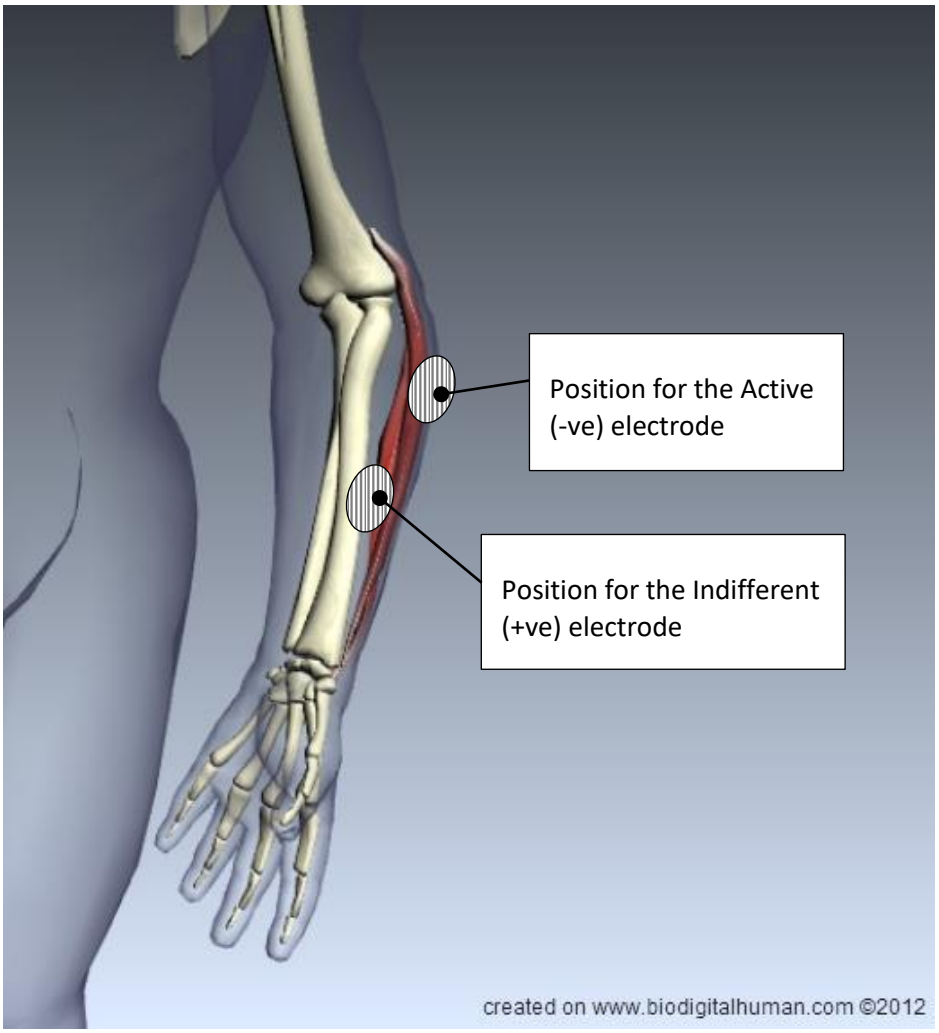

Figure 8 shows the FES electrode positions for stimulation of the wrist extensors and the posterior interosseous to achieve wrist extension with hand opening and thumb abduction.

(a) (b) (c)

Figure 9 is a series of images showing wrist and hand position.

a. Shows a position that is typical for a person who has high flexor muscle tone, this would be the positions from which any movement would begin.
b. Illustrates the desired wrist extension with hand opening and thumb abduction that produces a functionally useful opening of the hand.
c. Demonstrates an undesirable and non-functional finger hyper-extension of the fingers without any extension of the wrist.

3.2.2 **Elbow extension with wrist extension and hand opening**

This pattern of stimulation is an adaption of a method of stimulation that was first described by Naito (Naito, 2004) for use with tetraplegia. The technique uses the supinator function of the Biceps Brachii and the Brachioradialis (Figure 10) to achieve rotation of the forearm to a functional position for forming a grip. A further subtlety is to place the electrode stimulating the Brachioradialis over the deep branch of the radial nerve where the posterior Interosseous begins (Figure 10 Figure 11). The electrical stimulation circuit is then partially completed by current flowing back along the Radial nerve which causes two of the heads of the Triceps Brachii muscle to contract giving elbow extension. By stimulating so closely to the Posterior Interosseous it also produces wrist extension with hand opening.

Biceps Brachii is a double headed muscle beginning from two attachment points on the scapular and ending on the radius bone in the forearm. The longer head of the muscle performs predominantly as a supinator causing the forearm to rotate so that the palm of the hand faces upwards. It also works with the shorter head to flex the elbow. By concentrating the electrical stimulation on the longer head of the muscle and keeping levels below those that would cause flexion, it is possible to target only the supinator function.

Brachioradialis is also a flexor muscle, but it has the effect of pulling to rotate the forearm to a neutral position first that is midway between pronated and supinated. This means that a limb

which is pronated (rotated so that the palm is facing away from the body) will be supinated. Again by careful control of the stimulation it is possible to only target this function.

Triceps Brachii is a three headed muscle with the longest head beginning at the scapular and the other two from high up on the humerus. These two shorter heads are both innervated from the Radial nerve. All three heads come together at the elbow where they act to extend the forearm. Electrically stimulating the Radial nerve will cause two of the heads of Triceps to contract giving rise to elbow extension and promoting reach.

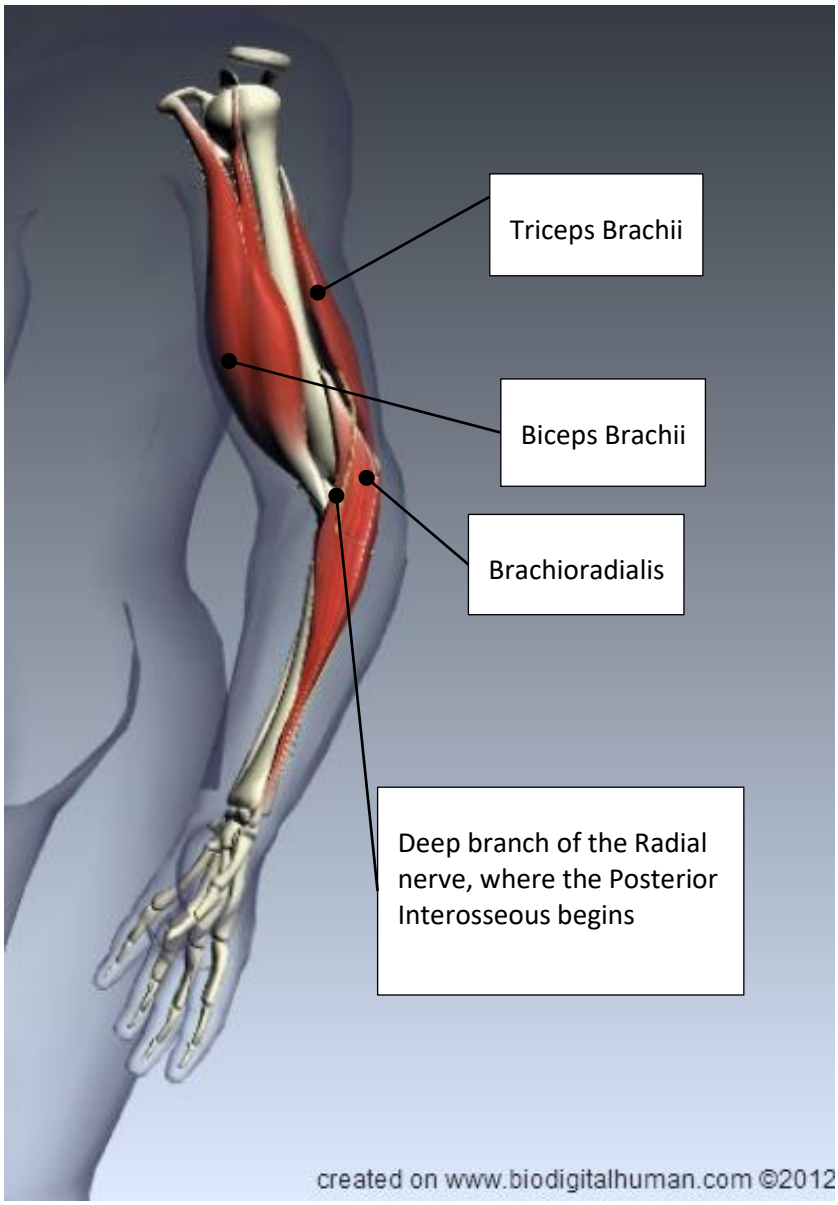

Figure 10 shows the muscles needed for supinating and extending the forearm. The long head of Biceps Brachii works with Brachioradialis to rotate the limb into a neutral position. While Triceps action is to extend the elbow. The posterior interosseous nerve sprouts from where the deep branch of the radial nerve emerges near Brachioradialis.

The method requires careful positioning of the electrodes in order to achieve the required functional movement. The active electrode is placed over Brachioradialis adjacent to where the deep branch of the Radial nerve emerges. The inactive electrode is positioned on the inside of the upper arm towards the rear edge of the long head of the Biceps. It is important that besides targeting these supinator muscles a current path is set up along the Radial nerve to ensure recruitment of the Triceps to promote elbow extension.

The active electrode placed over the Brachioradialis where the deep branch of the Radial nerve emerges will also be just ahead of the beginning of the posterior Interosseous, and stimulating the Posterior Interosseous will producing wrist extension with hand opening and thumb abduction.

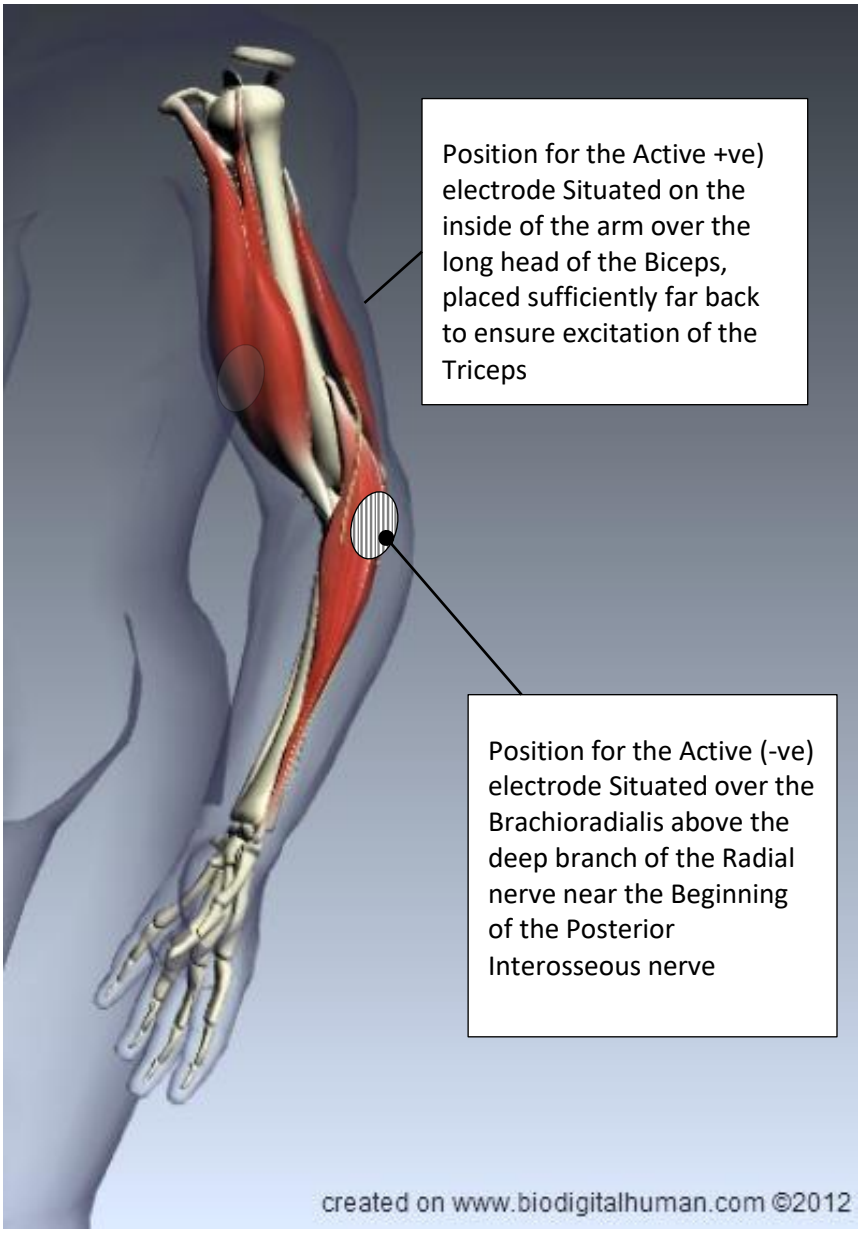

Figure 11 illustrates how the electrical stimulation electrodes are placed so that the current path is across the joint of the elbow. Stimulating the Posterior Interosseous nerve results in wrist and hand extension as well as excitation of the radial nerve to produce contraction of Triceps. While stimulation of the long head of Biceps and Brachioradialis supinates the forearm.

3.3 Multiple Axis Accelerometery

Early work with multiple axis micro-electro mechanical system (MEMS) accelerometers had demonstrated that it is both possible and practical to co-condition the output signals from these accelerometers to derive useful information about limb position and the wearer's volitional movement.

3.3.1 **MEMS Accelerometers**

Accelerometers consist of a damped mass that exhibits inertia in the presence of motion. This inertia is used to determine rate of change of motion. The damped mass is supported on a structure referred to as a beam. The beam is aligned to an orthogonal axis of movement. The inertia of the damped mass during periods of accelerations cause deflection of the beam and it is capacitive changes to the electrical properties caused by this deflection that are used to determine the acceleration. Multiple axis accelerometers have a beams for each of the axis.

MEMS accelerometers are manufactured from micro etching silicon substrates. The sub-miniature construction means that these devices are very responsive while being sufficiently robust for use in portable equipment. These devices have low power requirements which make them ideal for battery powered applications.

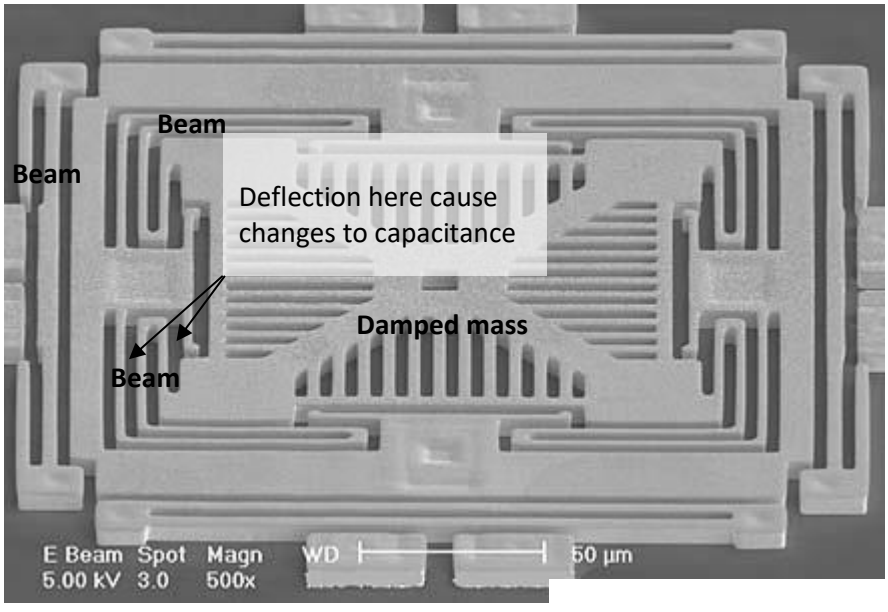

Figure 12 show an image of the etched silicon substrate of a three-axis MEMS accelerometer. The central mass is supported at each corner with spring beams that enable movement in all directions. Damping is achieved by gas sealed into the packaging container of the device. The entire sensor is approximately 200µm across.

A typically orientation for the accelerometer axis is shown in Figure 13. In this arrangement the z axis will usually display slightly different characteristics to the x and y which will be matched. This is because all of the beams lay on the same plane and whereas the facing surface area of the capacitive elements remains the same for x and y, the area of aligned elements reduces with deflection for z.

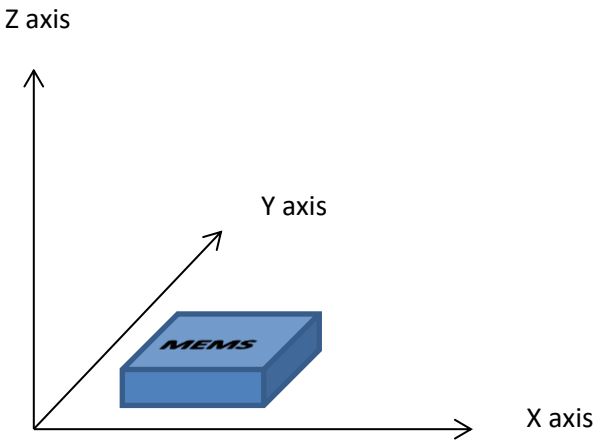

Figure 13 shows the orthogonal directions of measurement for a three axis accelerometer

3.3.2 **Signal conditioning**

The measurement response of accelerometers is categorised by the range of acceleration they are able to measure, the frequency response to changes in acceleration and the sensitivity or resolution of the readings. A typical device may offer a selectable operating range, for instance the Analog Devices ADXL345 can be set to measure full scale at 2g, 4g, 8g or 16g. The sensitivity remains constant at 10 bit resolution, so the resolution is finer at the lower range settings. The frequency response is determined by the bandwidth setting which for this device can be as high as 1.3 kHz. However the power requirement for the sensor increases with increased bandwidth so there is an incentive to set the bandwidth no greater than necessary.

Human body motion seldom exceeds a frequency of 10 Hz with most movement occurring at around 1 Hz (Winter, 1990) (Bronner, 2003). Gestures are typically faster and shorter movements than those associated with limb positioning.

If the accelerometer bandwidth setting is selected with a cut off frequency of 100 Hz then all body movement will be reliably captured and the device will be working at the lowest possible power

requirement for the application. Further processing of the signal is then required to separate the higher frequency gestures from the background limb position information.

The mass within the accelerometer is subject not only to initial forces resulting from motion, but also experiences the gravitational field of the Earth. When the accelerometer is stationary gravity will act upon the damped mass to cause deflection of the beams. As the orientation of the mass is altered by rotation of the device, the pattern of deflection of the beams changes. This relationship can be used to determine the angle of the device with respect to the ground (Figure 14).

Using the formula

$$s = g \sin\theta$$

Where

s is the output from the accelerometer

g is acceleration due to gravity

θ is the angle of inclination from the plane of the ground

Rearranging for angular displacement

$$\theta = \arcsin(s/g)$$

When the accelerometer is used to measure movement of a limb on the body the output can be conditioned to extract both the angular displacement and additional 'gesture' movements made by the wearer (Figure 15). These gestural movements can be used as control command signals.

When the signal from the accelerometer is low-pass filtered with a cut of frequency of approximately 2 Hz gravity referenced angular displacements can be determined (Figure 15 b).

When the signal from the accelerometer is high-pass filtered with a cut off frequency of approximately 10 Hz volitional gesture movements can be determined (Figure 15 c).

The 'dead-band' between 2 and 10 Hz provides sufficient separation for these two to be reliably identified (Winter, 1990) (Bronner, 2003). A problem often associate with movement following neurological disorder is 'intentional tremor'. This is where the limb will oscillate with a frequency of between 3 to 5 Hz as a movement is performed (Seeberger, 2005). The frequency of intentional tremor falls within the chosen dead-band.

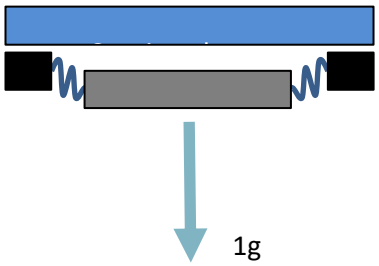

(a). Mass of the measuring beam aligned with the plane of the ground giving maximum displacement from the sensing element with respect to

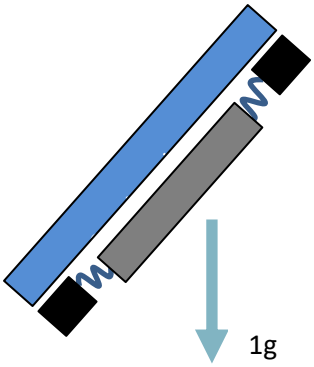

(b). Mass of the measuring beam only partially aligned with the plane of the ground displacement from the sensing element has reduced.

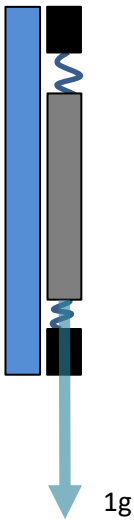

(c). Mass of the measuring beam completely unaligned with the plane of the ground displacement from the sensing element is at a minimum.

Figure 14 is a series of diagrams showing how the sensing element of an accelerometer is influenced by gravity

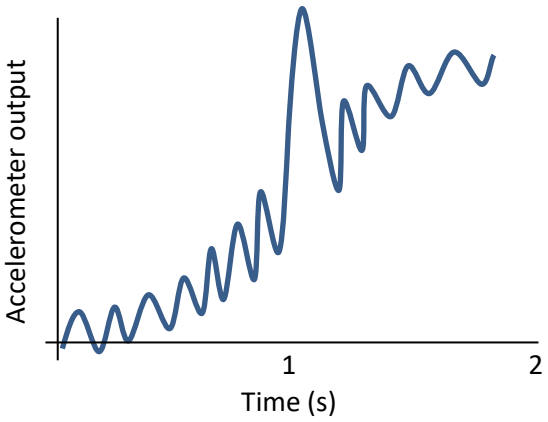

(a). Output from the accelerometer without any additional filtering. The signal contains both positional and volitional gesture information.

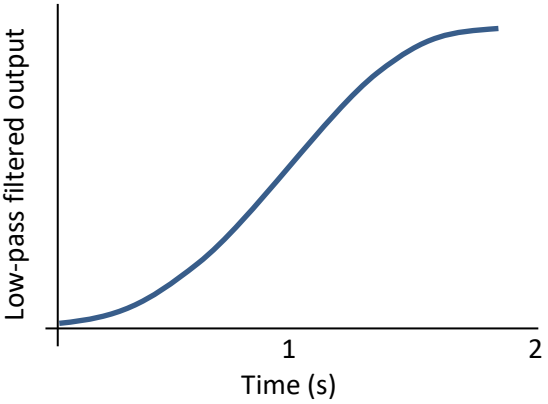

(b). Output from accelerometer with low-pass filtering to obtain the angular displacement

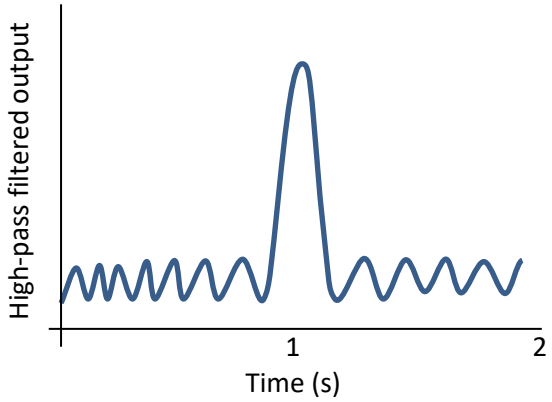

(c). Output from accelerometer with high-pass filtering to obtain volitional gesture movement

Figure 15 illustrates how the output from the accelerometer can be conditioned to extract angular displacement with respect to gravity and short duration volitional gesture movements.

Initial research to look at the use of accelerometers for movement tracking used a stimulator with a twin axis accelerometer mounted on the main printed circuit board within the device (Figure 16). When the stimulator was correctly positioned on the forearm it was possible to detect volitional forward, back and side-to-side movements as well as gravity referenced angular displacement in two planes.

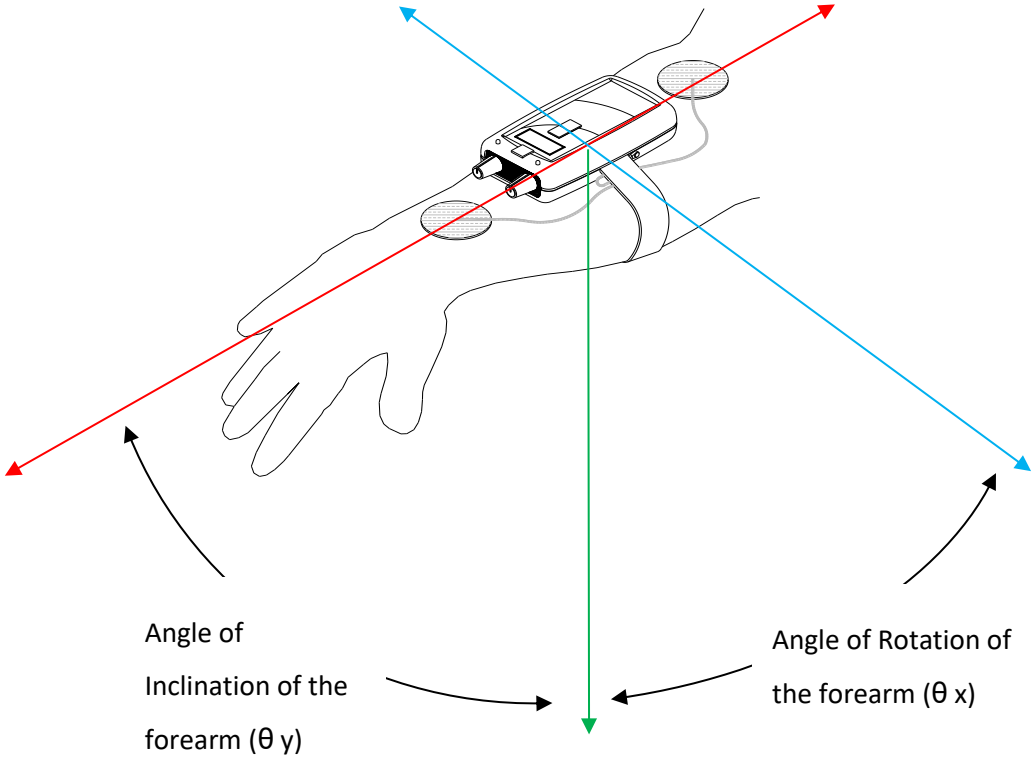

Figure 16 shows a stimulator containing a two axis accelerometer worn on the forearm. Using suitable signal conditioning methods the accelerometer was able to detect forward back and side-to-side movements as well as the forearm angle and rotation referenced to gravity.

The stimulator was designed to deliver controlled sequences of electrical stimulation capable of producing functional pattern of movement. The first study looked at assisted grasping where the stimulation produced wrist extension with hand opening and thumb abduction. Threshold triggers based on angular displacement and gesture were used to stage the progress through the sequence of the electrical stimulation. This gave the wearer control of timing for the pattern of stimulation so that the assistance of the functional electrical stimulation matched their volitional movement. If for example the user was able to move their arm forward, a threshold would be set to detect this movement and the stimulation triggered in response to the action.

This type of control has proved effective but remains susceptible to 'noise' from other movements unintended for control. It was found that a more robust method was to use thresholds based on absolute set point angles referenced to gravity. Triggers could then occur as

the limb either exceeds or falls below these set points. It is then possible to combine both of the above methods so that a forward motion will only act as a trigger after initially exceeding an angular displacement set point. This method was found to reliably produce immunity to non-control movement artefacts.

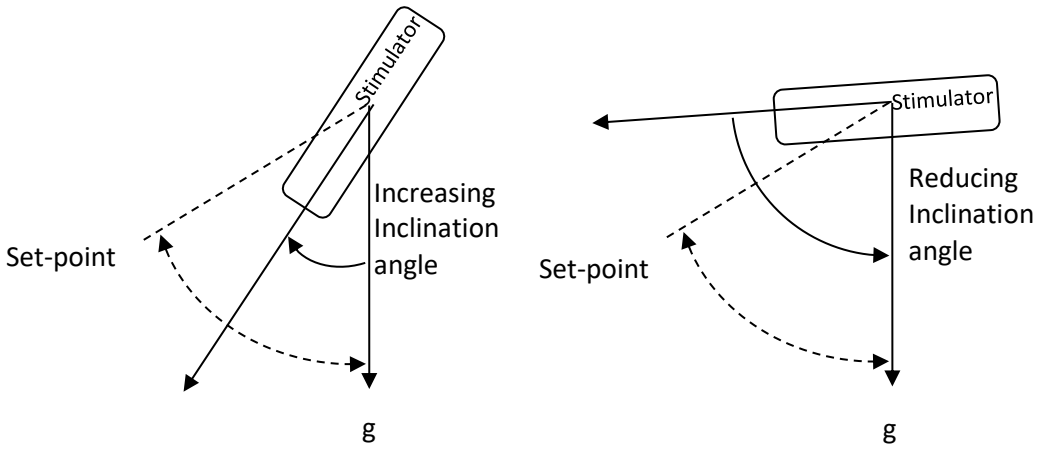

Case 1
The threshold is reached when the inclination angle exceeds the set-point angle.

Case 2
The threshold is reached when the inclination angle falls below the set-point angle.

Figure 17 illustrates how a single set-point angle can be used to provide two thresholds determined by the direction of approach.

3.4 Conclusions

Two functional upper-limb movements have been identified for the research. These are wrist extension with hand opening and thumb abduction, and elbow extension with wrist extension and hand opening. Practical methods for using FES to achieve these movements have also been identified. The two movements presents different challenges. For the wrist movement it important to ensure that the wrist has reached a neutral position before extending the fingers to prevent hyperextension of the finger from happening. For elbow extension it is important to ensure that the stimulated bicep muscle is only used for the initial supination function and not allow to develop into flexion. Control of both movement is therefore dependent upon knowing

the position of the limb about the associated joint with sufficient accuracy as the movement is happening.

MEMS accelerometers have been identified as an available method for measuring human body movement. They can be used effectively with modest processing requirements from a microcontroller and draw low amounts of power relative to other forms of sensors such as rate angle gyros or integrated inertial movement units. This means they are a practical and efficient solution for battery powered ambulatory devices.

Signal conditioning methods are available to extract information about the angular displacement of the limb upon which the device is being worn, along with volitional gestural movements made by the wearer. If sensible assumptions are made about the starting position of the limb and provided that the accelerometer signals are sampled at least five times faster than the gesture movements they can be filtered to provide meaningful information. Low pass filtering will reveal changes relating to the displacement of the limb with respect to gravity. High pass filtering will provide gesture movements made at a high frequency than the 'background' movement of the limb.

In addition the low frequency component that is used to determine the limb position can be used to initiate stages in sequence of FES. An example being the use of two channels of stimulation to extend the wrist and then open the hand. To prevent hyper extension of the fingers the second channel should not be commenced until the first channel has brought the wrist to a neutral position. Angular set points can be used to control progress through the sequence of FES to produce the functional pattern of movement in a timely way.

Chapter 4: Pilot Study using Accelerometer Triggered Functional Electrical Stimulation

4.1 Introduction

This work was carried by the author as part of a clinical research team looking at the use of FES for the upper-limb (Mann, et al., 2008). The author designed and manufactured the FES equipment for the trial. While working with the Physiotherapists and Occupational Therapists on the team to develop the protocol for its use on the trial. Before setting up the equipment for each of the participants and collecting results. The initial patient assessments and the impact on life outcome measures were carried out by others within the team.

4.2 Method

A compact battery powered neuromuscular stimulator incorporating a twin axes accelerometer as described in the previous chapter was designed to be worn on either the forearm or the upper arm, depending upon the required application.

Four programmable stimulation modes were available, one exercise and three functional.

The stimulator ran embedded state-machine software with sixteen discrete programme codes describing any of the available output conditions and transitions. These codes were programmed as a list of instruction that the stimulator would sequentially execute to produce a pattern of stimulation outputs.

For the exercise mode, the sequence was initiated by an internal timer. For the functional modes, signals from the accelerometer were used to control progress through the stimulation sequences. These 'triggers' were provided by performing low-pass digital filtering of the outputs from the internal accelerometer to convert the gravitational effect into an angular measure. Clinicians determined suitable angular 'set points' for each patient. Upon reaching the set point the sequence of stimulation is triggered to begin progressing through the pre-programmed pattern.

The stimulator offered two angular set points in each axis, and because each set point angle can be approached from either direction this gave a total of four trigger options in each axis.

4.3 Selection criteria

All of the volunteers were over 18 years of age, and had had a single stroke at least 6 months previously. They were medically stable, with no pre-morbid orthopaedic, neurological or other medical conditions that could affect their response to electrical stimulation.

The volunteers had sufficient cognitive ability to understand the trial, having scored 25 or more on the Mini Mental State Evaluation (Folstein & McHugh, 1975). They showed an absence of neglect syndrome, demonstrated through use of the star cancellation test (Halligan & Cockburn, 1990).

Volunteers had no fixed contractures of the elbow, wrist or fingers, and had a Modified Ashworth Scale (Bohannon & Smith, 1987) score of up to 3 in the flexor muscles for these joints. A minimum of 45^0 of flexion at the shoulder without simultaneously producing more than 30^0 of abduction or adduction was required, as well as an absence of shoulder subluxation or pain. It was necessary for volunteers to demonstrate wrist, finger and thumb extension in response to surface stimulation, and be able to tolerate the sensation.

4.4 Protocol

A total of six volunteers were seen for five visits at approximately two weekly intervals. At the initial visit the stimulator was set up with a non-functional exercise sequence. This was done so that the participants could become familiarised with operating the equipment. The volunteers were asked to use the system for two periods of exercise each day of up to 30 minutes each. At subsequent visits volunteers were assessed until they were ready to start using motion-triggered functional stimulation. The functional sequences were individually tailored to each volunteer's ability, with increased complexity of the sequences and triggering developed over the remaining visits.

4.5 Hardware Design

4.5.1 Neuromuscular electrical stimulator with inbuilt motion detection

For the initial investigative work into tracking movement using MEMS accelerometers to trigger stimulation a new FES stimulator was developed that included the following features;

- Twin-axis MEMS accelerometer

- Two independent output channels of stimulation
- Programmable state-machine controller for accelerometer triggering and stimulation output.

4.5.2 MEMS Accelerometer

A comparison was made of the available accelerometers. The results are shown in Table 1. The Analog Devices ADXL202 & 213 twin-axis accelerometer offered integrated circuitry for on-board signal conditioning with simple pin selection for sensitivity and filtering; along with a pulse-width-modulated output enabling simple interfacing to a microcontroller (Figure 18). Other available MEMS accelerometers were manufactured with analogue output signals, using one of these with a microcontroller required the use of analogue to digital conversion. Although the family of microcontrollers identified for use in the device had a built in analogue to digital convertor, the resolution of these devices was only 10bit. Whereas the ADXL202/213 PWM output could be read using a 16bit timer giving a higher resolution result.

Device	**Voltage**	**Current**	**Sensitivity**	**Comments**
Freescale MMA6270	2.2 – 3.6V	500 - 800uA	1.5g/2g/4g/6g	Analogue output Selectable gain setting Integrated low-pass filter Sleep function
ST LIS2L02AQ	2.4 – 5.25V	0.85 – 1.5mA	2g/6g	Analogue output
Analog ADXL213	3 – 6V	0.7 – 1.1mA	1.2g	PWM output Selectable bandwidth High accuracy for tilt sensing
Analog ADXL322	2.4 – 6V	450uA	2g	Analogue output
Analog ADXL202	3 – 5.25V	0.6 – 1.0mA	2g	PWM output Selectable bandwidth
Analog ADXL204	3 – 6V	500 – 900uA	1.7g	Analogue output Selectable bandwidth Integrated filter

Table 1 - A comparison of the accelerometers available at the time of the study that were considered to be suitable.

The Analogue Devices ADXL213 was selected for the following reasons;

- The high sensitivity of the 1.2g range made it the most suitable for detecting tilt and the relatively low-speed, human movement.
- The bandwidth could be set with a low-pass cut off frequency of 100Hz making it ideal for measuring human body movement.
- The Pulse width modulated digital output signal integrates very easily with the microcontroller (Figure 18).

One negative feature of the ADXL213 is that it draws slightly more current when operating than do any of the other devices; however this is outweighed by the savings to the power budget of the microcontroller by avoiding the need to use the ADC module.

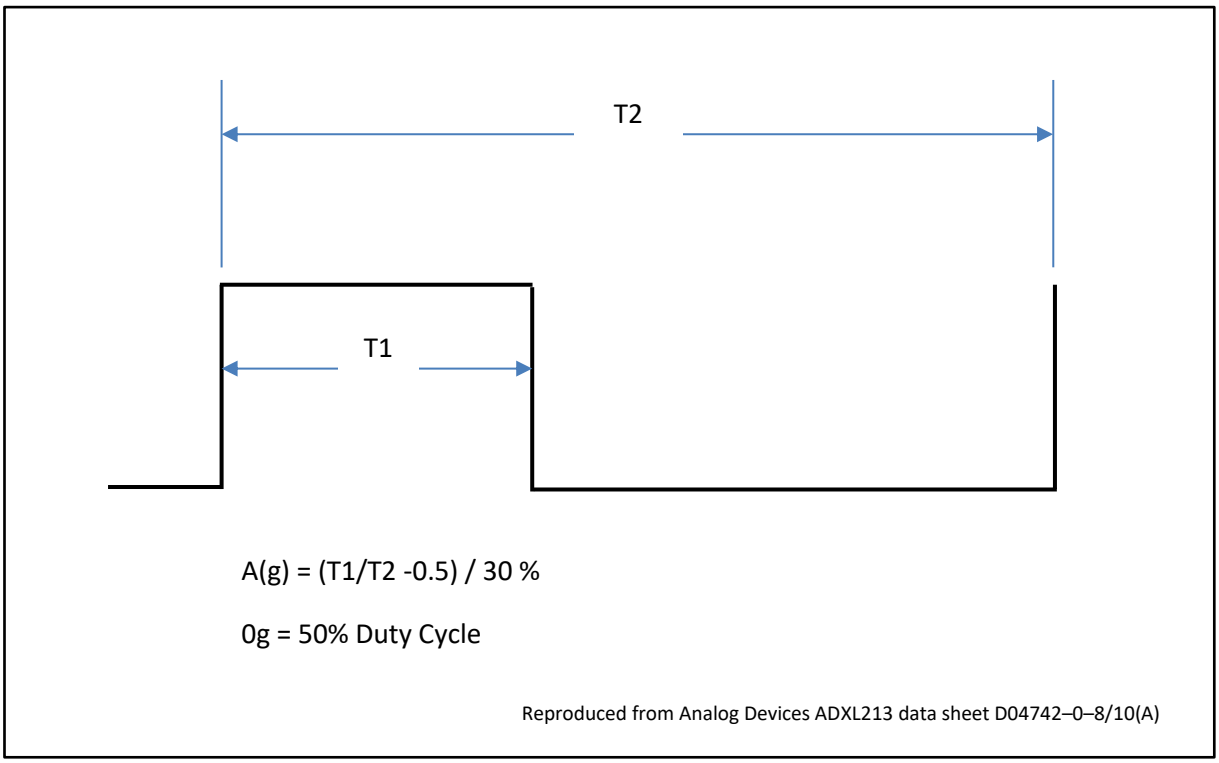

Figure 18 shows how the mark to space ratio of a timing signal is used to determine the acceleration reading from the ADXL202 & 213 MEMS accelerometer device

4.5.3 Neuromuscular electrical stimulator with two independent output channels of stimulation

The stimulator was designed to integrate with the wearer. The user would select an operating mode that has been programmed during a clinical set up for the functions they needed the assistance to perform. The stimulator would then use the movements detected by the accelerometer to trigger the stimulation (Figure 19). In all modes except for a cyclical 'exercise only' mode the stimulation was initiated by the user's movement.

The stimulator used a PIC18F series processor (Microchip Technology Inc. USA) which had an internal clock running at 8MHz. This clock signal was used to derive the stimulation pulses that drive the output stage of the circuit where a Darlington transistor pair provides the switching for the pulses. Digital potentiometers are used to attenuate the pulse signals to control the amount that the transistors are turned on by. The ADXL213 accelerometer was configured to produce a pulse-width-modulated output for each of the axis. The filtering characteristics and PWM period are pin selectable on this device and were fixed by the discrete components on the printed circuit board. Push buttons and a liquid crystal display make up the user interface. The output pulse signals from the digital stage are fed to the output circuit which further attenuated them through a rotary potentiometer for each output channel to give the user control over the output levels. This meant that when the device was programmed during the clinical set up, a safe maximum output current could be set via the digital potentiometers that the user would then be able to further reduce using the rotary analogue controls.

The battery voltage is stored in a pair of reservoir capacitors so that when the Darlington transistors are switched on a current of up to 1A can be delivered to the isolating transformers for the duration of the pulse. The transformers step the voltage up by ten times while ensuring that the outputs float independently of each other.

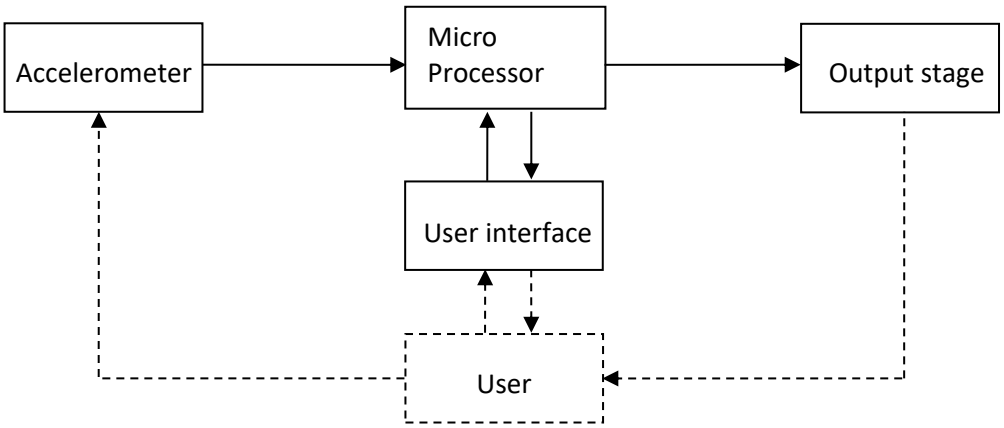

Figure 19 is a block diagram showing how the stimulator output is initiated by the user's movement.

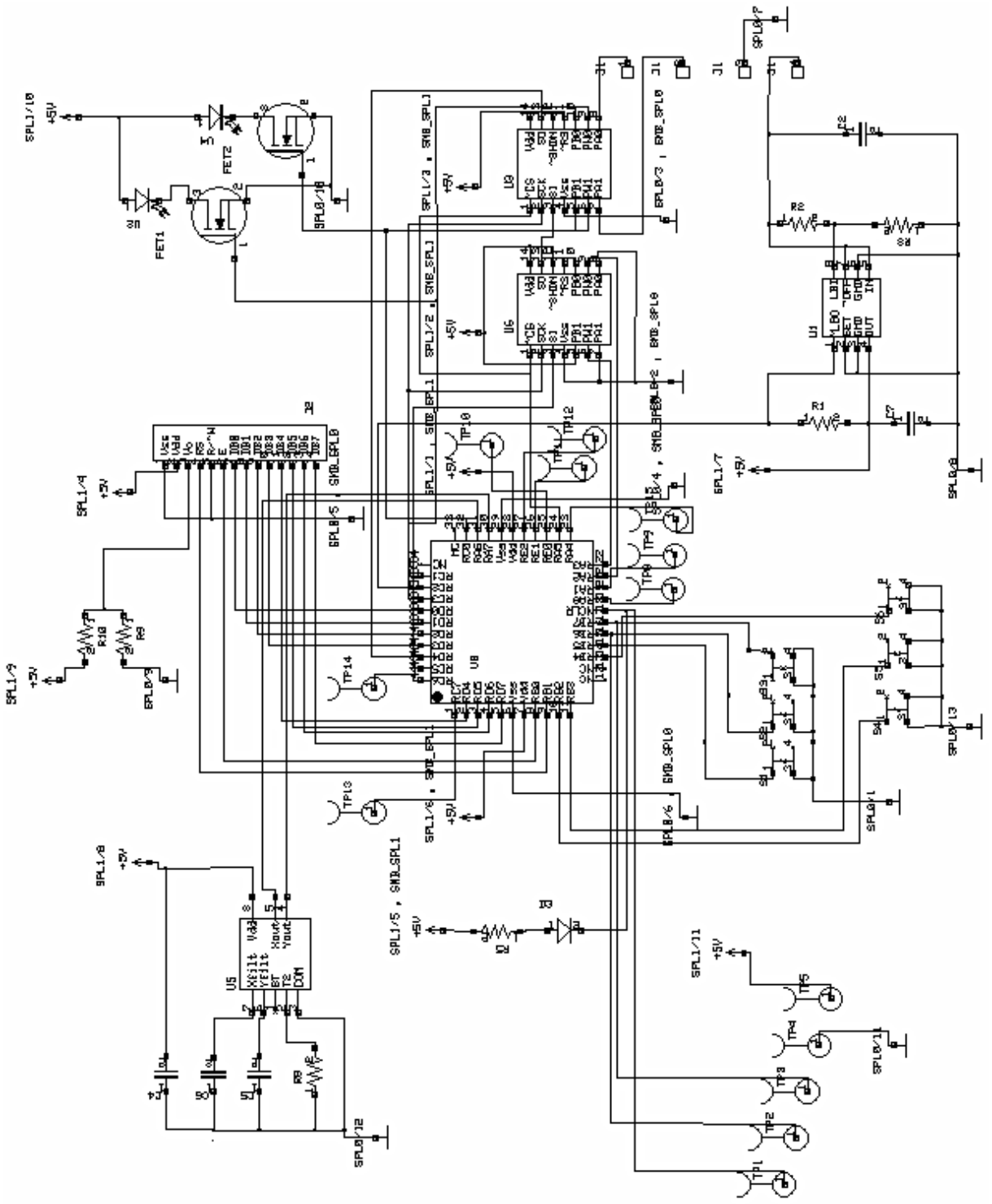

Figure 20 shows the circuit diagram for the neuromuscular stimulator developed for the pilot study using MEMS accelerometers triggered FES. U5 is the ADXL213 accelerometer.

4.5.4 Programmable state machine control

This device produced two channels of output stimulation that could be sequenced to work independently (Figure 20). In order to produce functional movement from electrical stimulation it is necessary to carefully control the timing and sequencing of the stimulation for each of the output channels. An example of why this is necessary would be for a reach and grasp movement sequence to enable small items to be picked up and moved around. The first channel of stimulation is applied to the wrist extensor muscles to extend and support the wrist while the second channel is applied to the finger and thumb extensors to open the hand. It is necessary for the wrist and hand stimulation to come on together at the outset so that the open hand can be placed around the object. The hand stimulation is then stopped to allow the hand to close under the patient's voluntary grip while the wrist stimulation remains on to keep the wrist supported.

When the wearer is ready to release their grip the hand stimulation needs to be brought back on. This is initiated by them moving the arm down through the set point angle used to control the stimulation sequence. Stimulation is commenced and the hand is able to release the object. Finally the wrist and hand stimulation are turned off and the arm can return to rest (Figure 21).

To be able to produce such patterns of stimulation a flexible control method was developed for the stimulator. The embedded software enables complex stimulation sequences to be programmed from simple sequential steps. It was identified that when using two output channels there were sixteen possible options that would be needed. These were referred to as segment codes and are shown in Table 2. Sequences are constructed by stringing together the individual segment codes.

The stimulator used the ADXL213 twin-axis accelerometer mounted on the main printed circuit board to enable detection of forward back and side to side movements. The sensing element within the accelerometer being subject to deflection due to the earth's gravitational field used this property as a gravity-referenced inclinometer. This allowed the separate detection of the inclination angle of the forearm and the degree of forearm rotation along with movements of the forearm up and down as well as side to side.

Digital filtering was used to perform the low-pass function. To ensure that the 8-bit microcontroller could perform the calculations quickly enough, a method that used binary bit-shifting maths was used which is both very fast and provides coarse and fine adjustment of the filtering parameters.

As an example of how the filter works consider the following equivalent 16-term moving average filter.

Start with the currently stored value, x and divide this by 16, then subtract this value from the original.

$$x - \frac{x}{16}$$

Then divide the remainder by 16

$$\frac{\left(x - \frac{x}{16}\right)}{16}$$

Take a new reading from the accelerometer, y and divide this by 16

$$\frac{y}{16}$$

And add this to previous result

$$\left(\frac{x - \frac{x}{16}}{16}\right) + \frac{y}{16}$$

Before multiplying by 16 to calculate a new current value

$$16\left(\left(\frac{x - \frac{x}{16}}{16}\right) + \frac{y}{16}\right)$$

Fine control of the filtering can be set by determining the number of 1/16th values that are replaced each time, the following formula will produces a faster response to change than the previous one.

$$16\left(\left(\frac{x - 2\left(\frac{x}{16}\right)}{16}\right) + 2\left(\frac{y}{16}\right)\right)$$

And this version faster again

$$16\left(\left(\frac{x - 3\left(\frac{x}{16}\right)}{16}\right) + 3\left(\frac{y}{16}\right)\right)$$

Segment Code	Function	Symbol
1	Channel 1 On (Ch1ON)	
2	Channel 2 On (Ch2ON)	
3	Ch1ON + Ch2ON	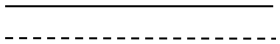
4	Channel 1 Ramp Up and stay On (Ch1RU & ON)	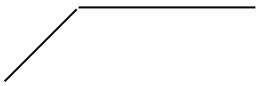
5	Channel 2 Ramp Up and stay On (Ch2RU & ON)	
6	Channel 1 Ramp Down and turn Off (Ch1RD & OFF)	
7	Channel 2 Ramp Down and turn Off (Ch2RD & OFF)	
8	Ch1RU & ON + Ch2 RU&ON	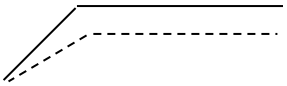
9	Ch1RD & OFF + Ch2RD & OFF	
10	Ch1ON + Ch2RU & ON	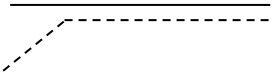
11	Ch1RU & ON + Ch2ON	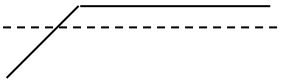
12	Ch1RD & OFF + Ch2ON	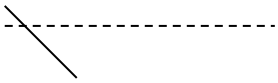
13	Ch1ON + Ch2RD & OFF	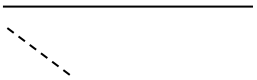
14	Ch1RU & ON+ Ch2RD & OFF	
15	Ch1RD & OFF + Ch2RU & ON	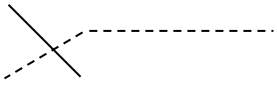
16	Ch1 & Ch2 OFF	

Table 2 - The segment codes that can be used to construct a pattern of stimulation

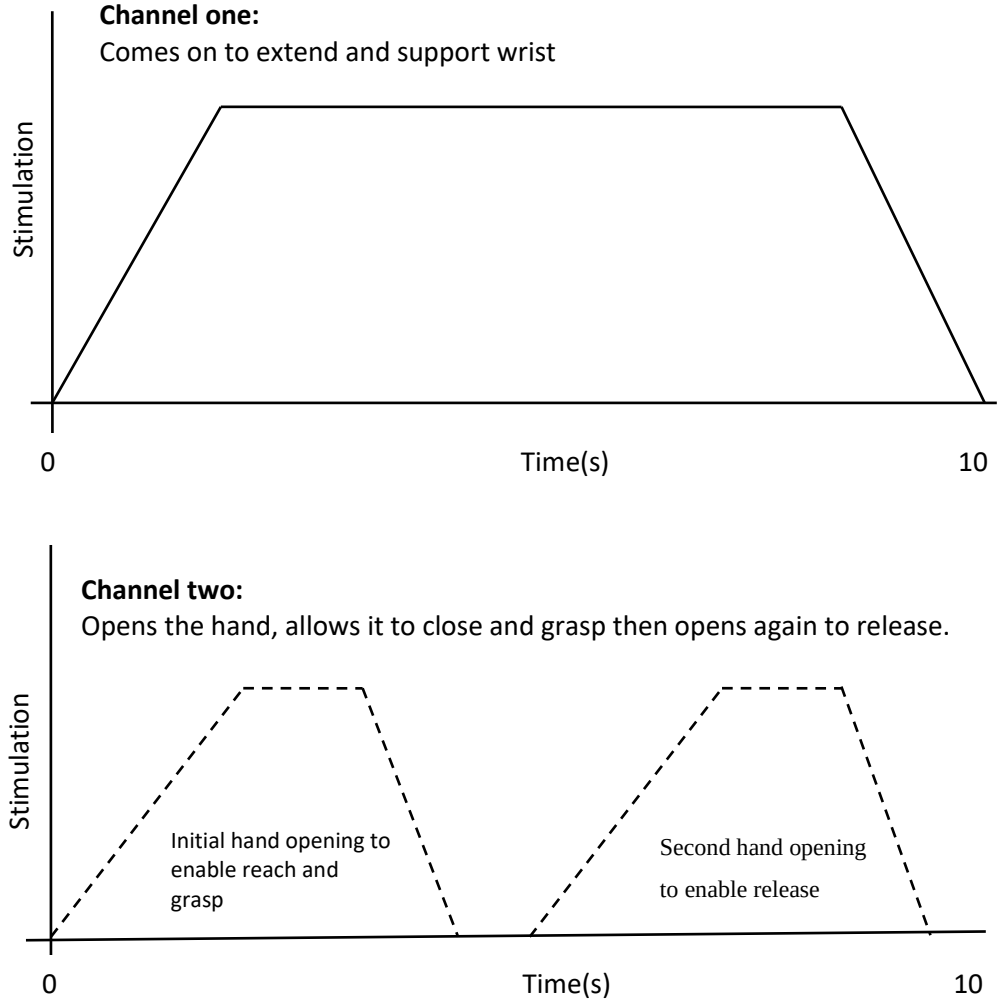

Figure 21 illustrates the pattern of stimulation necessary to produce the wrist and hand-opening movement described in the text. The second hand opening is initiated by the wearer moving the limb to take the stimulator passed an angular set point.

Using the segment codes given in Table 2 the sequence of stimulation shown in Figure 21 can be constructed from the following:

Code 08 - Both channels ramp on.

Code 13 - Channel 1 stays on, Channel 2 ramps off.

Code 10 - Channel 2 ramps back on again.

Code 09 - Both channels ramp off.

The transition between each of the states is determined either by time or by movement events detected from the accelerometer.

4.6 Results

4.6.1 Volunteer One

The volunteer was 51 year old male, 9 years post stroke who was right-side affected and right-side side dominant, with no previous use of FES.

Following an initial two weeks with the stimulator set up to exercise and strengthen the wrist and hand extensor muscles, the volunteer reported that the hand on the affected side had loosened.

An accelerometer triggered sequence was set up making use of his ability to rotate his forearm. Two channels of stimulation were used for extending the wrist and opening the hand.

During successive visits to the hospital clinic, the complexity of the stimulation sequences was steadily developed for tasks specific to the patient's work place needs. He became able to use a door handle and move small objects and hold a telephone handset with his affected hand.

4.6.2 Volunteer Two

The volunteer was a 65 year old male, 5 years post stroke who was left-side affected and right-side dominant with no previous use of FES.

After the initial exercise period, the volunteer was set up with a tilt trigger so that when the arm was raised beyond a set angle, stimulation would cause the hand to open.

The patient did not progress beyond this trigger and subsequently retired from the trial following a change of medication. He had however reported that he was now sometimes able to open his hand at will.

4.6.3 Volunteer Three

The volunteer was a 65 year old female, 5 years post stroke who was left-side affected and right-side dominant with no previous use of FES.

Following the two-weeks of exercise, a tilt trigger was set up to open the hand in reach. The volunteer failed to fully engage with the system and any benefit she gained from it was due to the support of carers and family.

The triggering and sequences were developed to allow the volunteer to carry out certain activities of daily living.

The volunteer was affected by increased muscle tone in standing making sitting down activities more appropriate.

4.6.4 Volunteer Four

The volunteer was a 61 year old female, 4 years post stroke who was right-side affected and right-side dominant who had previously used FES for wrist and finger extension exercise.

An initial exercise period was not required with this volunteer because of her familiarity with the therapy.

The first attempt to set up a trigger proved to be unreliable due to poor selection of the set point angles. When this problem was remedied at the next visit the device worked so reliably that no further adjustments were made for the rest of the trial.

Using the system the patient was able to perform numerous tasks she previously found difficult or impossible. These included food preparation, cooking and using door handles.

The volunteer reported that the system had reawakened an awareness of her hand while giving her the ability to use it again.

4.6.5 Volunteer Five

The volunteer was a 50 year old female, 4 years post stroke who was left-side affected and right-side dominant who had previously used exercise stimulation to reduce the subluxation and pain in her shoulder.

Because of this volunteer's familiarity with FES she was immediately set up with triggered activation to open her hand when her arm was raised from her side.

Although this worked it proved difficult to find set points that were not susceptible to inadvertent or false triggering. The volunteer progressed to more complex sequences but found them confusing so reverted back to simpler sequences.

The volunteer was also affected by an increase in tone when standing which contributed to the problems of finding suitable set points for the triggering.

4.6.6 Volunteer six

The volunteer was a 34 year old male, 2 years post stroke who was right-side affected and left-side dominant who was a previous FES user for dropped-foot.

The volunteer was familiar with FES so at the first visit the system was set up with triggered activation to produce hand opening on reach. Unfortunately he developed a tremor in the arm whenever he produced any effort. To remedy this, a period of desensitising exercise stimulation was required after which the condition improved and triggering was reintroduced.

By the end of the trial he was able to reliably repeat this action with little evidence of any residual tremor.

4.7 Discussion and conclusions

In all cases it was possible to open the hand using external FES and this could be initiated using a control signal derived from the accelerometer built into the stimulator unit that was worn on the forearm. The accelerometer was used to measure the angular displacement of the arm in relative to the Earth's gravitational field.

When the stimulator was used to induce movements for exercise, these were performed with the device strapped to the arm enabling the device to be carried around. Giving the user to ability to carry the unit around with them while exercising appeared to improve compliance with the treatment compared to standard exercise devices which are used while stationary.

Several users reported that they felt they were more aware of their affected limb.

Improvements in activities of daily living tasks were reported in some individuals.

In most cases, relatively simple control techniques were used and were shown to be the most practical. When more complex multiple stage sequences where implemented users found the device hard to control. They sometimes found it difficult to follow where they were in the sequence, then having lost where they were being unable to work out what they needed to do next.

More work is required to improve the detection of the intention to open the hand along with more intuitive control that requires less cognitive input from the user.

4.7.1 Illustrations of the hardware in use

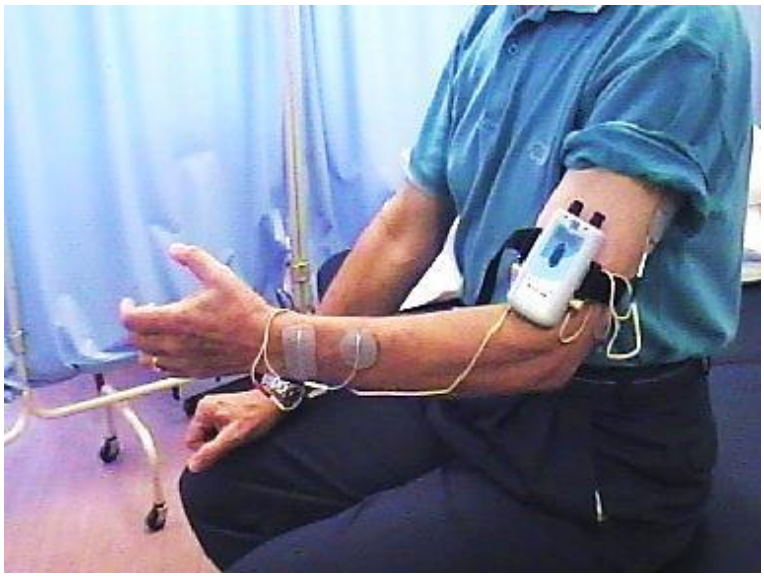

Figure 22 shows a photograph of a trial participant using the accelerometer control stimulator for a motion triggered FES to exercise hand opening.

Figure 23 shows a photograph of a trial participant using accelerometer triggered FES to help perform the daily activity of answering a telephone.

4.7.2 Programmable state machine control

The sixteen segment codes shown in Table 2 were inspired by a previous state machine control called F-Light that had been developed by Ben Heller from the Royal Hallamshire Hospital in

Sheffield. Heller's system used trapezoids with associated variables to describe each part of a sequence. Each section would consist of a rising ramp, an 'on' time and a falling ramp. Periods when the output was constant would be determined by setting the rising and falling ramp variables to zero. A drawback with F-Light was that the number of variables needed to describe a sequence is very large. Each stage of the sequence requires that the rising ramp duration, the on-time duration and the falling ramp durations are set for each channel. Programming the stimulator to customise it for each user's needs requires the use of interpretive software running on a PC.

The method developed for this research represented a simplification that improves the usability of the system without any loss of function. The development came with the realisation that the ramping rates are matched to the ability and physiology of each user and once established for the user can remain constant. This means that it is possible to clinically establish the correct rising and falling ramping rates for a user at the outset before the stimulation sequence is set. This means that it is no longer necessary to define the ramping parameters for each part of the sequence. The second realisation was that because rising ramps are not used in isolation they could be combined with a subsequent on duration for the stimulation. By combining the ramping and the on-time into a single function the number of required variables can be greatly reduced meaning that all possible sequence options for two channels of stimulation can be described with only sixteen segment codes.

The result is that the stimulator can be programmed from the user display on the device without need of a PC. The benefit of this is that it minimises the level of distraction for the patient. They will in many cases be having to work hard to produce the levels of concentration necessary to control the device, and the removal of distractions is important for them to maintain this during the set up process.

4.7.3 Further application of the two-channel stimulator

The two-channel stimulator developed for this study went on to be used in subsequent pilot studies and trials that demonstrated the effectiveness of FES triggered from accelerometers by the wearer's voluntary movement (Lane, et al., 2006) (Mann, et al., 2008) (Mann, et al., 2011).

The angular set point method has subsequently been used to redeploy lower-limb drop foot stimulators for upper-limb use. The tilt trigger built into some of these devices can be used to initiate hand opening as the user reaches forward.

Chapter 5: Electromyograms

5.1 Introduction

The nervous system has two main parts, the central nervous system and the peripheral nervous system. The central nervous system consists of the brain and spinal cord. The peripheral nervous system consists of the nerves that radiate out from the central nervous system and extend into the body.

The peripheral nervous system can be further broken down into autonomic nerves, sensory nerves and motor nerves. The autonomic nerves control involuntary actions and it has two divisions; the sympathetic and parasympathetic. Sensory nerves carry information from around the body to the central nervous system, these are afferent nerves. Motor nerves carry signals from the brain to skeletal muscle, these are efferent nerves.

Motor neurons originate from the ventral horns of the spinal cord and are responsible for activation of the muscle fibres of skeletal muscle that result in contraction. They consist of a cell body, dendrites and an axon projecting to the motor-point of the muscle, before branching out to form synapses with the muscle fibres. The arrangement is referred to as a motor unit and provides a path for action potentials to travel from the central nervous system to the muscle.

Most nerves are formed into bundles called fascicles that are formed from the nerve roots as they emerge from between the vertebrae of the spine. These fascicles contain both the afferent sensory nerves and the efferent axons that innervate muscle.

Every firing of a motor neuron produces a force twitch in its motor unit. If these force twitches are produced close together, they become superimposed producing what is known as a tetanic contraction that is capable of producing forces needed to move limbs. The force produced by the muscle is proportional to the rate of firing of the motor units.

The electrical activity caused by muscle contraction is measurable and the signals collected are referred to as electromyograms (EMG). EMG signals can be collected using percutaneous and transcutaneous methods. Percutaneous methods use specially designed needle electrodes that are inserted through the skin into the body of the muscle being measured. Whereas the transcutaneous methods are in contrast non-invasive, relying on measurement taken from electrodes placed over the muscle on the surface of the skin.

5.2 Capturing and conditioning EMG

EMG signals are measurable whenever a muscle contracts. This is true whether the contraction was as a result of volitional movement, movement in response to a reflex, or movement initiated by electrical stimulation. This property of EMG has potential as a feedback signal for the control of electrically stimulated movement.

Unfortunately, EMG signals do not readily lend themselves to being useful as control signals. EMG signals are spiky and random with the amplitude of the signal having a stochastic nature (Figure 24).

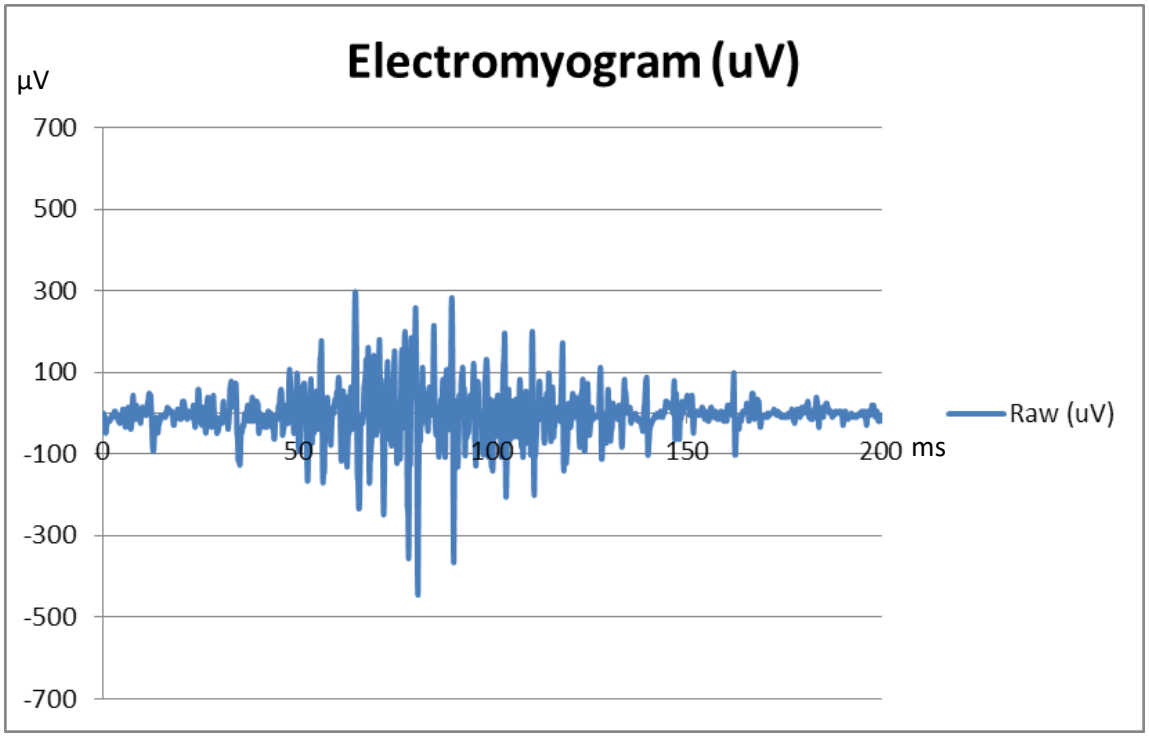

Figure 24 is an example of a raw EMG signal, the burst of higher amplitude coincides with contraction of the muscle.

Before the EMG signals can be used as control inputs it is necessary to suitably condition them. When an EMG signal is smoothed using a low-pass filter with a cut off frequency of 1 kHz the resulting waveform is approximately proportional to the isometric force produced by the muscle (Sinkjaer, et al., 2003). Whereas this is the case for static isometric measurement it does not hold true dynamically. The normal method to condition EMG for dynamic measurement is to extract the root mean squared (RMS) value of the EMG signal over a fixed period (Delsys Inc., n.d.). This is then rectified and either the mean rectified value or the integrated value can then be used as a control signal.

The conventional method is to use a precision rectifier to invert any parts of the signal that are below the ground reference voltage. This signal is then further conditioned to provide a DC level output representative of the EMG intensity measured. One of the problems with multi-stage signal processing is that the final output will be lagging behind changes to the input signal. The latency this introduces limits the speed at which the any control system relying upon the signal will be able to respond.

For the control purposes of this research it was desired to find a measurement method capable of rapidly detecting the onset of EMG bursts. The beginning of the burst coincides with commencement of the muscle being fired after which the associated limb will begin to move.

The novel approach taken to avoid the problems associated with latencies was to condition the EMG signal with a precision voltage clamp. The schematic for the precision clamp is shown in Figure 25 along with an indication of the effect of the clamp on the signal being conditioned by it.

The clamping circuit seeks to tie the lowest part of any waveform to a pre-set reference voltage. It works by using a blocking diode to hold any value that drops below the reference voltage, in effect shifting the entire waveform above the reference voltage. When a regular sine-wave is passed through the circuit the effect is to tie troughs of the output waveform to the reference providing a clean level shift. When a compound waveform like EMG is passed through the circuit the resulting level shift is less regular than for a pure sine wave, however rapid transitions in level become exaggerated. The effect of the circuit is to provide better detection of sudden level changes as happens at the onset of a burst of EMG.

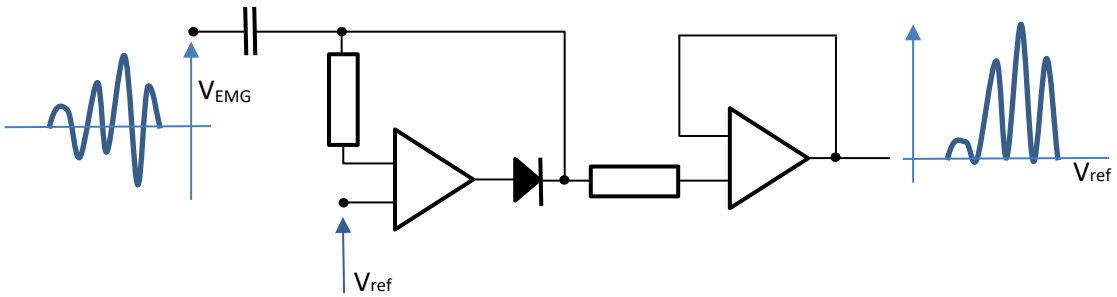

Figure 25 shows a precision clamp circuit used to tie the EMG waveform to the reference voltage applied to the first Op-Amp. The negative peaks are clamped to the level of the reference voltage. This has the effect of usefully distorting the waveform to show the onset of changes.

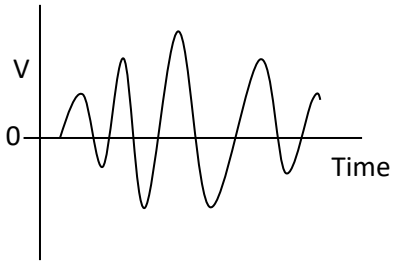

(a). EMG signal

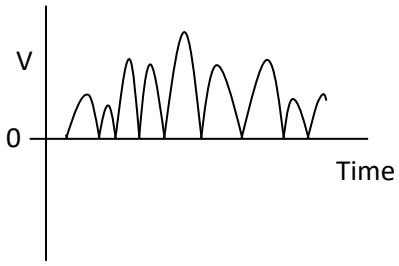

(b). Conventional rectification

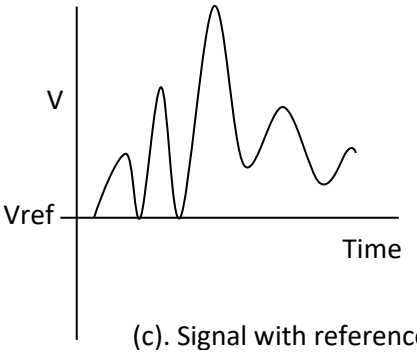

(c). Signal with reference voltage clamping

Figure 26 demonstrates the difference between rectification methods

(a) Is the raw EMG signal

(b) Is a representation of the signal after being conventionally rectified

(c) Is a representation of the same signal rectified when the clamp is used

5.3 A Comparison of Electromyogram Conditioning Methods

5.3.1 **Materials and Method**

The method was tested for detecting the onset of volitional limb movements by measuring and conditioning the EMG signal from the research supervisor's wrist extensor muscles. The measuring electrodes were located along the length of the extensor muscles with the reference electrode placed on the opposite arm.

An EMG signal was recorded using a capture oscilloscope (Pico Technology Ltd. UK). The captured signal was then processed offline by passing it through a conventional precision rectifier, and then a precision clamp, for comparison.

5.3.2 **Results**

The first plot shown in Figure 27 is the EMG measurement taken from the wrist extensor muscles during a wrist extension movement. The section of greater interest is the onset of the burst that is shown in Figure 28. This part of the burst occurs before movement of the muscle can be seen.

The plot in Figure 29 shows the results of conventional precision rectifying. A linear trend-line has been fitted to the plot to indicate the increase in intensity. The slope of this linear trend is 2.22 µV/ms.

The plot in Figure 30 shows the results for the precision clamp method. Again a linear trend-line has been fitted to the plot. This time the slope of the linear trend is 3.03 µV/ms.

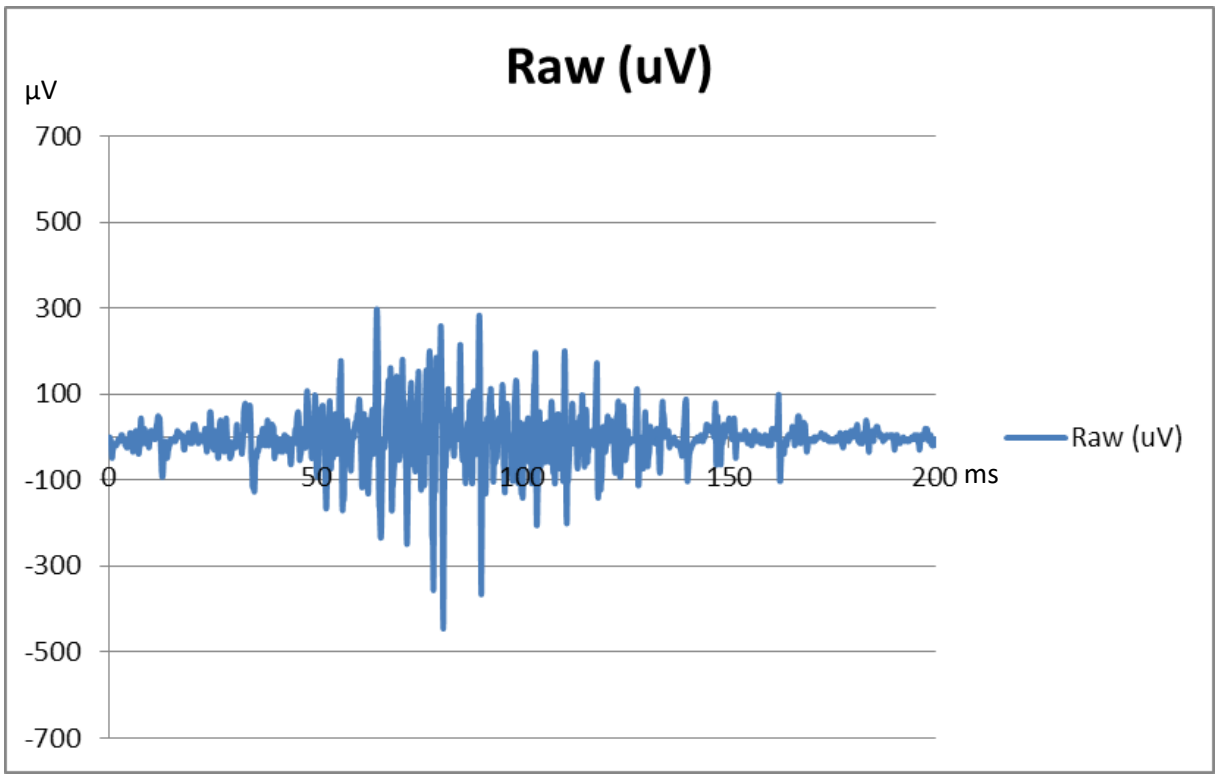

Figure 27 shows an electromyogram signal measurement made from the wrist extensor muscles of Paul Chappell's forearm during a wrist extension movement.

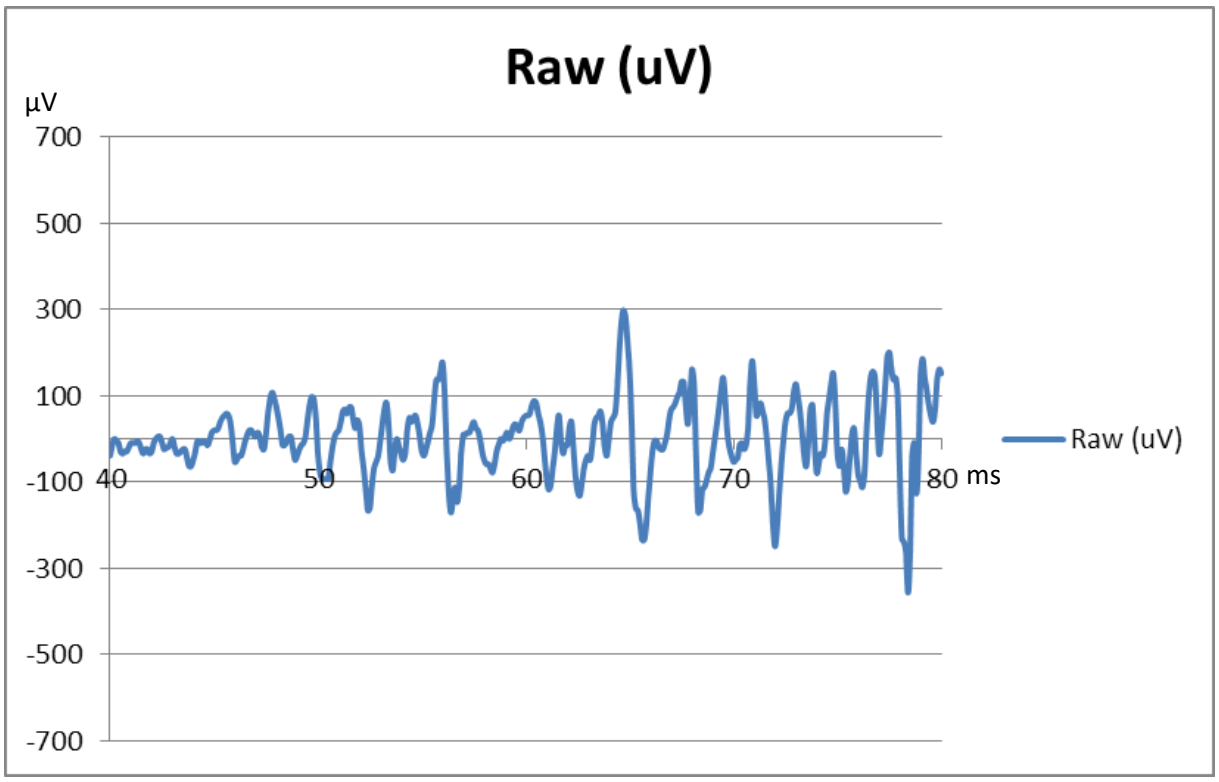

Figure 28 shows an enlarged section of the plot above covering just the early part of the onset of the EMG burst that occurs prior to visible movement of the muscle.

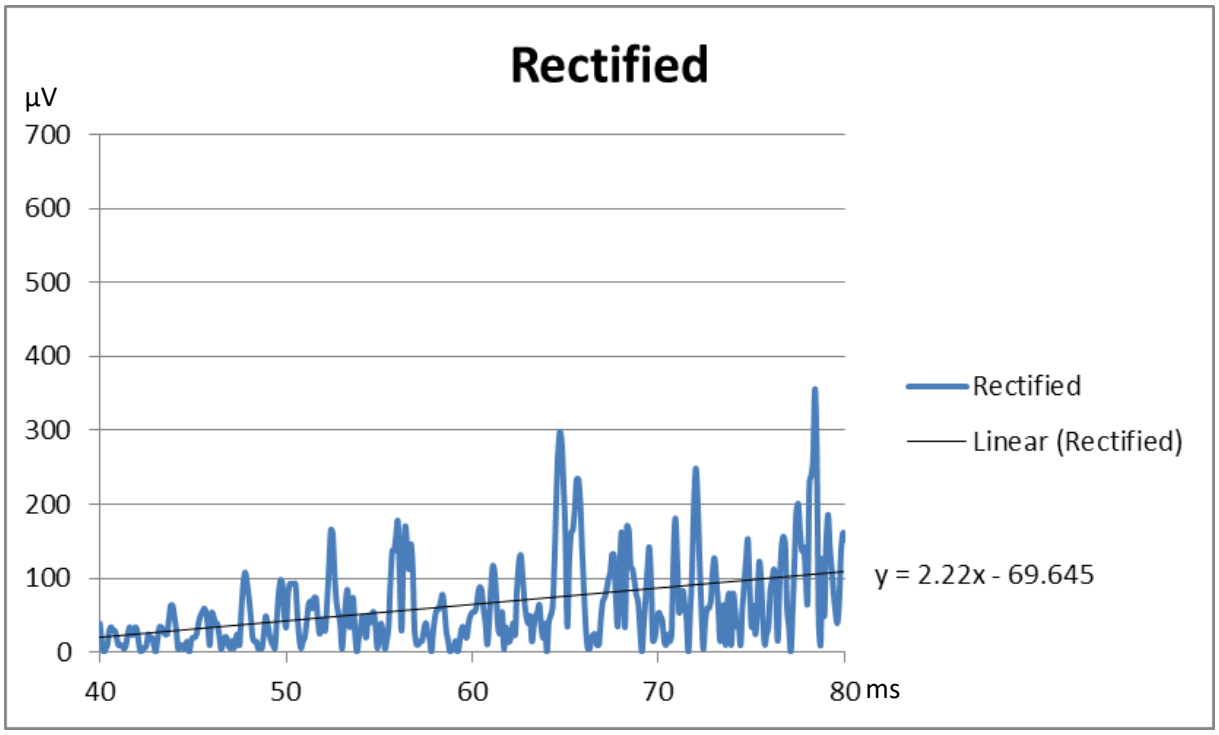

Figure 29 shows the signal after it has been passed through a conventional precision rectifier. The linear trend line gives an indication of the increase in intensity.

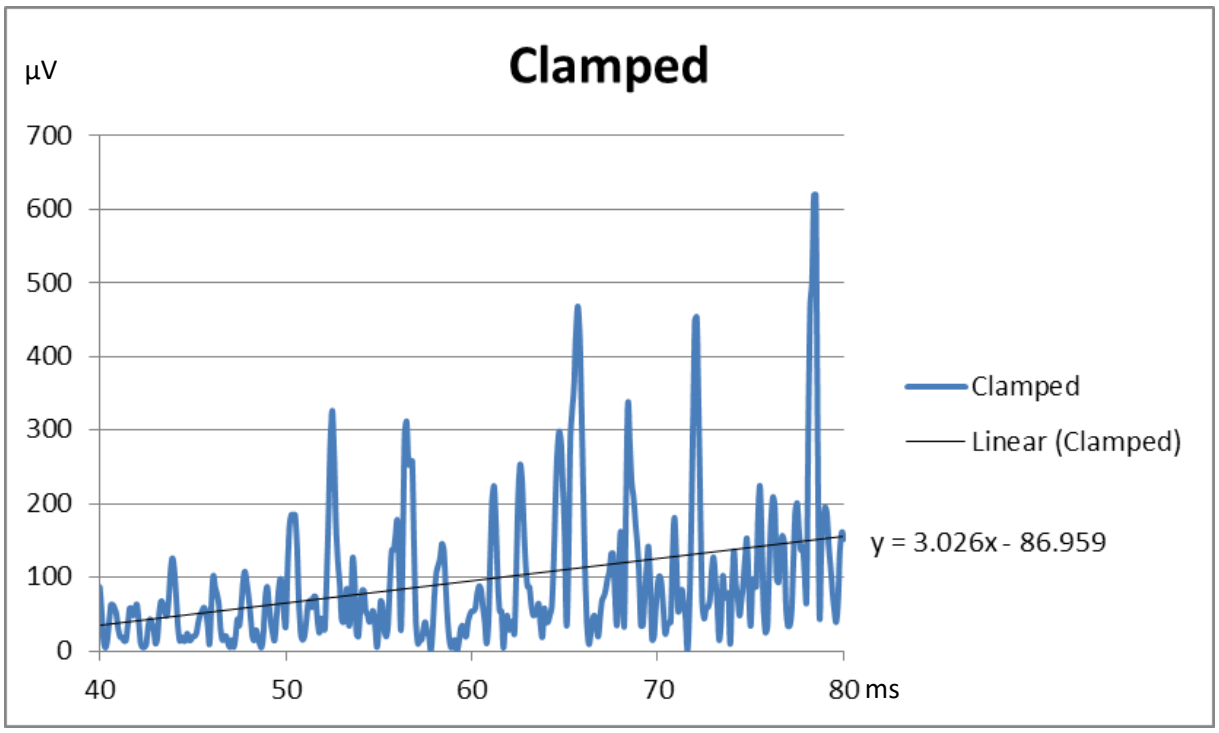

Figure 30 shows the same EMG signal after it has been passed through a precision clamp instead of the precision rectifier. The clamp has the effect of rectifying by level shifting the signal. Once again a linear trend line has been fitted to the plot, the slope of the trend is more than 25% greater than for the signal using the precision rectifier.

5.3.3 Discussion and Conclusions

The linear trend for the clamped signal shows a 26.6% increase over the same signal that has been conventionally rectified. The peak for the clamped signal shows a 42% increase over the rectified signal.

The clamping circuit distorts the signal and does not maintain the integrity in the same way that the rectifier does. This does not represent a problem as there is no requirement to break down or further analyse the signal.

The results show how an EMG signal that has been conditioned by a precision clamp will give a clearer indication of the onset of a burst than for a similar burst that has been conventionally rectified. The result means that this method of conditioning EMG signals will give a clearer indication of the intension to move a muscle.

5.4 Clinical testing of the EMG precision clamping method with spinal cord injury

A patient was identified as having the potential to benefit from an EMG sensing switch that could interface with his environmental control system. He had a high spinal cord neck injury that had resulted in tetraplegia although he remained able to breathe unaided.

A unit was built that was capable of collecting an EMG signal from the muscles used for raising an eyebrow.

The signal was processed using the precision circuit and switching was determined by exceeding a comparator threshold setting.

Prior to using the EMG switch the patient had used a tongue activated switch placed close to his cheek. He reported finding the EMG switch more convenient to use because;

- It was almost immune to accidental switching.
- He was now able to talk while using the switch.

This method of conditioning the EMG for use as a control signal became the subject of a granted patent (Lane & Nolan, 2009).

Having investigated the use of the precision clamp as a method to improve detection of EMG bursts, attention was turned to resolving the problems associated with the collection of these signals for use with FES.

5.5 Using EMG for control of an FES system

There is a fundamental problem with using EMG as a control input for FES systems. The amplitude of electrical stimulation pulses are in the order of 10 to 150V, whereas the much smaller EMG signals are in the order of 100μV to 100mV. The sensitive instrumentation amplifier needed to detect the EMG voltages is potentially swamped by the electrical stimulation and could be easily damaged. The conventional solution to this problem is to protect the EMG instrumentation amplifier by shutting it down for the period of the stimulation pulses. This method is known as blanking, see Figure 31.

The problem with blanking is that each time that the amplifier turns back on, the input is seen as a step change that usually requires a relatively lengthy settling period before EMG can be measured again. One way to address the problem of long settling times is by using a sample-and-hold arrangement. The EMG signal is sampled ahead of the stimulation pulse and held on the amplifier input for the duration of the blanking period. At the end of blanking the voltage, the EMG voltage is likely to be much closer to the previous signal voltage. A step change can still occur if the EMG value after the stimulation pulse does not match the sample-and-hold value, although this is likely to be smaller than for the first case.

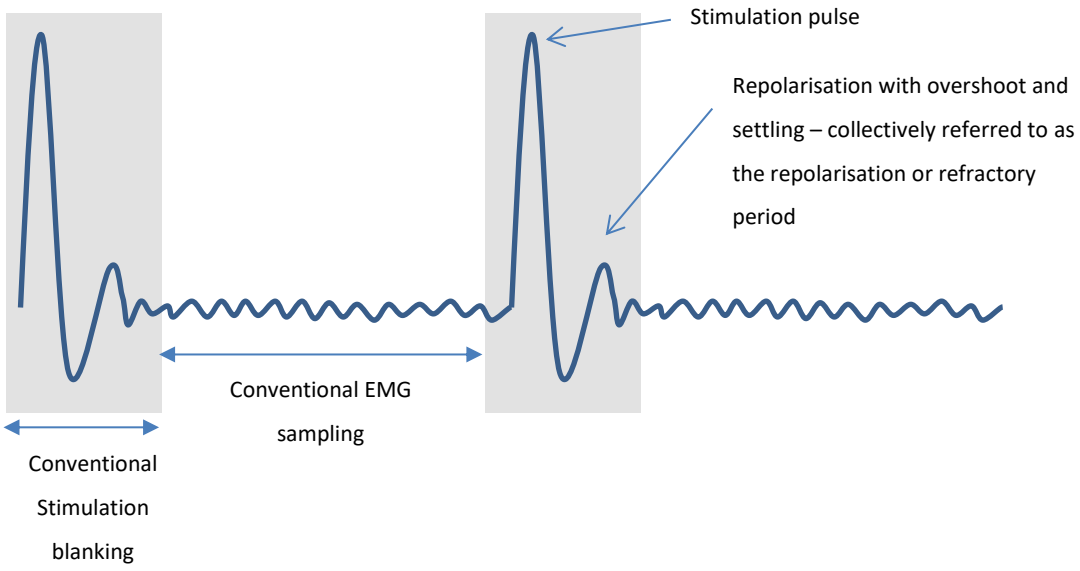

Figure 31 illustrates how conventional EMG sensors working with FES will have a 'blanking period' for the duration of the stimulation pulse to protect the EMG instrumentation amplifier. Any useful information that might have been contained in this period is therefore lost.

The solution adopted for this research was to develop an EMG amplifier capable of withstanding the FES voltage. To protect the amplifier a pre-filter was designed with inputs that are capacitively coupled. A low pass filtering arrangement between the inputs and the reference remove much of the stimulation pulse while causing the circuit to track the common mode signal with little drift (Figure 32).

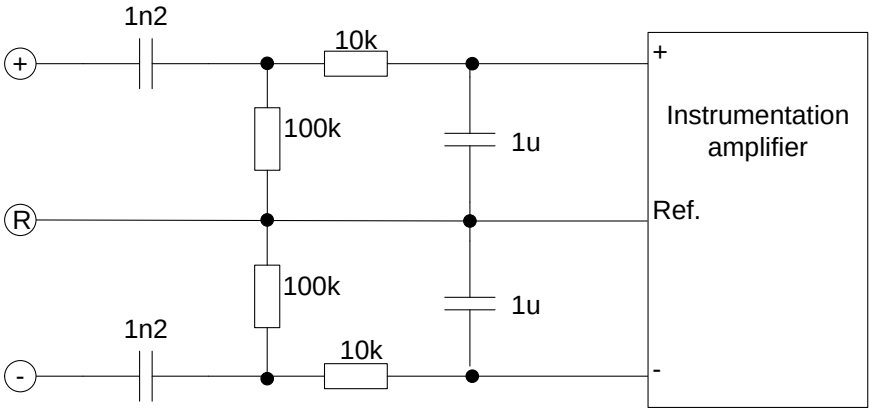

Figure 32 shows a schematic for the pre-filter used for the EMG amplifier.

A simulation using the Proteus circuit design software package (Labcenter Electronics, UK) was made to test the operation of the circuit shown in Figure 32. The output from the simulation is shown in Figure 33. The simulation was able to show that a pulse of similar duration to a stimulation pulse was heavily attenuated, while a 100Hz sine wave representing the frequency of EMG was passed intact.

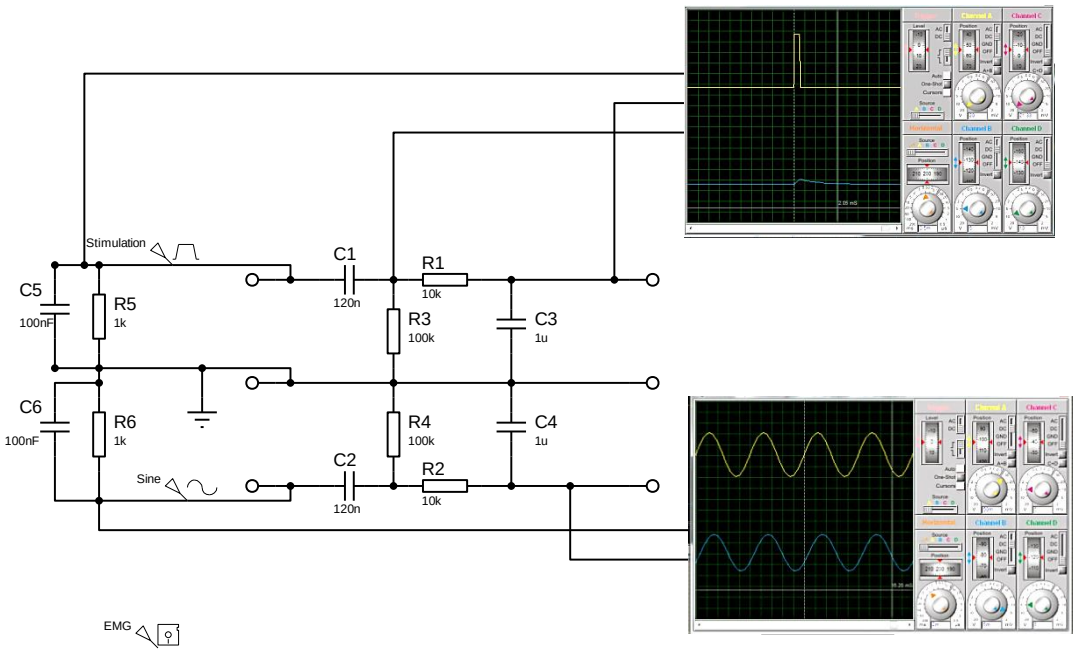

Figure 33 shows the simulation model of the EMG pre-filter circuit. The oscilloscope at the top shows how a 100V stimulation pulse (yellow) is heavily attenuated to 2.25v (blue) protecting the instrumentation amplifier, whereas the lower oscilloscope shows that the EMG frequency signal is passed.

5.5.1 EMG capture and conditioning circuit and hardware

Using the results obtained from the simulation, the pre-filter was incorporated into a design for an EMG capture and conditioning circuit

The pre-filter was placed on the input to an AD623 instrumentation amplifier from Analog Devices. This part was chosen because of the high slew rate and rail to rail operation.

MCP604 operational amplifiers from Microchip were used to create; a split rail generator for the instrumentation amplifier, a multi-stage 500kHz low pass filter, the precision clamp, and the output gain stage.

The device was then built and tested.

With this EMG pre-filter, the EMG measuring amplifier is able to track the stimulation artefact within the envelope that a conventional system would have normally blanked for (Figure 31). This meant that potentially useful information contained within the blanking period that would previously been inaccessible now became visible.

5.5.2 EMG signal detection during a stimulation pulse

While testing the EMG measuring systems ability to remain fully active during the stimulation pulse, changes in the signal were observed that varied with muscle contraction. For the first time it was possible to see an interesting artefact that occurred in the period that immediately follows the stimulation pulse (Figure 31). It was noticed that the amplitude of this part of the waveform varied with respect to contraction of the muscle for which EMG was being measured. Because muscle contraction directly relates to joint movement it was postulated that this may give rise to the ability to determine joint angle from the measured signal. By knowing the angle of a joint it is possible to interpret the position of the limb and so provide feedback to the system controlling the FES. Figure 34 shows the positioning for the electrodes while making the observation shown in Figure 35. The series of photographs in Figure 36 relate the observed changes to the position of the wrist. As the wrist is moved from fully extended to fully flexed the post stimulation region of the trace increases in amplitude. This increase was measured using the adjustable cursors on the oscilloscope. The peak of the turning point in the curve of the plot was used for the measurement. Cursor number one was placed at this location for the wrist extended. Cursor number two placed at this location for the wrist in flexion. The delta between the two cursors remained at approximately 250mV across numerous repetitions of the movement.

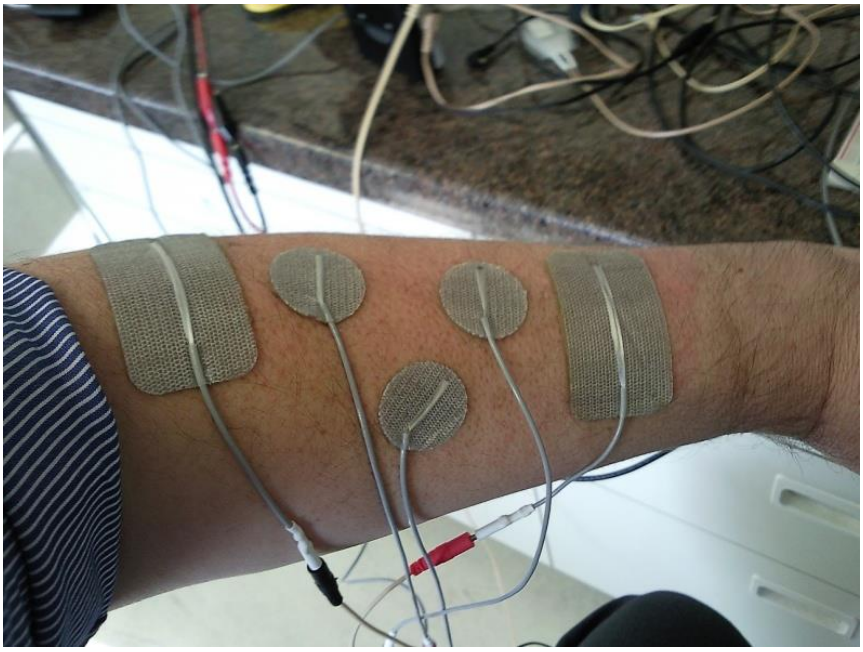

Figure 34 is an image showing two larger rectangular stimulation electrodes set up for wrist extension with hand opening and three smaller round electrodes used for EMG measurement.

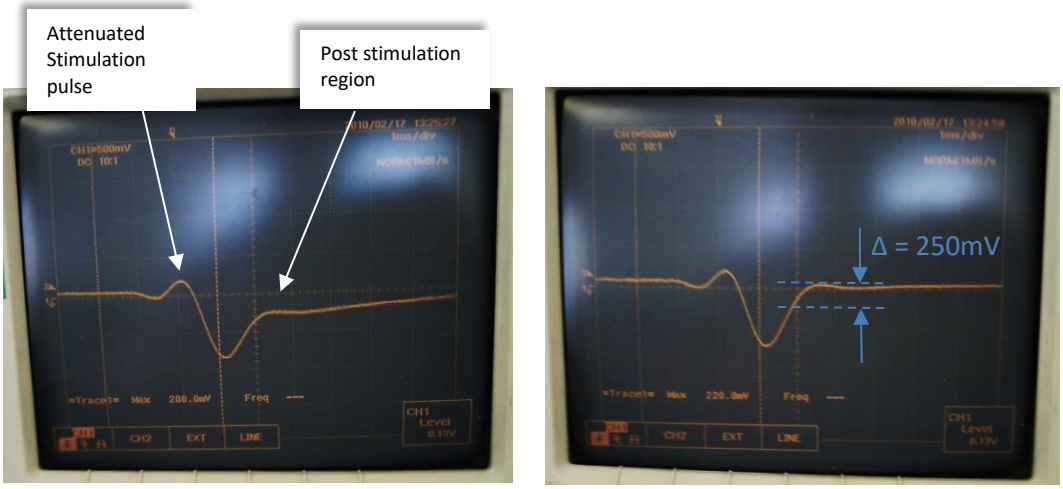

Figure 35 is an image showing a pair of oscilloscope traces the one on the left is with the wrist extended and the one on the right with the wrist flexed.

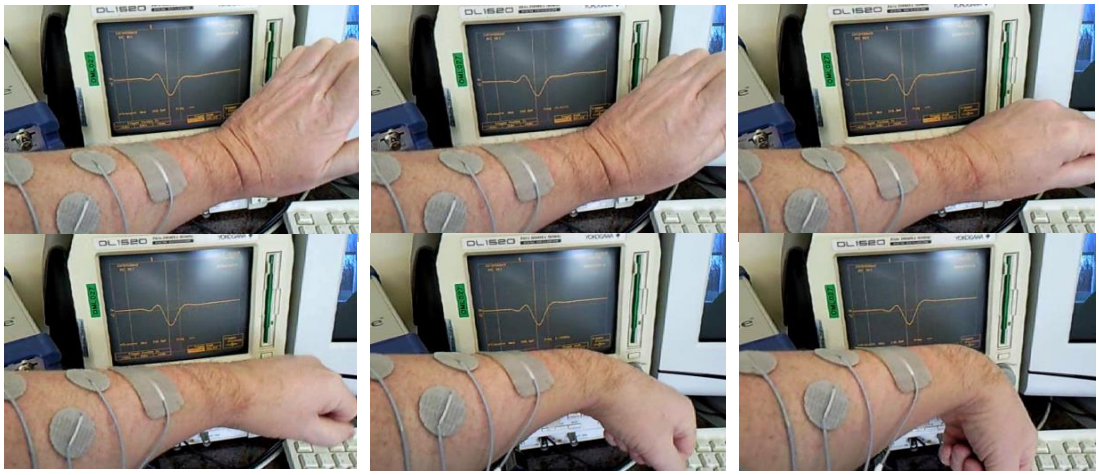

Figure 36 shows a series of photographs showing how the refractory part of the waveform varies as the wrist is moved from fully extended to fully flexed.

5.6 Movement artefact identified in stimulation pulse

5.6.1 Method

Using electrode positions similar the those shown in Figure 34, a single channel of FES was set up to produce a functional hand opening movement. The wrist was extended from a partially flexed position accompanied by finger extension and thumb abduction.

A data capture oscilloscope (Pico Technology Ltd. UK) was used to record the output from the EMG capture and conditioning board.

The wrist was placed into a partially flexed position that is typical in hemiplegia before electrical stimulation at 40Hz was gradually increased to produce wrist extension with hand opening.

The oscilloscope was used to capture the trace at the start and end positions.

5.6.2 Results

The trace shown in Figure 37 was while the wrist was partially flexed. It shows the amplitude of the overshoot following repolarisation reaching 2.215V and the slope of the final settling ripple to be $180Vs^{-1}$.

The trace shown in Figure 38 was while the wrist was extended. It shows the amplitude of the overshoot to be 2.185V and the slope of the final settling ripple to be $50Vs^{-1}$.

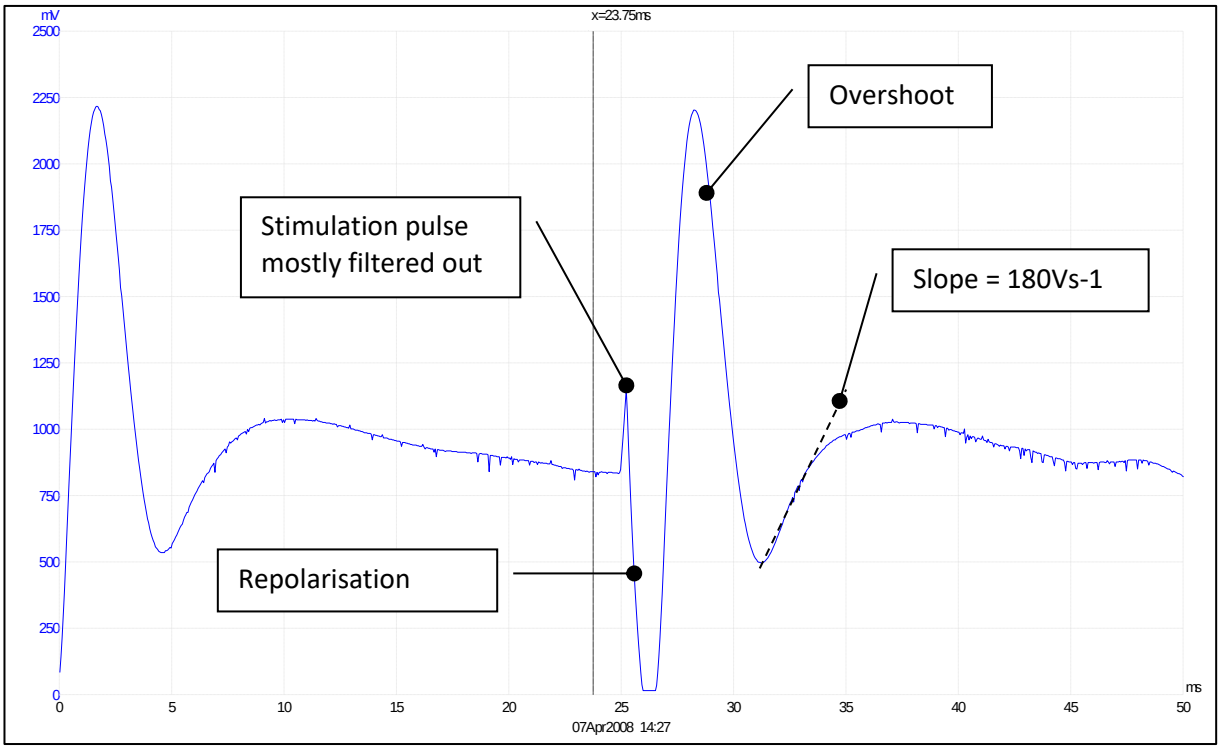

Figure 37 shows stimulation pulses and EMG signals measured from the wrist extensor muscles in the forearm with the wrist in a partially flexed position. The plot shows two stimulation pulses at 40Hz.

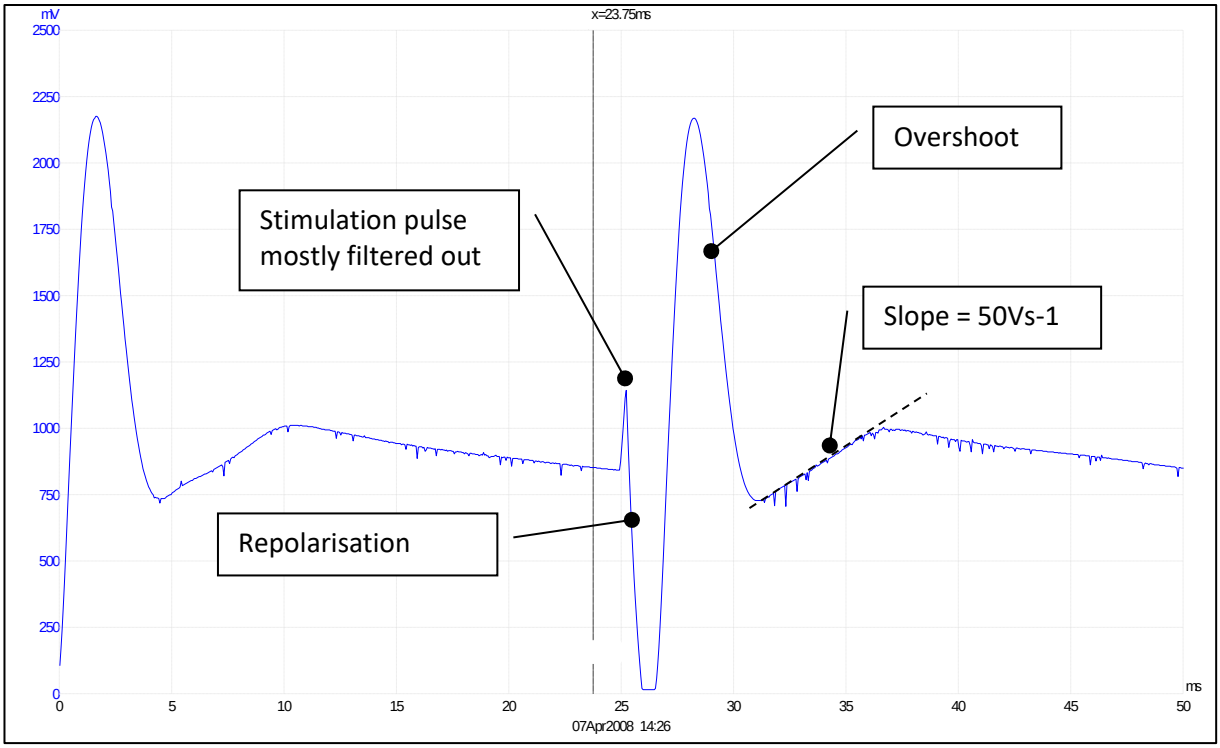

Figure 38 shows stimulation pulses and EMG signal measured from the wrist extensor muscles in the forearm with the wrist extended. The plot shows two stimulation pulses at 40Hz.

5.7 Discussion

The overshoot is a result of a large inductor in the form of a transformer that is used in the output stage of the stimulator. Following the end of the stimulation pulse a back emf (electro-magnetic force) is generated as the field within the inductor collapses. Fly-back diodes on the primary side of the transformer provide a safe route for any current induced in this period to short out. They are there to protect the transistors that are used to switch power into the transformer primary winding. The overshoot observed in the oscilloscope traces (Figure 37 and Figure 38) is a function of the threshold voltages of these fly-back diodes. The 9:1 winding ratio of the transformer means that induced current will stop flowing as the voltage on the secondary winding approach nine times the primary winding fly-back diode threshold voltage. This voltage then remains at the secondary and has to dissipate through the tissue of the limb to restore charge balance between the electrodes. The speed of the dissipation is a function of the impedance between the electrodes.

The clue to understanding the reasons for the effect came when it was observed that it could only be measured when the reference electrode was placed within close proximity to the other two EMG instrumentation amplifier electrodes. If the reference was placed distally as would be normal for a reference electrode then the effect was non-existent. The explanation for this came when studying a four-probe current sensing circuit for a completely different application used within the manufacture of silicon wafers as shown in Figure 39.

The arrangement of electrodes to detect a muscle response during a stimulation pulse had been found by experimentally trying different positions and observing the effects. This configuration placed the reference and sensing electrode along the line of the current path between the two stimulation electrodes. This had created a current probe capable of detecting the effect of small changes in the impedance of the tissue of the limb. Because this circuit is driven from the stimulator output, the stimulation pulse part of the waveform varies very little. Repolarisation during the refractory period that follows the stimulation pulse is however not driven, so the current flows back through the limb to achieve a state of equilibrium between the electrodes. The time it takes to reach a charge balance is affected by the impedance the flow of current encounters which is detected by the changes in the measured potential.

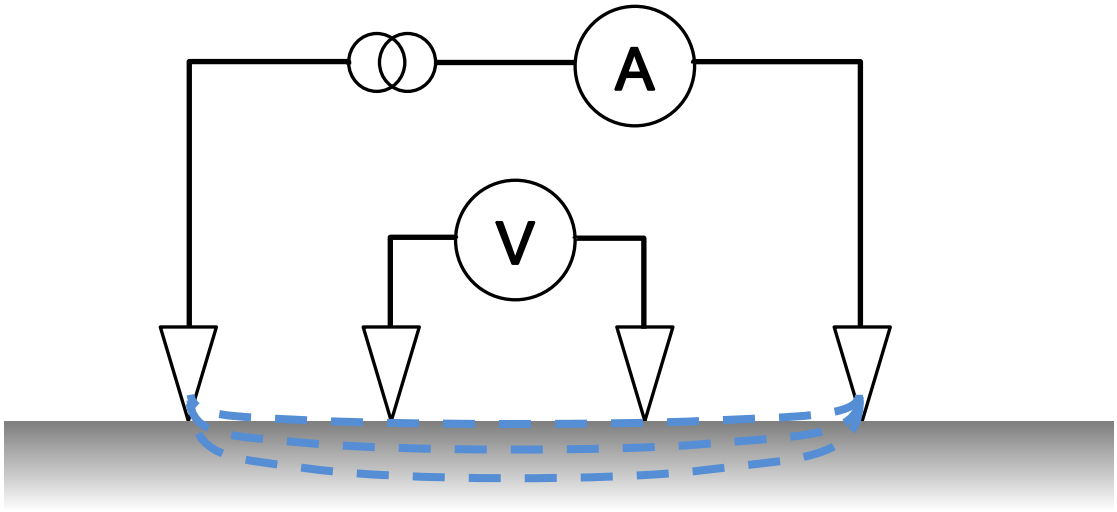

Figure 39 showing a typical arrangement for a four point current probe. A constant current is driven through the outer pair of contacts through the surface of the material. Using the voltage measured at the centre pair of contacts it is possible to determine very low resistances. This type of four terminal sensing is also known as Kelvin sensing.

A full understanding for the effect could not be immediately established. The observation did however invite further enquiry because it offered the potential to address two commonly occurring problems encountered when attempting to use EMG as a control signal for FES.

The first of these is the F-wave disturbance where a 'reflected' motor action potential generated at spinal cord level reinforces the EMG signal.

When an electrical stimulation pulse is applied through the skin to excite a motor nerve for the purpose of evoking an action potential, the evoked potential will then travel along the nerve fibres in both directions, orthodromic and antidromic.

Orthodromic – this is when the flows along the nerve is toward the motor point that joins the muscle, resulting in activation of the muscle. This is known as an M-response. The activation of the muscle produces EMG bio-signals which grow in intensity with the strength of the contraction.

Antidromic – this is when the flow is towards the motor neurons in the spinal cord. When the antidromic evoked potential reaches the motor neurons it is partially reflected, with this reflected portion becoming orthodromic action potential capable of producing a response when it reaches

the muscle. This reflected potential is known as an F-wave. The muscles response to the F-wave will be much weaker than the initial M-response and will occur after a delay determined by the nerve conduction speed and distances between the stimulating electrodes, the motor neurones and the stimulated muscle. Activation of the muscle from the F-wave also produces EMG bio-signals.

Measured and suitably conditioned EMG bio-signals can be used to determine the intention to move a limb and then the volitional effort made by a patient. FES can then be used to provide assistance with making the movement commensurate with the patient's intent. For real-time control of this type of system it is necessary to make measurements of the EMG in between the stimulation pulses. Where the level of measured EMG relates to the volitional effort of the patient and determines the degree of FES assistance required. Initially the patient will make a large effort the initiate movement, which will be matched by a high level of FES. Then as the limb begins to reach the desired position the patient will reduce their effort and the level of intensity of FES can be reduced to arrest further movement beyond the desired position.

The problem for an FES system that relies upon EMG magnitude as a measure of volitional effort to provide the control signal for stimulation matched to the user's need, is that F-wave disturbance can lead to unwanted positive feedback. Which can then result in the limb being over stimulated into hyperextension. This is because the F-wave occurs during the inter stimulation pulse period which is the time when the EMG needs to be measured. Removing an F-wave artefact from the control signal derived from the measured EMG is less than straightforward. The timing of the F-wave is a function of the distance between the site of the electrical stimulation and motor neurones located at the spine. This produces variability that makes determining which part of the EMG signal has been affected by the F-wave difficult to determine without first directly measuring the nerve conduction speed before ignoring or attenuating the relevant part of the signal.

The second issue is a problem regarding the antagonist muscle co-contraction known as the 'clasp-knife' effect. Stimulation of the extensor muscles has to steadily increase until a point is reached where the force generated by the extensors will overcome the force generated from the spastic flexor muscles. At this point the force generated by the flexor muscle reduces rapidly as a result of becoming stretched and losing mechanical advantage. This causes the joint to quickly go into hyperextension rather like the blade of a clasp-knife snapping shut. Hyperextension is undesirable for functional use and can be painful.

Having the ability to monitor joint angle would make it possible to detect the threshold prior to onset of the clasp-knife effect. The stimulation intensity could then be reduced to a level sufficient to maintain the limb positon but low enough to prevent hyperextension from occurring.

5.8 Conclusions

Measured EMG bio-signals can be used as a control signal for FES although the latencies associated with conditioning them can be problematic for low power ambulatory devices. The onset of an EMG burst begins prior to the muscle beginning to contract, making this a good way to detect a patient's volitional intent. Traditional signal conditioning methods of rectification and converting to a DC voltage level are slow at detecting the onset of EMG bursts. A better method for detecting the EMG burst onsets is the use of precision clamp tied to a known reference voltage. This method enhances the detection of change at burst onset by favourably distorting the waveform in that region.

The desire to avoid the difficulties associated with the use of blanking periods during the time when the electrical stimulation pulse is delivered led to the development of a ruggedized EMG sensor. The sensor had a pre-filter capable of substantially rejecting the higher frequency stimulation pulse while accurately capturing the lower frequency EMG signal. It was while using this sensor that an artefact of the stimulation pulse was related to limb position. The conclusion was drawn that this artefact was a function of impedance changes within the tissue of the limb.

Moreover these bio-impedance changes were by inspection a good dynamic indicator of the position of the limb during a movement made in response to electrical stimulation.

Chapter 6: Experimental Investigation of Impedance Variation with respect to the angular change between two limb segments

6.1 Introduction

The observed variations in the waveforms described in the previous chapter were by inspection consistent with changes to the joint angle and the effect was repeatable. It was also noticed that there were regions where the relationship between the changes to the joint angle and the changes to the waveform appeared linear. A method was needed to accurately capture the change in the joint angle so that a direct comparison to the waveform could be made. After considering the use of various mechanical goniometer arrangements it was decided to use an electronic goniometer (from the SG range manufactured by Biometrics Ltd. UK). These units provided a straightforward and adaptable method that would work equally well on the wrist or elbow joint as the work of the research developed.

Using the Biometrics goniometer enabled accurate measurement of movement about the wrist joint, which were then compared to changes in identified features of the captured bio-impedance plots.

A tracking system from Vicon Motion Systems that used cameras to capture motion in three dimensions was considered as an alternative method for measuring the movement. Use of the system was rejected however, because it offered no accuracy advantages over the Biometrics goniometers and was far less convenient to use.

6.2 Goniometer interfacing

Biometrics provides a computer interface for their goniometers that comes supplied with a software package for reading and capturing data. This interface did not fully meet the needs of the research and proved to be difficult to interact with in any way other than how its designers had intended. To avoid these problems, a drive circuit was designed and constructed to capture the raw output from the sensor into an oscilloscope. Because the manufacture's interface had now been replaced it was necessary to calibrate the goniometer output against a known standard before it could be used it in any experiments. To calibrate the goniometer it was first aligned onto the axis of a mechanical goniometer otherwise known as a clinical protractor (Figure 40).

The biometrics goniometer was powered from a 5V DC supply with the output captured using an oscilloscope. The mechanical goniometer was adjusted to a series of set angles covering the full range of movement and the output from the Biometrics device was recorded at each of the angles. The recorded readings were then plotted against the mechanically measured angle to check the correlation.

6.2.1 **Goniometer calibration test**

Figure 40 is an image of the Biometrics electronic goniometer attached to a mechanical one for checking the calibration

The Biometrics goniometer calibration measurements for each of the 10^0 set angles measured using the clinical protractor are given in

Table 3. These results were then plotted in Figure 41. A Correlation (r^2) of 0.9994 was obtained from the plot, indicating that the output from the Biometrics goniometer was closely matched to readings obtained from the protractor.

The error bars on the plot display the ±5% margin either side of the Biometric values on the y axis. The trend line fitted to these points falls comfortably within this margin of error.

Positive Angles		Negative Angles	
Mechanical Goniometer set angle in degrees	Biometrics goniometer output in µV	Mechanical Goniometer set angle in degrees	Biometrics goniometer output in µV
0	0	0	0
10	470	-10	-440
20	950	-20	-840
30	1380	-30	-1270
40	1860	-40	-1700
50	2290	-50	-2110
60	2740	-60	-2520
70	3150	-70	-2880
80	3560	-80	-3290
90	3990	-90	-3670

Table 3 – Calibration readings for the Biometrics goniometer output compared to set point angles on a mechanical goniometer

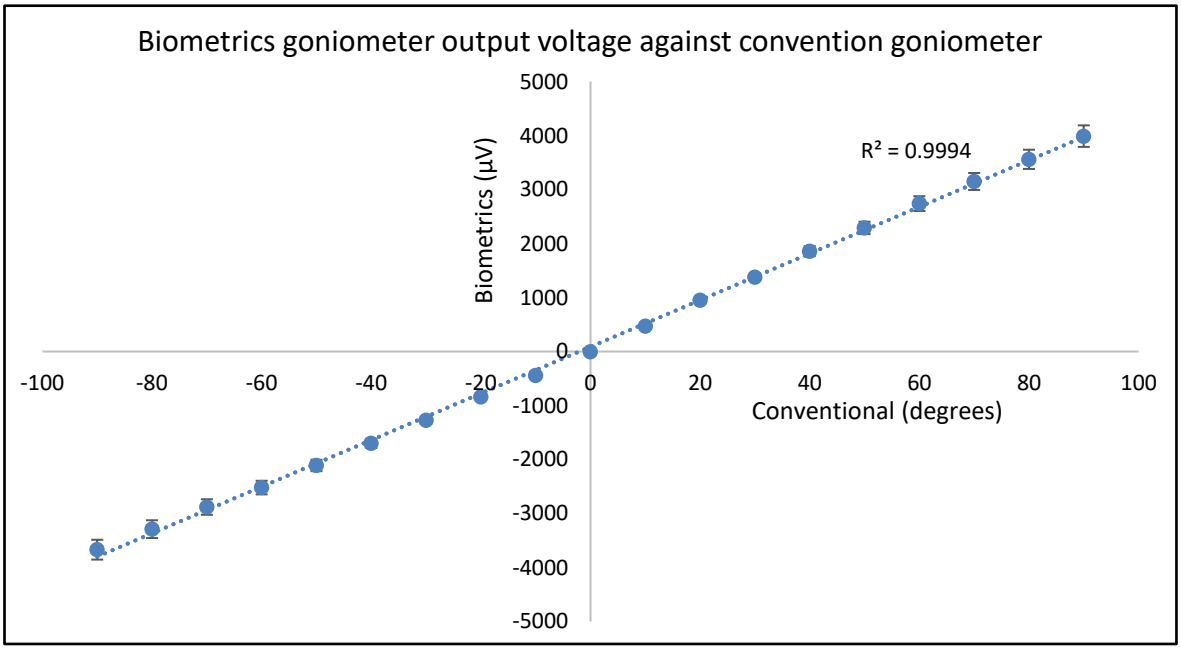

Figure 41 shows the goniometer calibration results for the Biometrics electronic goniometer output readings plotted against conventional mechanical goniometer readings. The error bars display a ±5% error margin for the y-axis values.

6.3 First experiment using a goniometer

6.3.1 Method

With the stimulation electrodes positioned to produce wrist extension with hand opening, the Biometrics goniometer was fixed across the wrist with one end of the device secured to the back of the hand and the other end to the forearm above the wrist. It was ensured that a complete range of wrist movement could be measured from full flexion to full extension (Figure 42).

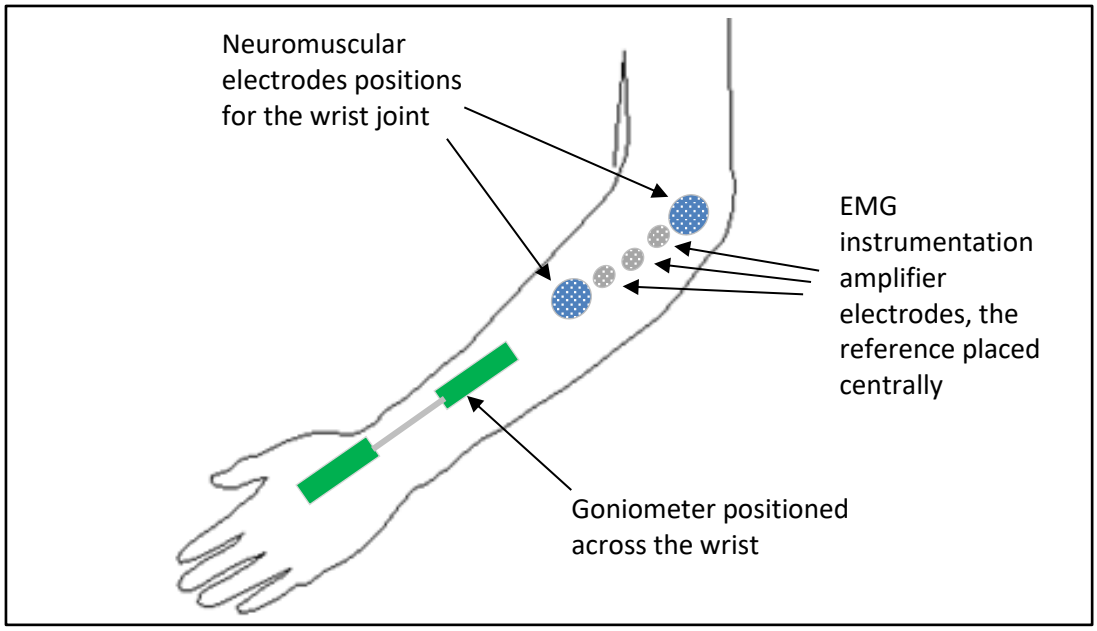

Figure 42 illustrates the position of stimulation electrodes and EMG amplifier electrodes on the forearm. A goniometer was placed across the wrist to measure joint angle changes resulting from the stimulation.

To collect measurements a PicoScope 2204 (Pico Technology Ltd. UK) two-channel data capture oscilloscope was used. The EMG sensor instrumentation amplifier was connected to one of the channels and the goniometer to the other. Common time-bases and sample rates were used on

both channels for the captures so that the traces containing the information about impedance could be directly compared to the trace from the goniometer output.

The electrical stimulation was adjusted to the level where it could be felt and seen to begin to affect the muscle but was still below the level needed to produce a contraction that would cause movement.

Data was then collected while the wrist was volitionally moved from fully flexed through to fully extended and then back to fully flexed again in one smooth movement lasting approximately two seconds.

The following parameters were used;

- Electrical stimulation was set to deliver pulses at a frequency of 40 Hz
- Data capture was at a frequency of 20 kHz

The analysis compared the value of the waveform peak in the refractory period that immediately follows stimulation with the outputs from the goniometer. The wave form peaks in this region had previously been shown to be an effective indicator of joint position (Figure 35, Figure 36), as had the slope of the change leading up to the peaks (Figure 37, Figure 38). However the stated overall objective of the research was to arrive at a practical and intuitive method to initiate and control FES assisted upper-limb movement, for a patient group who find difficulty in straightening their hand and opening the fingers and thumb to be able to reach and grasp an object (page 38). To this end where the desire is for a small and light-weight system based around a microcontroller architecture, the level of processing required for effective control can have significance upon the size of the battery needed for the power source. Because establishing maxima is a comparatively simpler task for this type of embedded control than measuring a slopes leading up to maxima, determining peak values was chosen as the preferred method.

During the refractory period the charge that was introduced into the body by the stimulation pulse has to settle as electrical equilibrium is restored in the circuit. The time and the manner in which it settles is a function of the circuit made up from the stimulator output, the electrodes and the body.

The data was exported into Excel (Microsoft Corporation, USA) where a filter was applied to extract the amplitude of the signals at a regular point in the refractory period of each stimulation cycle. This produced two sets of data with a common interval of 25ms which were then plotted with time on the x axis (

Figure 43).

The regions of the plot that were of particular interest were where the wrist reached and crossed the midway position from either direction. The importance of being able to identify this neutral position when the hand is pointing directly forward has previously been explained as necessary to avoid problems with hyperextension of the fingers. Any use of the method to control FES would require the system to reliably determine when the neutral point was reached so that the stimulation could then be modulated to maintain the position while the hand was being used. An angular range of approximately 20^0 either side of the neutral position was identified and looked at in greater detail.

To enable identification of underlying trends in the absence of noise a 10 term moving average filter was applied to the waveform data to act as a low pass filter. The goniometer output was plotted against the filtered peak waveform data and a curve fitted to the plot as a measure of correlation.

6.3.2 **Results**

Figure 43 shows the plot for the two set of values captured by the oscilloscope. These were from the EMG instrumentation amplifier with pre-filter and from the goniometer. The results are presented on the same time base for direct comparison.

The plots show a visual relationship between the amplifier measurements and the goniometer output for the wrist going from flexion to extension, and for returning from extension to flexion.

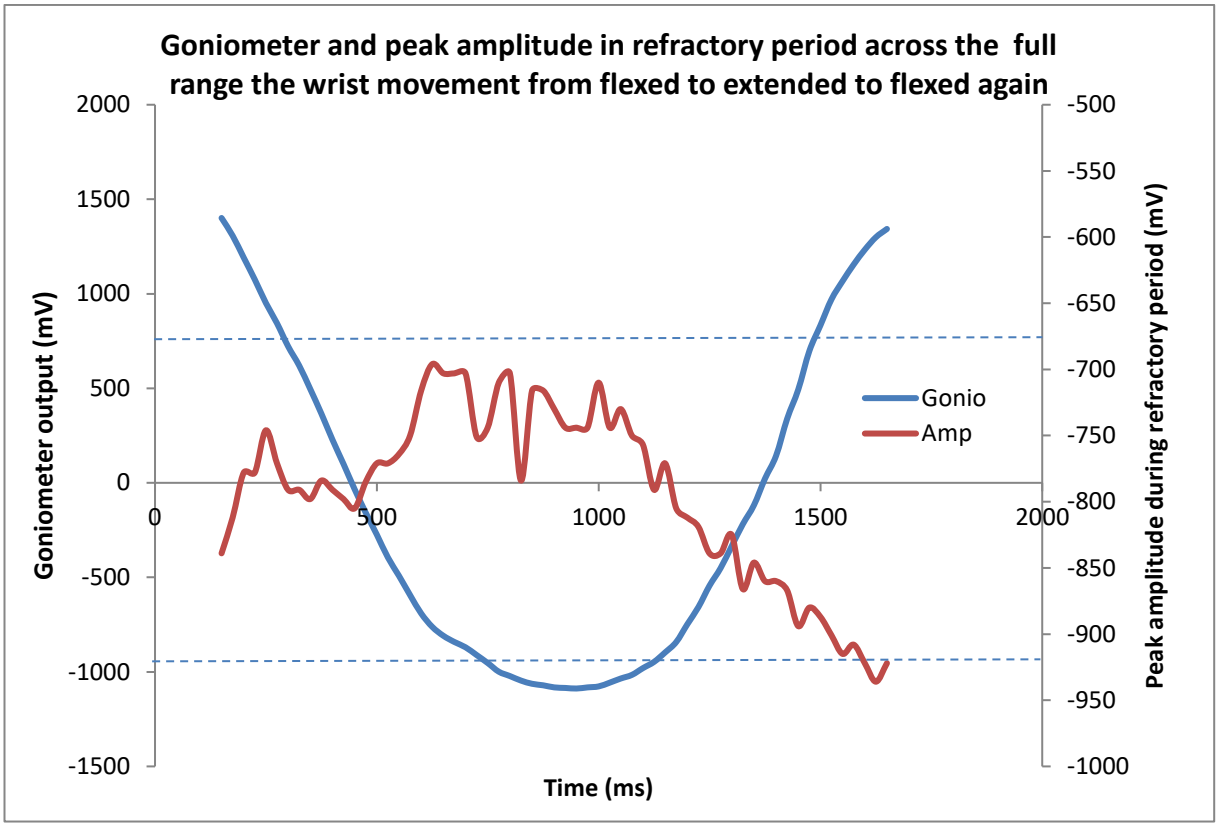

Figure 43 plots the goniometer and EMG amplifier readings collected while the wrist was moved through from full flexion to full extension and back to full flexion. Where the x-axis crosses the y-axis relates to the wrist being in a neutral position midway between fexion and extension. The two dotted blue lines relate to 20^0 either side of the midway neutral position.

Sections of the smoothed data were extracted for the movement of the wrist as it crossed the neutral position. This data was then plotted against the goniometer output reading with respect to time and a linear trend line fitted.

The plots shown in Figure 44 is as the wrist crosses the midway neutral point from flexion into extension.

The plot shown in Figure 45 is as the wrist crosses the midway neutral point from extension to flexion.

The standard error is indicated by the error bars. The standard error is the standard deviation of the sampled values, and is a measurement of the accuracy that each sampled value represents within the range of values used to populate the plot. In both plots the fitted trend line falls within

the range defined by the standard error bars for the region of interest as the wrist crosses the neutral position.

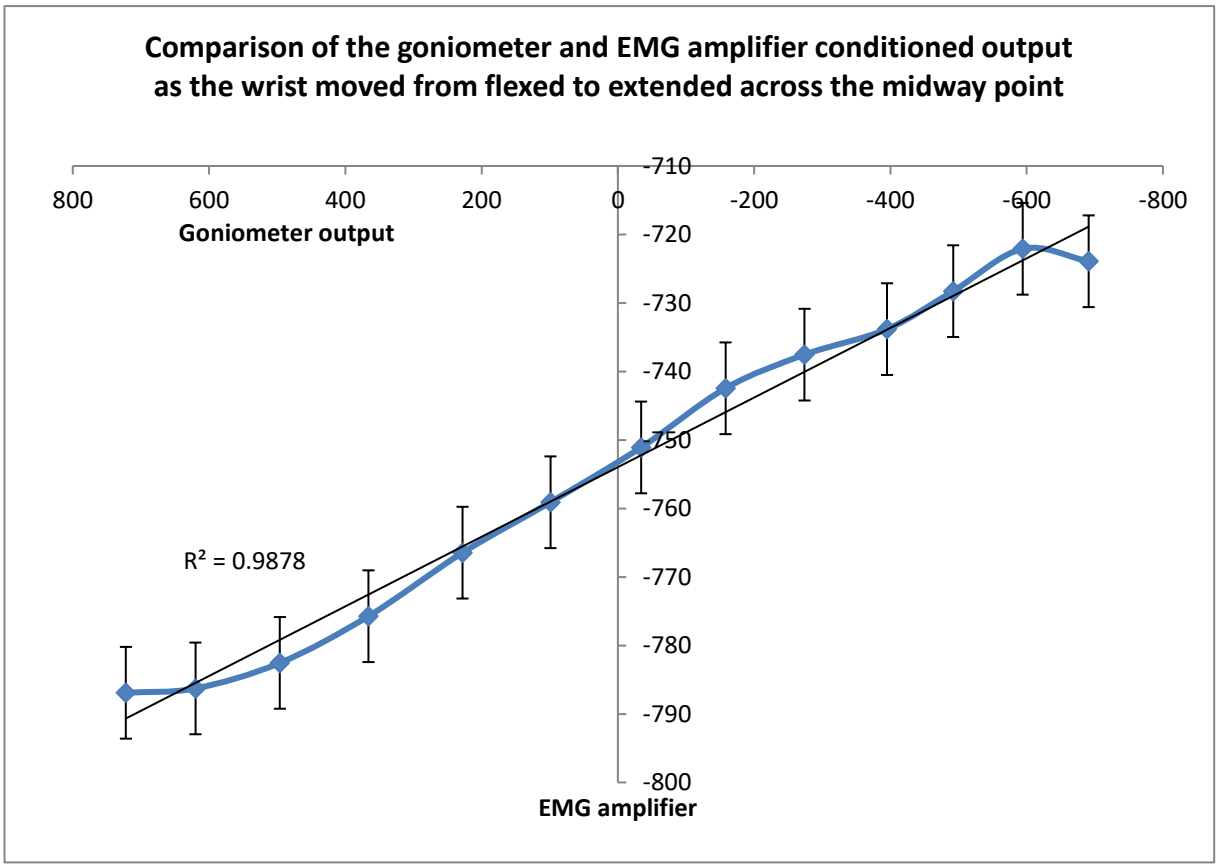

Figure 44 shows the correlation between the goniometer and EMG amplifier measurements after a low pass filtered was applied to the peak amplitude in the refractory period that follows the stimulation pulse. The plot is for the wrist movement as it passes through the neutral position from approximately 20^0 flexion to 20^0 extension. The error bars show the standard error for each value.

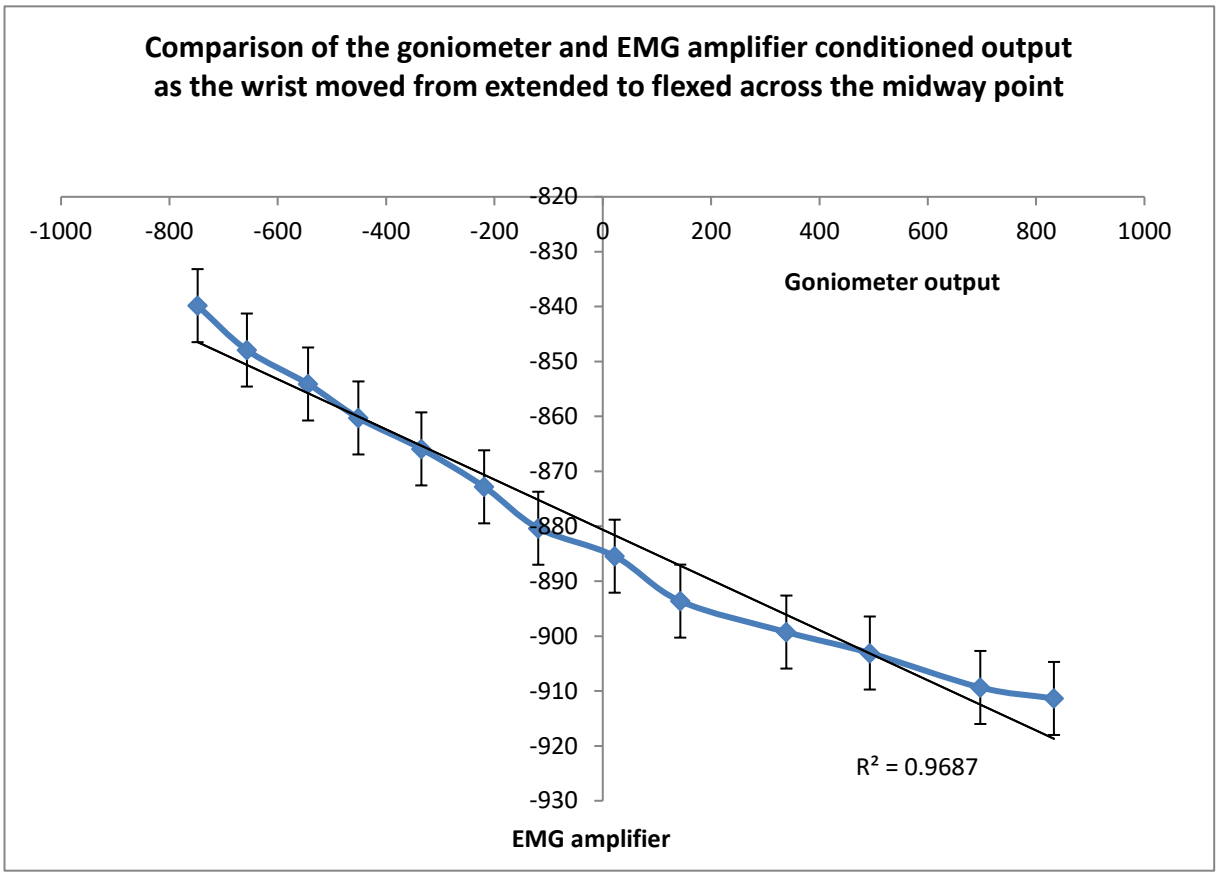

Figure 45 shows the correlation between the goniometer and EMG amplifier measurements after a low pass filtered was applied to the peak amplitude in the refractory period that follows the stimulation pulse. The plot is for the wrist movement as it passes through the neutral position from approximately 20^0 extension to 20^0 flexion. The error bars show the standard error for each value.

6.4 Discussion

The plot in Figure 43 shows the goniometer plot starting at a high level when the wrist was fully flexed, then slopping down as the wrist went passed the neutral position and into extension, before sloping up again as the wrist was taken back into flexion. Where the x-axis crosses the y-axis relates to the midway point of the movement or neutral position.

There is a noticeable increase in the amplitude of the amplifier signal as the wrist moves towards extension from being flexed. This is matched by a similar decrease as the wrist moves back toward flexion from being extended. A component of the signal that is higher than the frequency of the movement is evident and superimposed on the underlying trend relating to the movement.

The source of the high frequency component was not fully understood but the most likely reason for it would be alignment reorganisation of the muscles and tendons in the forearm as the movement progressed. This could lead to rapid changes in to current path taken between the skin surface electrodes. After applying a low-pass filter to the data using a non-recursive moving average, the underlying trend was exposed. The correlation of the low-pass filtered data to the goniometer for the neutral-crossing periods shown in Figure 44 and Figure 45 confirmed the linearity of the relationship that had been predicted from the original oscilloscope observations.

It was proposed that the observations could only be explained by impedance changes taking place in the circuit made up from the stimulator output, the electrodes and the tissue of the body. The relationship between all of these components is complex. The electrode interface with the skin contains capacitive and resistive elements. FES electrodes have a conductive layer designed to spread the charge they deliver over as wide and area of the electrode as possible. This is assisted by using an adhesive gel to affix the electrodes that has resistive properties. The effect is that the charge from the stimulation pulse reaches the electrode and spreads out before crossing the gel layer. The charged layer forms one plate of a capacitor with the tissue underlying the skin forming the other.

The Stratum Conium is the outer layer of the epidermis of the skin and is made up from many layers of cells known as the lipid-coenocyte matrix. These cells behave very differently depending upon the electrical potential across them. Initially they are very poor conductors but become highly conductive after sufficient potential has been applied across them when electropores become established (Keller & Kuhn, 2008). Passing through the lipid-coenocyte layer are appendages such as hair follicles and sweat gland. Prior to the electropores becoming opened up these represent an easier path for electrical current and can be a potential source of discomfort or even burns. The resistive gel used on the electrodes is designed to limit current concentrations from occurring along these appendages prior to the electropores being established. This results in the capacitance formed from the electrode held on the skin with the gel layer reaching a peak just prior to the electropores opening when it falls away rapidly as current is conducted through the skin.

If the assumption is made that after electroporation has occurred the conduction through the electrodes becomes stable, any remaining changes in impedance should be due to the changes to tissue underlying the skin.

6.5 Conclusions

The comparatively more straightforward method of measuring the peak amplitude of the charge balancing after each stimulation pulse had been delivered proved effective while requiring fewer resources than calculating the slope of the plot during this period.

There is a detectable impedance variation with respect to an angular change between the two limb segments. The investigation was able to demonstrate a near linear relationship between variations attributed to body tissue impedance changes and the angle of the wrist joint about the neutral position. This relationship was true for both directions of travel through the neutral position as the wrist moved from flexed to extended and back.

These results gave an early indication of how the initially observed and now measured impedance effect had the potential for use as a control signal for FES. A further understanding of bioimpedance was now needed to make full use of these findings.

Chapter 7: Bioimpedance

7.1 Description of Bioimpedance

Bioimpedance is the name given to impedance as it relates to the electrical properties of biological tissue. This impedance is measure of the voltage response to current conducted through the tissue. Bioimpedance is a complex impedance made up from purely resistive elements and reactive elements due to capacitances within the body tissue (Preedy, 2012). When Bioimpedance is measured transcutaneously it is these capacitances that contribute to the tissue being a very poor DC conductor. To avoid this DC blocking property of the tissue an AC signal is used when measuring Bioimpedance.

7.2 Measuring Bioimpedance

In order to characterise the impedance of biological tissue it is necessary to measure the following two parameters, the voltage dropped across the tissue and the extent of any phase changes. From these it is possible to determine the resistive and reactive components. Two methods for measuring the complex impedance are presented here.

7.2.1 Four Electrode method

One method of obtaining these measurements is to use four electrodes. These are arranged in a line along the limb to be measured as shown in Figure 46. The outer pair is used to introduce current from a constant current source while the middle pair is used to make the impedance measurements from.

An AC signal from a constant current source is introduced into the limb via the current electrodes which are placed as far apart as can be practically achieved on the limb. This gives the current the maximum opportunity to spread through the tissue of the limb. The second pair of electrodes is then used to measure the voltage across the part of the limb of interest between the current electrodes. This voltage is fed into the high impedance inputs of an amplifier. A comparison is made between the measured voltage and the injected signal to determine phase shift.

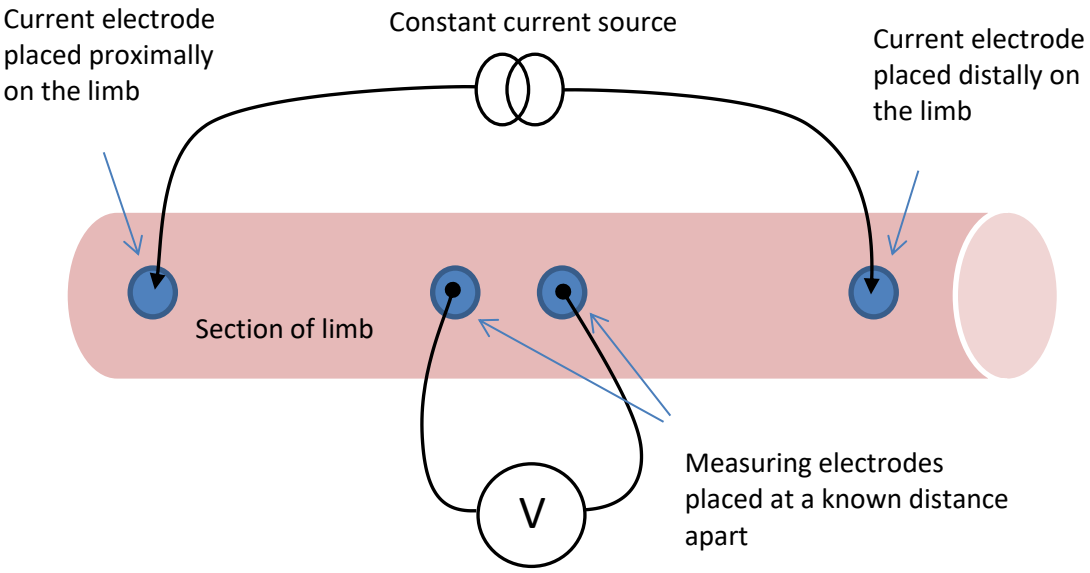

Figure 46 illustrates a typical four electrode bioimpedance measuring method

The four electrode impedance measurement method has the advantage of being unaffected by the impedance of the electrodes being used. The constant current source automatically accounts for any electrode impedance by driving at the necessary voltage needed to maintain the current flow. The high impedance of the voltage amplifier input does not permit current flow through the measuring electrodes and so is unaffected by their impedance. The four electrode method is the most accurate method of measuring tissue impedance.

The drawbacks with the methods are that placement of four electrodes is required and geometry of the measurement electrodes placement needs to be done accurately because the voltage measured is a function of the distance between these electrodes. It is also uncertain which path the current will have taken when flowing through the limb which can have implications on the amplifier gain for the measuring system.

7.2.2 **Two electrode method**

An alternative to the four electrode method is the two electrode method. A known AC signal is injected into the limb using two electrodes placed over the area of the limb of interest. Voltage drop and phase shift changes to this signal are measured directly.

The advantages of this method are that the area of the limb of interest is being excited and measured directly while only requiring placement of two electrodes. The main drawback with the method is that the impedance of the electrodes is included in the measurement of impedance.

This can be removed following an initial calibration process if required. For any application where it is only a relative change in impedance that is required to be known, the two electrodes method can be an acceptable approach.

7.3 An investigation using the two electrode method to measure limb movement about the elbow over a range of sampling signal frequencies

7.3.1 Introduction

The literature on impedance myography shows that changes to an AC signal used to excite the tissue for making the measurements are the usual method for determining the impedance It has also been shown that a previously unwanted movement artefact that gave problems in the field of impedance myography can be used to determine limb position. The two electrode method of measuring bioimpedance offer certain advantages over the four electrode method in terms of simplicity of use that lend it to the type of ambulatory systems that this research is focussed upon. The goal being that movement could be detected by using a pair of electrodes that were also used for delivering FES, such that the electrical stimulation could be delivered while any resulting bioimpedance changes are measured from the same electrodes.

The literature suggested that frequencies below 50 kHz when used as the sampling sine-wave for impedance myography have been identified as being more susceptible to movement artefact. It was decided to investigate frequencies up to 50 kHz to find out which would be most receptive to movement.

7.3.2 Method

An FES stimulator was used to establish a functional electrode position across the elbow joint with the electrodes positioned to produce forearm extension with supination, wrist extension and hand opening of the type described shown in Figure 11 (page 67). The elbow was chosen in preference to the wrist because of the larger range of the movement involved, making any effects of the frequency more easily detectable.

Having found the correct electrode position to produce a functional arm movement the stimulator was disconnected and the electrodes connected up to a signal generator.

The signal generator produced a 2V peak to peak sine wave. The signal was conducted through a current sensing resistor before making a circuit through the body with the electrodes as shown in Figure 47.

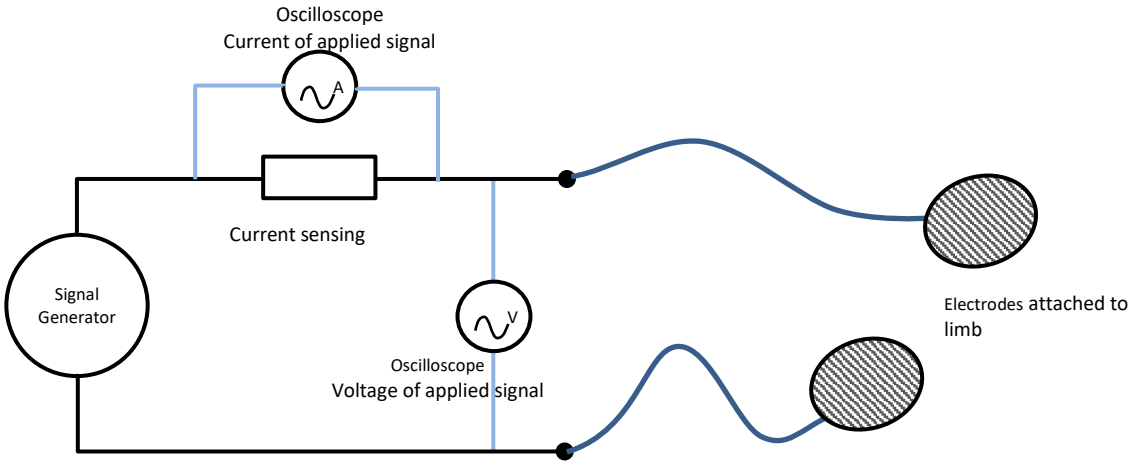

Figure 47 illustrates the circuit used to investigate response to an applied signal at different frequencies.

A two-channel oscilloscope was set to sample at a rate of 250 kHz. One of the channels was connected across the electrodes to monitor the signal voltage applied across the electrodes and the other channel to measure changes across the current sensing resistor.

The data logging oscilloscope had insufficient data buffering capacity to store an entire movement at the higher data rate of 25 MHz that was necessary to avoid aliasing errors and provide adequate resolution of the sampled signal. Measurements of 5000 data points (a 200µs time window) were captured at three set points at the beginning, midway and end of the range of movement.

Four sets of measurements were made at each of the frequencies 20, 30, 40 and 50 kHz

Readings were taken by inspection from the captured oscilloscope plots using the measurement tools that are part of the PicoScope oscilloscope software to record the amplitudes of the voltage applied across the electrodes and voltage drop across the current sensing resistor.

7.3.3 **Results**

The results of the investigation into the effect of frequency on amplitude measurement are shown in Table 4. These results can be seen plotted in Figure 48**Error! Reference source not found.** for graphical comparison.

Frequency (kHz)	Flexed (mV)	Midway (mV)	Extended (mV)
20	821	825	832
30	642	646	653
40	534	541	548
50	442	453	457

Table 4 – Table showing a comparison of the peak values for the amplitude of the signal across the sampling electrodes for each of three limb positions at a range of measuring signal frequencies.

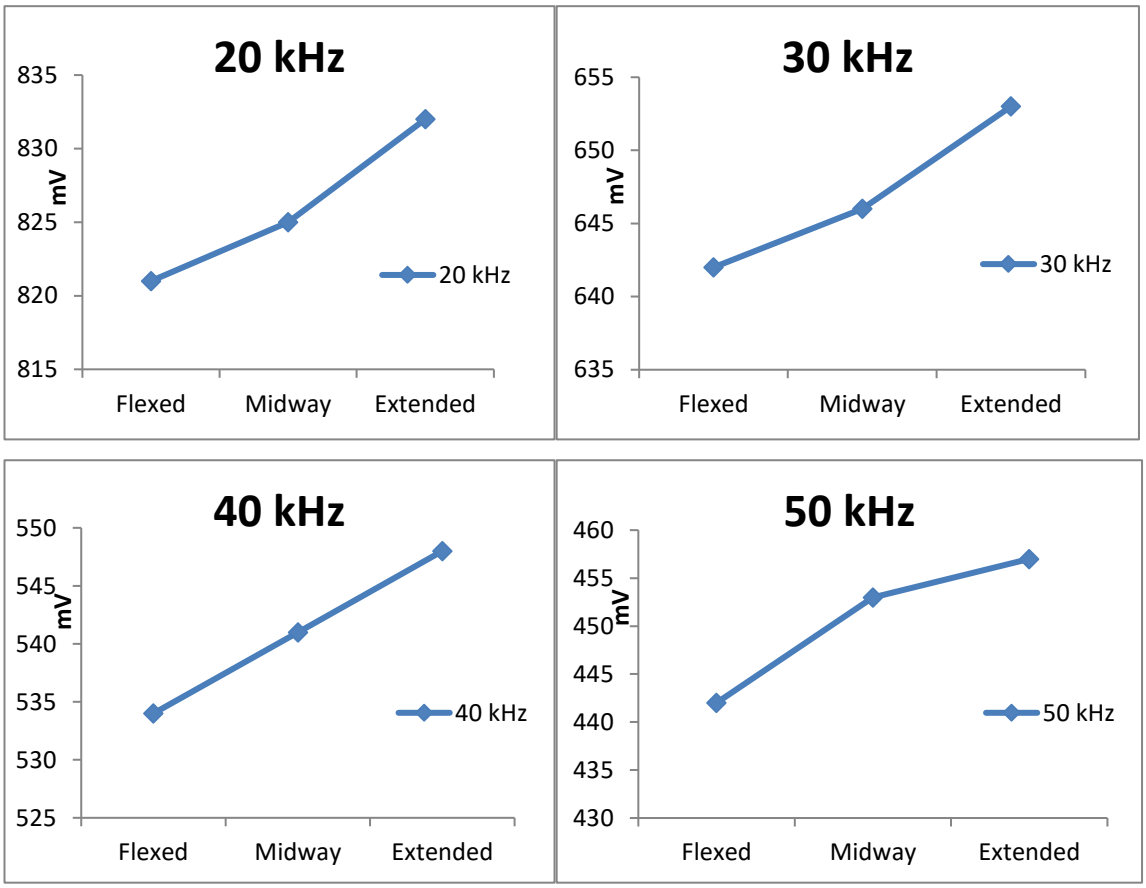

Figure 48 is a set of plots of the results given in the Table 4**Error! Reference source not found.**. They show little relative variation between plots at different frequencies.

7.4 Discussion

The four electrode impedance measurement method disregards the effect of the electrodes being used, because a constant current source automatically accounts for any variation in electrode impedance by driving at the voltage necessary to maintain stable current flow. While the high impedance of the voltage amplifier ensures that the measuring electrodes remain unaffected by their impedance. Two drawbacks for this method were identified, the need for accurate placement of the four electrodes to ensure consistency and the uncertainty about the current path through the limb. Each of these are discussed turn.

The four electrode method is used to make absolute measurement of bio-impedance. The technique is used to chart the progress of chronic muscle disease. The electrodes are accurately and repeatedly placed with reference to anatomical prominences and many sets of measurements will be made over many weeks or months. The method is used to determine absolute changes in impedance over the course of the muscle disease rather than relative changes due to transients such as movement. Indeed movement will produce an unwanted artefact when these types of measurements are being made.

The uncertainty over which path the current will have taken when flowing through the limb is of little significance when taking impedance measurement form a static limb. Consistency of electrode placement between measurements will remove much of this error, and the amplifier gain can be set to match the signal under measure. The uncertainty about the path of current flow does however present difficulties when measuring a dynamic limb, when the changes of current path due to altered limb segment orientation across the movement represent an artefact to the absolute bio-impedance measurement. The path of the current will be dynamic throughout the movement with potential for uncertainty for this path between repeated movements due to subtle differences of limb position between each repetition. Moreover the changes in the current path could result in the gain setting of the amplifier becoming out of range for parts of the movement sequence.

The two electrode method has the drawback of being unable to disregard the impedance of the measuring electrodes and so is less appropriate for measuring absolute impedance than the previous method. The method does however have a number of advantages when used to dynamically track the movement of limbs. The electrode can be placed in close proximity to the

muscles that produce the limb movements so impedance changes between the electrodes are much less likely to be influenced by the sort of changes in the current path that effect the four electrode method. Because the current path remains unaffected in this way, the gain settings of the measuring amplifier can remain constant over the entire range of the movement.

The results of using the two electrode method to track points across the range of elbow flexion movements showed a measurable change in the impedance that related to the movement. The results showed little relative variation between plots when different frequencies were used for the sampling signal. This is a useful finding when considering the end goal for an ambulatory system. This is because the processing requirement for sampling and processing a 20 kHz signal are significant lower than for a 50 kHz one, which has consequential benefits on power requirements.

7.5 Conclusions

Four electrode bioimpedance measurement systems are the preferred method for obtaining absolute measurements of bio-impedance. They do however require additional electrodes, can lack sensitivity and require assumption on current paths.

Two electrode bioimpedance measuring system are simpler and capable of measuring relative changes in impedance. With measurements of bioimpedance from a two electrode system used to determine the progress of muscle contractions that result in movement of a limb about a joint.

The frequency of the AC signal used for making the impedance measurements had little influence across the range of 20 to 50 kHz. Therefore 20 kHz would be used for further investigations as this imposes lower demands on sampling and processing signals.

The performance criteria that a system using bioimpedance as a method to measure limb movement would be required to display are;

- reliable and repeatable identification of the important stages of the movement,
- immunity from any artefact introduced by electrical stimulation,
- capable of real time operation,
- suitability for a clinically practical application.

Chapter 8: Investigation into measuring the effects of bioimpedance changes while using neuromuscular stimulation

8.1 Introduction

The previous chapters demonstrated the effectiveness of the two electrode method for measuring bio-impedance as a way to determine three points of limb position within a movement. The next stage of the work was to demonstrate how bio-impedance measurements could be captured across the entire range of the movement so that these could become a control signal for the FES. In the previous chapter the amplitude of the voltage across a current sensing resistor was used to determine the impedance, this however ignored any phase shift components. So a method was developed to capture both the amplitude and phase shift so that the complex impedance could be fully characterised. The resistive component of the impedance was determined from changes in amplitude of the voltage across a current sensing resistor as before. While the phase shift changes were determined by measuring the interval between the zero-crossings of the current sensing voltage and the signal voltage applied across the electrodes.

The Picotech PicoScope software that came supplied with the data capture oscilloscope to be used for the investigations was not well suited to the needs of the research, not allowing data to be streaming at the required rate for a sufficient length of time. Referring to the Picotech's documentation for the oscilloscope it was clear that the device was capable of streaming the data at the required rate. Picotech offered a software development kit (SDK) to enable investigators to create their own software to exploit this feature. The SDK had drivers for use with LabVIEW (National Instruments USA) that would allow a LabVIEW virtual instrument to be developed for the application. A virtual instrument to run on LabVIEW was developed capable of streaming data from the oscilloscope to the computer for storage for the time needed to complete a full limb movement.

The sample rate was fast enough to enable phase shift measurement from zero-crossings. Peak amplitudes were obtained by monitoring maxima over a number of successive waveforms. Matlab scripts were written to process the captured files so that the zero-crossings and amplitude peak values could be extracted from a moving time window.

Equipment was designed to enable the bi-impedance measuring system to be used in conjunction with FES. This was so that the feasibility of obtaining positional information about the limb while the muscles were being electrically stimulated could be tested. If this proved possible it would have the potential to be developed into a real-time control for FES stimulation intensity to change and maintain limb position. This would achieve the stated aims of the research.

The neuromuscular stimulation followed a conventional pattern, delivered in pulses of approximately 200µs duration at a frequency of 40Hz. This gave a period between the pulse of 25ms, and of this up to 15ms was needed to achieve a charge balance following each pulse leaving a period of around 10ms to measure the impedance.

To protect the impedance measurement circuit (Figure 47) isolation was required from the electrodes for the period while the stimulation was delivered. Isolation was achieved using a twin-pole high speed relay with a timing signal from the stimulator used to switch the connection to the electrodes between the stimulator output and the impedance measuring circuit. A two channel oscilloscope was used to measure the voltage and current waveforms as before. In addition one of the channels was also used to capture the goniometer output during the period when the stimulation was being delivered. A second high speed switching relay was used to make the connection to the goniometer, this was also controlled by the timing signal from the stimulator. Meaning that both oscilloscope inputs were switched at the same time, as the electrodes were switched between the stimulator output and a 20 kHz sine wave from the signal generator used for the impedance measurement (Figure 49).

The first of the oscilloscope inputs was set to capture the voltage across the electrodes when the signal generator output was connected, and disconnected during the stimulation pulse.

The second input was connected across the current sensing resistor when the signal generator output was connected to the electrodes, then during the stimulation pulse connected to record the goniometer output signal.

Three parameters were captured on the same time base;

- Voltage across the electrodes
- Voltage across the current sensing resistor
- Voltage output from the goniometer

8.2 Test equipment for measuring bio-impedance while electrically stimulating

8.2.1 Bio-impedance measurement

The PicoScope 2204 manufactured by Pico Technology was identified as a two-channel oscilloscope with signal generator capable of delivering the 20 kHz sine wave of 2V amplitude needed for making the bio-impedance measurements. The oscilloscope has data storage capacity and a USB interface to a host computer. This oscilloscope is capable to simultaneously producing the required sine wave output and measuring the resultant waveforms. Data can be internally buffered or streamed over the USB link to the computer.

The PicoScope oscilloscope therefore satisfactorily formed the basis of the impedance measuring method and was built into the test equipment.

8.2.2 Equipment for sequentially switching the electrode connections

The test equipment needed to sequentially connect the electrodes placed on the limb to the stimulator output and the impedance measuring circuit (Figure 49). To protect the impedance measuring circuit from the stimulation pulses it was necessary to ensure that there was complete isolation. A further requirement was to collect measurements from the goniometer circuit while stimulation was in progress.

The arrangement used for switching the connection to the electrodes is shown in

Figure 49. High speed double pole single throw switching relays were chosen to guarantee complete isolation and provide a convenient way to connect to the goniometer circuit. Details of how the relay connections are switched are given in Table 5.

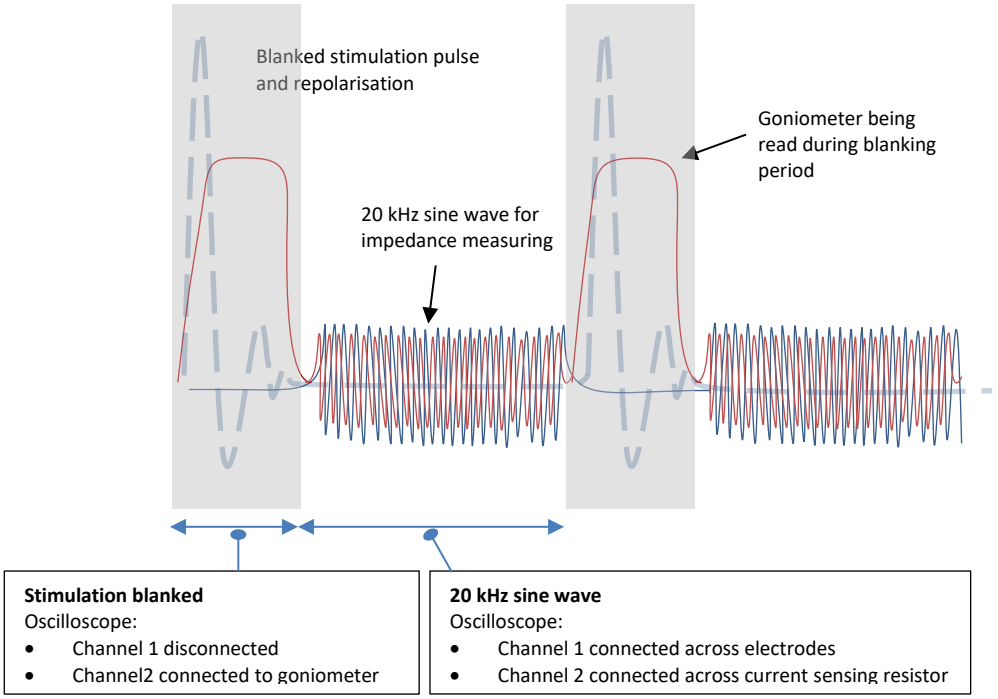

Figure 49 shows how the oscilloscope input channels are switched between connections to the sine wave used for impedance measurement and the goniometer to accord with the regular 40 HZ stimulation pulses.

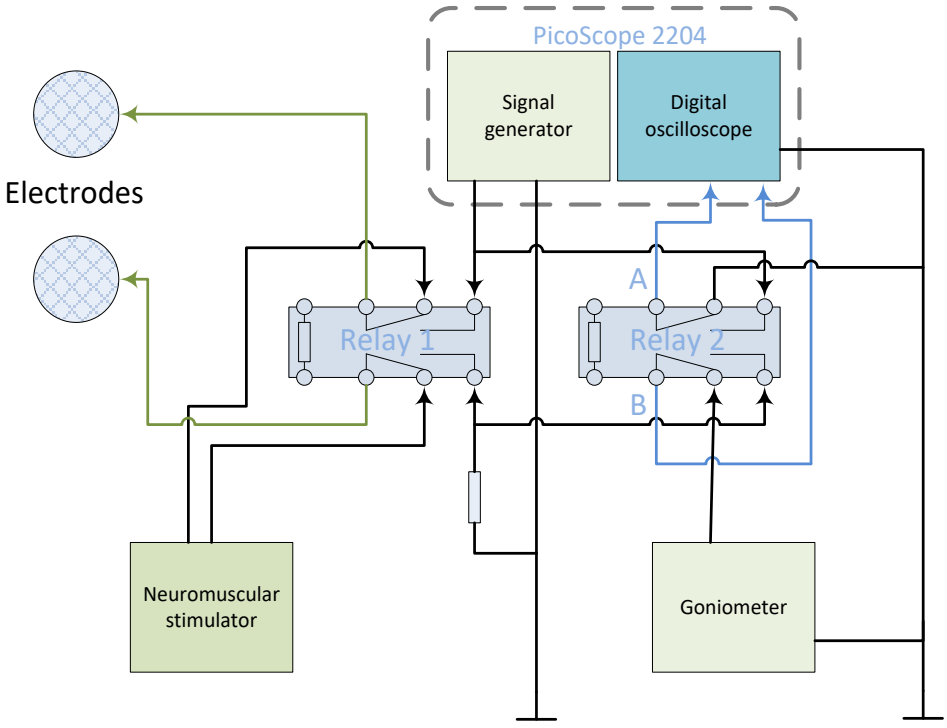

Figure 50 shows how the double pole electromechanical switching relays were arranged to ensure complete isolation of the electrical stimulation from the

impedance measurement circuit, and also to enable connection of the goniometer circuit.

Relay state	**Relay 1** – Source devices	**Relay 2** – measuring device
De-energised	Electrodes are connected to the neuromuscular electrical stimulator	Channel A – Ground Channel B - Goniometer
Energised	Electrodes are connected to the 20kHz sine wave from the signal generator	Channel A – Impedance (V) Channel B – Impedance (I)

Table 5 – Details the operation for the switching relays. Relays are activated by a common timing signal from the stimulator so that energising and de-energising is synchronised to the stimulation pulse.

8.2.3 The goniometer circuit

The Biometrics goniometer carried its own signal conditioning circuitry within the device. To use this circuitry it was only necessary to provide a stable 5V supply.

8.2.4 Neuromuscular electrical stimulator for use with impedance measurement

8.2.4.1 Pace stimulator

At the time of conducting this research the author was designing a neuromuscular electrical stimulator to treat dropped-foot. This was the Pace stimulator produced by Odstock Medical Ltd in the UK (OML). It was a version of this stimulator that was modified to work with the impedance measuring equipment. The information given in this thesis has been taken from the patent document (Lane, et al., 2011) which is within the public domain.

This Pace stimulator offered an advantage over the version that had been used so far in the research, benefitting from a more developed version of the state-machine control. The device was limited to a single output channel of stimulation however this was all that was necessary for the investigation into impedance.

A number of changes were necessary before the standard version of the Pace stimulator could be used for the investigation into impedance.

As a dropped-foot stimulator the Pace would normally have a foot-switch lead plugged into a socket on the unit. The function of this socket was changed so that it could be used to output a

timing signal for controlling switching of the relays used in the test equipment. This is shown in Figure 51 as the blue and green timing signal lines going to the relays, labelled as A and B.

The standard Pace unit has 'Test' and 'Walk' functions that are commenced by pressing the appropriate buttons. In normal use either of these functions will produce a stimulation output. The 'Walk' function was modified to produce a timing signal with the stimulation output inactivated.

Changes were made to the wording used in the user display menus so that it was obvious to the casual observer that this was no longer a conventional Pace stimulator and should not be used as such.

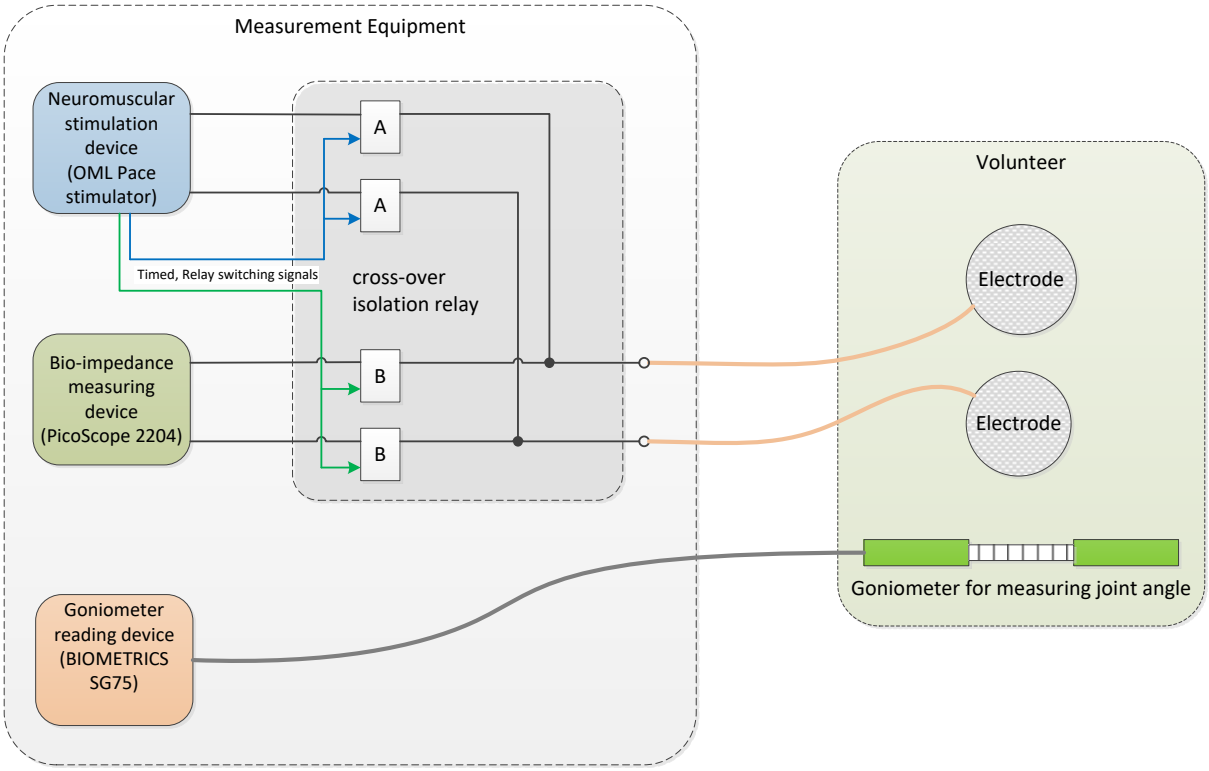

Figure 51 shows a block diagram of how each of the parts was integrated.

8.2.5 **Housing the test equipment**

The test equipment was assembled and housed into an equipment case. This was done partially to keep everything together and partially because a properly packaged piece of equipment would be better received by the participants of the study.

An aluminium equipment case was sourced from Maplin Limited UK. To ensure that it would be suitable for housing all of the parts of the system a computer aided design (CAD) model was created in SketchUp (Trimble Navigation Limited) before producing the final assembly (Figure 52).

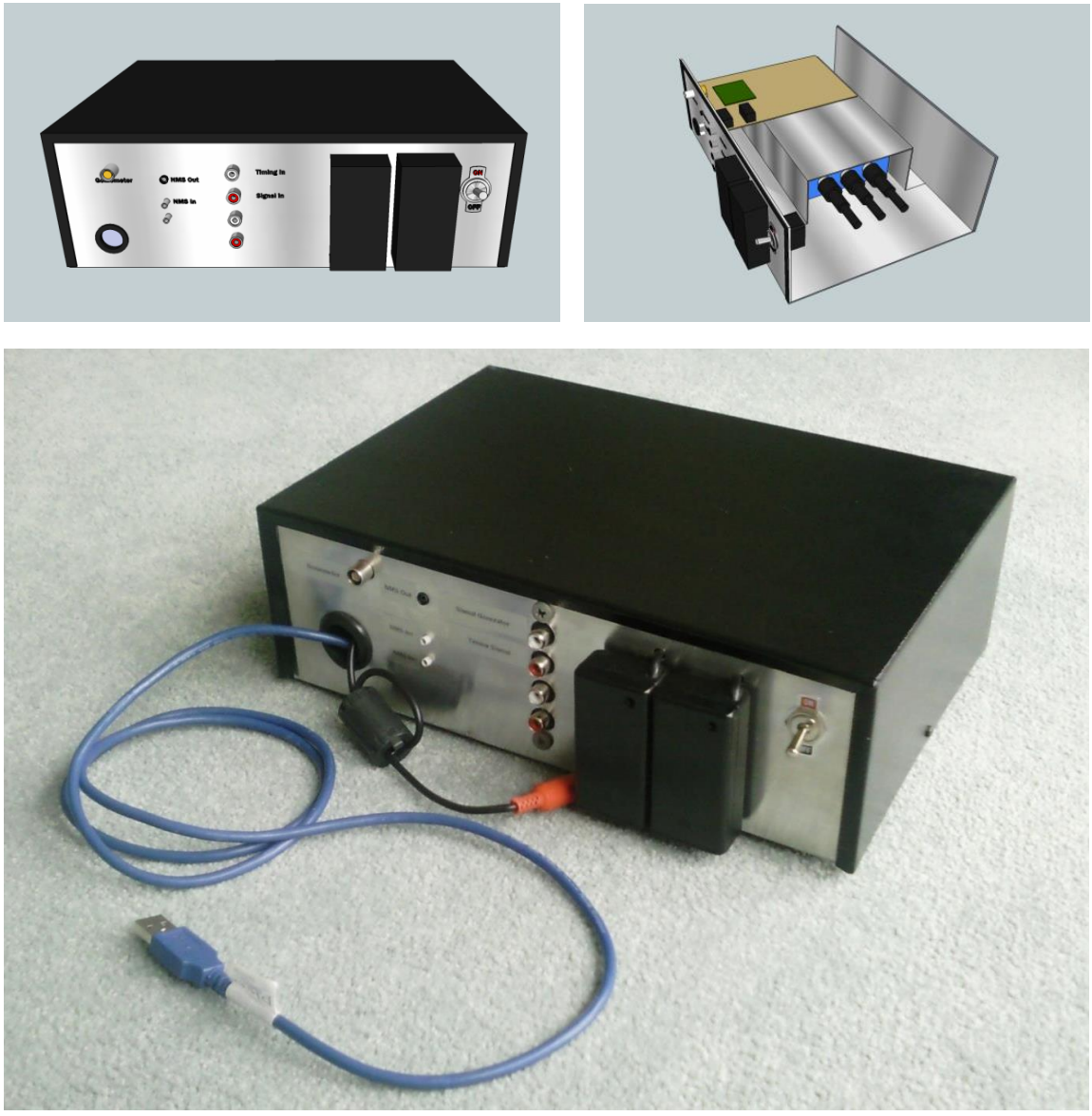

Figure 52 shows the 3D CAD design and finished test equipment.

8.2.6 **Equipment testing**

The switching relay arrangement had been chosen to ensure full isolation between the circuit delivering the stimulation and the circuit measuring impedance. These relays had an unintended

consequence that made it difficult to use the automated Matlab scripts written for processing the data files captured by the oscilloscope. The Matlab scripts had been written to identify the repeated patterns in the data to enable the phase shift, amplitude and goniometer readings to be extracted. Unfortunately this proved unreliably because of variability in the switching of the relays. During the period while a solution to the problem was being investigated Pico Technology released an updated version of their PicoScope oscilloscope software. This new version enabled the data streaming capability previously lacking and removed the need for the National instruments virtual machine that had been created using the SDK. This also meant that the inbuilt measurement tools that come with PicoScope became available which avoided the need to use Matlab. The PicoScope tools offered a very convenient way to detect the peak amplitude changes by to measuring the ACRMS for the period when the 20 kHz sine wave is applied between the stimulation pulses. Measuring in this way reflects the peak amplitude changes while averaging the measurement over a large number of waveforms.

The decision was taken to use the newer version of the PicoScope software in place of the National Instruments virtual machine and Matlab scripts. The work was still at an investigation stage so manually processing the data using the PicoScope software was preferable to further developing the automated data processing method using Matlab at this stage.

The PicoScope software did not provide an easy means by which phase shift measurements could be taken from the captured traces. Amplitude changes had previously been shown to be an effective measure of impedance change (Table 4). It was therefore decided to only measure amplitude changes using the ACRMS tool for this initial investigation to see if dynamic bioimpedance changes could be detected while using FES.

8.3 Method

Measurements were taken from the authors arm using the test equipment connected to the PicoScope software which were later analysed using Microsoft Excel.

Three treatments were chosen for the investigation.

- Voluntary movement of the limb about the joint under investigation without any electrical stimulation – this was to establish a baseline result for normal movement.
- Voluntary movement of the limb while a constant low level electrical stimulation was being applied – this was to investigate whether the bio-impedance measurements could

be carried out during stimulation. The parameters for the stimulation remained constant through the test.

- Movement evoked by FES – this was to investigate whether the bio-impedance measurements could be made while the parameters of the neuromuscular electrical stimulation were changing during an evoked movement.

A protocol was developed for capturing and processing the data that made use of the tools available within the PicoScope software and Microsoft Excel.

8.3.1 Pico Technology oscilloscope setup

Setting	Value
Time base	500ms/div
Number of samples	500k samples (equates to 100k samples/s)
Channel A (voltage)	+/- 5V
Channel B (current)	+/- 100mV
Sine wave generator	20 KHz at 2V peak to peak

Table 6 – Oscilloscope setting used for the data capture

8.3.2 Stimulator settings

Setting	Value
Output current	Nominally 20mA
Low level stimulation	20% of maximum output
Functional level	50% of maximum output

Table 7 – FES stimulator settings the 50% functional level reflected the standard operating procedure for the Pace stimulator used.

8.3.3 Treatment protocol

Movement type	Protocol
Volitional movement without stimulation	• Ensure that the electrode lead is connected to the test unit • Press '>' to active timing signal without any stimulation output • Start scope capturing • Ask the participant to make the limb movement

Volitional movement with stimulation	• Go into setup menu of the stimulator -> FURTHER SETTING -> TIMING MODE select 'No time out' exit menu • Set output to low level stimulation • Press TEST to activate timing signal and stimulation output • Start scope capturing • Watch display to see for the end of the rising ramp to show that the stimulation is up to full intensity • Ask the participant to make the movement
Non-volitional movement produced by the stimulation	• Go into setup menu -> FURTHER SETTING -> TIMING MODE select 'adaptive timing' exit menu • Set output to functional level stimulation • Start scope capturing • Press TEST to activate timing signal and stimulation output

Table 8 – Protocol for collecting readings for each of the treatments

8.3.4 **Data measurement**

Activity	**Protocol**
Collecting measurements	• Ensure that the Pico Technology oscilloscope is connected to the computer to enable the post filtering function for captured signals • Set the filter for Channel A to 20 kHz low pass • Set the filter for Channel B to 100 Hz low pass with x2 magnification • Enlarge view to include one burst of 20 kHz on Channel A and the subsequent goniometer reading on Channel B • Place both time rulers at the end of the of the burst, then using the delta reading position one of the time ruler at approximately 1ms in from the end of the burst inside of any switching noise. • Place the other time ruler at approximately 10ms ahead of the first cursor with the aim to produce a 10ms sample window that avoids any of the switching noise that maybe present at either end of the burst.
Taking measurements	• Channel A - ACRMS between the rulers with the waveform 20kHz low pass filtered • Channel B – use the cursor to read of the amplitude of the goniometer output at a point approximately 5ms after the end of the burst on Channel A
Analysing the measured data in Excel	• Set up the data in the following way; • Column A - Time values from 0 in 25ms steps

	• Column B - 20 kHz LP filtered values • Column C - Goniometer output

Table 9 – Measurement protocol

The protocol was applied to wrist movements made by the author with the stimulation electrodes positioned to produce functional movement (Figure 8).

8.4 Results

The results are presented as a comparison between ACRMS values and the goniometer output on a common time base, with values plotted at 25ms intervals. The ACRMS values are those of the voltage measured across the electrodes when the 20 kHz sine wave was being applied during the period between stimulation pulses.

The results for three treatments are shown for the wrist movements in Figure 53 to Figure 58.

- Voluntary movement of the limb with no electrical stimulation
- Voluntary movement of the limb with low-level electrical stimulation
- Involuntary movement evoked by functional electrical stimulation

The plots are presented in pairs for each of the treatments.

- The first plot in each pair shows the raw data.
- The second plot shows the same data after a 200ms moving average filter has been applied.

8.4.1 Movement about the wrist joint – volitional – no electrical stimulation

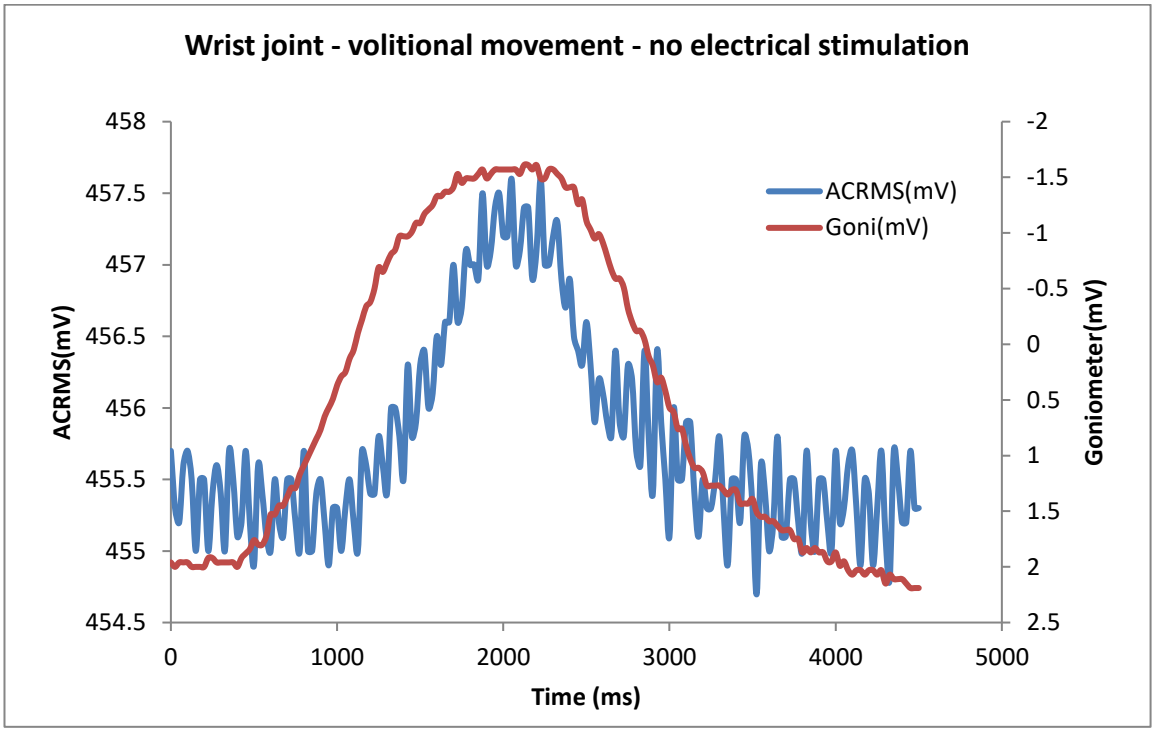

Figure 53 shows ACRMS of voltage across the measuring electrodes and the goniometer output readings on a common time base. Zero on the goniometer axis relates to the midway position as the joint between flexed and extended.

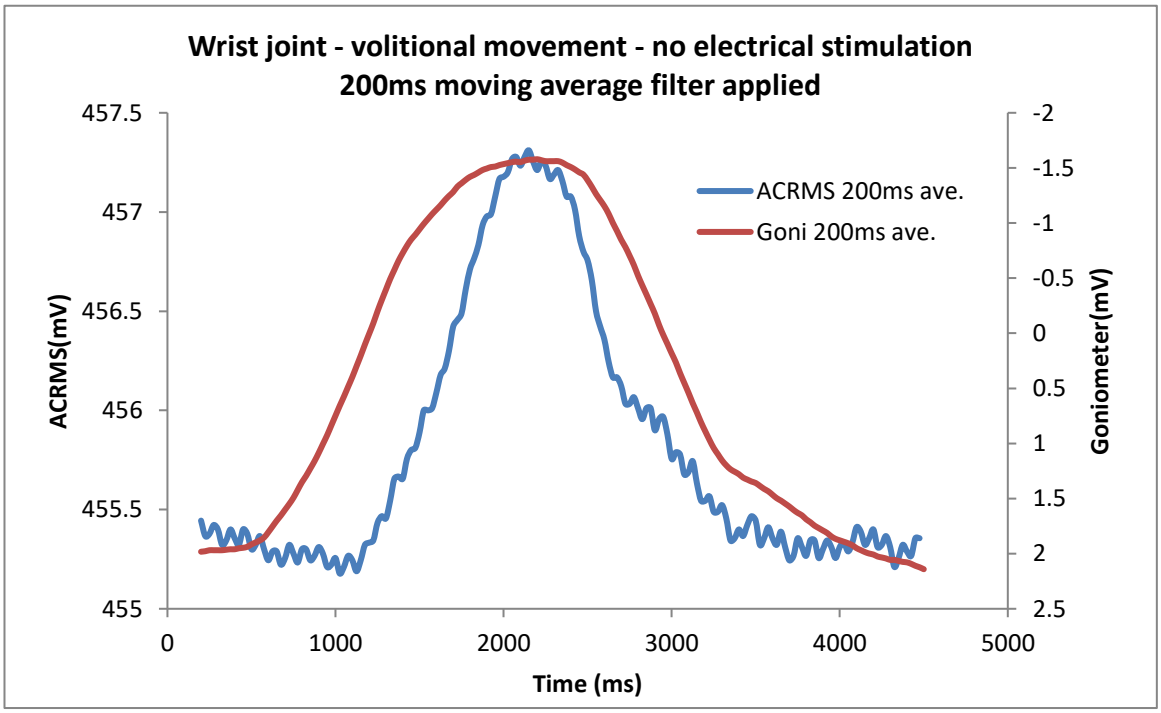

Figure 54 shows the same data as the previous plot but with a 200ms moving average filter applied

8.4.2 Movement about the wrist joint – volitional – constant low-level electrical stimulation

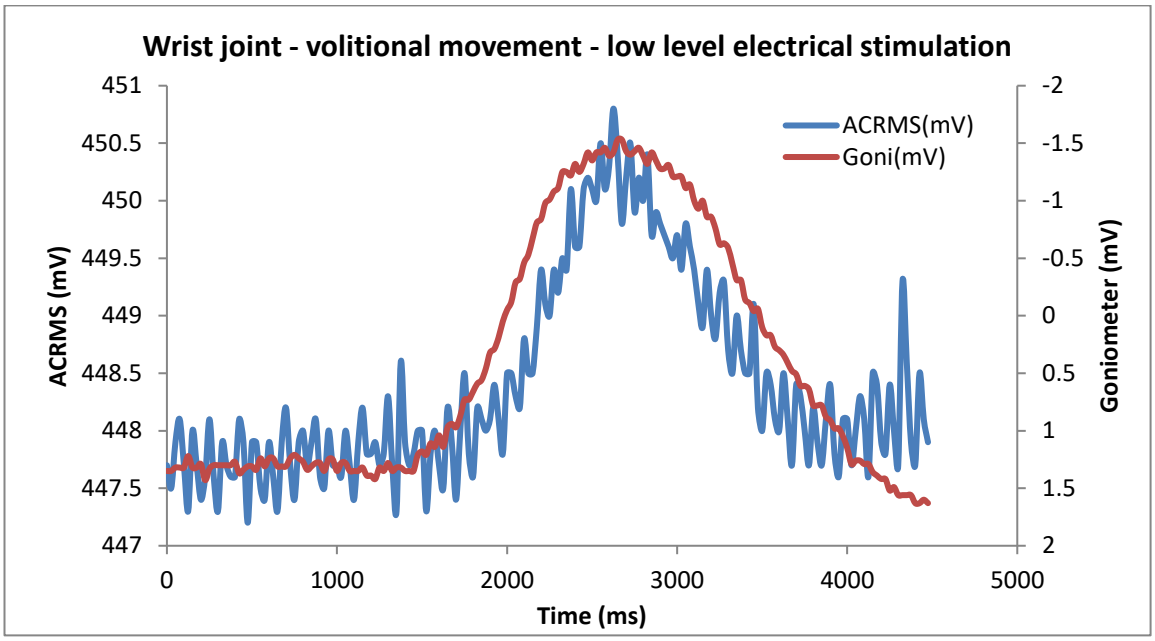

Figure 55 shows ACRMS of voltage across the measuring electrodes and the goniometer output readings on a common time base. Zero on the goniometer axis relates to the midway position as the joint between flexed and extended.

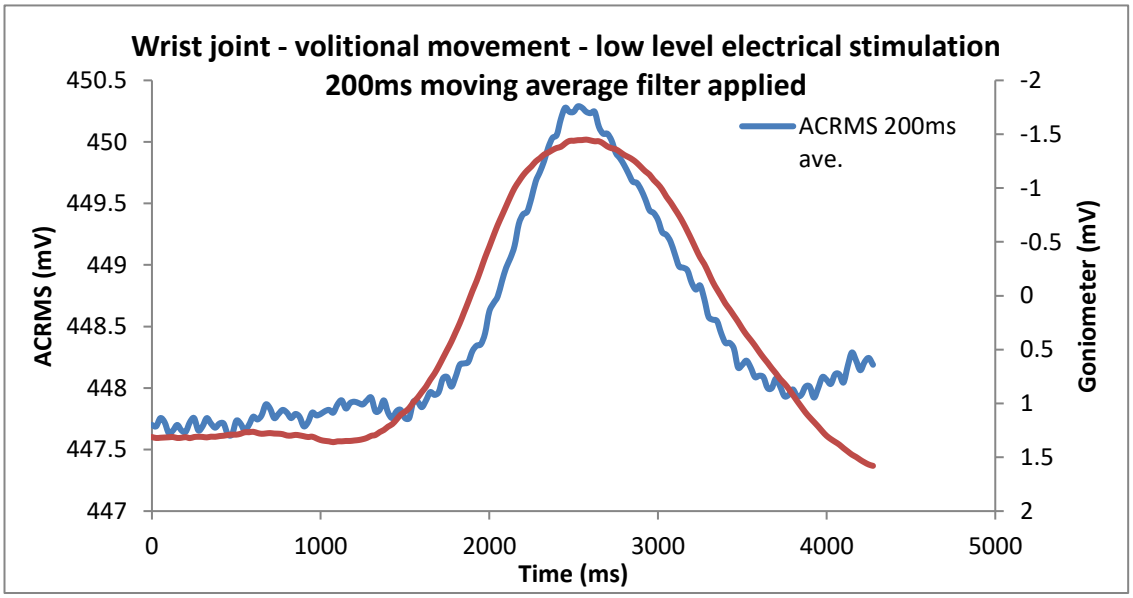

Figure 56 shows the same data as the previous plot but with a 200ms moving average filter applied

8.4.3 Movement about the wrist joint – involuntary – functional electrical stimulation

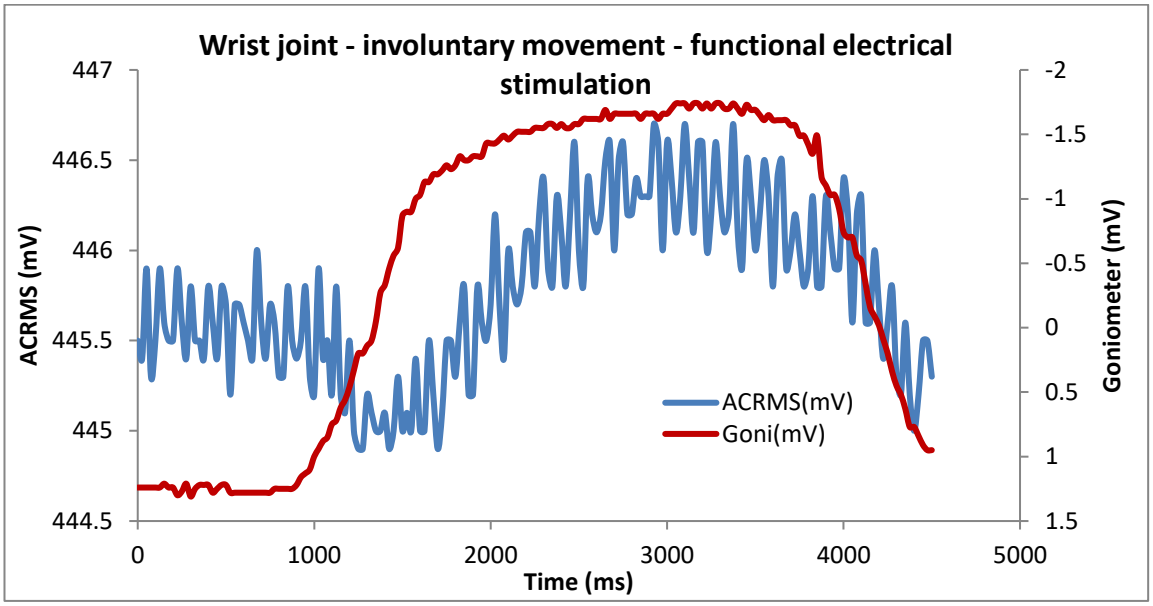

Figure 57 shows ACRMS of voltage across the measuring electrodes and the goniometer output readings on a common time base. Zero on the goniometer axis relates to the midway position as the joint between flexed and extended.

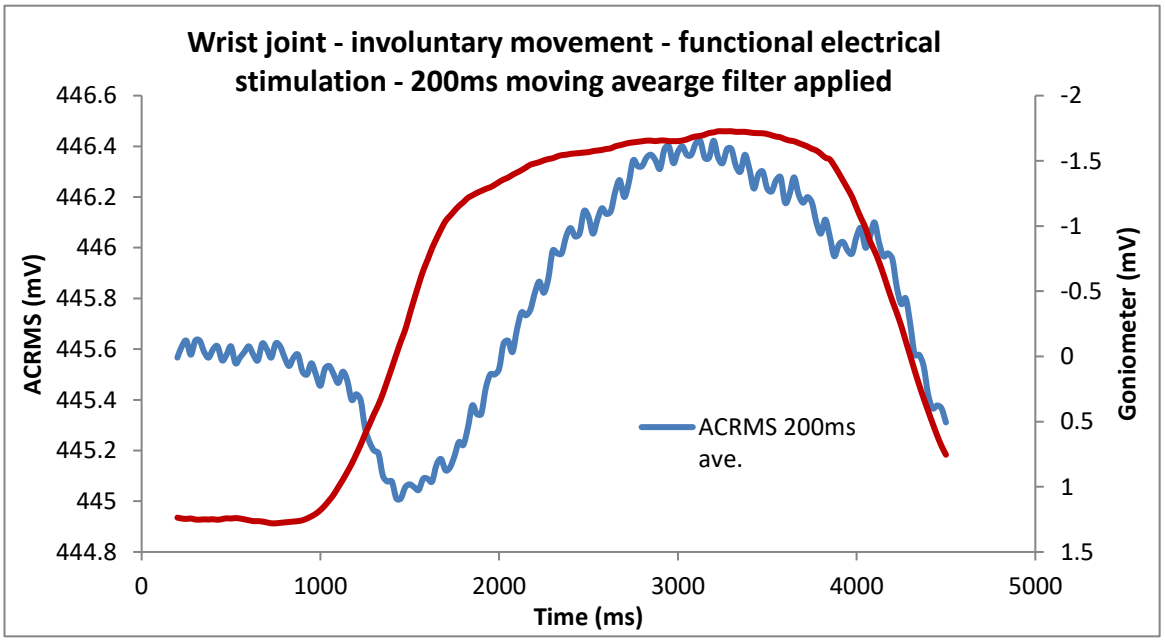

Figure 58 - shows the same data as the previous plot but with a 200ms moving average filter applied

8.5 Discussion

The results show a clear relationship between the impedance changes taking place within the tissue of the limb and the position of the limb about the joint as measured by the goniometer.

For the volitional wrist movement without electrical stimulation (Figure 53) the ACRMS plot is behind the goniometer as the wrist goes from flexed to extended, yet leads the goniometer plot as the joint returns. This is far less noticeable when low level constant electrical stimulation is applied (Figure 55). A possible explanation is that the stimulation may have caused 'pre-tensioning' to have occurred in the muscles. This does not explain why the ACRMS is lagging the goniometer when Functional levels of stimulation are involved (Figure 57). This movement was however involuntary, and so may have had little involvement from the antagonist muscles.

Of interest is the drop in the ACRMS that accompanies the onset of the FES between 1000ms and 1400ms of about 5mV. The peak that occurs at around 3000ms is also lower than peak voltage the previous FRES treatments by a similar amount of about 5mV. This suggests that the entire plot has been offset by about 5mV as a result of the FES reaching full intensity. This argument is supported by the upward flick at 4000ms which accords to the period when the FES was ramping down in intensity. The most likely explanation for this observation would be a small build-up of residual charge remaining in the tissue between the stimulation pulses. This charge has to dissipate during the inter-pulse period. When the delivered energy of the FES goes beyond the level at which there becomes insufficient time for it to fully dissipate during the finite inter-pulse period, any residual charge will remain. The AC sampling signal would then be superimposed onto this during the impedance measurement interval giving the offset result seen.

This offset represent a potential source of error if bioimpedance is to be used as a feedback signal to control FES. Solutions could be found to account for the effect by careful signal post-processing, but a better solution would be find a method to prevent any residual charge due to the FES from being able to building up.

8.6 Conclusions

The method of using a pair of electrodes that were common to the FES and to an AC signal used to measure the bio-impedance proved possible. The results produced were directly comparable to the previous method of using the EMG amplifier to measuring the amplitude of the refractory period, so it can be concluded that this method is at least as effective for determining a limb joint angle during movement resulting from electrical stimulation.

The method was compromised by an offset due to the influence of the FES as it built in intensity to a level needed to produce involuntary movement. A solution is need to overcome this problem, either by providing signal post-processing the account for the effect or more correctly by addressing the elements of the electric stimulator design that lead to the problem.

The results were obtained by manual processing of the captured data. For the method to be used for a practical ambulatory system an automated solution is required to provide real-time control.

Chapter 9: Hardware design for an integrated system capable of measuring Bioimpedance and delivering Functional Electrical Stimulation

9.1 Introduction

Having demonstration that measurements of tissue impedance could be made on a muscle group while it was being electrically stimulated, and that these measurement could be made through a common pair of electrodes, the need to refine the method was evident.

The objectives were;

- a reliable method of making repeatable measurements of the impedance
- an integrated electrical stimulator with full control over pulse timing and intensity
- goniometer measurement
- a robust method of isolating the impedance circuit from the stimulation voltage that introduced minimal artefact
- live data streaming for analysis on a PC

A new piece of test equipment was specified and designed to be capable of meeting these objectives. Each feature of the design was considered prior to final integration into a system.

9.2 Impedance measurement

The AD5933 Impedance converter (Analog Devices Inc.) shown in Figure 59 was identified as suitable device for making the impedance measurements. The AD5933 is a high precision impedance converter in a single integrated system-on-chip. It combines an on-board frequency generator with a 12-bit analogue-to-digital converter (ADC) capable of running at 1 mega samples per second. The frequency generator allows an unknown complex impedance to be excited with a known frequency. The response signal from the impedance is sampled by the on-board ADC and a discrete Fourier transform is processed by an on-board digital signal processing engine. The discrete Fourier transform algorithm returns the results of the impedance measurement as a pair of real and imaginary numbers. Communication to the device is via an I2C standard compliant bus. The AD5933 is targeted at bioelectrical applications and so is an ideal choice for this investigation.

9.2.1 Block diagram

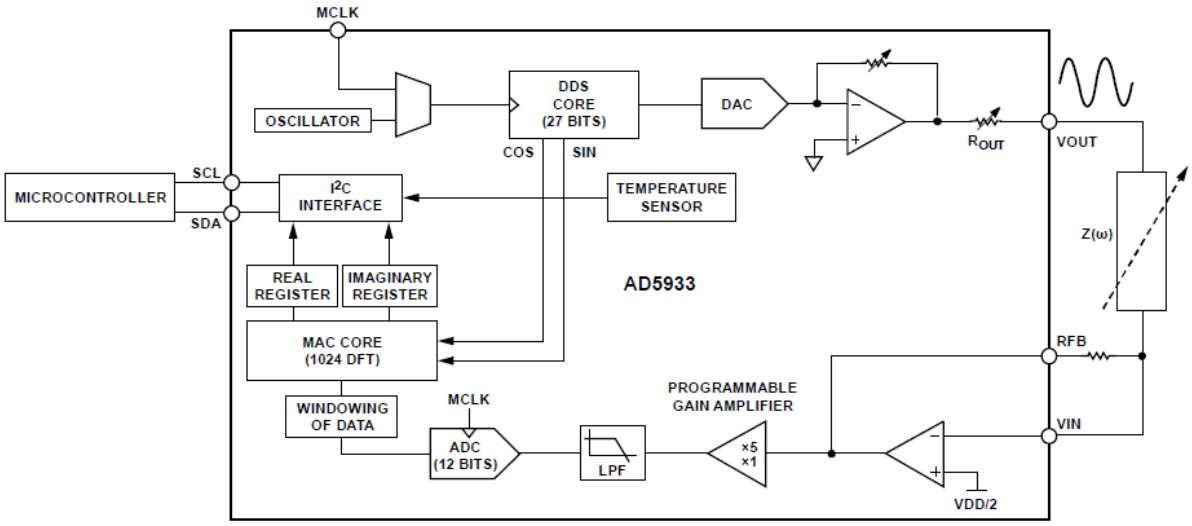

Figure 59 shows the block diagram for the AD5933 impedance measuring device manufactured by Analog Devices. This image was reproduced from the manufactures data sheet.

The frequency and amplitude of the excitation signal are controlled by writing to registers within the device. An internal oscillator or an external clock can be used to set the frequency, the internal oscillator was considered sufficiently accurate for this application and so was adopted. The frequency can be set from between 1 kHz to 100 kHz in 0.1 Hz step sizes. The output voltage has four selectable peak to peak settings available (Table 10). These are biased to ensure that the returning input signal sits within the rail voltages of the input operational amplifier.

Range	Output Excitation Voltage (V Peak to Peak)	Output VDC Bias Level
1	1.98	1.48
2	0.97	0.76
3	0.383	0.31
4	0.198	0.173

Table 10 – Shows the range of selectable voltage available for the AC excitation signal used for the impedance measurements, along with the DC offset voltage used to ensure that the signal remains within the rails of the input op-amp.

As well as being able to set the amplitude of the excitation signal there are two further methods of ensuring that the measured signal makes best use of the ADC range. A feedback resistor (RFB) can be used to fix the gain to the input stage (Figure 59). This is followed by a programmable gain

amplifier with the options of parity or five times gain. It is important that the ADC is allowed to work within the linear region of operation to ensure that saturation cannot occur.

Following each successful conversion of the impedance the results are stored into two registers for the real (R) and imaginary (I) parts of the complex form that can be accessed via the I2C communications.

These can be used to calculate;

$$Magnitude = \sqrt{R^2 + I^2}$$

$$Phase = tan^{-1}(I/R)$$

The magnitude calculated in this way must be further multiplied by a scaling factor before taking the reciprocal to arrive at the impedance value. The scaling factor is determined by calibrating the configured system using a known value of impedance.

$$Impedance = \frac{1}{Scaling\ factor \times magnitude}$$

9.3 Electrical stimulation

A flexible approach was needed in order to provide the maximum amount of adjustment to be able to integrate the stimulation generator with the impedance measurement system.

The meant that control was required for;

- the amplitude of the stimulation voltage
- the duration of the stimulation pulses
- the duration of the period between the pulses
- the polarity and form of the stimulation pulses

A full explanation of the relevance of these parameters is given in Appendix A.

The solution adopted used an inductor based boost switching regulator with settable output voltage via a programmable feedback resistor. Pulse timing was under the control of a microcontroller as was an output 'H' bridge that determined the polarity of the pulses as they were delivered.

An MCP1650 boost controller (Microchip Technology Inc.) was chosen for the switching regulator. The part was subjected to bench testing before being integrated into the final design circuit. The device proved capable of allowing voltages above 100V to be generated from a 5V supply.

The AD5245 digital potentiometer (Analog Devices Inc.) was selected for control of the feedback circuit to enable the output voltage to be set. This device has 256 positions which are selected by writing to the device via an I2C compatible communications bus.

The voltage generated by the switch mode boost regulator was stored in 5µF of capacitance before being switched through an 'H' bridge made from PHC2300 complimentary enhancement mode MOS transistors (NXP B.V.). These devices are able to easily withstand the stimulation voltage, can be controlled directly from the microcontroller and have acceptable turn on and turn off times. The typical combined turn on time is the fastest and least important. The typical turn off time is 53ns but can be as high as 65ns. Stimulation pulse durations are typically from 25 to 250µs, so it is only at the lower end of the pulse duration range that the turn off time begins to matter making around 0.25% of a difference that might need to be to be accounted for.

9.4 Goniometer measurement

The goniometer was powered from a stable 5V supply with the voltage returned in the range of 0 to 4.99V. This was read by the ADC of the microcontroller. An 8 bit resolution was used for the ADC and the goniometer was calibrated from 20^0 to 270^0 giving a working resolution of very slightly better than 1 step per degree.

9.5 Isolation of the impedance measuring circuit from the stimulation voltages

The impedance measurement circuit and the electrical stimulation circuit share a common connection to the skin contact electrodes. The AD5933 used in the impedance measurement circuit needs to be isolated from the electrodes to protect it during the period while the stimulation voltage is being applied. To provide this isolation ASSR-401C solid state relays (Avago Technologies) were selected. These devices are able to withstand up to 400V and can be rapidly switched on and off in under 1ms. They also have low on-resistance and output capacitances and so have little influence on the impedance measurement circuit.

9.6 Data streaming

The microcontroller was provided with a link to a PC via a USB to UART cable (FTDI Ltd.) enabling serial communication between the microcontroller and the PC running a terminal programme (Figure 60). A simple numeric menu was written for the microcontroller so that the stimulation and impedance measurement parameters could be remotely set from the PC. During data capture the goniometer angle and impedance were written out as coma separated values to a text file on the PC.

9.7 System block diagram

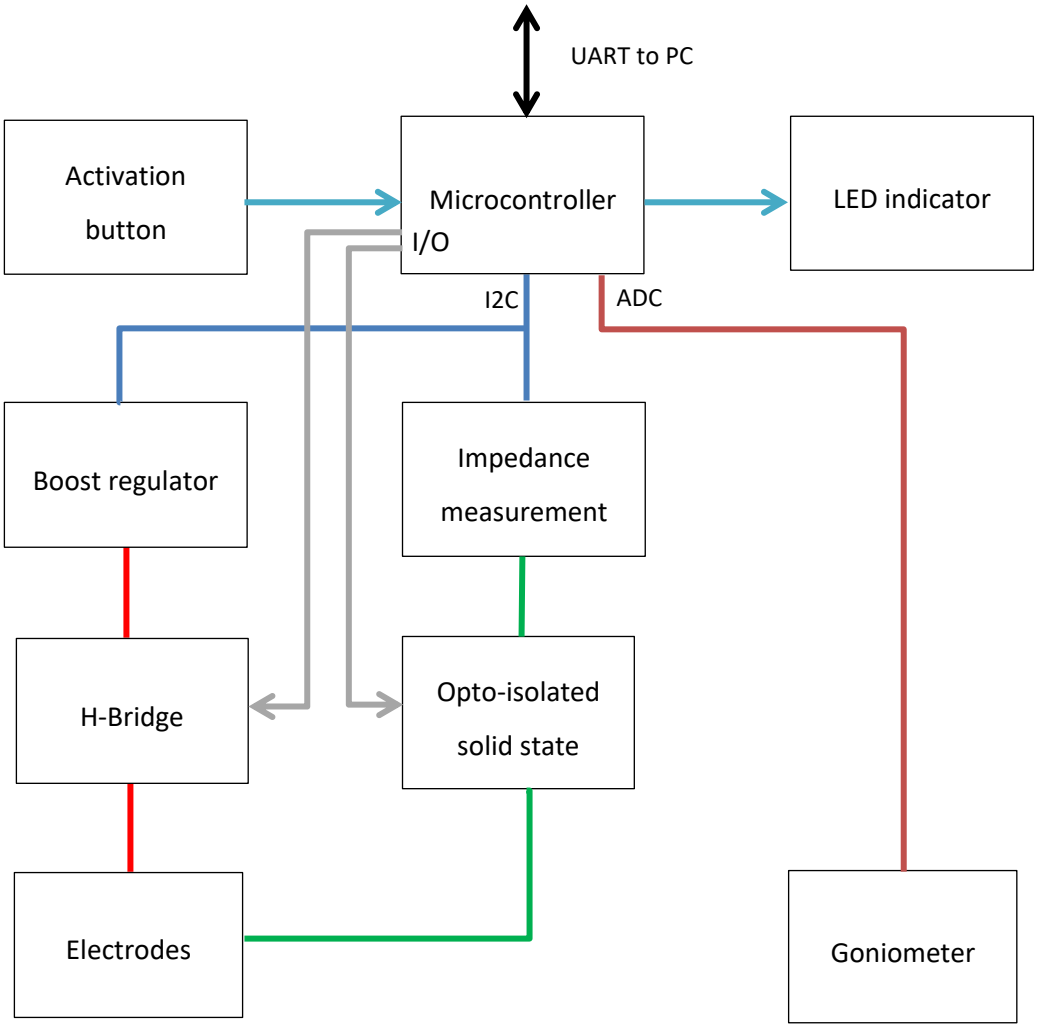

Figure 60 shows the block diagram for the integrated Bioimpedance measurement and FES system with provision to read from a goniometer.

In addition to capturing the output data the UART connection to the PC was also used to access an operating menu running on the microcontroller. This menu enables the set up registers of the AD5933 impedance converter to be initialised with the parameters for the impedance excitation voltage frequency and amplitude with values inputted via the PC. The menu also allowed the output voltage setting of the boost regulator to be adjusted and enabled.

Two operating modes were implemented. The first of these makes repeated impedance and goniometer readings and reports these out continuously over the UART as a coma separated pair on a common time base. The second mode does the same functions but now includes the electrical stimulation. After choosing this option from the menu the stimulation it is started by pressing an activation button and will continue for as long as the button remains held down. The goniometer angle and impedance value are reported as before.

The circuit diagrams and layout for the integrated bioimpedance and FES system are shown in Appendix B. The code listing for the microcontroller firmware is shown in Appendix C.

9.8 Stimulator output voltage testing and calibration

It was necessary to test and record the output voltage from the boost regulator in response to changes to the value of the digital potentiometer in the feedback path.

With the board powered from a stable 5V supply and the boost regulator enabled the value written into the memory of the digital potentiometer was steadily increased and the resulting voltage recorded shown in Table 11.

Register value	Output voltage
0x10	10.1
0x20	10.7
0x30	11.3
0x40	12.1
0x50	13.0
0x60	14.0
0x70	15.4
0x80	17.0
0x90	19.1
0xA0	22.0
0xB0	25.9
0xC0	31.6
0xD0	41.0
0xE0	58.8
0xF0	62.9

Table 11 – The output voltages from the MCP1650 boost regulator circuit in response to the register values loaded into the AD5245 digital potentiometer

The output voltage followed an exponential progression such that at start up when the wiper of the digital potentiometer defaults to the mid-way point a safe default voltage of around 17V was produced.

9.9 Impedance measuring system

The impedance measuring sub-system that was based upon the AD5933 and shown in Figure 60 required calibrating before being used. To do this an impedance of known values was needed. A circuit based on the simplified Shiffman tissue model (Shiffmann, et al., 2008) was chosen for the calibration. This is the circuit that is routinely used within the field of impedance myography.

The use of the AD5933 impedance measuring device enabled a choice of excitation frequency up to 100 kHz. The implications of this were that the reasons for choosing an excitation frequency of 20 kHz for the previous investigation could be revisited. 20 kHz had been selected because it gave an acceptably similar result to the higher frequencies but had more appropriate power implication for an ambulatory device. Now that the excitation frequency was a function of the system-on-chip device this was much less of a consideration. Returning to the previous bioimpedance result shown in Figure 48 on page 125 it can be seen that the 40 kHz excitation frequency resulted in the most linear plot. Moreover referring to Table 4 on page 125 the difference between the peak voltages across the range of the movement were 11mV for the 20 and 30 kHz frequencies and 14 and 15 mV for the 40 and 50 kHz frequencies. The shows that the relative difference in peak voltage was greater at the higher frequencies and therefore more indicative of the impedance changes influencing them. An excitation frequency of 40 kHz was selected for the further impedance measurements for this next part of the research. The 50 kHz frequency was not selected over 40 kHz as it offered little additional benefit in terms of peak voltage difference and had produced a less linear results.

The selected 40 kHz frequency also sits between the alpha and beta dispersions described in Chapter 7:Bioimpedance and so is unaffected by these regions.

9.9.1 **Calibration**

Calibration was carried out using the simplified Shiffman tissue model which consists of a 1kΩ resistor in parallel with a 100nF capacitor.

From $$Z = \frac{1}{\sqrt{\left(\frac{1}{R}\right)^2 + (\omega C)^2}}$$

At the chosen circuit excitation of 40 kHz

where $R = 1 \times 10^3 \Omega$

and $C = 100 \times 10^{-9} F$

$Z = 39.757 \Omega$

The impedance of the Shiffman model circuit was measured and the correction factor set to provide the correct calibration. Following calibration the impedance of the circuit was tested initially without a stimulation voltage present between each measurement (Figure 61). The test was then repeated with a 40V stimulation pulse of 200µs duration applied across the circuit between each impedance measurement (Figure 62).

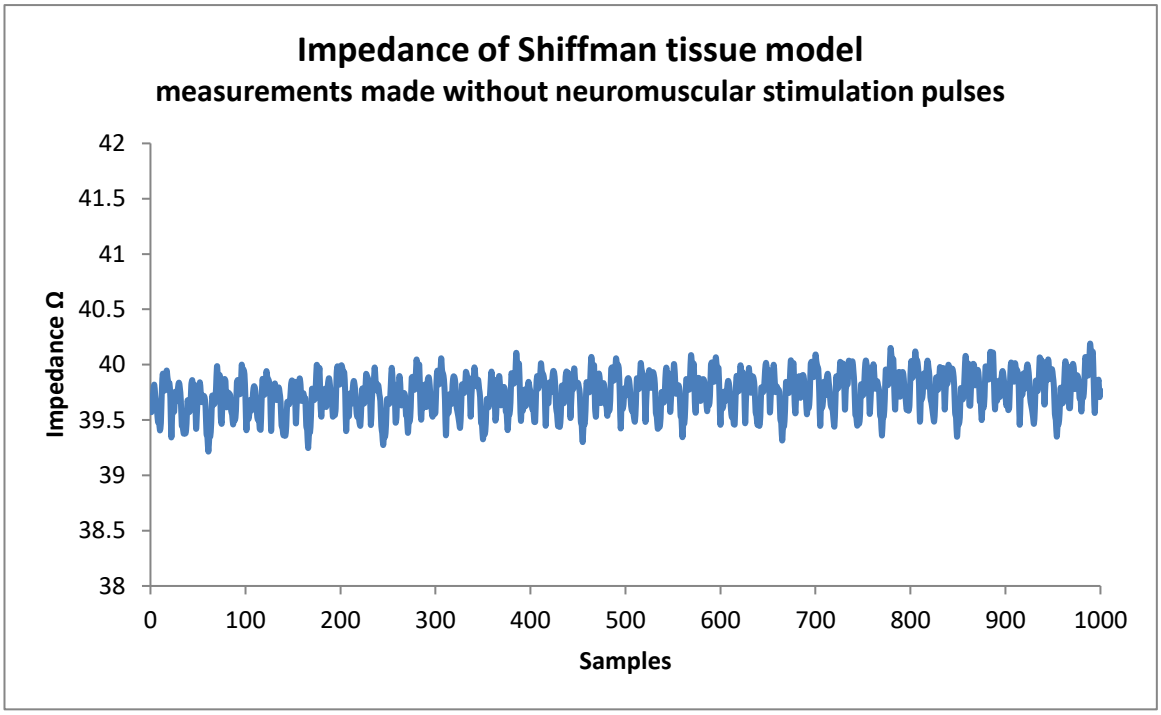

Figure 61 shows a plot for 1000 reading made from a Shiffman tissue model circuit using a 40 kHz excitation frequency.

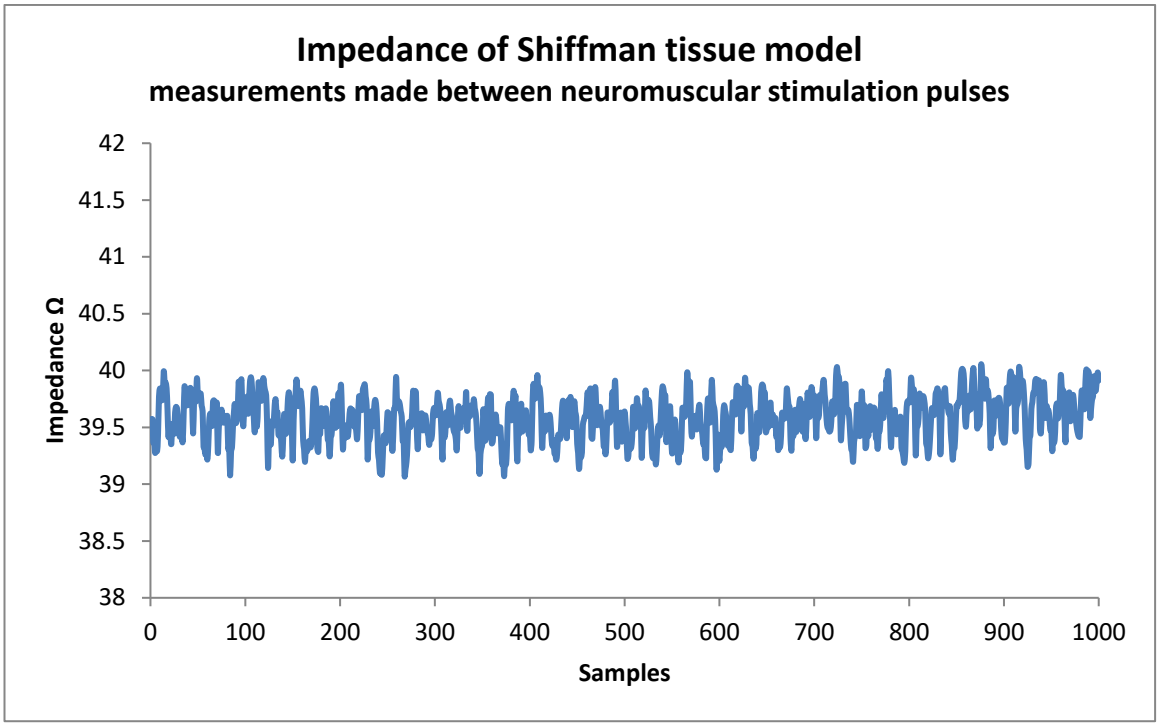

Figure 62 shows the plots for a 1000 reading made from the same Shiffman tissue model with the reading made between 40V stimulation pulses applied to the same model.

9.9.2 Selecting a sampling strategy

The data sheet for the AD5933 impedance converter integrated circuit recommends that to improve the accuracy of the conversion process repeated reading are taken and the average determined. The drawback is that each repeated read takes additional time. As the time available between the neuromuscular stimulation pulses is not indefinite it was important to understand and optimise the best strategy for averaging the impedance readings.

9.9.3 Single reading and conversion

This method took a single reading upon which the conversion to calculate the impedance was made. One thousand data points were measured for the impedance in this way and the results plotted. The frequency distribution for the data was is shown as a histogram (Figure 63).

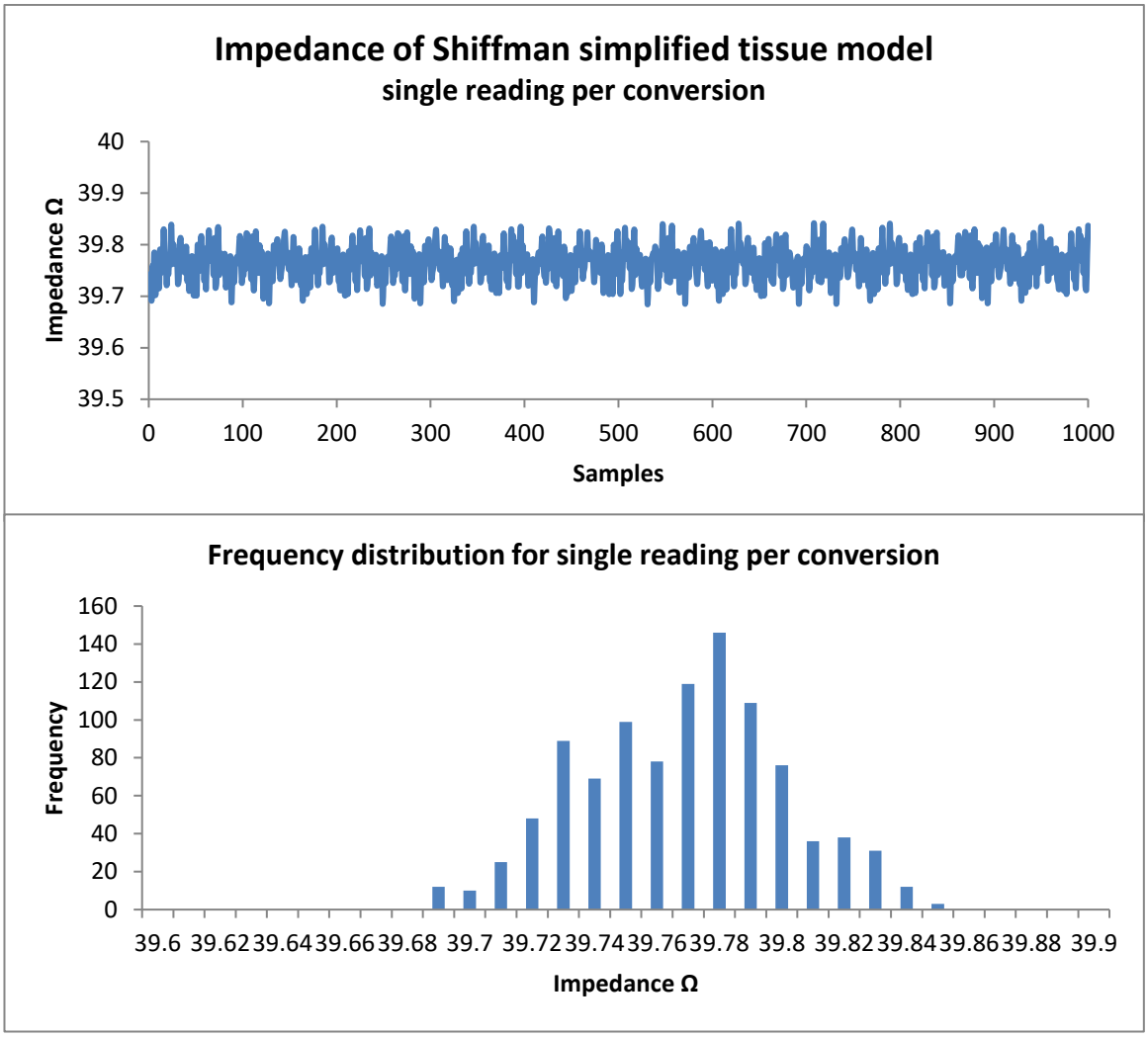

Figure 63 shows the plots for 1000 single readings of the impedance without averaging with the distribution of the converted values shown in the histogram

9.9.4 Five repeated readings and conversion

This method took 5 concurrent reading and determined their average upon which the conversion to calculate the impedance was made. One thousand data points were measured for the impedance in this way and the results plotted. The frequency distribution for the data was is shown as a histogram (Figure 64).

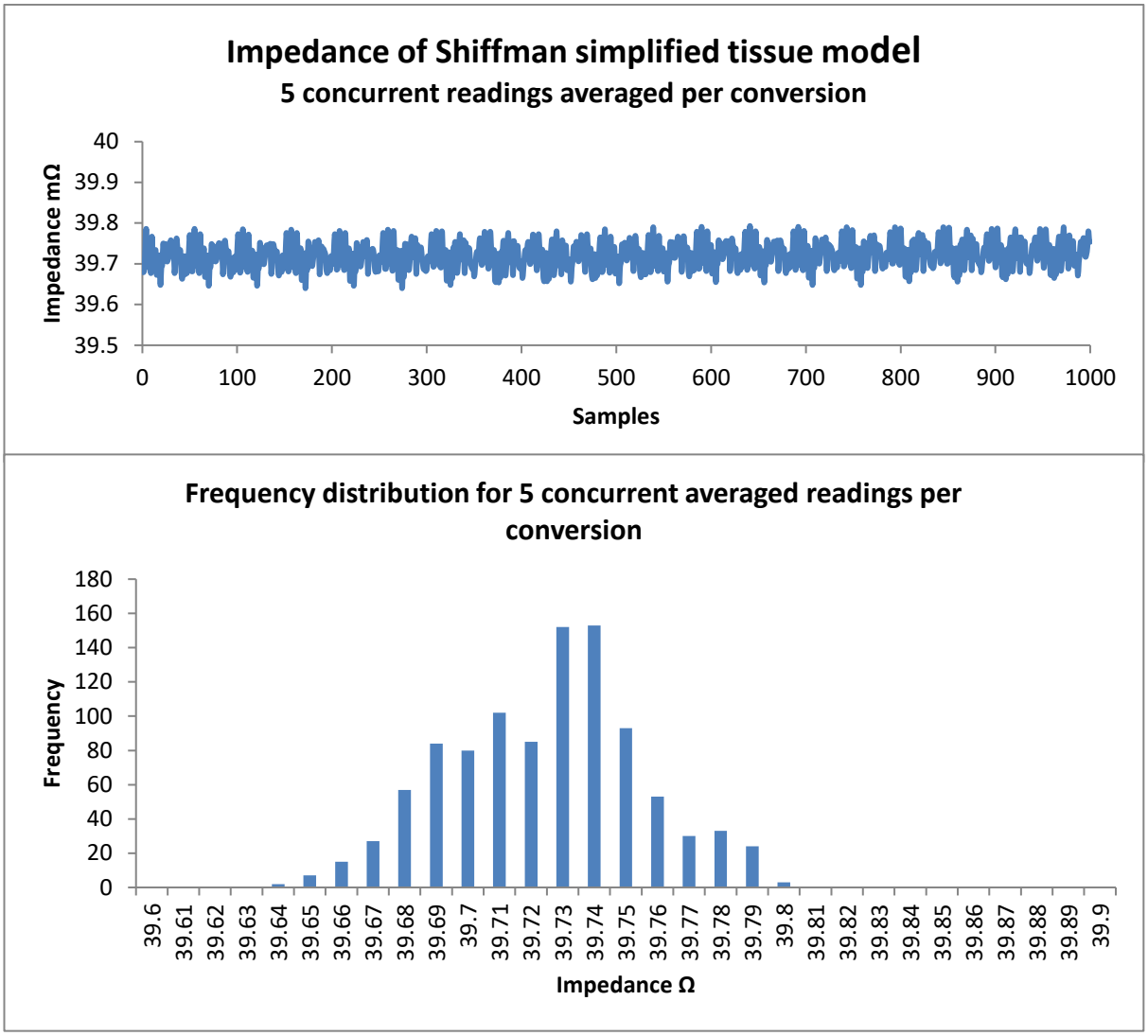

Figure 64 shows the plots for 1000 data points from 5 readings that were averaged of the impedance, the distribution of the converted values are shown in the histogram

9.9.5 Twenty five repeated readings and conversion

This method took 25 concurrent reading and determined their average upon which the conversion to calculate the impedance was made. One thousand data points were measured for the impedance in this way and the results plotted. The frequency distribution for the data was is shown as a histogram (Figure 65).

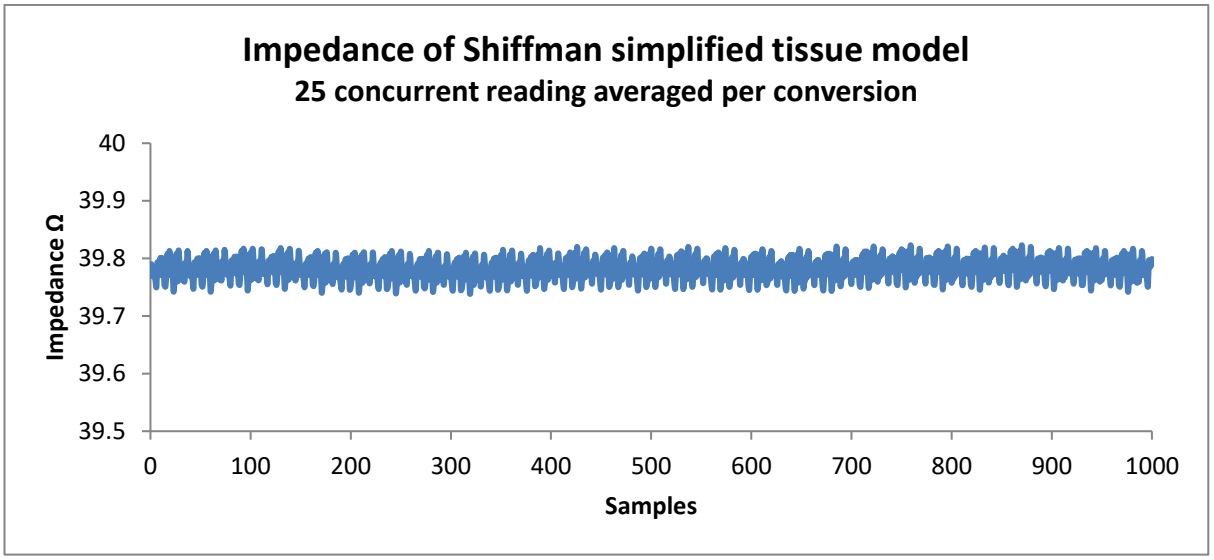

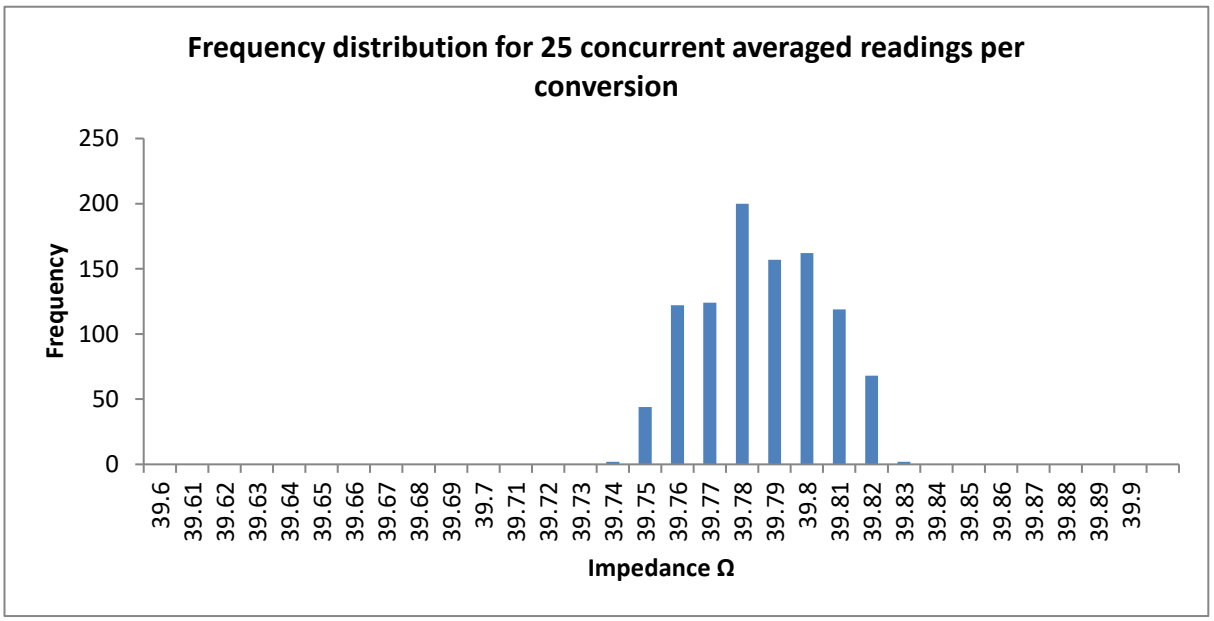

Figure 65 shows the plots for 1000 data points from 25 readings that were averaged of the impedance, the distribution of the converted values are shown in the histogram

9.9.6 Five repeated readings and conversion with additional filtering

This method took 5 concurrent reading and determined their average upon which the conversion to calculate the impedance was made. The results of the impedance calculation were then passed to a five-term moving average filter. One thousand data points were measured for the impedance in this way and the results plotted. The frequency distribution for the data was is shown as a histogram.

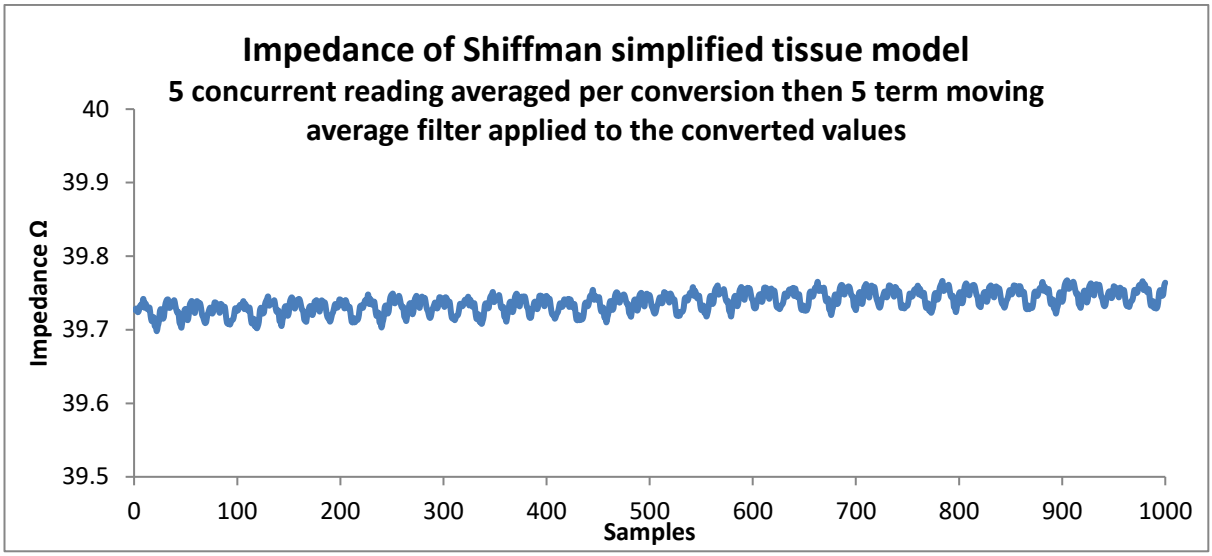

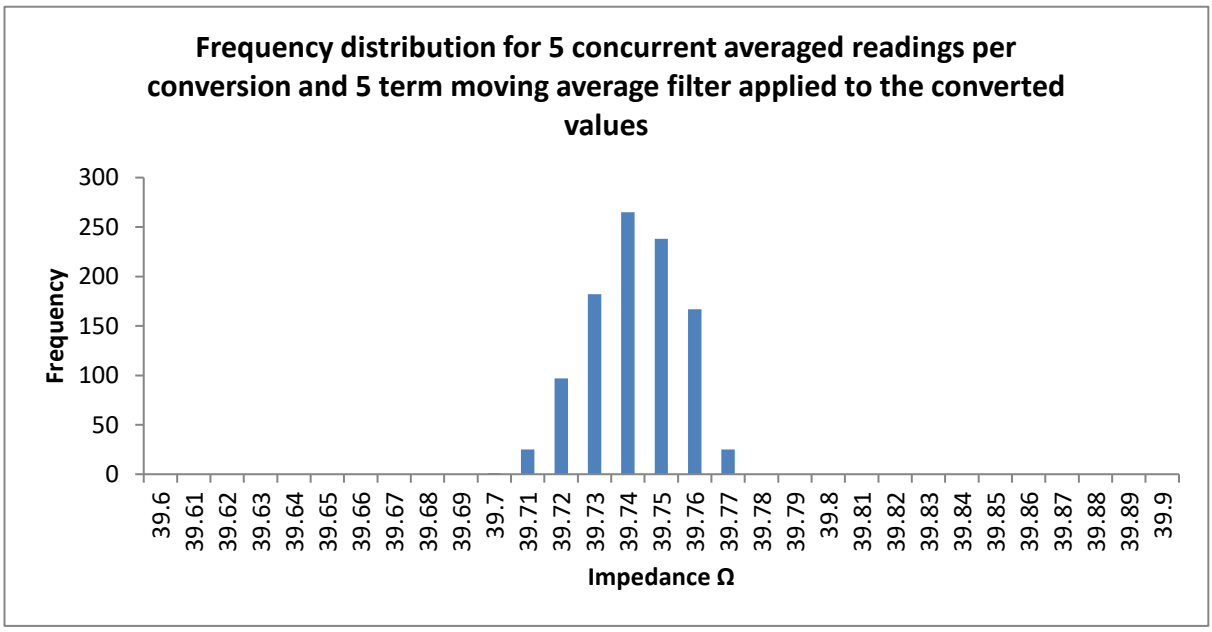

Figure 66 shows the plots for 1000 data points from 5 readings that were averaged of the impedance before an additional five-term moving average filter was applied, the distribution of the converted values are shown in the histogram

9.9.7 **Discussion**

The single read and conversion is the fastest method at approximately 3.5ms and can easily be completed within the interval between neuromuscular stimulation pulses. However it is also the least precise with the reading across a wide spread (Figure 63).

The five readings averaged method does little to improve the spread but does concentrate more of the values into the centre region (Figure 64). The time needed for the measurements and

conversion is approximately 17.5ms and so is still practical for use with FES running at a frequency of 20Hz.

The twenty five reading averaged method addresses the spread producing a much tighter concentration of the results from the impedance calculations (Figure 65). However as the method takes approximately 87.5ms per conversion result it is too slow to be used with FES.

The final method makes use of the five readings averaged method which has the effect of concentrating the values about the centre when compared to the single read method. The FES stimulation is delivered between each the blocks of five reads and so can comfortably run at 20Hz. The five-read averaged impedance values are then further filtered using an infinite impulse response digital filter that behaves similar to a 5 term moving average filter (Figure 66). The output of the method offers results comparable to the twenty five readings averaged method and achieves it over five 50ms stimulation cycles totalling 250ms. The method has a reduced rate of response when compared to the 87.5ms of the 25 read averaging method but will produce acceptable results while allowing stimulation at a rate necessary for effective FES.

9.10 Conclusion

Each of the individual parts of the system was shown to be effective. The electrical stimulation voltage pump was capable of producing voltages of a sufficient level for upper-limb FES. The output switching H-bridge was able to switch quickly enough with a calculated pulse duration of comfortably less than 1% across the entire range. The impedance measuring circuit could be isolated from the electrical stimulation voltage. Readings from the goniometer could be made with these and the impedance calculations steamed in real-time to a PC for offline analysis.

When run together the integrated electrical stimulation and impedance measuring system is able to make impedance measurements from a calibration circuit while the same circuit was being subjected to functional levels of electrical stimulation.

The accuracy of the impedance readings can be improved by taking multiple reading between the stimulation pulses. However these repeated readings introduce unacceptable amounts of latency when the go above 5 reading. 25 reading was shown to produce very good results but was far too slow for use with effective FES. A multiple of 5 readings only produces a small advantage over a single reading. But when multiples of 5 readings are made and these are then averaged over 5 of pulses 25 readings can be included into the smoothing calculation. This method offers the ability to run the neuromuscular stimulation at a frequency necessary for FES with the pulses delivered

between the each block of 5 impedance readings. It was anticipated that the small latency penalty introduced by this method would be acceptable.

Chapter 10: Impedance measurements and FES

10.1 Introduction

The objectives for this part of the work was broken down into three parts.

- An investigation into the effectiveness of the impedance measurement system when used with conventional FES skin contact electrodes. With these electrodes positioned correctly for achieving functional movement when used with FES.
- An investigation into the ability to obtain useful measurements of bioimpedance while neuromuscular electrical stimulation is being applied through the same pair of electrodes. Initially looking at voluntary movement with low levels of stimulation and then at functional levels able to produce involuntary movement.
- An investigation into the use of the results obtained in the second investigation to establish parameters for a control strategy capable of limiting the extent of movement in response to the measured impedance change.

10.2 Bio-impedance measured using conventionally FES electrodes

The first part of this investigation measured the impedance of the wrist extensor muscles with the wrist supported and held stationary. A period for the measurement was chosen to be similar to the time needed for making the dynamic measurement in the second part of the investigation. The objective was to find out how reliably bioimpedance measurement could be made using conventionally functionally poisoned conventional FES electrode.

The second part of the investigation used the same electrodes unaltered form the first part of the investigation to measure the impedance during repeated voluntary wrist movements. These movement were measured using a goniometer on a similar time-base for comparison.

The objective was to find out how well any changes in impedance related to the movement.

10.2.1 Bioimpedance measurement made with the wrist joint held stationary

10.2.1.1 Method

Conventional FES electrodes (Axelgaard Manufacturing Co. Ltd. – product code CF5000) were placed on the forearm over the extensor carpi longus and brevis muscles in a position to produce wrist extension when electrical stimulation was applied (Figure 8 page 63).

The forearm was supported with the wrist resting in a neutral position midway between flexed and extended. The impedance across the electrodes was measured with the wrist was held stationary. One thousand measurements were recorded over a period of 50 seconds.

10.2.1.2 Results

The impedance measurements were plotted against time, shown in Figure 67. Despite the wrist remaining stationary the impedance varied within a range of 2Ω over the period of the measurements.

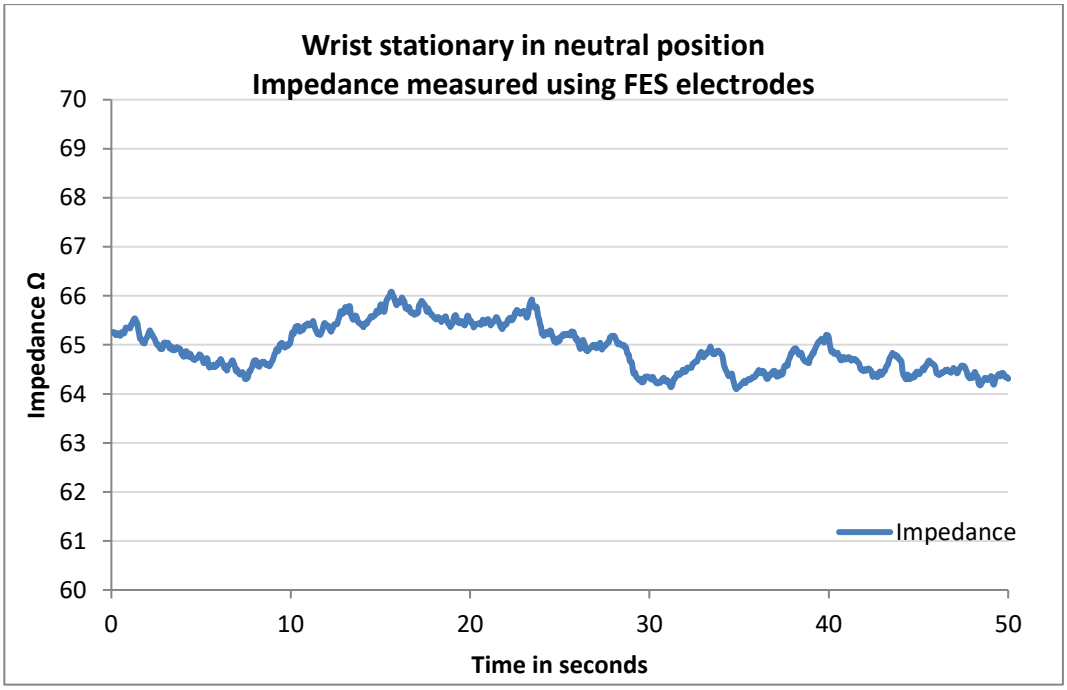

Figure 67 shows the impedance across the FES electrodes applied to the forearm while the limb remained still with the wrist in a neutral position. The impedance measured is the combined impedance of the tissue and the electrodes. The impedance varied within a range of 2Ω over a 50s period.

10.2.1.3 **Discussion**

The investigation showed the variation in the bioimpedance over a period of 50s. This is similar to the time that would be needed to make the series of voluntary movements planned for the next part of the investigation. The results establish a baseline for comparison purposes.

The impedance plot for the stationary wrist joint shows a variability in the impedance as measured across the electrodes even when the joint is held at rest (Figure 67). The measured values varies within a 2Ω range of between 64Ω and 66Ω over the 50s period. This would further support the previous conclusion drawn in section 7.4 Bioimpedance on Page 126 that this type of 2 electrode method measurement may not be suitable as an absolute measurement to determine joint angle.

10.2.2 **Bioimpedance measurements of voluntary wrist movements**

10.2.2.1 **Method**

The electrodes and placement used in 10.2.1.1 where retained and a goniometer was fitted across the wrist joint. The impedance between the electrodes measured while the wrist was volitionally moved over a number of repetitions within a range of fully flexed and fully extended.

Goniometer and bioimpedance readings were streamed to a PC for analysis.

10.2.2.2 **Results**

The goniometer angle is shown of the left y-axis and the impedance on the right y-axis, both have been plotted against time.

On the goniometer axis 240^0 relates to fully flexed and 140^0 relates to fully extended, the neutral position occurs at 180^0.

The reciprocal wrist movements produced a sinusoidal plot from the goniometer.

The sinusoidal goniometer plot has been overlaid on the impedance plot showing to show any relationship between changes in impedance to the movement (Figure 68). It does not show a close relationship between the measured bioimpedance and the repeated movement pattern recorded by the goniometer.

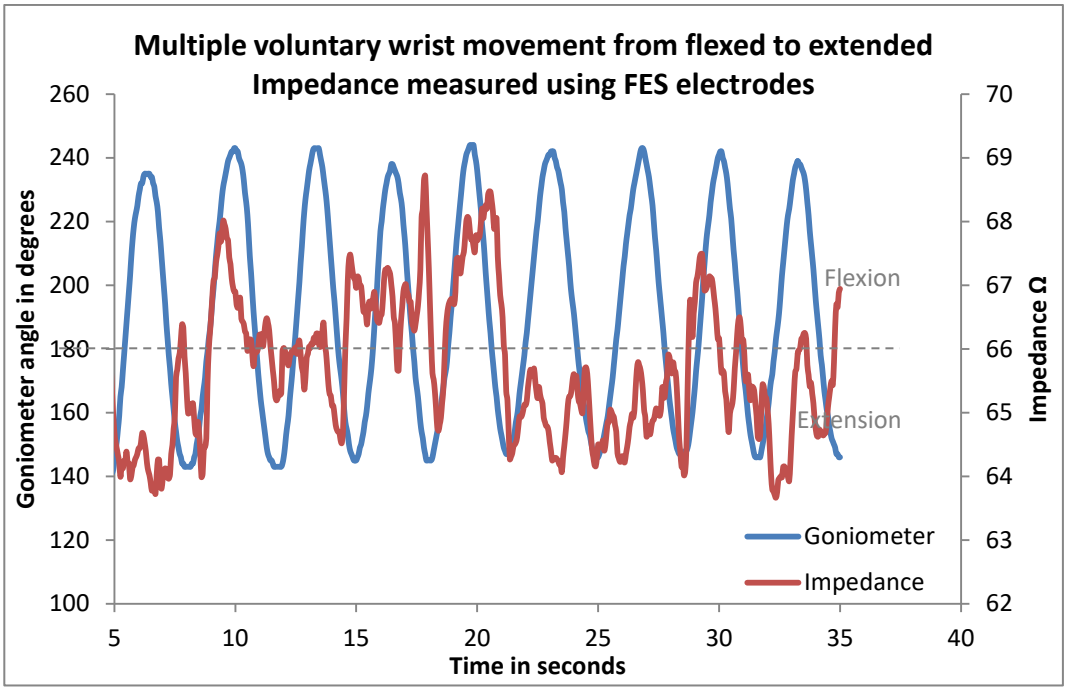

Figure 68 shows the measured impedance overlaid on the goniometer plots for a number of repetitive wrist movements from extension into flexion and back. The plot for the impedance changes shows some relationship to the movement recorded by the goniometer.

10.2.3 **Discussion**

When the plot for the dynamic joint is studied (Figure 68) it can be seen that the range limits of the impedance is increased in both direction from 63.5Ω to 69Ω giving a range of 5.5Ω. It is uncertain from these results whether the 2Ω variation seen in the stationary measurements (Figure 67) is evident in the dynamic measurements but the increase in range implies that the movement is having an influence.

The rapid changes in the impedance plot (Figure 68) show some relationship to the changes of movement captured by the goniometer. In that the direction changes produce peaks and troughs in the bioimpedance plot. However although the joint is passing through the same range of movement repeatedly, the pattern for the impedance for the same place in the movement is not regular between each cycle of the movement. The dynamic measurements further confirms the unreliability of this type of impedance measurement as an absolute determinant of the joint angle for voluntary movement.

10.3 Bioimpedance measurement of voluntary movement with low levels of stimulation

This next investigation looked at impedance measurements made across the electrodes while electrical stimulation was being applied. With the measurements of the bioimpedance being made during the period between the stimulation pulses. The electrical stimulation was applied at 20Hz with a pulse duration of 175µs.

For the investigation an amplitude of 20V was used for the stimulation. This level induced a small amount of force from the stimulated extensor muscles which was sufficient to apply a low level of torque about the wrist and served to tighten these muscles. The resulting light muscle tension was noticeable but easily overcome to allow voluntary movement about the wrist.

The objectives for the investigation were to establish the effectiveness of measuring bioimpedance while electrically stimulating, and to see if tensioning of the actuating muscles made any effect on the dynamic measurements.

10.3.1 **Method**

The electrodes and placement used in 10.2.1.1 where retained along with the goniometer fitted across the wrist joint in 10.2.2.1.

The electrical stimulation was applied at frequency of 20 Hz with a pulse duration of 175µs and amplitude of 20V.

The impedance between the electrodes was then measured while the wrist was volitionally moved over a number of repetitions within a range of fully flexed and fully extended. 240^0 relates to fully flexed and 140^0 relates to fully extended, the neutral position occurs at 180^0.

Goniometer and bioimpedance readings were streamed to a PC for analysis.

10.3.2 **Results**

The goniometer angle is shown of the left y-axis and the impedance on the right y-axis, both have been plotted against time.

On the goniometer axis 240^0 relates to fully flexed and 140^0 relates to fully extended, the neutral position occurs at 180^0.

The reciprocal wrist movements produced a sinusoidal plot from the goniometer.

The sinusoidal goniometer plot has been overlaid on the impedance plot showing to show any relationship between changes in impedance to the movement (Figure 69). The measured bioimpedance has range limits of approximately 62.25Ω and 64.25Ω giving a range of 2Ω. The light tensioning of the muscles from the electrical stimulation produced a closer relationship of the bioimpedance to the dynamic measurements than for the unstimulated results in the previous investigation. By inspection repeated maxima can be related to event in the repeated movement as the wrist goes form flexed to extended, and from extended to flexed.

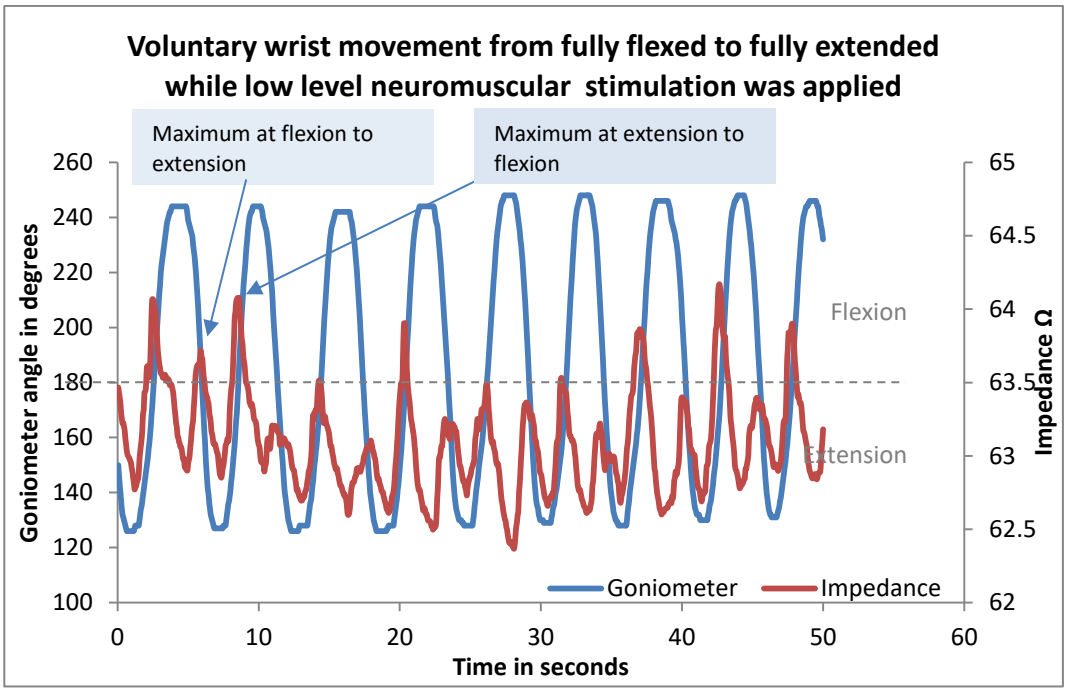

Figure 69 shows the measured impedance overlaid on the goniometer plots for a number of volitional repetitive wrist movements from extension into flexion and back while low levels of electrical stimulation is being applied. The stimulation is holding the extensor muscles partially tightened. The impedance changes relate to the changes in muscle length for the movement captured by the goniometer.

10.3.3 **Discussion**

When a comparison of the bioimpedance measurements of the voluntary movements is made between the unstimulated in Figure 68 and with low levels of stimulation in Figure 69 a number of things become apparent. The overall range of the measurements has reduced from 5.5Ω to 2Ω, this can be explained by the reduced the variability that is evident within the plot. The impedance shows a much closer relation to the movement for the movement with the low level

stimulation. For example when looking at Figure 69 the plot for the movements show minima when the wrist is either fully flexed or fully extended. There are maxima as the wrist moves towards extension from flexion. These peaks coincide with the wrist crossing the neutral point. There are complimentary maxima as the wrist crosses the neutral point again for the extension to flexion movement. The absolute values for these minima and maxima vary between cycles of the repeated movement and so cannot directly be used as threshold to determine limb position. However by following the sequence of the minima and maxima it would be possible to track progress through the movement.

The electrical stimulation by holding the muscles in light tension improves the relationship between the bioimpedance measurements and the dynamic movement. The reason might be due to reducing the influence of any initially slack elements within the tissue.

10.4 Bioimpedance measurement of involuntary movement with functional levels of stimulation

For this investigation the electrical stimulation was increased to functional levels where the resulting movements were involuntary.

The previous investigations had revealed by inspection an identifiable relationship between bioimpedance and the limb movement. So that the strength of this relationship could be measured one hundred repetitions of the stimulated involuntary movement were made, sufficient for statistical analysis.

10.4.1 **Method**

The electrodes and placement used in 10.2.1.1 where retained along with the goniometer fitted across the wrist joint in 10.2.2.1.

The forearm was horizontally supported and the wrist allowed to rest in a flexed position under the effect of gravity.

The stimulation was delivered at 20Hz with a pulse duration of 200µs and 40V amplitude. Stimulation was commenced by pressing and holding down an activation button on the stimulator unit. The stimulation was stopped by releasing the activation button after the wrist had reached fully extended. Between each repetition the wrist was allowed to return to rest in the flexed position under the influence of gravity. The approximate duration from the start of a repetition to commencing the next was 8s.

The goniometer was used to measure the rotation about the wrist joint from fully flexed to fully extended for each repetition of the movement. Goniometer and bioimpedance readings were streamed to a PC for the period when the stimulation was active meaning that only the flexion to extension part of the movement was recorded. This is the part of the movement of most interest for clinical application of the control of FES.

10.4.2 **Results**

The plot shown in Figure 70 and Figure 71 have the goniometer angle on the left y-axis and the impedance on the right y-axis, with both plotted against time. On the goniometer axis 240^0 relates to fully flexed and 140^0 relates to fully extended, the neutral position occurs at 180^0.

The plots in Figure 70 shows all of the 100 repetitions. The goniometer plot in blue has very little variation across the start of each of the curves at the top, showing that the starting point for each repetition when the wrist had returned to flexion was consistent over the movements. The ends of the curves at the bottom show greater variability across the repetitions. Recording stopped when the button controlling the stimulation was released. The differences seen are due to variability with when the button was released for each repetition. The bioimpedance curves in red are by inspection mainly of similar proportion. There is a ripple of drift of approximately 1Ω magnitude that is underlying the measurement of the individual repetitions. The bioimpedance can be seen to move down over the first 50s from starting the involuntary movement repetitions.

The plots in Figure 71 shows ten of the repetitions of the sequence in Figure 70 in expanded detail. The features of the bioimpedance curves can now be seen. In each case the bioimpedance reduces with a rapid slope downwards as the stimulated limb is moved away from the flexed position. When the wrist is approaching the neutral position the bioimpedance curve turns and starts to climb. The bioimpedance curve turns once more just after the neutral point has been passed. All of the curves show these characteristics although some show more fluctuation around the turning points than others.

The occurrence of the first minima after the initial downward slope were looked at in more detail. The value of the bioimpedance at these minima were extracted from the data and then compared to the wrist joint angle at the time when they occurred. The results of the statistical analysis of these first minima is set out in Table 12.

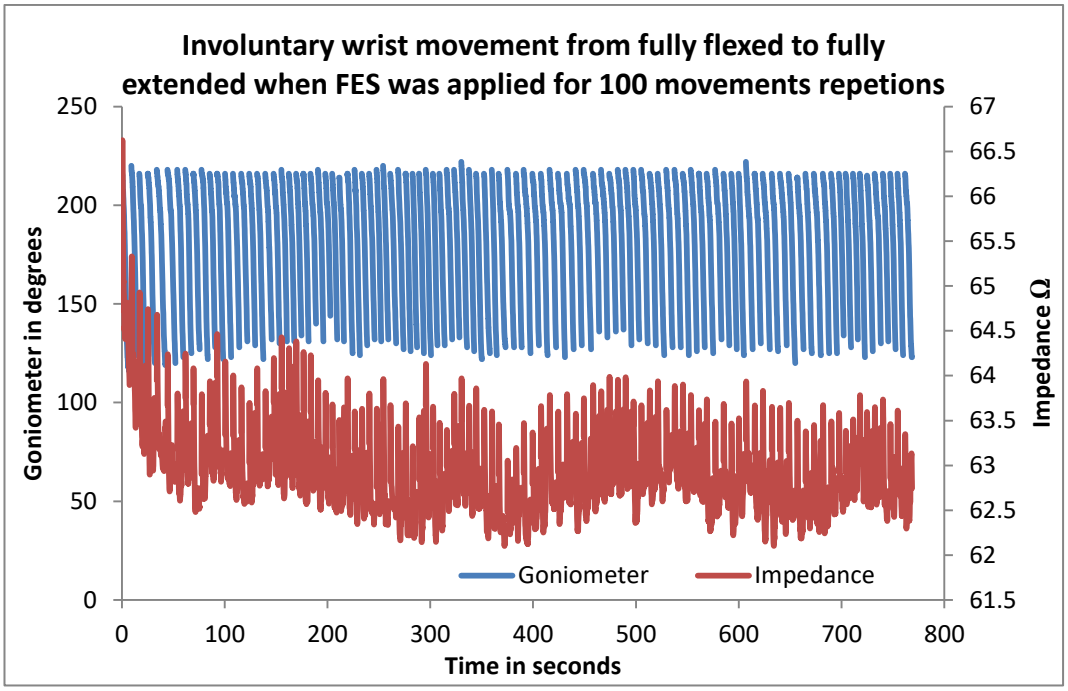

Figure 70 Impedance and Goniometer plots for 100 repetitions. The impedance can be seen to drift down over the initial 50s before varying within a 1Ω range for the remaining repetitions of the involuntary movement.

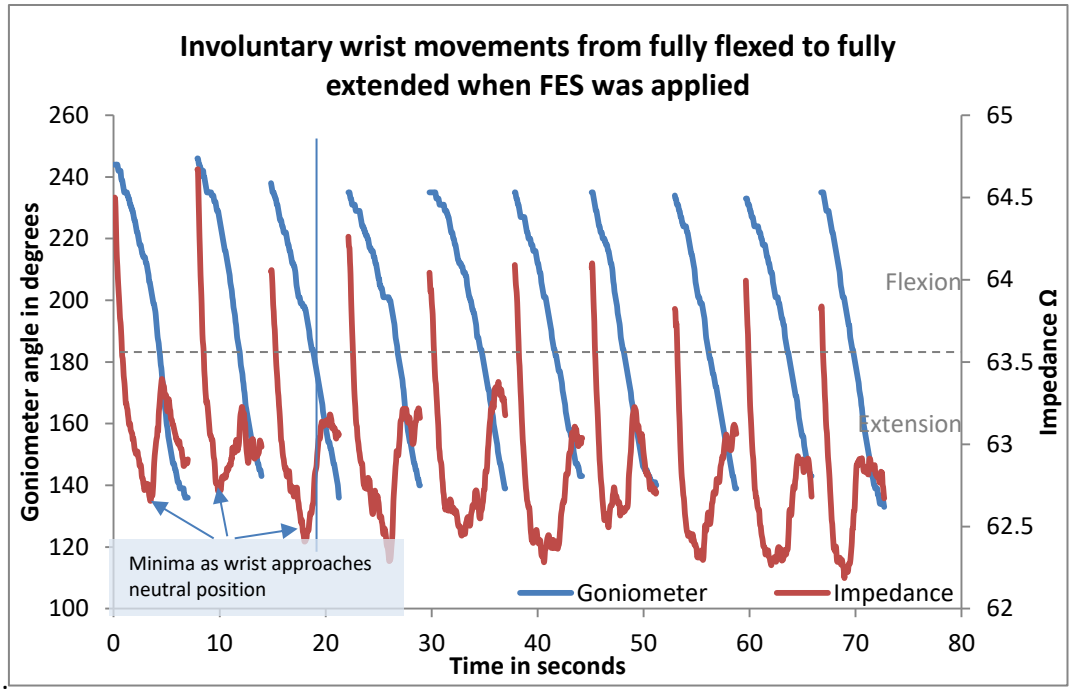

Figure 71 shows the impedance overlaid on the goniometer plot for wrist movements evoked using FES. For each of the repeated movements the impedance shows minima as the wrist approached the mid-way neutral point.

Statistical analysis of first minima in the bioimpedance curves related to the wrist joint angle at the time at which they occurred	
Minimum	186^0
Maximum	212^0
Range	26^0
Mean	201.12^0
Median	202^0
Mode	205^0
Standard Deviation	5.431^0
Sample Variance	29.495^{0^2}
Kurtosis	0.176
Skewness	-0.556
Correlation to measured impedance	
Correlation between Impedance and angle	0.29

Table 12 Statistical analysis of the minima of the first turning point in each of the bioimpedance measurement with respect to the angle they occurred at measured by the goinimeter.

The results of the statistical analysis show a very poor correlation between the absolute value of the bioimpedance at the time of the minima and the joint angle at the time when they occurred.

The joint angles relating to the minima all fell within a 26^0 range. The standard deviation shows that most of these were with the range of 206.6^0 to 195.7^0. The skewness and kurtosis suggest that the minima tend toward the lower angles and that the distribution is spread in this direction. The histogram plot in Figure 72 confirms this. The histogram was calculated using a 1^0 bin size, being the best resolution of the data possible. The spike in the plot that can be observed at 190^0 accounts for the negative skewness and positive kurtosis results.

The scatter plot in Figure 73 shows the angle that the wrist joint had reached when the minima in the bioimpedance curve occurred plotted against the bioimpedance values at the time, for all 100 repetitions of the stimulated involuntary movement. The plot show a tight clustering either side of the 201^0 mean value, as the standard deviation had indicated. The few outliers to the right of the main cluster relate to readings made during the initial 50s settling period, these also lay close to the 201^0 mean value.

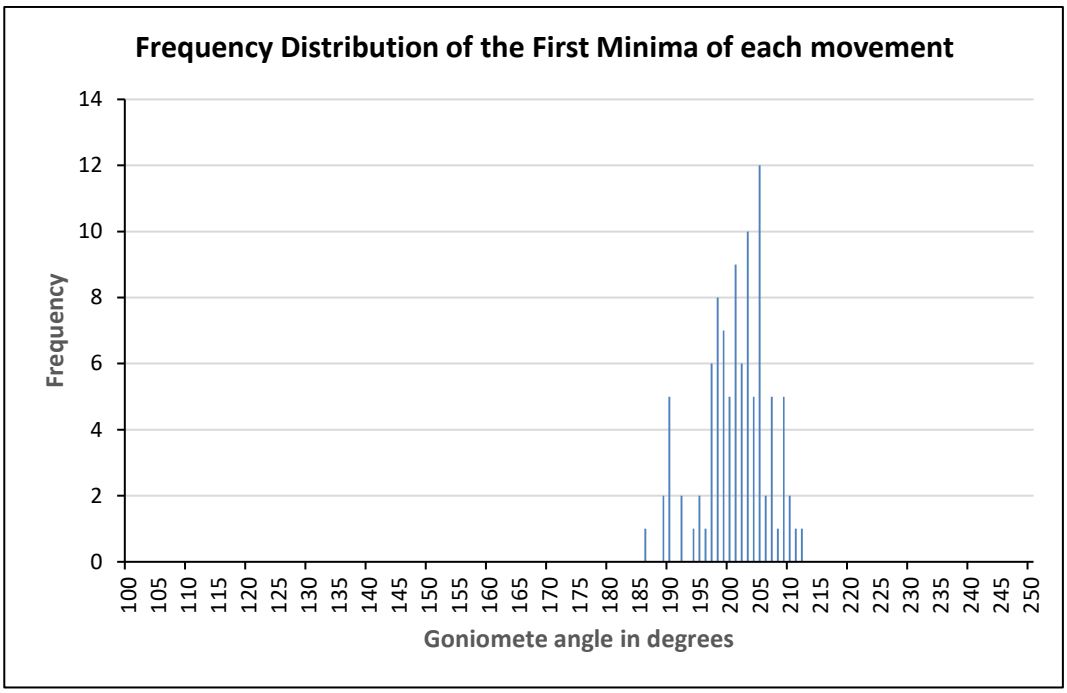

Figure 72. Histogram showing the frequency distribution of the wrist joint angle at the time of the first minima in the bioimpedance curves for a data set of 100 repetition of the stimulated involuntary limb movement.

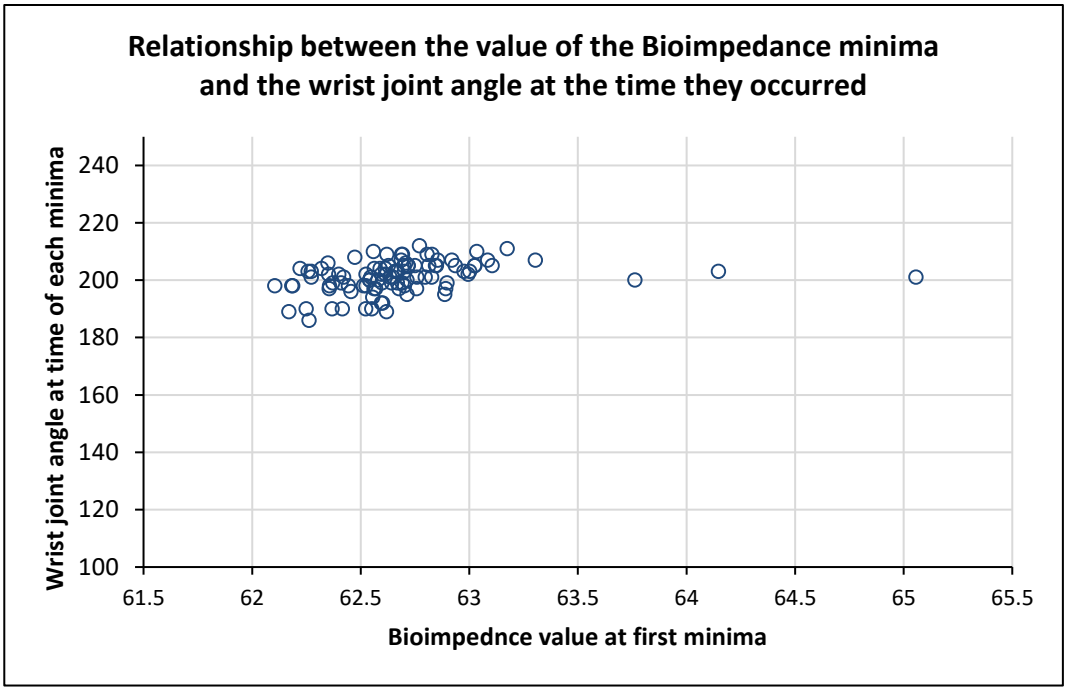

Figure 73. Scatter plot showing the angle at which the first minima occurred in each bioimpedance measurement for each repetition, plotted against the bioimpedance value at those minima. The plot show results for 100 successive involuntary stimulated wrist movements.

10.4.3 **Discussion**

Looking the results for the 100 involuntary stimulated movements shown in Figure 70 there are two previously identified features to discuss.

The downward settling of the bioimpedance over the first 50s after starting covering the first 6 repetitions of the movement. The effects of tissue charging as identified as a probable cause of an offset in section 8.5 on page 142 can be discounted here. The design of the stimulator that was used in that part of the research, and which directly contributed to the effect, had been replaced for this investigation with a design that specifically avoided the problem. Moreover the intervals between the repetitions which repeated every 8s would have given ample time for any such residual charge to dissipate. Which would suggest that the effects were due to physiological changes taking place over the period. It is outside of the scope to investigate within this research but a likely explanation would be the effects of adenosine triphosphate (ATP) and phosphocreatine (PC) as part of the ATP – PC system. ATP is the biochemical way the body stores energy for immediate use at the onset of movement. There are a number of stages in the processes of the ATP system. Put simply, ATP is initially found in the myosin cross-bridges which are the contractile parts of muscle. Upon recruitment of the muscle the ATP is broken down to release energy so that the muscle is able to contract. This produces ATP by-products of adenosine diphosphate (ADP) and phosphate (Pi). In the next stage of the process phosphocreatine (PC) is broken down by a combination of enzyme activity and the newly released Pi from the first stage. This releases more energy which allows the ADP and Pi to re-join and form more ATP which can then be broken down to release energy to supply the muscle. The ATP – PC system provides instant energy at the onset of exercise. During heavy exercise this system can be become depleted within 10 to 20s. For the relatively gentle effort the limb developed during the trial to ATP – PC system could reasonably have been expected to extend beyond 20s. The changes in the bioimpedance over the first 6 repetitions of the movement could have been due to changes in the ATP stored in the contractile tissue of the muscle affecting the conductance of the tissue.

The second previously identified feature was the underlying ripple that affected the relative positions of the bioimpedance curves. This ripple bares similarity to the base-line measurements shown in Figure 67 on page 160 and so probably results for similar reasons. It is also likely to have contributed to the poor correlation between the absolute impedance values and the joint angle given in Table 12.

The expanded plot segment shown in Figure 71 gives greater detail on the shape of the bioimpedance curves. The profiles of these curves share important similar characteristics that make it possible to determine when the wrist joint is approaching the neutral position. The significance of this was explained in section 3.2.1 on page 61 showing the importance of the wrist being in a neutral position before beginning to extend the fingers to avoid hyperextension. From the results the first minima can be used as an identifier that the wrist is will be at 200^0 plus or minus 50, that is to say somewhere between 25^0 and 15^0 before the neutral position is reached (180^0). The histogram in Figure 72 and scatter plot in Figure 73 reveal more information about these minima that invite further discussion.

The spike which occurs at 190^0 in Figure 72 is contributed to by 5 of the 100 repetitions which makes it interesting. When these five reading are looked at greater detail by expanding the cluster for that region within the scatter plot shown in Figure 73 the results are as shown below in Figure 74. The red circle drawn onto the plot identifies all of the minima that are associated with spike and it can be seen that they all fall just outside of the main cluster. This suggests that this spike might be due to a separate population of data that relates to a different muscle group to the ones being directly stimulated. If this is the case it not necessarily a surprising result as there are many muscles in that part of the arm which could have been involved within the conduction path for the impedance measuring signal. It would also have contributed to the poor correlation.

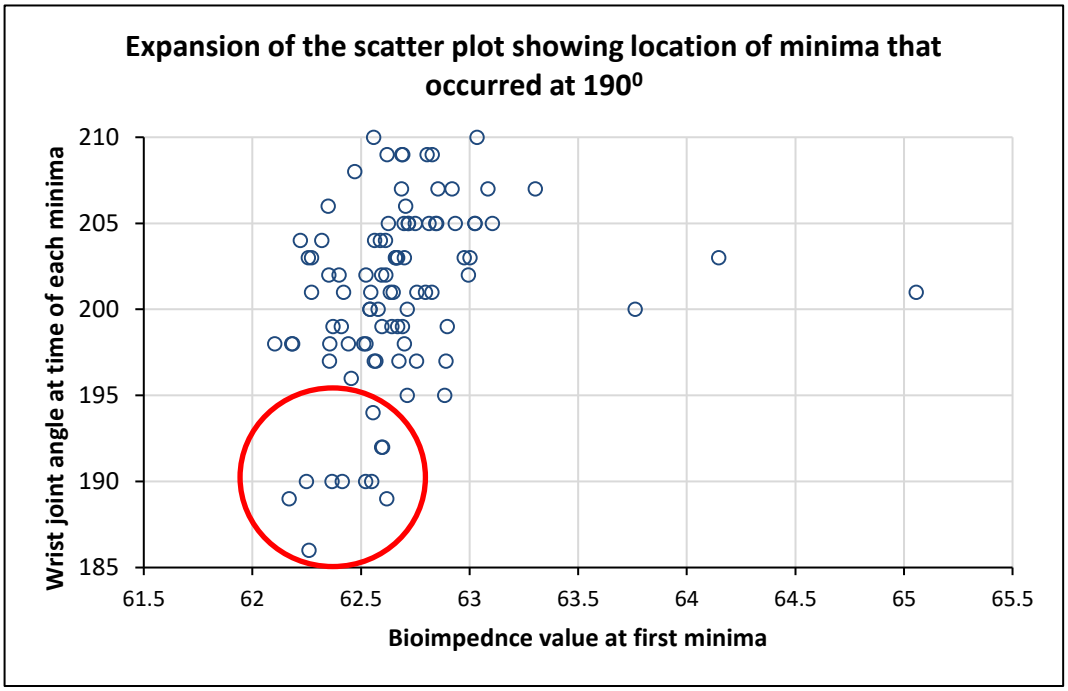

Figure 74 showing the scatter plot for the wrist joint angle against bioimpedance values for the region around 190^0 in detail. Five minima occurred at this angle and all can be found to the lower end of the impedance range of the cluster.

A feature previously identified in the scatter plot in Figure 73 are the outliers to the right of the main cluster. These all relate to the minima form the bioimpedance curves form the first few repetitions during the initial 50s from beginning. The argument was put forward above that the ATP – PC system could have contributed to this increase in impedance at the start. The significant thing to notice is that despite the elevated impedance the minima all occur close to the mean value for the cluster. The implication is that the first minima remains useful as an indication of the wrist approaching the neutral position under these conditions.

As has already been said in the discussion for early sections of this chapter, when comparing Figure 69 and Figure 71 the measurements for the impedance while stimulating it is apparent that the range of the measurements has reduced. The range sits within the 2Ω band seen for the limb at rest in Figure 67. At the same time the variability has also reduced meaning that the impedance now has closer relation to the movement. For example when looking at the plot for the voluntary movements in Figure 69 the plot for the movements show minima when the wrist is either fully flexed or fully extended. There are maxima as the wrist moves towards extension from flexion. These peaks coincide with the wrist crossing the neutral point. There are complimentary maxima as the wrist crosses the neutral point again for the extension to flexion movement. The absolute values for these minima and maxima vary between cycles of the repeated movement and so cannot directly be used as threshold to determine limb position. However by tracking the sequence of the minima and maxima it would be possible to track progress through the movement.

There are a number of possible explanations as to why the impedance shows a clearer relationship to the movement for the electrically stimulated limb. The stimulation is holding the muscles in light tension and therefore keeping them taut. This might be reducing the variability in any movement of the tissue across the range of the limb movement by reducing the influence of any initially slack elements within the tissue. Possible evidence of this is the reduced spread of the impedance measurements compared to the un-stimulated results. An alternative explanation comes from the differences in the way that muscles are naturally recruited, compared to when they are recruited with evoked action potentials from electrical stimulation. Voluntary postural movement of this type would normally use the type 1 ‘slow twitch’ muscle fibres whereas electrical stimulation preferentially recruits the type 2 ‘fast twitch’ fibres. Type 2 fibres have a larger diameter and greater z-line width than type 1 fibres and so once recruited these larger fibres could be influencing the impedance results.

When two cycles from the voluntary movement are expanded in Figure 75 the maxima already discussed can be more clearly seen. There is are maxima in each case as the wrist returns from extension to flexion. Followed by minima relating to full flexion and then second maxima as the wrist approaches the neutral position when moving from flexion to extension. When referring back to the original unexpanded plot in Figure 69 it can be seen that this pattern is repeated for each cycle of the movements.

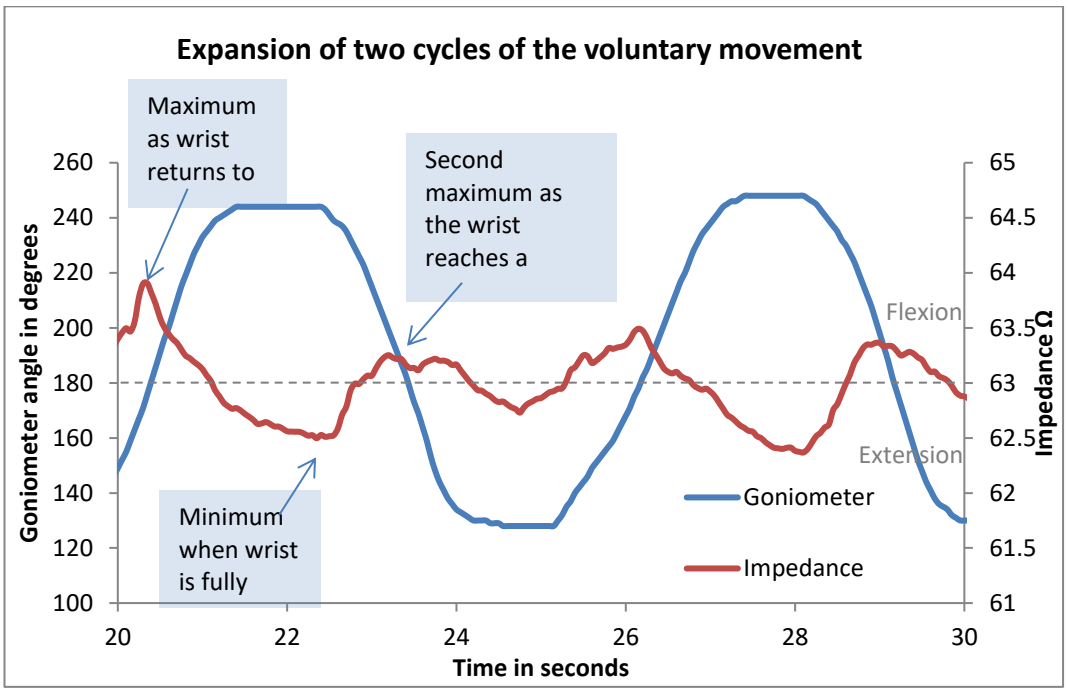

Figure 75 shows an expansion for two cycle of the movement show in Figure 69 above. There are maxima associated with the neutral crossings for both directions of the movement with a minimum between them for each cycle of the movement.

When functional levels of stimulation are used a substantially similar pattern of impedance change is also evident. This pattern has easily identifiable features which are repeated across successive movements (Figure 71). This is more clearly explained by the expansion of two cycles of the FES evoked movement that are shown in Figure 76. When these two cycles are expanded as shown the similarity to the volitional movement can be more obviously seen. There is one apparent difference in that the curve although similar seems to be delayed relative to the stage in the movement compared to the voluntary movement. In both cases the minima coincides with approaching the neutral position of the wrist movement. A difference between the voluntary functional movements is that the voluntary movement was a smooth up and down producing the sinusoidal response from the goniometer, whereas for the functional movement the stimulation acted upon a flaccid flexed wrist at rest. The delay in the impedance curve may be a function of the muscle fibre recruitment pattern causing initially tightening of the muscle as the joint is

moved from rest. In the volitional movement there is likely to still be a large proportion of the type 1 fibres being volitionally recruited, whereas the evoked action potentials from the stimulation will be recruiting predominantly the type 2 fibres. These are the fibres with the greater z-line width meaning a longer contraction distance for the sarcomere as the muscles pull on the wrist, this greater distance with respect to type 1 fibres may account for the slower rate of the impedance curve for the functionally stimulated movement.

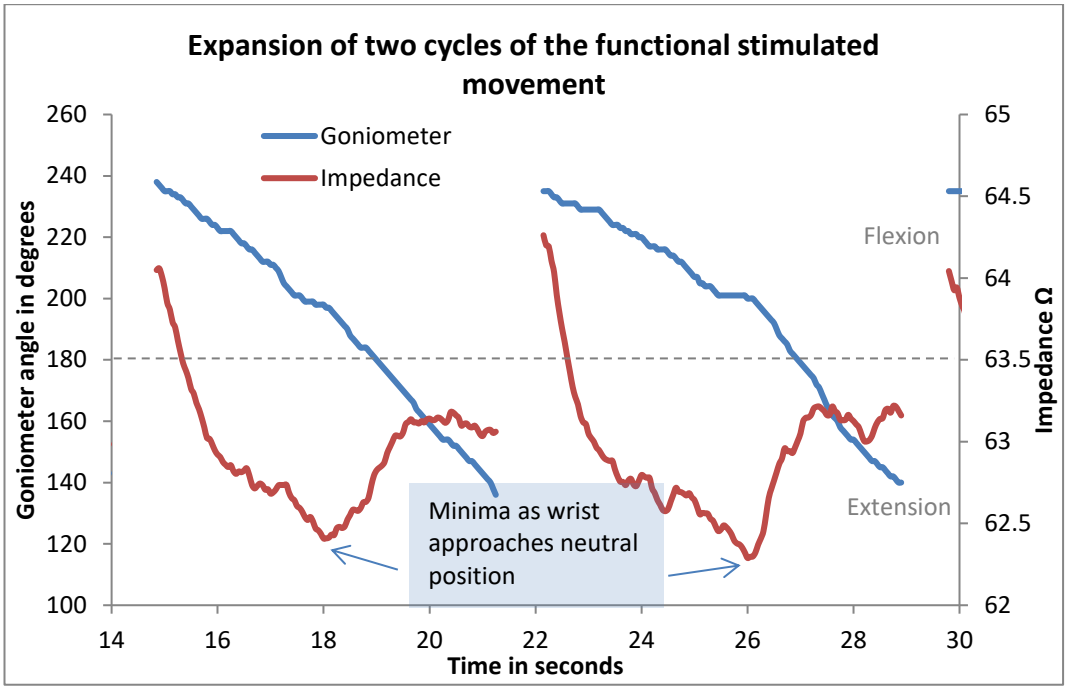

Figure 76 shows two cycles of the FES evoked movement where minima are seen as the wrist approaches the mid-way neutral point from flexion.

The important physical event is the ability to identify when extension of the wrist is approaching or has reached the neutral position. The expanded plot in Figure 76 shows that there is a difference of at least an Ohm between the minimum value for the impedance as the neutral position is approached and the value when the 180^0 neutral position is subsequently reached. When the original unexpanded plot in Figure 71 is referred back to it can be observed that this relationship holds true despite the variability of the absolute values for each cycle of the movement.

10.5 Bio-impedance tracking to detect the wrist neutral position and arrest further movement though control of the FES

For this investigation the identification of the first minima in the bioimpedance curve was used to track when the wrist joint was approaching the neutral position. This would then be used as a control signal for the FES to arrest progress beyond the neutral position.

10.5.1 **Method**

A tracking algorithm capable of identifying the first minima in the bioimpedance reading was developed and embedded into the microcontroller of the stimulator. The algorithm used the moving average low-pass digital filter described in section 9.9.6 on page 155 to calculate the trend of the bioimpedance measurements. The details of stages that the tracking algorithm are set out in Table 13.

The electrodes and placement where retained along with the goniometer fitted across the wrist joint from the previous investigation.

As with the previous investigation in section 10.4 on page 165, the stimulation was delivered at 20Hz with an amplitude of 40V. Unlike the previous investigation where the pulse width was set as 200µs, for this investigation the stimulation was progressive from the start of each repetition. Stimulation started at a 10µs pulse duration which was then progressively increased by 4µs steps with each new pulse. This gave a ramping rate of 10 to 200µs pulse duration within a period of 2.5s.

When the stimulation is started and the limb begins to move the trend for the bioimpedance is to decrease as the wrist moves away from flexion. As the wrist nears the neutral position the first minima is reached at which point the trend charges direction and begins to increase. A threshold of was set at 0.25Ω above the minimum value at the turning point. The reason for choosing this value is explained by referring to Figure 71 on page 167 which shows the expansion of involuntary movement bioimpedance curves. The difference in the minimum impedance at the turning point at the end of the initial downward slope and the maximum value at the next turning point is approximately 0.5Ω. Both of these turning points have relevance to the neutral position, with the minima occurring before the neutral position and the following maxima happening just afterwards so the mid-point of 0.25Ω is an approximation of the neutral position.

When the impedance threshold value was reached the ramping of the stimulation was stopped and in addition the pulse duration by 10% to arrest further movement. After which that the pulse

duration remained constant, with the objective of establishing whether this would arrest any further movement of the limb.

The impedance tracking algorithm and FES control functions were written into the firmware that was then loaded into the embedded microcontroller to manage the electrical stimulation, bioimpedance reading and goniometer reading (Chapter 9: Hardware design). The bioimpedance and goniometer values were streamed to the PC for later analysis.

Firmware Tracking Algorithm		Muscle Stimulator
Stage	Description	Activity
Filtering	The impedance signal are conditioned as described in 9.9.6 on page 155. The impedance measurement is repeated five times and between each stimulation pulse. These readings are then averaged to produce an inter-pulse average impedance. The inter-pulse average impedance is then passed into to a five-term moving average filter that calculates the average of the five most recent inter-pulse averaged impedances. This then become the latest impedance result.	The stimulator starts at a low intensity. The intensity is slowly increased using gentle ramping. This first initiates and then progresses the movement of the limb about the wrist joint. Starting from flexion moving toward the neutral position.
Comparison	A tracking comparator compares the latest impedance result to a stored tracking value.	
Tracking down	If the latest impedance value is less than the stored tracking value the stored tracking value is updated to the value of the latest impedance value. Meaning that the stored tracking value will follow the impedance as it moves down the initial slope of the curve towards the first turning point (Figure 71).	
Tracking at the minima	If the latest impedance value is equal to or more than the stored tracking value the stored tracking value is not updated. This means that the stored tracking value will record the minimum value at the turning point in the curve.	
Detecting the upturn	If the latest impedance value has exceeded the stored tracking value by more than 0.25Ω this is used as an indication that the neutral position at 180^0 has been reached.	Stimulation intensity is reduced by 10% and the ramping suspended to arrest any further movement toward extension.

Table 13 Details of the stages of the impedance tracking and FES control algorithm

10.5.2 **Results**

The plot shown in Figure 77 have the goniometer angle on the left y-axis and the impedance on the right y-axis, with both plotted against time. On the goniometer axis 240^0 relates to fully flexed, the neutral position occurs at 180^0.

The results show that in all of the goniometer curves the progress of the limb was slowed or arrested prior to reaching the 180^0 neutral position. In most cases the neutral position then went on to be exceeded.

In all cases the bioimpedance curves having reached the minima stayed within that region without any previously seen characteristics of a turning point.

In all cases the stimulated involuntary movement about the wrist was arrested before becoming fully extended.

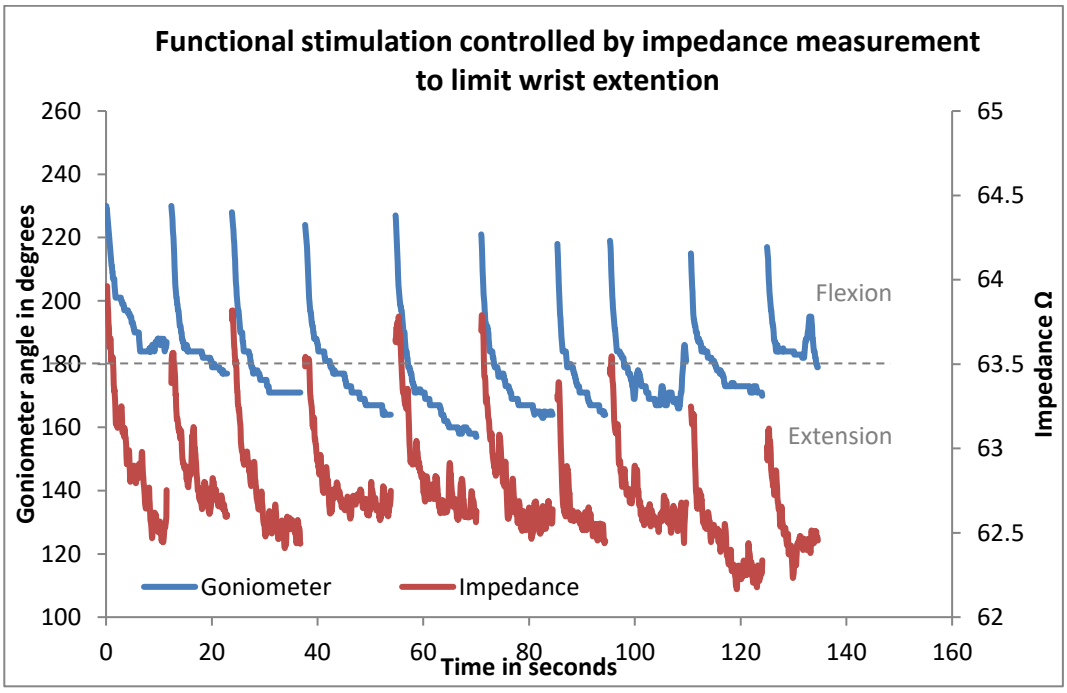

Figure 77 shows the effect of an algorithm used to track the bioimpedance to identify the minimum that occurs as the wrist approached the neutral position. The algorithm then allowed the impedance to increase by 0.25Ω above the tracked value before halting the FES ramping to arrest further movement.

10.5.3 **Discussion**

The results show movements that were relatively slower than for the previous FES investigation. The reflects the additional time needed for the ramping of the stimulation pulse duration from the low starting level before seeing a movement response. The gentle rate of ramping that was used would also have contributed to a slow rate of change for the movement. However the speed of the movement remained within normal limit for functional requirements.

The tracking algorithm demonstrated the ability to detect a threshold set above the first minima value that was associated with the wrist joint neutral position at 180^0, and to prevent the ramping of the FES after this threshold had been reached.

When comparing these results with the uncontrolled stimulated movements shown Figure 70 it can be seen that the movement about the wrist has been reduced. In the uncontrolled functional movements the goniometer shows the wrist moving fully into extension at 140^0. In the tracked results the movement is being arrested in response to the threshold having been exceeded a long way short of full extension.

In most cases the limb then continued to progress beyond the 180^0 target angle. This should not have been too much of a surprise because once the tracking value had reached the threshold, the control of the FES was open-loop. After the target threshold had been reached it triggered cessation of the pulse duration ramping to prevent further progress, and a 10% reduction in the pulse duration to check any overshoot. The results show that this type of predictive open-loop control was not entirely effective in preventing a slow drift toward extension. This accords with (Allin & Inbar, 1986) and (Bajzek & Jaeger, 1987) observations that the response to electrical stimulation is non-linear and requires closed-loop control.

The logical next development would be to introduce a missing closed-loop element to the control.

10.6 Bio-impedance feedback control of FES to detect the wrist neutral position and maintain the position using a closed-loop controller

The purpose of this investigation was to build on the previous investigation (10.5) where the bioimpedance tracking was used only to identify a threshold at which electrical stimulation no longer increased in intensity. This investigation would continue to track the bioimpedance after the threshold had been reached so that the FES intensity could be modulated to maintain the target angle for the limb position.

10.6.1 **Method**

The tracking algorithm used in the previous investigation (10.5) was further refined with the aim of providing better control of the movement about the target 180^0 neutral joint angle. When the 0.25Ω limit was reached the firmware controlling the FES was made to modulate the pulse duration while continuing to track the impedance. Upon reaching the threshold the pulse duration was dropped back immediately to arrest the progress of the wrist travel. It was then ramped back up slowly while continuing to track the impedance and dropped back again every time the threshold was exceeded. The control algorithm was non-symmetric about the threshold. Meaning that the increase in the stimulation pulse duration through the ramping on the approach to the thresholds was slow relative to the immediate rate of reduction after it had been exceeded. The details of stages that the tracking algorithm are set out in

Table 14.

As with the earlier investigation in section 10.5, the stimulation was delivered at 20Hz with an amplitude of 40V. Stimulation started at a 10µs pulse duration which was then progressively increased by 4µs steps with each new pulse. To give a ramping rate of 10 to 200µs pulse duration within a period of 2.5s.

The electrodes and placement where retained along with the goniometer fitted across the wrist joint from the previous investigation.

The impedance tracking algorithm and FES control functions were written into the firmware that was then loaded into the embedded microcontroller to manage the electrical stimulation, bioimpedance reading and goniometer reading (Chapter 9: Hardware design). The bioimpedance and goniometer values were streamed to the PC for later analysis.

Firmware Tracking Algorithm		Muscle Stimulator
Stage	Description	Activity
Filtering	The impedance signal are conditioned as described in 9.9.6 on page 155. The impedance measurement is repeated five times and between each stimulation pulse. These readings are then averaged to produce an inter-pulse average impedance. The inter-pulse average impedance is then passed into to a five-term moving average filter that calculates the average of the five most recent inter-pulse averaged impedances. This then become the latest impedance result.	The stimulator starts at a low intensity. The intensity is slowly increased using gentle ramping. This first initiates and then progresses the movement of the limb about the wrist joint. Starting from flexion moving toward the neutral position.
Comparison	A tracking comparator compares the latest impedance result to a stored tracking value.	
Tracking down	If the latest impedance value is less than the stored tracking value the stored tracking value is updated to the value of the latest impedance value. Meaning that the stored tracking value will follow the impedance as it moves down the initial slope of the curve towards the first turning point (Figure 71).	
Tracking at the minima	If the latest impedance value is equal to or more than the stored tracking value the stored tracking value is not updated. This means that the stored tracking value will record the minimum value at the turning point in the curve.	
Tracking the threshold	(1). If the latest impedance value has exceeded the stored tracking value by more than 0.25Ω this is used as an indication that the neutral position at 180^0 has been reached. This is set as the threshold value for maintaining the target joint angle.	The stimulation intensity is immediately reduced to arrest further movement toward extension.
	(2). The impedance drops in response to the immediate reduction in the FES intensity and tracking resumes	Ramping of the stimulation intensity resumes
	(3). Until the set threshold has been exceed again and the process repeats from (2).	Stimulation intensity is immediately reduced.

Table 14 Details of the stages of the impedance tracking and closed-loop FES control algorithm

10.6.2 **Results**

The plot shown in Figure 77Figure 78 have the goniometer angle on the left y-axis and the impedance on the right y-axis, with both plotted against time. On the goniometer axis 240^0 relates to fully flexed, the neutral position occurs at 180^0.

The results show that in all of the goniometer curves the progress of the limb was arrested close to the 180^0 target neutral position.

In nearly all cases the bioimpedance curves having reached the minima stayed within that region without any previously seen characteristics of a turning point. The exception being the final curve in the sequence when the limb was accidently knocked against the edge of the table causing a small additional movement toward extension. This produced a spike in the bioimpedance curve as the algorithm brought it under control.

In all cases the stimulated involuntary movement about the wrist was arrested as it moved away from flexion and then controlled close to the target neutral position of 180^0.

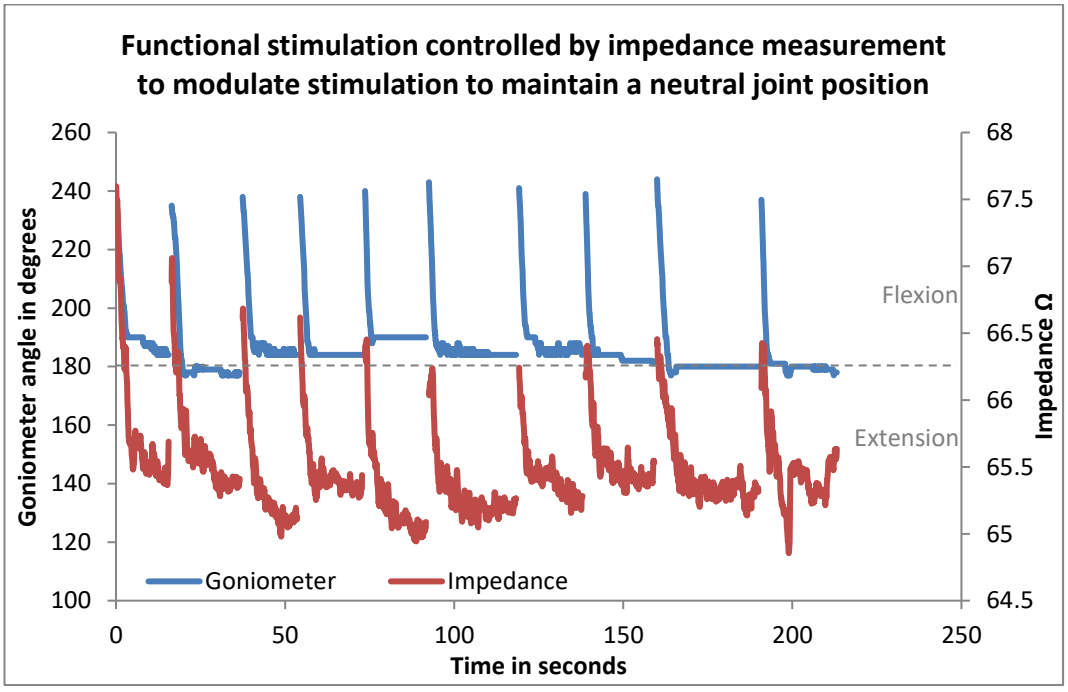

Figure 78 shows the effect of the improved algorithm used to track the bioimpedance to identify the minimum that occurs as the wrist approached the neutral position. The algorithm allowed the impedance to increase by 0.25Ω before modulating the FES while continuing to track the impedance to maintain the wrist in a neutral position. The final repetition shows evidence of an unintended perturbation being controlled.

The expansion of the first two repetitions is shown in Figure 79. The plots show linearised regions within the targeted region of control. When this linear region for these two plots were subjected to statistical analysis to results shown in Table 15 were obtained.

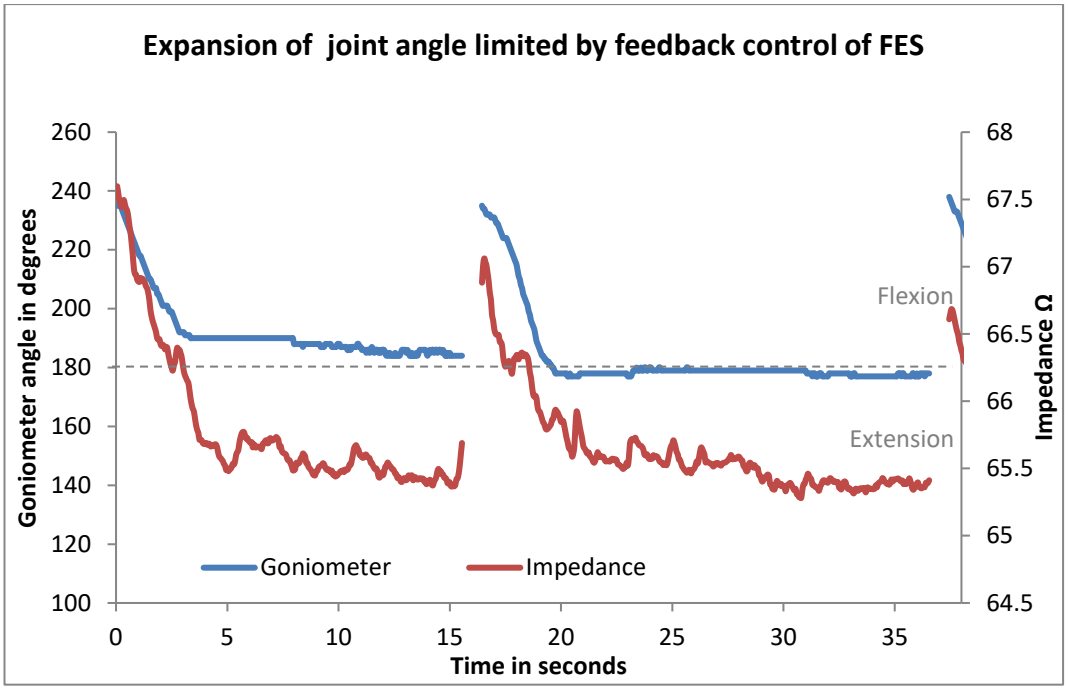

Figure 79 shows an expansion for the first two movement cycles from Figure 78. The goniometer plot shows how by tracking the impedance the system was able to maintain a constant position.

Statistical analysis	Movement Cycle 1		Movement Cycle 2	
	Goniometer	Bioimpedance	Goniometer	Bioimpedance
Mean	187.4095	65.53878	178.2680723	65.49295181
Median	187	65.516	178	65.494
Mode	190	65.48	179	65.543
Standard Deviation	2.209875	0.104728	0.857068647	0.125411218
Sample Variance	4.883546	0.010968	-0.226589605	0.693702775
Range	6	0.406	3	0.641
Minimum	184	65.365	177	65.281
Maximum	190	65.771	180	65.922
Count	232	232	332	332

Table 15 – statistical analysis of the linear region of the movement cycles one and two shown in Figure 79. This the period when the stimulation control algorithm is tracking the impedance to maintain the position of the limb.

10.6.3 **Discussion**

The initial attempt to limit the movement by controlling the FES in response to bioimpedance changes (Figure 77) used a very simple open-loop control algorithm. The bioimpedance was tracked until the minimum value was reached indicating that the movement was approaching the neutral position. As soon as the impedance exceeded this value by 0.25Ω the stimulation intensity was reduced to a lower level which had the effect of slowing the rate of additional progress toward extension. After being reduced the level was maintained which explains why the wrist movement continued beyond the 180^0 target. Because of the reduced intensity of the stimulation this latter part of the movement was at a much reduced rate. The result had shown that the bioimpedance tracking method was able to determine the wrist position as the movement approached the neutral position and respond to control the FES. But that the predictive open-loop control had not been fully effective in arresting the movement. For the system to be clinically useful the wrist position would need to be controlled within a range of 10 degrees either side of the target.

Having demonstrated that control of the FES was possible improvements were then made to the algorithm to be able to continue to track the bioimpedance after the threshold value was reached. Such that the FES intensity having been initially reduced was then modulate at a level needed to maintain the bioimpedance at the target value. When the results for the closed-loop algorithm shown in Figure 78 are compared to the open-loop results shown in Figure 77 they demonstrate much better control. The movement is initially arrested before the limb position is then maintained.

When the expansion of the first two cycles of the movement is observed in Figure 79 it can be seen that the target value of 180^0 was not reached during the first cycle and slightly exceeded in the second. Table 15 shows the median value for the first cycle as 187^0 and the second as 178^0. However having commenced control of the FES the algorithm is able to maintain the limb in a stable position. The range of the bioimpedance changes were well within an Ohm in both cases and the standard deviations show that the two thirds of the measurement were within 0.25Ω.

The final movement in the sequence in Figure 78 was highlighted in the results for showing evidence of an inadvertent perturbation within the controlled region. This invites closer inspection and further discussion. Figure 80 is an expansion of this final repetition of the movement. The dip in the bioimpedance during the controlled period is accompanied by additional extension of the movement about the wrist. The dip in the bioimpedance resulted in a correction by increasing the intensity of the FES. The bioimpedance is returned to the previous

level as the wrist move back toward the target position and the goniometer records this change in displacement. The statistical analysis shown in Table 16 shows that the range of the bioimpedance was greater than for the first two cycles shown in Table 15 which is consistent with the additional movement.

The recovery from this inadvertent perturbation suggested at the potential for robustness from the control algorithm which now required further investigation.

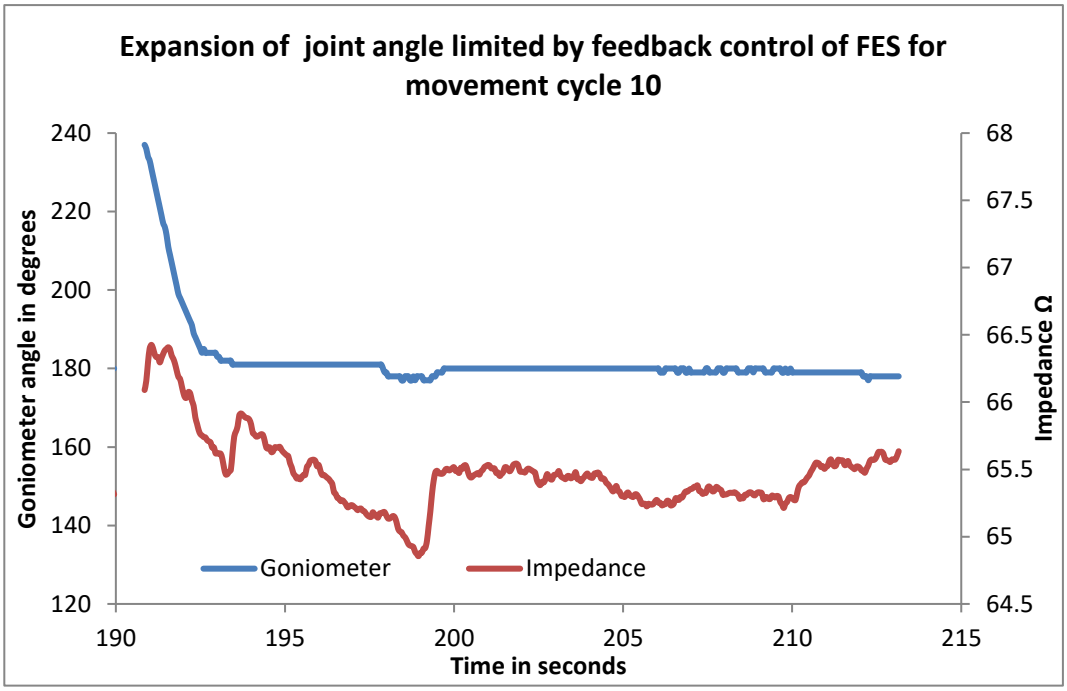

Figure 80 shows an expansion of Figure 78 for movement cycle number ten. The dip in the bioimpedance during the controlled period is accompanied by additional extension of the movement. When the FES is controlled to correct this the bioimpedance returns and the wrist move back toward the target neutral position.

Statistical analysis	Goniometer	Bioimpedance
Mean	179.9545	65.41858
Median	180	65.441
Mode	180	65.459
Standard Deviation	1.459391	0.190481
Skewness	1.68857	-0.15477
Range	12	1.118
Minimum	177	64.855
Maximum	189	65.973
Count	418	418

Table 16 statistical analysis of the linear region of the movement cycles one and two shown in Figure 80. This the period from 192 s when the stimulation control algorithm is tracking the impedance to maintain the position of the limb.

10.7 Further investigation into the response of the bioimpedance tracking closed-loop control to an external disturbance

The closed loop control from the previous investigation had demonstrated the ability to bring the wrist joint to the neutral position and then maintain this position through control of the FES intensity. The results had also hinted at the ability to cope with unexpected external disturbances, this next investigation was designed to explore this potential. For any system using bioimpedance closed-loop control to be considered clinically useful it would need to be able to, identify the target angle, and then maintain this within a tolerance of plus or minus 10 degrees.

10.7.1 **Method**

The tracking algorithm used in the previous investigation (10.6) was retained with the stimulation delivered at 20Hz at an amplitude of 40V. Stimulation started at a 10µs pulse duration which was then progressively increased by 4µs steps with each new pulse. To give a ramping rate of 10 to 200µs pulse duration within a period of 2.5s.

As with the previous investigation the stimulation was commenced by pressing the activation button (Figure 60 on page 148). For the previous investigations the stimulation was only active while the button remained held down. For this investigation the function of the button was altered to enable a timed period of stimulation to be dispensed following a single press and release of the button. The period was set at 7.5s, this being long enough to allow 2.5s for the pulse duration ramping followed by 5s in which to test the response to a perturbation. This measure was introduced to produce timing consistency across repetitions of the movement.

The electrodes and placement where replicated along with the goniometer fitted across the wrist joint that were used in from the previous investigations as described in section 10.2.1.1 on page 160.

The stimulation was started by pressing the activation button. The stimulation intensity automatically ramped to produce limb movement about the wrist from the flexed position (Figure 81a). The system tracked the bioimpedance to locate the neutral position of the wrist and began modulating the stimulation intensity to maintain this position. After the wrist had reached the settled position an external disturbance was applied in the form of a poke on the back of the hand causing the wrist to go into involuntary partial flexion (Figure 81b). The system was then left to recover from the perturbation Figure 81c).

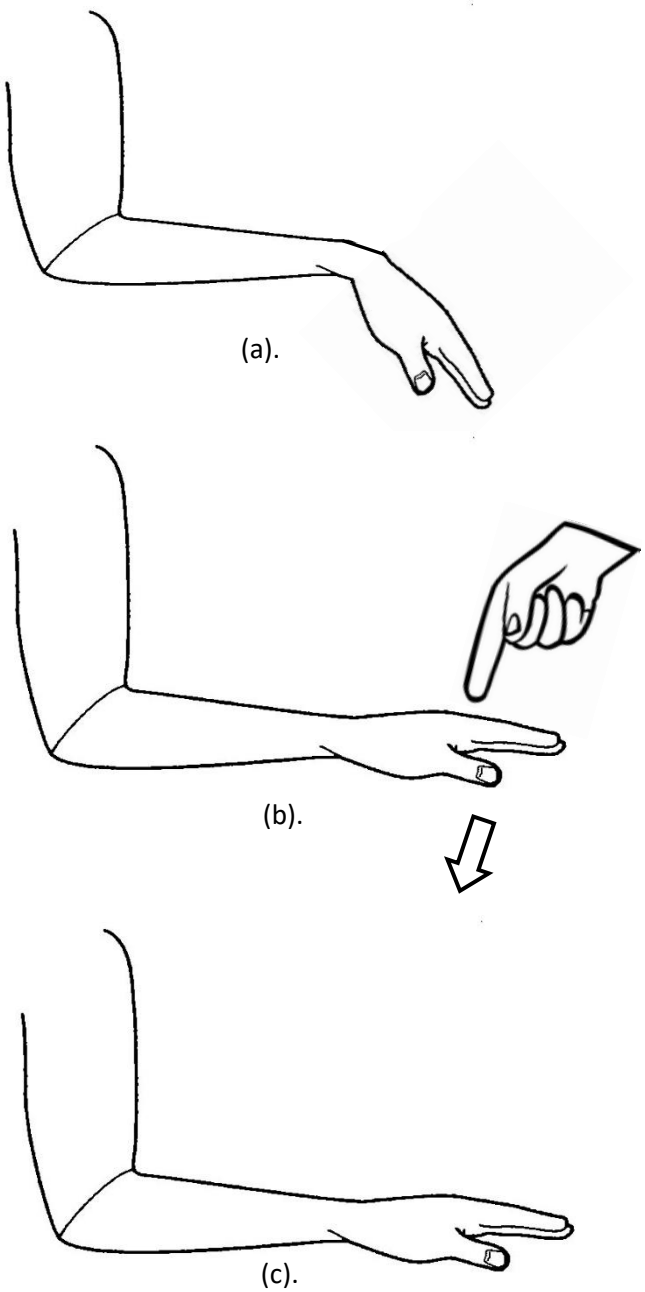

Figure 81 Illustrates how the external disturbance was applied to the limb while the position was being maintained by the bioimpedance closed-loop control.

(a). shows the starting position with the wrist in flexion.

(b). shows how after the wrist had reached a settled position the disturbance was applied to the back of the hand to push the wrist back into partial flexion.

(c). shows the settled position after the control system had recovered from the disturbance.

Ten repetition of the movement were made with the impedance and goniometer readings streamed to the PC for analysis.

10.7.2 **Results**

The plot shown in Figure 82 shows the ten repetitions of the movement over a period of 80s, with each repetition lasting for 7.5s.

The goniometer plots show an initial downward slope as the wrist moves from flexion to the target 180^0 neutral position. This is matched by the fall in the bioimpedance until the threshold value above the first minima is recorded and the stimulation is modulated to maintain this position.

The applied disturbance after the limb had settled can be seen as the spike that follows as the hand was pushed back into partial flexion. When the disturbance was removed the modulated stimulation returned the limb position to the recovered settled position.

In all cases the initial settling position and the recovered settling position were within 10^0 either side of the 180^0 target value.

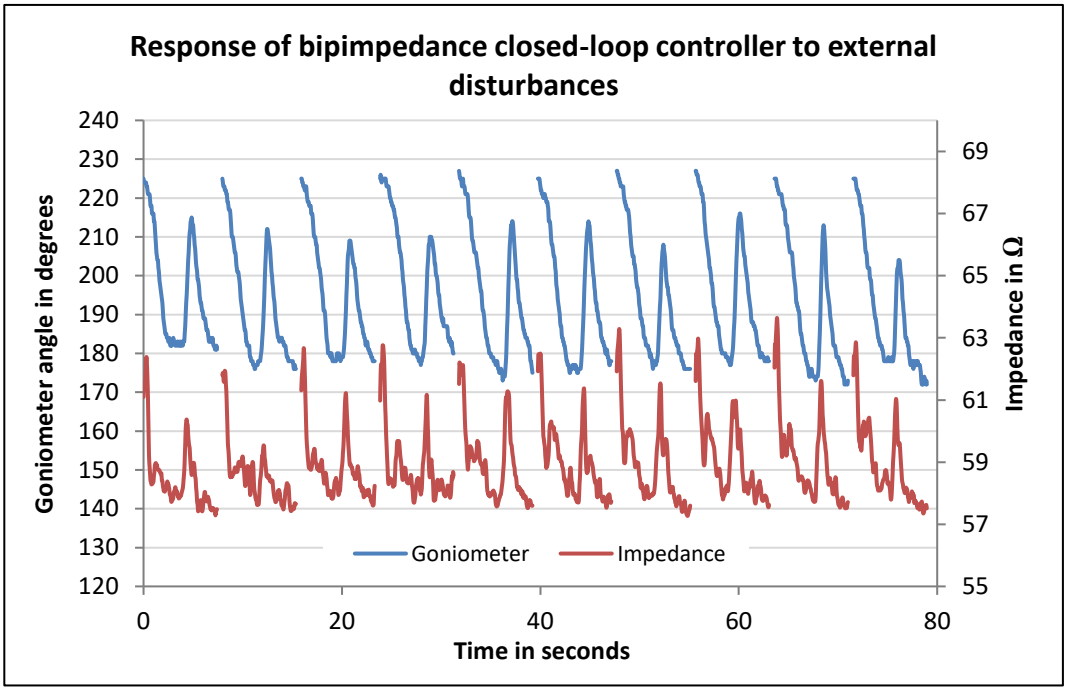

Figure 82 shows the results from ten repetitions of controlled wrist movements. After the initial position had settled the external disturbance can be observed as the spike. This is followed by the recovered settling position after the response of the closed-loop control to the disturbance. In all cases the initial settling angle and the recovered settling angle remain within 10^0 either side of the 180^0 target.

10.7.3 Discussion

The results show that the closed-loop control system is capable of tracking the initial limb movement to find and maintain the neutral position for the wrist. When the external disturbance that causes the wrist to go back into flexion is applied, the system is able to recover the target position.

I all cases the recovered position is very similar to the initial settling position before the disturbance. The variability to the achieved accuracy to the target is similar to the previous investigations (Figure 78). In all cases the initial settling and recovered settling angles were with 10^0 either side of the target value. In the introduction to this investigation it was stated that for the system to be considered clinically useful this would need to be the case.

10.8 Investigation of the closed-loop control to disturbance when the subject is blindfolded

To remove any effect of the subject visually influencing the recovered position achieved by the closed-loop control following the external disturbance, the previous investigation was repeated blindfolded and with the aid of an assistant.

10.8.1 Method

The same method was used as was used for 10.7, with the following additions.

- The subject was blindfolded to remove any effects of visual influence. Before the stimulation was commenced the subject was informed. The subject was unable to see when the wrist had settled or when the disturbance was about to be applied.
- An assistant was used to activate the stimulation and to apply the disturbance after the limb had been observed to settle.

10.8.2 Results

The plot in Figure 83 shows the results for the ten repetitions of the stimulated involuntary movement while the subject was blindfolded. They show that the closed-control system was able to find the initial settling position and that in all cases the initial settling position and the recovered settling position were within 10^0 either side of the 180^0 target value.

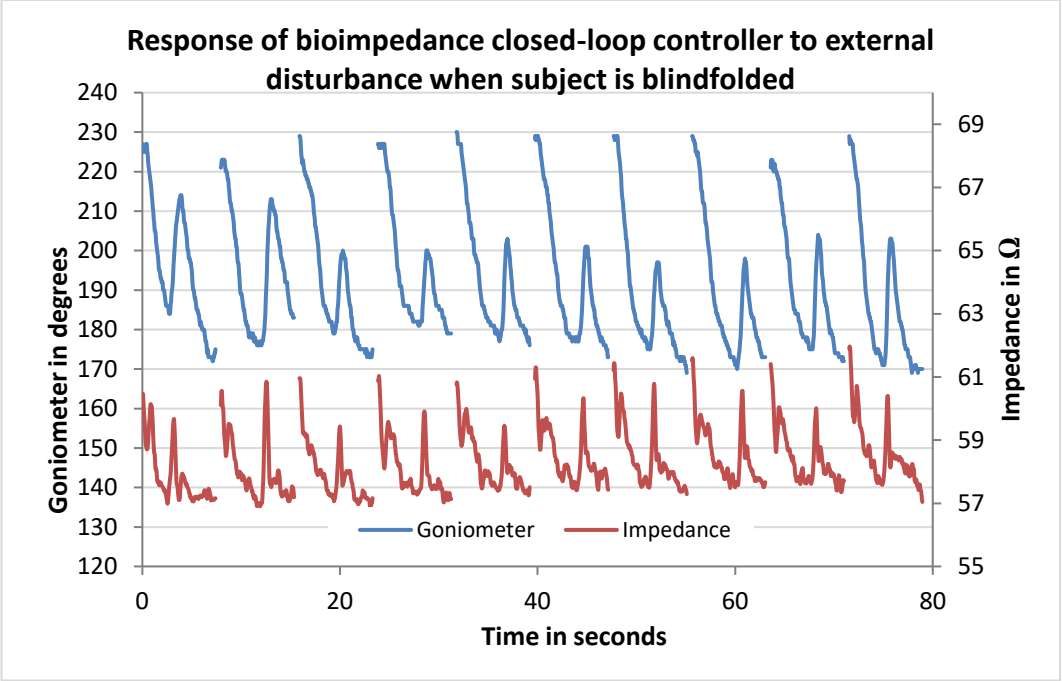

Figure 83 shows the results from ten repetitions of controlled wrist movements when the subject was unable to visually influence results. The initial settling angle and the recovered settling angle are within 10^0 either side of the 180^0 target.

10.8.3 **Discussion**

There are a number of things to draw from the results of this investigation.

The first of these is to highlight the variability in the sizes of the disturbances applied by the assistant when compared to those in Figure 82 for the non-blindfolded test. Repetition number 4 had a 17^0 disturbance applied, whereas repetition number had 27^0 applied. The controller was able to recover from the disturbances each time equally effectively. Repetition number 2 had the largest disturbance at 35^0. This was applied relatively late into the settling period following the initial movement with the result that the 7.5s of stimulation had timed out before the recovered settling position was achieved. The trajectory suggests it was in the right direction.

Repetitions numbers 8 and 10 show that the target was overshot by the acceptable limit of 10^0. The previous non-blindfolded investigation stayed within 7^0 of the target. This could be an indication that the subject was able to visually influence the non-blindfolded results, or it could just be normal variability. The difference of 3^0 is very small and would be difficult to visually judge.

More results are required to determine how well the closed-loop control works and also how well it behaves over an extended period.

10.9 Closed-loop control with the subject blindfolded over an extended period of two hours

The results of the previous investigation demonstrated that the bioimpedance closed-loop control was probably suitable to be considered clinically useful. An extended test was required to see whether the system remained functional over a longer period.

10.9.1 **Method**

The same method was used as for 10.8 in the previous investigation to look at the effect of blindfolding the subject. The method was extended over a 2 hour period with 10 movement repetitions being measured at 15 minute intervals.

The subject was free to remove the blindfold and move between each set of repetitions.

The arm was returned to a similar starting position with the forearm supported and the hand free to hang down before each set of measurements.

The assistant operated the stimulation and provided the disturbances as before.

10.9.2 **Results**

The plots in Figure 84 to Figure 92 show the goniometer and bioimpedance results for measurement made at 15 minute intervals over a 2 hour period.

The results demonstrate that the target value of 180^0 was identified and maintained is at or within the plus or minus 10^0 range needed to be considered clinically useful. This was also demonstrated for the recovery settling positions following the disturbances.

An upward shift in the bioimpedance measurements can be observed that reaches around 1Ω by 45 minutes (Figure 87) after the start. This have moved down again by 75 minutes (Figure 89) where it remains for the rest of the time. At the start most of the impedance is below 57Ω, whereas after 45 minutes nearly all of it is above 57Ω. After 75 minutes it is at a similar level to the start and after 105 minutes it nearly all below 57Ω. The ability of the tracking algorithm to remain within the range for the target angle is unaffected by this.

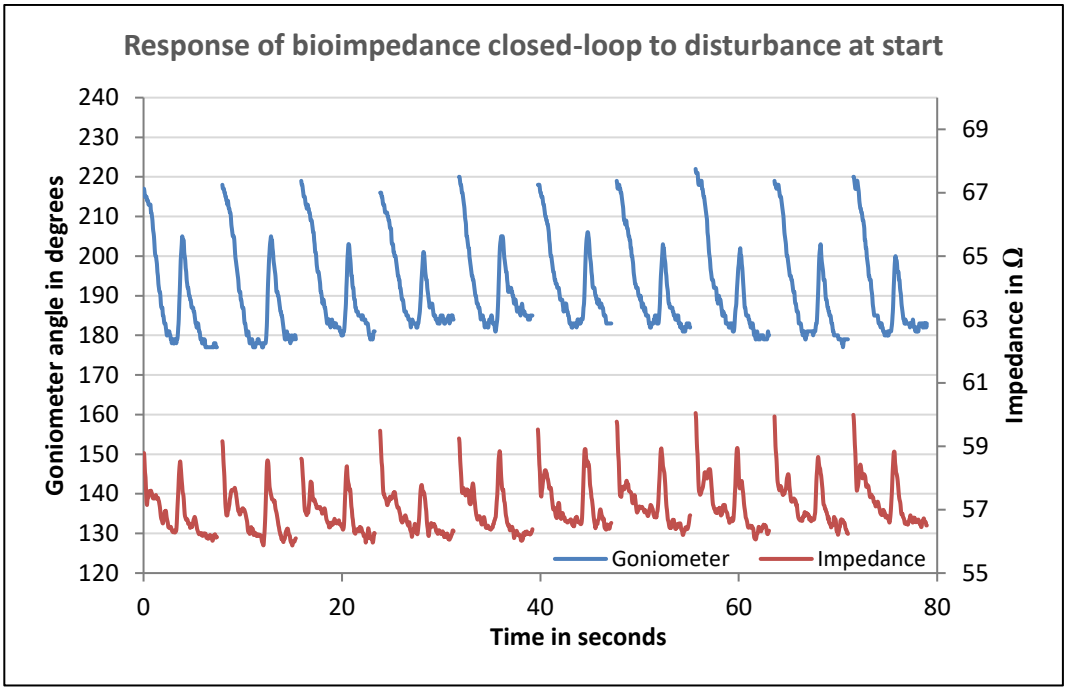

Figure 84 showing ten repetitions of bioimpedance closed-loop controlled stimulated movement with external disturbance and recovery.

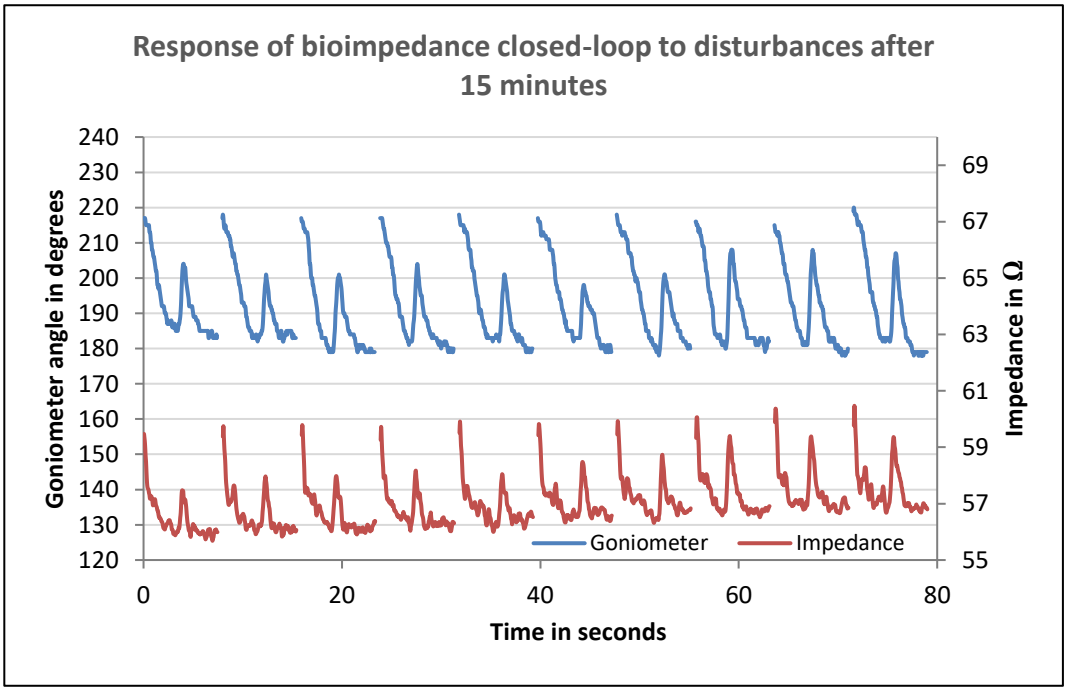

Figure 85 showing ten further repetitions after 15 minutes of bioimpedance closed-loop controlled stimulated movement with external disturbance and recovery.

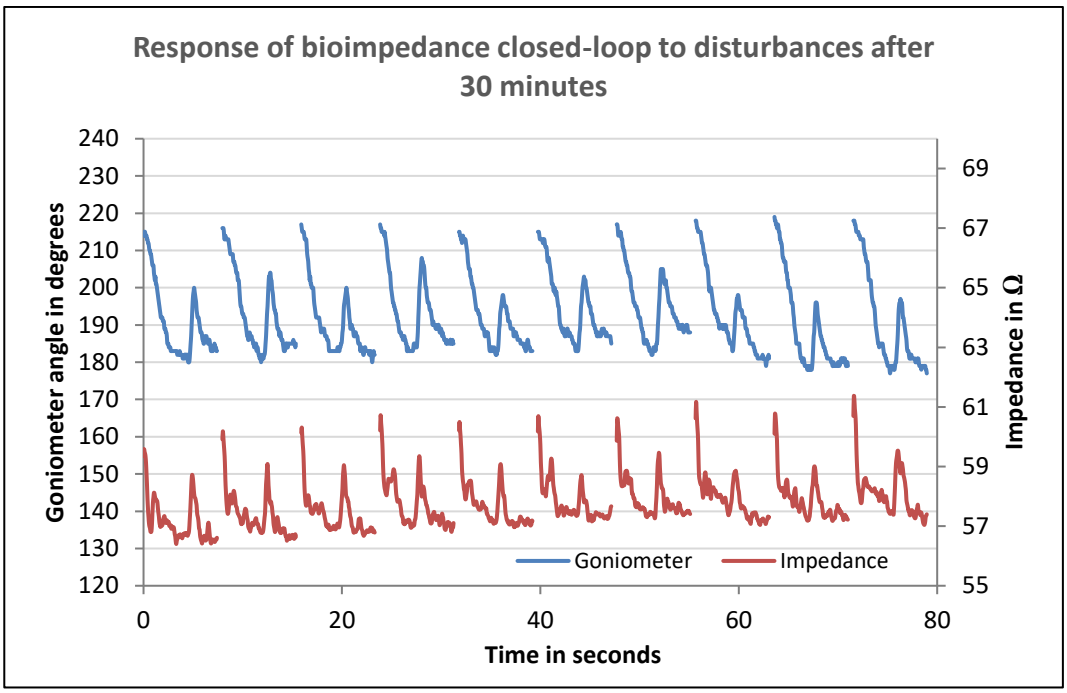

Figure 86 showing ten further repetitions after 30 minutes of bioimpedance closed-loop controlled stimulated movement with external disturbance and recovery.

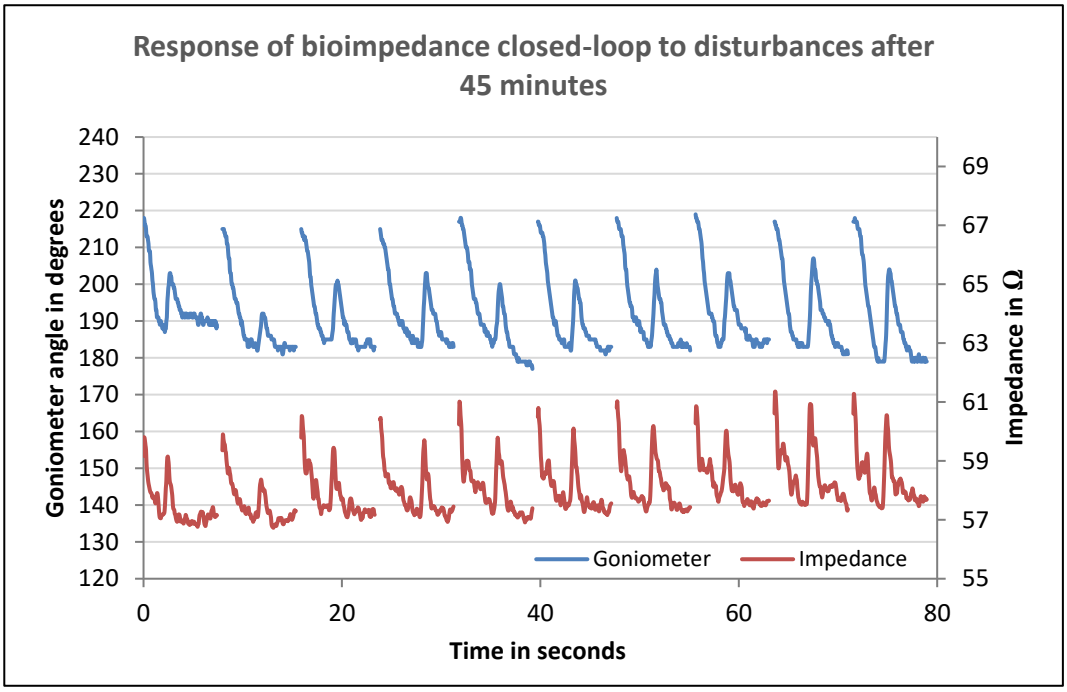

Figure 87 showing ten further repetitions after 45 minutes of bioimpedance closed-loop controlled stimulated movement with external disturbance and recovery.

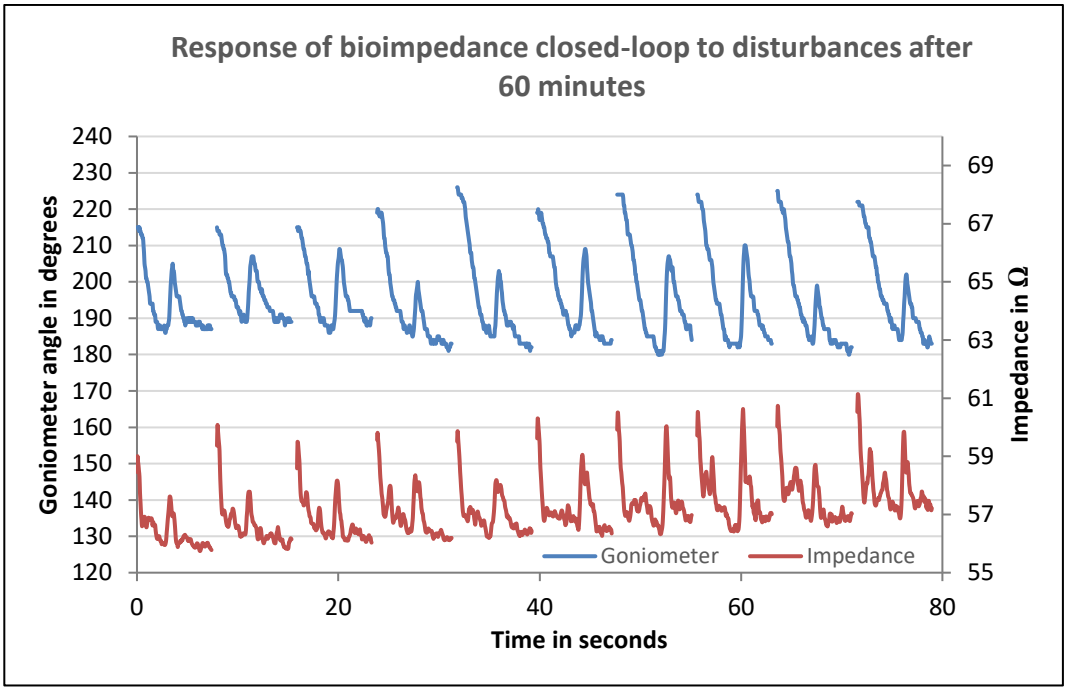

Figure 88 showing ten further repetitions after 60 minutes of bioimpedance closed-loop controlled stimulated movement with external disturbance and recovery.

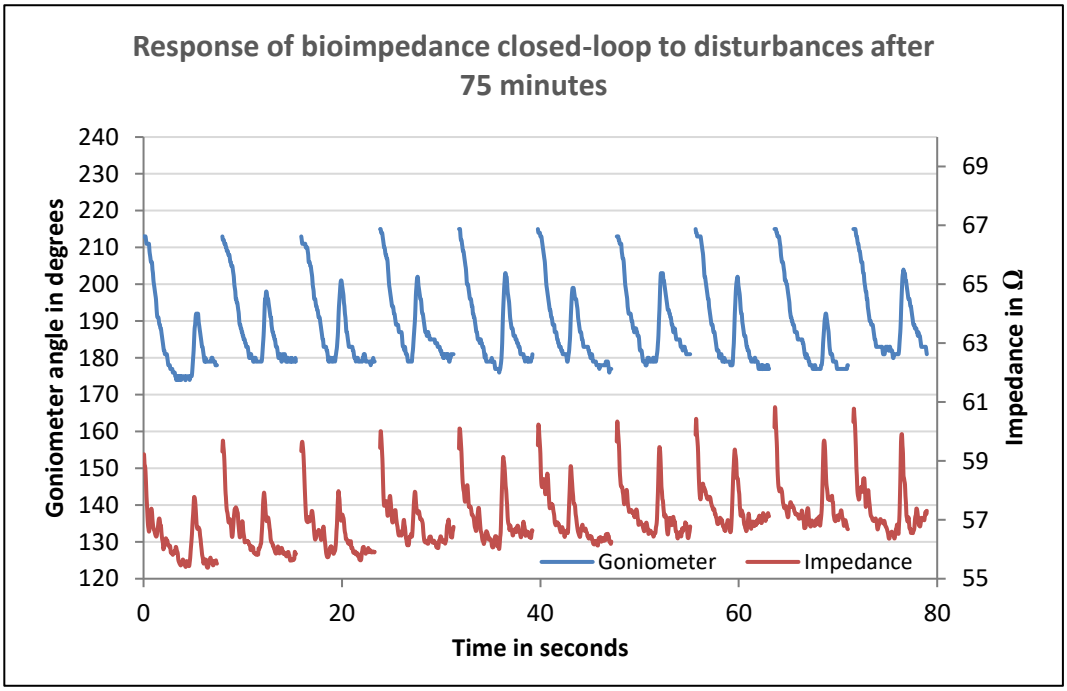

Figure 89 showing ten further repetitions after 75 minutes of bioimpedance closed-loop controlled stimulated movement with external disturbance and recovery.

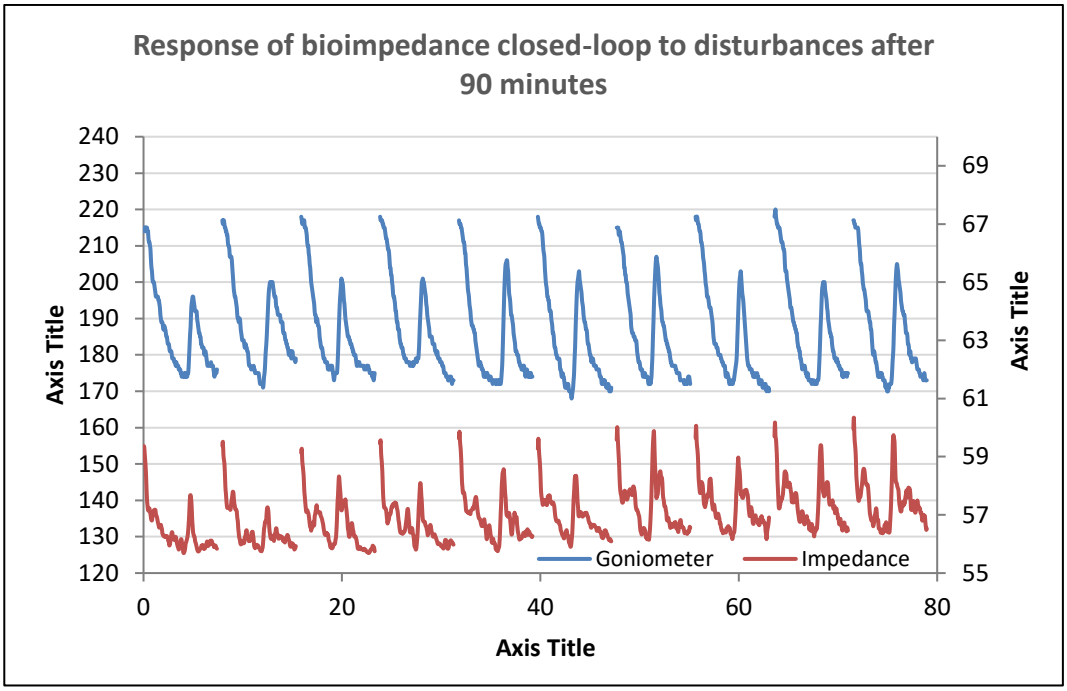

Figure 90 showing ten further repetitions after 90 minutes of bioimpedance closed-loop controlled stimulated movement with external disturbance and recovery.

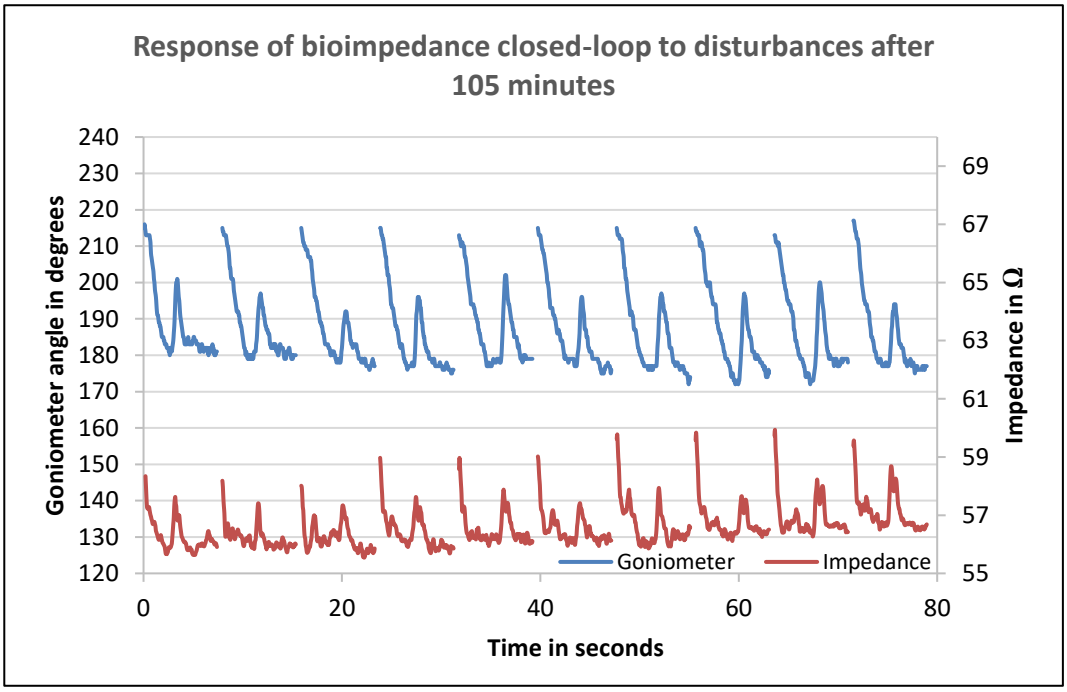

Figure 91 showing ten further repetitions after 105 minutes of bioimpedance closed-loop controlled stimulated movement with external disturbance and recovery.

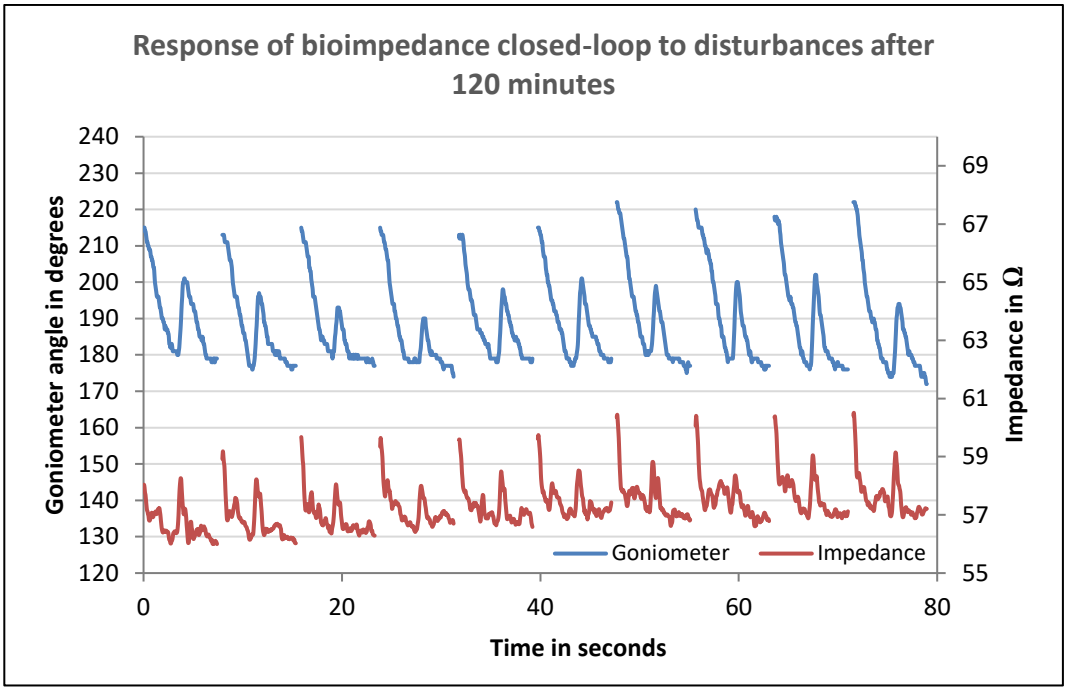

Figure 92 showing ten further repetitions after 120 minutes of bioimpedance closed-loop controlled stimulated movement with external disturbance and recovery.

10.9.3 **Discussion**

The results amount to 90 repetitions of the stimulated involuntary movement carried out over 2 hours. With the possible exception of the first movement at 45 minutes (Figure 87) the results demonstrated that the bioimpedance closed-loop control was able to find and maintain the target angle within the clinically useful tolerance of plus or minus 10^0. The system was then able to recover from a perturbation to return the limb position to within this range.

The 45 minute plot was identified in the results because of the evidence of a shift in the impedance which had reached a maximum by this stage. This observation is interesting not only for the reason that it does not appear the have had any particularly adverse effects upon the functioning of the system, but also as to the likely cause of the difference in impedance observed. The investigation was started within an hour of the subject having eaten breakfast and the likely cause of the effect will have been changes in blood sugars over that time. There is increasing evidence that bioimpedance can be used as a method to noninvasively measure glucose levels (So, 2012) (Kamat, 2014). At the start of the investigation the blood glucose levels of the subject would have been increasing as the food was being digested, this would have been countered by the body producing insulin to bring the levels down again to normal levels. The effect of this insulin would then have tapered off. Bioimpedance decreases as glucose levels increase, so the bioimpedance will be increased by the effects of insulin. The change in the impedance that builds

up and recedes either side of the 45 minute measurements might therefore be due to effects of the subject's body producing insulin to counter the effects of sugars from the meal. If this is the case then it is a useful finding as it would indicate the bioimpedance closed-loop control would remain functional through the course of a normal day.

10.10 Bioimpedance measurement taken from a manually manipulated limb

It was decided to investigate the bioimpedance measurements obtained when a joint was manually manipulated by a third part. There was not any direct reason for doing this other than for thoroughness to see what it might reveal.

10.10.1 **Method**

The following two set of readings were made,

- Bioimpedance measurement while the wrist was manipulated form flexed to extended and back again over a number of repetition cycles without any electrical stimulation.
- Bioimpedance measurement while the wrist was manipulated form flexed to extended and back again with low-level electrical stimulation keeping tension on the extensor muscles.

Similar electrode positions and goniometer arrangements were use as previously. For the second part of the investigation with electrical stimulation a 175µs pulse duration at amplitude 20V with a frequency of 20Hz was applied.

10.10.2 **Results**

The plot in Figure 93 shows the results for the wrist being manipulated when no electrical stimulation was applied. The bioimpedance plot shows a relationship to the goniometer readings. Allowing for the 'noise' the bioimpedance plots follows the sine wave produced by the movement measurements of the goniometer. The bioimpedance waveform appears to be 180^0 out of phase with the movement.

The plot in Figure 93 shows the results for the wrist being manipulated while low level neuromuscular electrical stimulation was applied to maintain a gentle tension on the extensor muscles. The relationship of the bioimpedance changes are less easily related to the movement than for the non-stimulated results.

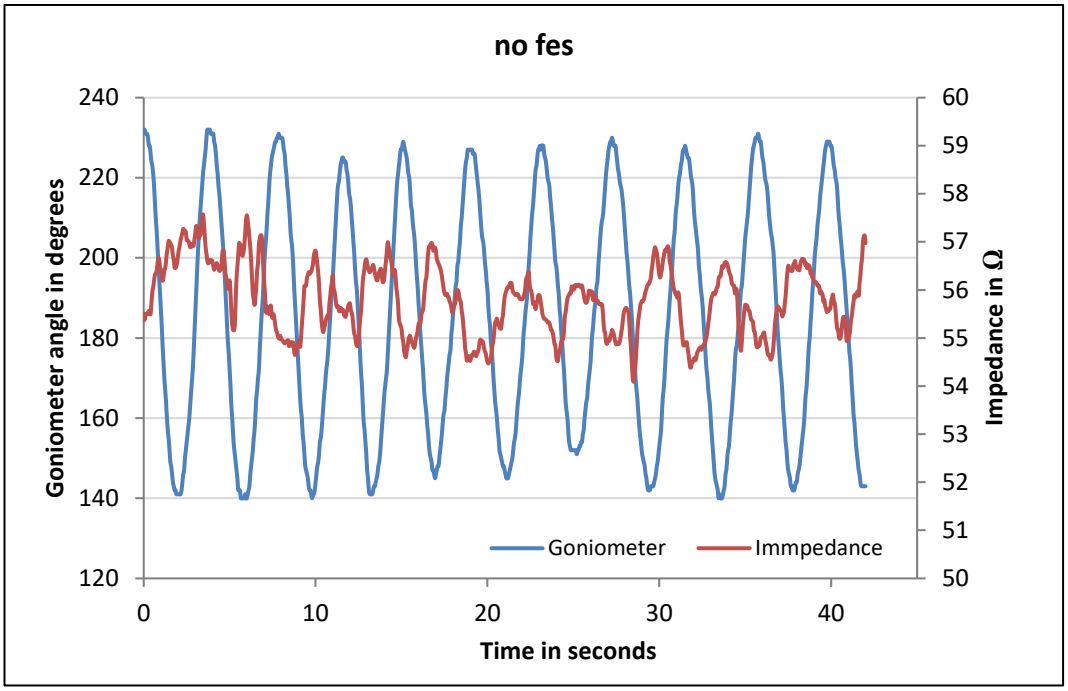

Figure 93 shows the bioimpedance results for a wrist which was manually manipulated by a third party. The bioimpedance shows changes that have some relationship to the movement.

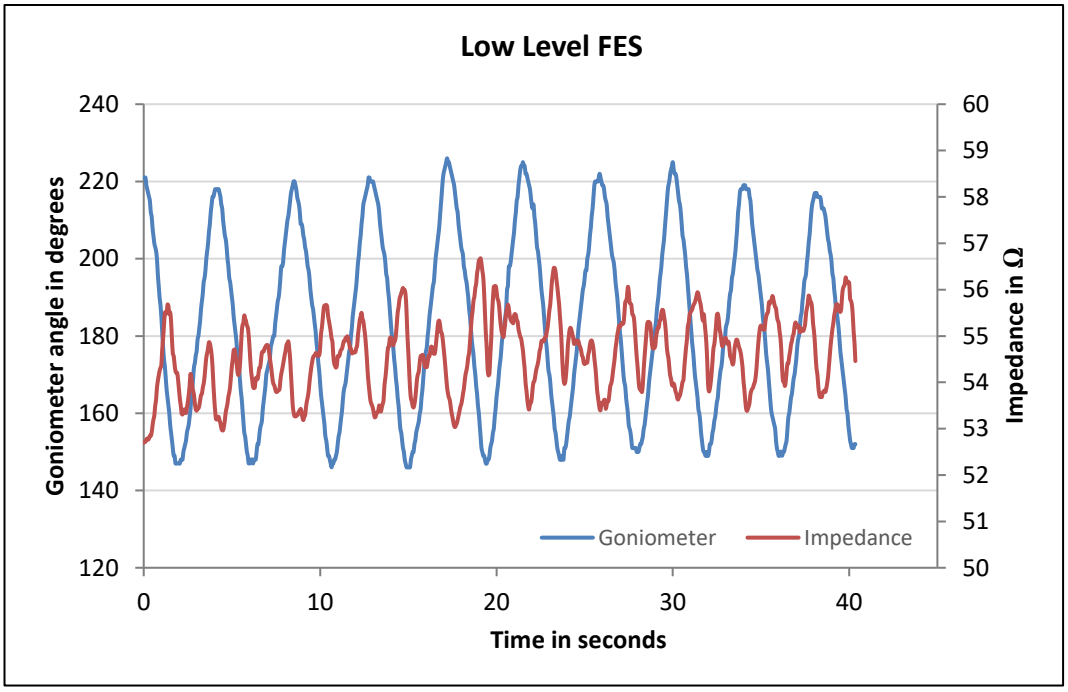

Figure 94 shows the bioimpedance results for a wrist which was manually manipulated by a third party while low level neuromuscular electrical stimulation was applied. The bioimpedance shows changes that have some relationship to the movement. These are less easily identifiable than for the non-stimulated results.

10.10.3 **Discussion**

The results for the wrist manipulation look at a type of movement not looked at in any of the previous investigations. These investigations used voluntary movement without stimulations and with low-level stimulation, and involuntary movement resulting from stimulation. The involuntary movement applied during this investigation was from a third party for both the non-stimulated and stimulated measurements.

The major difference to consider is muscle recruitment. In the previous investigation the extensor muscles were being recruited, either volitionally or non-volitionally to produce the wrist movement.

In this investigation when the wrist was manipulated up and down, Figure 93 shows a change in bioimpedance that is lagging the movement. This suggest that the upward movement of the wrist toward the relaxed extensor muscle did not produce any immediate change in muscle length. When the wrist was moved down again, somewhere beyond the halfway point the extensor muscles began to stretch producing the change in bioimpedance. Similarly on the next upward movement it was beyond the halfway point before the muscles began to be pushed to contact. Producing the out of phase response.

The impedance plot for the stimulated muscle is less easily interpreted. The extensor muscles were held in light tension by the stimulation and then stretched and returned by the involuntary manipulation. The bioimpedance plot shows similar changes relating to the movement, but with a significant differences. The electrical stimulation produced tensioning of the muscle. This would have been most noticeable when the wrist had been manipulated into the fully flexed position when the extensor muscles were fully stretched. The second point of interest is the crossing of the halfway or neutral position that follows as the wrist is manipulated toward extension, these is where the extensor muscles have gained full mechanical advantage.

This is shown in greater detail in Figure 95. There is an upward swing in the bioimpedance as the wrist changed direction from extension back to flexion (i). This is followed by a fluctuation as the halfway or neutral position is crossed (ii). This shows that the tensioning of the extensor muscles maintains the features of the bioimpedance in alignment to the movement.

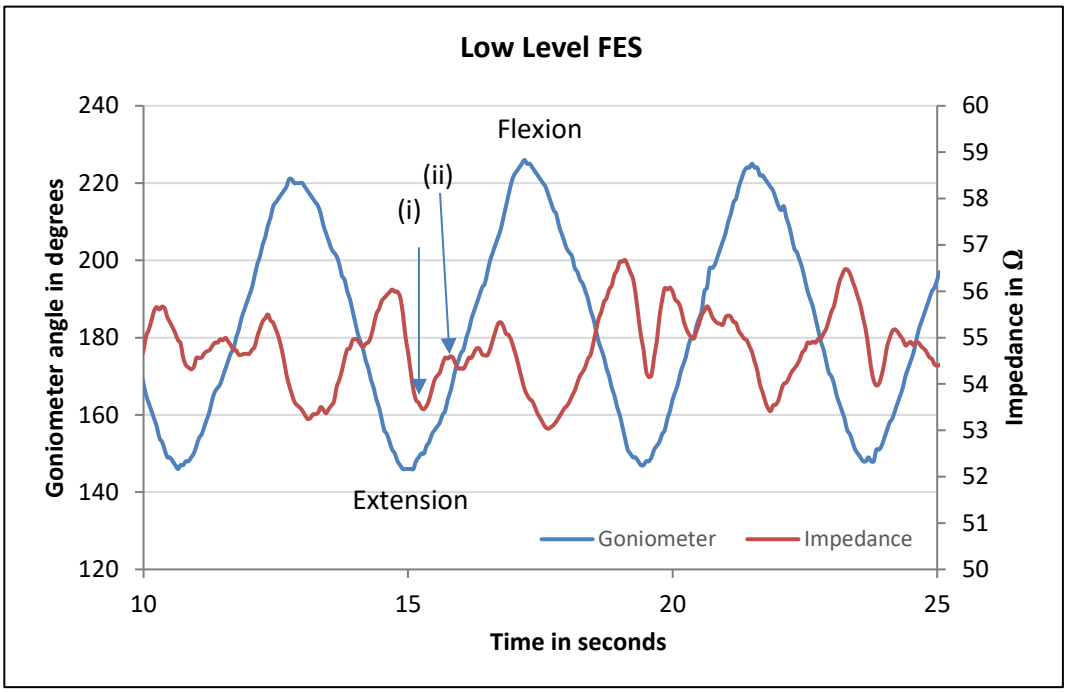

Figure 95 shows a section of the stimulated manipulation in greater detail. There is an upward swing in the bioimpedance associated with the change in direction of the wrist from as it reaches full extension (i). This is followed by fluctuations as the wrist passes the midway or neutral position (ii).

It should also be noted that although the extensor muscles were being stimulated the flexor muscles were not, so there would have been little or none of the normal antagonist activity associated with movement.

10.11 Bio-impedance measurements of a compound movement across the elbow joint

As a final investigation measurements were made of the bioimpedance across the elbow joint while functionally stimulating to produce the compound movement shown in Figure 11 on page 67. When using FES with electrodes in this position to open and reach out the arm it is important to know when the movement has reached an optimum limb position. If the FES were to continue increasing beyond this point it would results in hyper-extension of the elbow, which would cause high levels of discomfort while placing the limb in a less than functional position. The objective of

this investigation was to see if clinically useful measurements of the bioimpedance could be obtained for controlling the FES intensity to prevent the limb from being over stimulated into hyper-extension.

10.11.1 **Method**

FES electrodes were placed on the arm, positioned to produce a compound movement. The movement began by supinating of the forearm, then extended of the wrist while extending the elbow. The stimulation produces a smooth compound movement where each part of the movement overlapped into the next.

The limb was placed in a starting position prior to each repetition. The arm was held with the forearm pronated, and the wrist and elbow flexed. This is typical of the arm position that a hemiplegic patient would present with.

The electrical stimulation was delivered at frequency of 20Hz with an amplitude of 40V. The stimulation started at a 10µs pulse duration which was then progressively increased by 4µs steps with each new pulse. To give a ramping rate of 10 to 200µs pulse duration within a period of 2.5s.

The goniometer was placed across the elbow joint. With the elbow flexed it was at 80^0 and when extended was at 140^0

10.11.2 **Results**

The plot in Figure 96 shows the results for ten repetitions of the electrically stimulated upper-limb movement. The results show variability in the pattern of the bioimpedance between the repetitions with no immediately easily identifiable similarity of the features between repetitions.

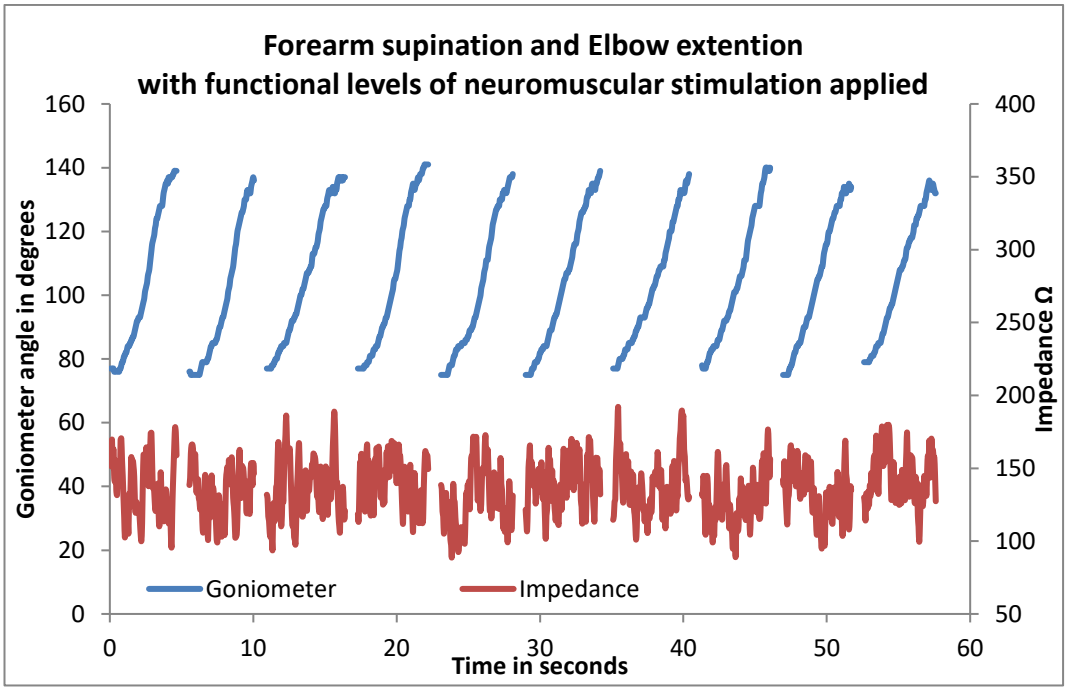

Figure 96 shows the bioimpedance and goniometer plots for ten electrically stimulated compound upper-limb movements about the elbow. The goniometer is measuring the elbow joint angle.

10.11.3 **Discussion**

The objective of the investigation was to determine whether it was possible to tell when the elbow had reached or was approaching 140^0 by from measuring changes in the bioimpedance.

This compound movement of the upper-limb is more complex than the wrist movements looked at previously. Which results in a more complex bioimpedance plot that is less easy to interpret than the plots for the wrist. There are features of the bioimpedance changes which can be seen to relate to parts of the movement when the expansion of three of the movements shown in Figure 97 is studied. Although there are similarities in the impedance plots for each repetition of the compound movement sequence these are not as immediately identifiable as for the results with the wrist.

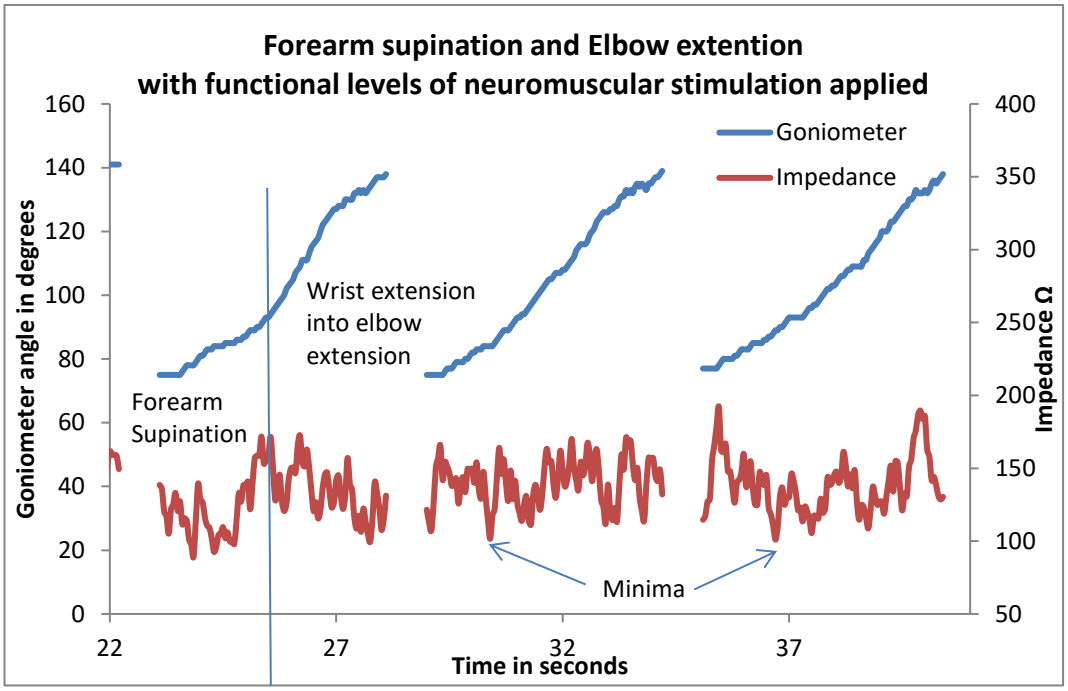

Figure 97 shows and expansion of three of the movements shown in Figure 96. There are identifiable minima relating to the supination of the forearm.

The impedance plots shows minima relating to the period when the forearm is supinating. This is followed about a second later by a series of peaks that are less easy to interpret but occur as supination ends and the wrist extends. In each case there is a trough as the elbow moves into extension and again this is not easily interpreted.

Whereas the wrist movement was produced by stimulation of two extensor muscles the compound elbow and arm movement was the result of stimulating many more. For the wrist movement the main changes with respect to the measurement conditions was the bellying of the extensor muscles beneath the position where the electrodes were placed. Whereas the upper-limb compound movement had electrodes placed either side of the elbow joint with the only muscle along the conduction path being Biceps Brachii, used for the supinator function. The relevance of this to the measured bioimpedance change is that the only muscle impedance measured was for the partially recruited Biceps Brachii near the beginning of the sequence. Whereas the later parts of the plots relate to impedance change across the elbow joint as it extends. The variability in the current path across the joint between repetitions could explain the differences seen in the plots for this part of the movement.

The ability to use the identified minima in the early stages of the sequence for determining forearm supination may be of clinical benefit. The method would need further refinement before it could be used reliably to control FES.

10.12 Isometric bioimpedance measurement

This investigation followed on from the results obtained in 10.2 for bioimpedance measurements made on a stationary limb. Measurements of bioimpedance were made during an isometric contraction of the extensor muscles of the forearm. The measurements were made under the three treatments studied previously of no stimulation, low-level stimulation and functional stimulation. The objective was to see how measurements of bioimpedance made during isometric contractions compared to bioimpedance measurements of muscle contractions that result in movement.

10.12.1 **Method**

The forearm was supported with hand and wrist in neutral position. A constraint was placed above the back of the hand to prevent extension about the wrist during isometric recruitment of the extensor muscles. The arrangement of the constraint is shown in Figure 98. The constraint was made strong enough to resist the maximum effort applied against it.

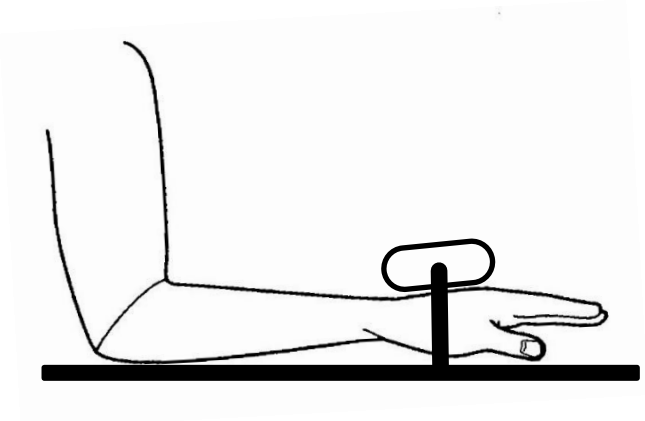

Figure 98 shows the arrangement used to prevent movement of the hand and wrist during isometric recruitment of the extensor muscles.

Isometric muscle contractions were made at maximum voluntary effort (MVE) and held for 20s while the bioimpedance measurements were made. MVE was chosen for the tests as it provided the best way to ensure consistency between each of the treatments. This is because any level of effort less than MVE could not be accurately quantified to ensure consistency. A five minute rest period was allowed between each treatment to give the muscles time to recover.

Measurements were taken for three treatment conditions,

- Isometric contraction with no electrical stimulation
- Isometric contraction with low-level electrical stimulation

- Isometric contraction with function levels of electrical stimulation with movement

The low-level stimulation was set at 20V with a pulse-duration of 175µs at a frequency of 20Hz. This level was chosen for sufficient to begin recruitment of the muscles but insufficient to produce movement.

The functional stimulation was set at 40V with a pulse-duration of 200µs at frequency of 20Hz. At this level the stimulation was high enough to produce involuntary movement.

In each case the subject was making MVE against the constraint at the start of the readings

10.12.2 **Results**

The three plots in Figure 99, Figure 100 & Figure 101 show the results for the bioimpedance for the three treatments.

The range of the readings is greater for the results where there was no electrical stimulation (Figure 99) having a spread of 2.7Ω. This was reduced by the low-level electrical stimulation (Figure 100) to 1.4Ω, and further reduced with functional electrical stimulation (Figure 101) to 0.93Ω.

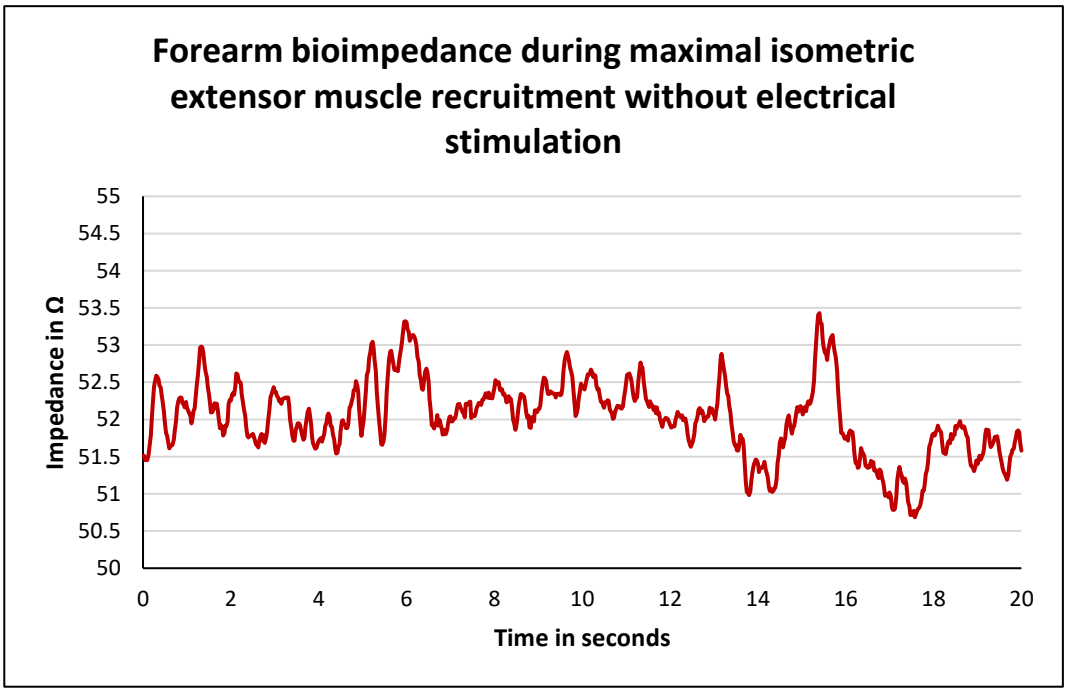

Figure 99 shows bioimpedance measurements made of the forearm during maximal isometric contraction of the extensor muscles without electrical stimulation.

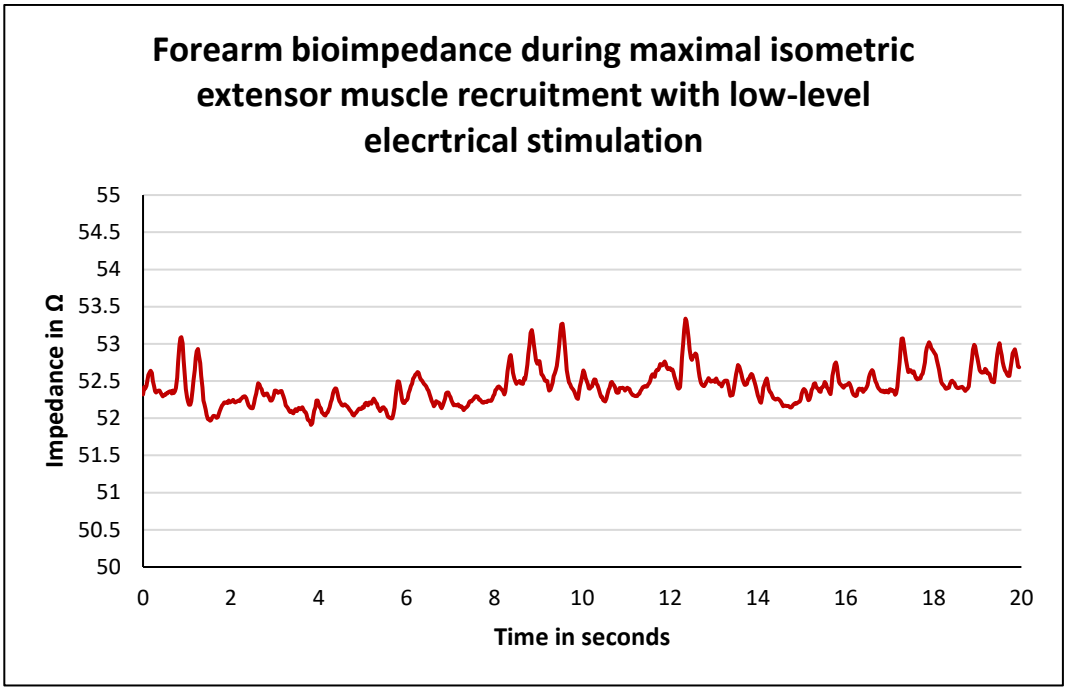

Figure 100 shows bioimpedance measurements made of the forearm during maximal isometric contraction of the extensor muscles with a low-level of electrical stimulation that was sufficient to recruit the muscles but not sufficient to produce movement.

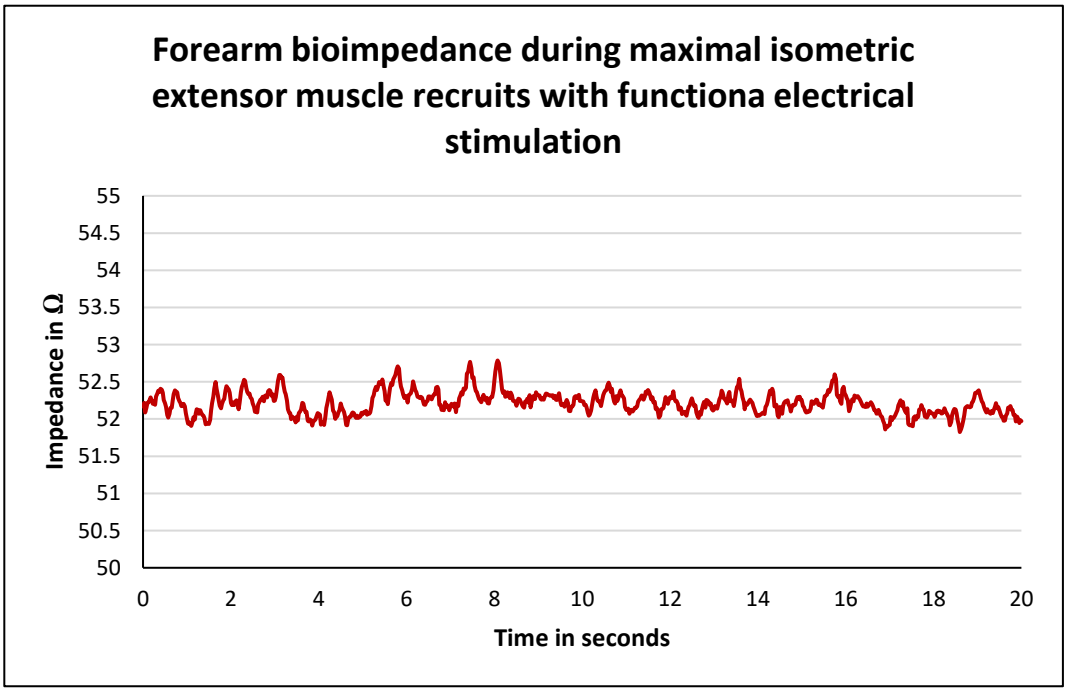

Figure 101 shows bioimpedance measurements made of the forearm during maximal isometric contraction of the extensor muscles with functional levels of electrical stimulation capable of producing movement had the joint not been constrained.

10.12.3 **Discussion**

The bioimpedance shows greatest fluctuation for the results with no electrical stimulation. The fluctuations are progressively reduced with the introduction of greater levels of stimulation.

There are a number of explanation to discuss to explain this observation.

The volitional movement was made using all of the extensor muscles in the forearm. Any small differences in the balance between how these were recruited could have influenced the path that the impedance measuring signal took through the limb. When the electrical stimulation was introduced an order was imposed upon the muscle recruitment reducing the variability of the current path for the measuring signal.

The way in which muscle is recruited volitionally compared to with electrical stimulation is different. When skeletal muscle is volitionally recruited over an extended contraction it is the slow twitch fibres that are predominately activated. When the body recruits this postural muscle it will introduce fibres into the contraction and then relax them as it introduces other fibres. This is done to prevent fatigue by resting fibres within the duration of the contraction. Electrical stimulation however favours the larger fast twitch fibres and will recruit these continuously for the duration of the contraction. This alteration of the muscle fibre recruitment could influence the current path taken by for the impedance measurement system. When the electrical stimulation is used that results in a more uniform fibre recruitment the current path of the impedance measuring signal will remain similarly uniform.

A final explanation could be due to how electropores are opened through the skin. The stratum corneum is a layer of the skin made up from many layers of cells. When an electrical potential is applied across these layers they become increasingly conductive. When the tissue has become conductive in this way an electropores is said to have been opened. The voltage of the impedance measurement signal is unlikely to have produced the same level of sustainably opened electropores as the functional levels of electrical stimulation. Meaning that variations in skin impedance could also be influencing the results.

The bioimpedance measurement across all of the treatments remains within a similar range. They also showed little variation over the duration of the isometric contraction. The accords with the observations from the previous studies where the bioimpedance was a poor indicator of absolute limb position, but showed relationship to dynamic change. In this case there was no dynamic change and the bioimpedance remained constant.

The results may have a clinical relevance in that they show that measurements of bioimpedance can be made from stimulated muscle that is being volitionally recruited. This has potential importance because a patient who is using an FES system is likely to have some weak use of the muscle for which they are using FES to provide additional assistance to.

10.13 Conclusions

The results in 10.2 demonstrated that it was possible to make measurements of bioimpedance using conventional FES hydrogel electrodes. Bioimpedance measurements made on a stationary forearm showed variations within a 2Ω range over a 50s period. When voluntary movements were made, the range of the bioimpedance increased to 5Ω. This was accompanied by some of the characteristics of the bioimpedance measurements relating to the pattern of movement. The position of the limb could not be determined from the bioimpedance measurement. This confirms the earlier findings that this method of bioimpedance measurement is a poor indicator of the absolute position of the limb. Moreover it also an unreliable method of capturing relative change for this type of voluntary movement.

The introduction of low-level neuromuscular electrical stimulation in 10.3 produced bioimpedance measurements with a close relationship to voluntary movements. The range of the measured bioimpedance was reduced to 2Ω by the electrical stimulation. The measured bioimpedance remained a poor indicator of absolute limb position.

When the neuromuscular electrical stimulation was administered at functional levels capable of producing involuntary movement of the limb in 10.4 the relationship between the bioimpedance measurements and the movement remained. When the bioimpedance measurement are plotted and compared to the limbs angular displacement about the wrist, there are easily identified minima relating to a functionally useful limb position. There is poor correlation between the measured bioimpedance and the angular displacement at the point where the minima occur, however using the timing of these minima it is possible to interpret the absolute position of the limb from the bioimpedance measurement alone.

When a bioimpedance tracking algorithm of the type given in 10.5 is used, a clinically useful position for the limb can be identified and the stimulation intensity reduced to arrest further movement. When the tracking algorithm was further enhanced to include modulated control of the electrical stimulation as in 10.6, it demonstrated closed-loop feedback control for maintaining the target angular displacement of the clinically useful limb position. The closed-loop control was

shown to be able to recover from external disturbances when maintaining this target displacement in 10.7, and also while the subject was blind folder in 10.8. The closed-loop control remained effective when tested over an extended period of 2 hours in 10.9. During the period the baseline of the bioimpedance measurement showed fluctuations that the closed-loop control was unaffected by.

Measurements of bioimpedance while the limb was manually manipulated by a third party in 10.10 were in line with previous results. When manipulated without electrical stimulation the bioimpedance showed a relationship to the movement but could not be used to determine position. When low-level electrical stimulation was introduced there were identifiable features of the bioimpedance that related to limb position.

Measurement of bioimpedance across the elbow of a stimulated limb in 10.11 produced no clinically useful results. There is some indication that the technique could identify supination of the forearm from Biceps Brachii activity.

Measurements of bioimpedance made during isometric contractions demonstrated more regular results from stimulated muscle. A clinically useful finding was that stable bioimpedance measurements could be made from functionally stimulated muscle while the subject was also volitionally recruiting the muscle.

Chapter 11: Closing discussion

In the literature review at the outset to this research it was concluded that FES is an established treatment and rehabilitation for patients with neurological disease that results in partial paralysis, which can be applied to functionally assist with the activities of daily living. The use of FES for the leg is well established, with many versions of dropped-foot systems in regular daily use. But there are less options available for FES for the arm existing outside of a clinical laboratory setting. This reflects the additional difficulties associated with administering and controlling electrical stimulation to produce functional results in the arm when compared the correcting a dropped-foot. Percutaneous FES electrodes placed on the skin are the simplest and most accessible clinical option for patients. A shortcoming is that the displacement of the electrodes from the muscle compared to implanted options introduces recruitment uncertainty, which can be further complicated by the non-linear response of muscles to the stimulation. These two confounding

factors compromise the use of simple open-loop control for upper-limb FES of the type found with dropped-foot systems. Closed-loop control strategies have been demonstrated to address these issues. With the feedback used for these systems derived from either MEMS sensors or Bio-signals. Both methods have potential application, to enable initiation and proportional control of FES assisted movement. An EMG will register volitional intent to move as well as having a dynamic component during subsequent movement, but does not readily provide information about limb position or the starting orientation prior to the movement. MEMS sensors are able to provide starting orientation and limb position information. They have proved effective but complex, meaning that they remain predominantly laboratory based with little wider clinical application. Bioimpedance has been demonstrated as a method for determining the extent of muscle contraction and so can be related to the joint angle to give limb position. Bio-signals in the form of EMG and bioimpedance have been shown to be effective but have proved difficult to use clinically with FES. Further investigation was needed to combine the benefits of the MEMS and bio-signal methods into a clinically useful solution.

There were two clinically functional upper-limb movements identified for the research. These were wrist extension with hand opening and elbow extension with wrist extension and hand opening. Practical methods to use FES to achieve these movements were understood but in both cases needed an effective control method for them to become clinically practical. The challenges were, for the wrist movement to identify a functional position and prevent hyper-extension, and for the elbow extension to ensure that bicep activation ends with supination before flexion is allowed to develop. Accurate control of these movements relies upon real-time tracking of the limb position. The limb position can be tracked either by monitoring movement of limb segments or inferred by determining joint angles. MEMS accelerometers were identified as a method for measuring human body movement. With modest processing and power requirements they are a practical solution for the type of battery powered ambulatory devices needed for a clinically useful device. With suitable signal conditioning information about the angular displacement of the limb can be extracted as well as recognising volitional gestural movements made by the wearer. Low pass filtering reveals changes relating to the displacement of the limb. High pass filtering provides the gesture movements.

When a pilot study was carried out to investigate the use of accelerometers for the control of FES assisted sequenced movements, it was in all cases found to be possible to initiate FES assisted hand opening from interpreting gestures made by the user. The accelerometers were also used to measure the angular displacement of the arm for controlling progress through the sequence of stimulated movement. The effect for the users of the system was to increase awareness of their

affected arm and improve their ability to perform daily activities. These are clinically important outcomes because long term recovery from a brain insult requires practicing movement so that neuroplasticity can take place within adjoining undamaged areas of the brain. A patient following brain trauma can be left with neglect for the affected limb, anything which works to overcome this neglect will have a benefits on rehabilitation outcomes.

Work done to investigate the role that EMG could have to integrate and improve control of upper-limb FES threw up some interesting results. An arrangement of electrodes to detect a muscle response during a stimulation pulse had been found by experimentally trying different positions and observing the effects. The configuration had created a current probe capable of detecting the effect of small changes in the impedance of the tissue of the limb. Results obtained from using this system invited further enquiry, because it offered the potential to address two commonly occurring problems encountered when attempting to use EMG as a control signal for FES. The first is the F-wave disturbance where a 'reflected' motor action potential generated at spinal cord level reinforces the EMG signal. When an electrical stimulation pulse is applied through the skin to excite a motor nerve for the purpose of evoking an action potential, the evoked potential will then travel along the nerve fibres in both directions, the antidromic portion is reflected back from the spine as a F-wave which further stimulates the muscle during the period when EMG needs to be measured and can lead to a positive feedback loop. The second issue is the antagonist muscle co-contraction known as the 'clasp-knife' effect. Failure to carefully control FES intensity around the point where the antagonist muscles begin to loose mechanical advantage can result in rapid and undesirable hyperextension. The current probe arrangement was influenced by changes in bioimpedance which showed relationship to joint angle. The ability to measure joint angle makes it possible to modulate the FES to maintain a target angle for the joint that avoids the problems of F-wave EMG reinforcement while detecting the threshold prior to onset of the clasp-knife effect.

Investigations into the relationship between bioimpedance changes and joint angle were carried out. At this stage the changes in impedance we being determined from changes in the stimulation pulse being applied for the FES. The results showed regions of linear relationship during the period when there was movement about the joint. Alignment reorganisation of the muscles and tendons in the forearm as the movement progressed lead to rapid changes in to current path taken between the skin surface electrodes producing spikes in the results of a higher frequency than the underlying movement. These were easily removed with low-pass filtering.

The subject of bioimpedance was studied further with the relative benefits of different measuring methods compared. The two probe method was taken forward for further study because it gave

better measured results local to the electrode site and had the potential to be used with conventional FES electrodes. For this investigation the stimulation pulse was replaced with an AC excitation signal to make the measurements with. A range of frequencies from 20 kHz to 50 kHz were tried for comparison. The results showed little relative variation between the different frequencies used for the sampling signal. This was a useful finding when considering the end goal for a clinically practical ambulatory system, because the processing and power requirement for sampling and processing a 20 kHz signal are significant lower than for a 50 kHz one should that become an issue. The next investigation combined this method of measuring the bioimpedance with FES to produce movement about the wrist joint. A clear relationship between the impedance changes taking place within the tissue of the limb and the position of the limb about the joint as measured by the goniometer was evident.

This led to the development of dedicated hardware better able to integrate with the requirements of the FES. This was an important stage in the research towards a system that would be clinically useful. The hardware was made up of the voltage multiplier and switching arrangement needed for the FES, the impedance measuring with isolation and a port for taking readings from the goniometer. Impedance calculations and readings from the goniometer were steamed in real-time to a PC for offline analysis. The system was calibrated and suitable sampling settings set to capture bioimpedance in real time from stimulated muscle while measuring the joint angle. The new hardware was then used to carry out a number of further investigations.

The practicality of using the hardware to measure bioimpedance with conventional FES electrodes was investigated. It effectively captured bioimpedance from a stationary forearm and established a baseline for the next stage in the investigation which looked at voluntary movement. The dynamic results for the bioimpedance showed some relationship to the movement but could not be used to interpret the absolute position of the joint. When this was repeated with a low-level of electrical stimulation the pre-tensioning of the extensor muscles served to produce bioimpedance changes with close relationship to the movement. The results did not relate well to the absolute position of the joint, but the sequence of peaks and troughs matched the movement. This was an important finding because it meant that relative changes within the bioimpedance dynamically related to joint position within the voluntary movement. This was further supported when the FES was increased to functional levels and the movements became evoked. A characteristic of the bioimpedance was observed to relate to a point where the wrist joint was approaching a functional position. When this point was statistically analysed two findings were made. The point at which the characteristic occurred showed close relationship to the joint angle. Whereas the value of the bioimpedance when the characteristic occurred showed no correlation

to the joint angle. These findings confirmed the previous observations that the bioimpedance measurements were a poor indicator of the absolute joint position, whereas the timing of the waveform characteristics showed close relationship. The importance of this finding was that for bioimpedance to be used as a control input for and FES system, the system would need to track for relative changes rather than look for absolute levels. When a tracking algorithm was implemented it was able to identify the target joint angle from the changes in the bioimpedance and reduce the FES intensity to prevent further progress. The algorithm was further improved to provide modulated control of the FES to maintain the target angle. This proved effective to external disturbances regardless of whether the subject was able to observe them or nor, and proved equally effective over an extended period. These were very important findings. In a real world application for the system to be clinically useful the stimulation will need to adapt to perturbation. As touched upon earlier, as part of rehabilitation clinicians will get patients to engage in two handed activity. This lessens to effect of neglect and encourages cortical reorganisation to occur. Typical tasks would be catching a ball or holding a tray. When catching a ball the weight in the hand suddenly increases requiring a control system capable of correcting for the additional load. Similarly when holding an empty tray that an object is then placed upon an adjustment is required.

When the investigation was repeated for a compound movement of the elbow is produced far less easy to interpret results. The movement was far more complex than the wrist movements looked at previously. Which resulted in more complex bioimpedance plots. There are features of the bioimpedance changes which can be seen to relate to the supinatory part of the movement and so could have clinical relevance.

The final investigation found that the bioimpedance showed little relative change during isometric muscle recruitment. This was an important finding because it showed that stable bioimpedance measurements could be made from functionally stimulated muscle while the subject was also volitionally recruiting the muscle. Clinically this is as important as the ability to recover from perturbation described above. FES is seldom used in isolation, more normally being applied to provide assistance to augment the patient's own efforts.

Chapter 12: Future work

The overall aim at the outset of this research was arrive at a clinically useful method for controlling upper-limb FES. The research demonstrated effective methods of using MEMS sensors

to capture and interpret patient's intentional gestures, and to use these to initiate sequences of FES. The attempt to use MEMS sensors track progress within a movement to provide sequenced patterns of stimulation was less than optimal, and only properly worked with very simple sequences. The MEMS system provided no feedback control to the FES, it functioned by switching between phases of a sequence based on passing pre-set thresholds with in the movement. FES intensity levels were pre-set for each part of the sequence.

The bioimpedance measuring system combined into an FES stimulator that was developed as part of this research demonstrated a practical and robust method for real-time tracking of limb joint angle while stimulating. The system was able to find and maintain a target joint angle and recover from external disturbance. It was demonstrated to work reliably over an extended period despite variation in the background bioimpedance.

The next task should be to combine the information about absolute limb position that can be obtained from MEMS sensors with the real-time control available from tracking measurements of bioimpedance. Clinically this would then provide an orthotic and rehabilitation device capable of adapting to patient requirements. The system could be set up on the patient and readings steamed from it for observation and interpretation on a PC. The clinician could then set threshold for the gesture recognition and limits for phases of the movement. Bioimpedance characteristics could then be identified for modulated control of the FES with the levels tuned to provide accurate movement. The current system was able to maintain the joint to within plus or minus ten degrees of the target. Functionally this adequate and represents a significant improvement over the patients existing ability to attain and maintain a given joint position. It should however be the subject of future work to refine the control algorithm to provide closer control to the target. Later on methods should be sought to automate as much of the initial set up as possible by making it self-tuning. Ideally the clinician would be able to place the system in learning mode and 'walk' to patient through the desired movement by manually influencing the extents and limits of each part the movement. The system would then attempt to replicate the movement until the clinician was satisfied. This matches the way in which clinicians like to work, with their focus remaining on the patient rather than the systems user interface.

Effort should also be put into refining the method the compound movement of the arm. The bioimpedance results did show some relation the supination of the forearm early in the movement. It would be useful to further investigate the later parts of the movement.

Chapter 13: References

Abbot, L. F., 1999. Lapicque's introduction of the integrate-and-fire model neuron (1907). *Brain Research Bulletin,* 50(5/6), pp. 303-304.

Abdul malik, N., Chappell, P. H., Wood, D. & Taylor, P. N., 2010. *Event detection for gluteal or hamstring stimulation during walking in neurological patients.* Vienna, The 15th Annual Conference of the International FES Society (IFESS).

Allin, J. & Inbar, G. F., 1986. FNS control schemes for upper limb. *IEEE Trans. Biomed. Eng.,* 33(9), pp. 818-828.

Alon, G. et al., 1998. Efficacy of a hybrid upper limb neuromuscular electrical stimulation system in lessening selected impairments and dysfunctionns consequent to cerebral damage. *Neurorehabil Neural Repair,* 12(2), pp. 73-79.

Alon, G., McBride, K. & Ring, H., 2002. Improving selected hand functions using a noninvasive neuroprothesis in persons with chronic stroke. *Journal of Stroke and Cerebovascular Diseases,* 11(2), pp. 99-106.

Alon, G. & Ring, H., 2003. Gait and Hand Function Enhancement Following Training with a Multi-Segment Hybrid-Orthosis Stimulation System in Stroke Patients. *Journal of Stroke and Cerebrovascular Diseases,* 12(5), pp. 209-216.

Aoyagi, Y. & Tsubahara, A., 2004. Therapeutic Orthosis and Electrical Stimulation for Upper Extremity Hemiplegia After Stroke: A Review of Effectiveness Based on Evidence. *Topics in Stroke Rehabilitation,* 11(3), pp. 9-45.

Axelgaard manufacturing company, 2015. *Axelgaard Education.* [Online]
Available at: http://www.axelgaard.com/Education

Bagwell, P. J. & Chappell, P. H., 1995. Real time microcontroller implementation of an adaptive myoelectric filter. *Med Eng Phys,* 17(2), pp. 151-160.

Bajzek, T. J. & Jaeger, R. J., 1987. Charecterisation and control of muscle responcse to electrical stimulation. *Annals of Biomedical Engineering,* Volume 15, pp. 485-501.

Baker, L. L. et al., 2000. *Neuromuscular Electrical Stimulation.* 4 ed. s.l.:Los Amigos Research and Education institute Inc..

Barker, R. N., Gill, T. J. & Brauer, S. G., 2007. Factors contributing to upper limb recovery after stroke: a survey of stroke survivors in Queensland Australia. *Disability and Rehabilitation,* 29(13), pp. 981-989.

Benton, L. A., Baker, L. L. & Waters, R. L., 1981. *Functional Electrical Stimulation - A Practical Clinical Guide.* Rancho Los Amigos, Downey CA: Ranchos Amigos Hospital Rehabilitation Engineering Center.

Bigland-Ritchie, B. et al., 1983. Changes in motoneurone firing rates during sustained maximal voluntary contractions. *J. Physiol.,* Volume 340, pp. 335-346.

Billian, C. & Gorman, P. H., 1992. Upper extremity applications of functional neuromuscular stimulation. *Assistive Technology,* 4(1), pp. 31-39.

Bohannon, R. W. & Smith, M. B., 1987. Interrator reliabilty of a modified Ashworth scale of muscle spacticity. *Phys. Ther.,* 67(2), pp. 206-7.

Bronner, S., 2003. *Instrumented Analysis of Human Movement,* Adam Centre Brooklyn: Long Island University.

Burridge, J. H. & Ladouceur, M., 2008. Clinical and Therapeutic Applications of Neuromuscular Stimulation: A Review of Current uUse and Speculation into Future Developments. *Neuromodulation,* 4(4), pp. 147-154.

Carpaneto, J. et al., 2003. A sensorized thumb for force closed-lood control of hand neuroprostheses. *IEEE Transactions on Neural Systems & Rehabilitation Engineering,* 11(4), pp. 346-353.

Chae, J. et al., 1998. Neuromuscular stimulation for upper extremity motor and functional recovery in acute hemiplegia. *Stroke,* Volume 29, pp. 975-979.

Chen, M. et al., 2010. *A foot drop FES envelope design method using tibialis anterior EMG during healthy gait with a new walking speed control strategy.* Buenos Aires, 32nd Annual International Conference of the IEEE EMBS.

Chen, R., Cohen, L. G. & Hallett, M., 2002. Nervous system reorganization following injury. *Neuroscience,* 111(4), pp. 761-773.

Chen, Y. L., Li, Y. C., Kuo, T. S. & Lai, S. L., 2001. The development of a closed-loop controlled FES in gait training. *Journal of Medical Engineering & technology,* 25(2), pp. 41-48.

Chou, L. W. & Binder-Macleod, S. A., 2007. The effects of stimulation frequency and fatigue on the force-intensity relationship for skeletal muscle. *Clinical Neurophysiology,* Volume 118, pp. 1387-1396.

Coutinho, A., Jotta, B., Pino, A. & Souza, M., 2012. *Behaviour of the electrical impedance myography in isometric contraction of biceps bracii at different elbow joint angles.* First Latin-American Conference on Bioimpedance (CLABIO 2012), Journal of Physics: Conference Series.

Crago, P. E., Mortimer, T. J. & Peckham, H. P., 1980. Closed-loop control of force during electrical stimulation of muscle. *IEEE Trans. Biomed. Eng.,* 27(6), pp. 306-312.

Dai, R. et al., 1996. Application of tilt sensors in functional electrical stimulation. *IEEE Trans. Rehabil. Eng.,* 4(2), pp. 63-72.

Delsys Inc., n.d. *Technical Note 103: EMG Signal Analysis.* Boston, MA: s.n.

Donaldson, N. et al., 2000. FES cycling may promote recovery of leg function after incomplete spinal cord injury. *Spinal Cord,* 2(38), pp. 680-2.

Feiereisen, P. & Duchateau, J., 1997. Motor unit recruitment order during voluntary and electrically induced contraction in the tibialis anterior. *Exp Brain Res,* 114(1), pp. 117-123.

Ferrari de Castro, M. C. & Cliquet, A., 2000. Artificial grasping system for the paralysed hand. *Artificial Organs,* 24(3), pp. 185-188.

Ferrari de Castro, M. C. & Cliquet, A., 2000. Artificial grasping system for the paralysed hand. *Artif. Organs.,* 24(3), pp. 185-188.

Folstein, F. S. & McHugh, P. R., 1975. Mini-Mental State - A practical method for grading the cognitive state of patients for clinicians. *J. Physiol. Res,* Volume 12, pp. 189-198.

Frick, H. & Morse, S., 1926. The electric capacity of tumours of the breast. *Cancer Research,* Volume 16, pp. 340-376.

Fugelvand, A. J. & Keen, D. A., 2003. Re-evaluation of muscle wisdom in human adductor pollicis using physiological rates of stimulation. *J Physiol,* 549(3), pp. 865-875.

Galvani, L., 1842. *Collezione delle Opera.* http://books.google.com/ ed. Bologna: Academia delle Scienze dell' Instuto.

Gregory, C. M. & Bickel, C., 2005. Recruitment patterns in hman skeletal muscle during electrical stimulation. *Physical Therapy,* 85(4), pp. 358-364.

Grill, W. M. & Mortimer, T. J., 1996. The Effect of Stimulus Pulse Duration on Selectivity of Neural Stimulation. *IEEE Transactions on Biomedical Engineering,* 43(2), pp. 375-385.

Halligan, P. W. B. & Cockburn, J., 1990. A short screening test for visual neglect in stroke patients. *Int. Disabil. Stud.,* 12(3), pp. 95-99.

Hart, R. L., Kilgore, K. L. & Peckham, P. H., 1998. A comparison between control methods for implanted FES hand-grasp systems. *IEEE Trans. Rehabil. Eng.,* 6(2), pp. 208-218.

Hendricks, H. T., IJzerman, M. J., de Kroon, J. R. & Zilvold, G., 2001. Functional electrical stimulation by means of the 'Ness Handmaster Orthosis' in chronic stroke patients: an exploratory study. *Clinical Rehabilitation,* 15(1), pp. 217-220.

Hodgkin, A. L., 1954. A note on conduction velocity. *J. Physiol.,* Volume 125, pp. 221-224.

Hodgkin, A. L. & Huxley, A. F., 1952. A quantitative description of membrane current and its applications to conduction and excitation in nerve. *J. Physiol.,* Volume 117, pp. 500-544.

Holsheimer, J. et al., 2000. *Implantable dual channel peroneal nerve stimulator.* Ljubljana, Proceedings of the Ljubljana Fes Conference.

Hussain, Y., 2013. *Measurement of the electrical impedance between two electrodes attached to the skin's surface,* University of Southampton: A report submitted for the award of MEng Electronic Engineering.

International Functional Electrical Stimulation Society (IFESS), 2002. *INTRODUCTION AND HISTORY OF FUNCTIONAL ELECTRICAL STIMULATION [FES].* [Online]
Available at: http://ifess.org/sites/default/files/general_considerations.pdf

Jones, D. A., Bigland-Ritchie, B. & Edwards, R. H. T., 1979. Excitation frequency and muscle fatigue: mechanical responces during voluntary and stimulated contractions. *Exp Neurol,* Volume 64, pp. 401-413.

Kamat, D. F. D. B. P. P. M., 2014. Blood Glucose Measurement Using Bioimpedance Techniques. *Advances in Electronics,* Volume 2014, p. 5.

Kebaetse, M. B. & Binder-Macleod, S. A., 2004. Strategies that improve human skeletal muscle performance during repetitive non-isometric contractions. *Arch J Physiol ,* Volume 448, pp. 525-532.

Kebaetse, M. B., Lee, S. C. K. & Binder-Macleod, S. A., 2001. A Novel stimulation pattern improves performance during repetitive dynamic contractions. *Muscle and Nerve,* Volume 24, pp. 744-752.

Keith, M. W., 2001. Neuroprostheses for the upper extremity. *Microsurgery,* 21(6), pp. 256-263.

Keller, T. & Kuhn, A., 2008. Electrodes for transcutaneous (surface) electrical stimulation. *Journal of Automatic Control,* 18(2), pp. 35-45.

Kimberley, T. J. et al., 2004. Electrical stimulation driving functional improvements and cortical changes in subjects with stroke. *Exp Brain Res,* Volume 154, pp. 450-460.

Kim, K. et al., 2004. *A New Bio-impedance Sensor Technique for Leg Movement Analysis.* Melbourne, IEEE ISSNIP.

Kim, S. C. et al., 2003. Optimum electrode configuratio for detection of arm movement using bio-impedance. *Med. Biol. Eng. Comput.,* Volume 41, pp. 141-145.

Knaflitz, M., Merletti, R. & De Luca, C. J., 1990. Inference of motor unit recruitment order in voluntary and electrically elicited contractions. *American Physiological Society,* 68(4), pp. 1657-1667.

Konrad, P., 2005. *A Practical Introduction to Kinesiology Electromyography.* s.l.:Noraxon, USA.

Kraft, G. H. & Hammond, M. C., 1992. Techniques to improve function of the arm and hand in chronic stroke. *Arch Phys Med Rehabil,* 73(3), pp. 220-227.

Krakauer, J. W., 2005. Arm function after stroke: from physiology to recovery. *Seminar in Neurology,* 25(4), pp. 384-395.

Kyle, U. G. et al., 2004. ESPEN Guidlines - Bioelectrical impedance analysis - part 1: review of principles and methods. *Clinical Nutrition,* Volume 23, pp. 1226-1243.

Lane, R. P., 2012. Multisensor Controls Advance Ambulatory System Designs. *European Medical Device Technology,* March, 3(2), pp. 8-12.

Lane, R. P. & Chappell, P. H., 2013. *Apparatus for use for providing information on at least one muscle in a patient.* PCT, Patent No. PCT/GB2013/000325.

Lane, R. P., Esnouf, J. & Taylor, P. N., 2006. *Use of accelerometry to control an FES device for restorationof hand function following stroke.* Miyagi-Zao, Japan, Annual Conference of the International FES Society.

Lane, R. P. et al., 2011. *Apparatus for functional electrical stimulation of the body.* International PCT/GB, Patent No. WO 2011/042736 A1.

Lane, R. P. & Nolan, D., 2009. *EMG device for controlling equipment.* UK, Patent No. WO2009093063 (A1).

Lane, R. P. & Taylor, P. N., 2004. *Issues surrounding the proportional control of surface FES from surface measurements of EMG.* Boston, Annual ISEK Conference .

Lapicque, L., 1907. Recherches quantitatives sur l'excitation electique des nerfs traitee comme une polarization. *J. Physiol. Pathol. Gen,* Volume 9, pp. 620-635.

Lee, R. G. & Donkelaar, P., 1995. Mechanisms underlying functional recovery following stroke. *Canadian Journal of Neurological Science,* 22(4), pp. 257-263.

Lieberson, W. T., Scot, D. & Dow, M., 1961. Functional electrotherapy: stimulation of the peroneal nerve synchronised with the swing phase of the gait of hemiplegic patients. *Arch Phys Med Rehabil,* 101(5), p. 42.

Li, L., Tong, K. Y. & Hu, X., 2008. The effect of poststoke impairments on brachialis muscle architecture as measured by ultrasound. *Arch Phys Med Rehabil,* Volume 88, pp. 243-250.

Lyons, G. M., Sinkjær, T., Burridge, J. H. & Wilcox, D. J., 2002. A review of portable FES-based neural orthosis for the correction of dropped foot. *IEEE Trans Neural Syst Rehabil Eng,* 10(4), pp. 260-79.

Mann, G. E., Taylor, P. N. & Lane, R. P., 2011. Accelerometer triggered electrical stimulation for Reach and Grasp in chronic stroke patients. *Neurorehabil Neural Repair,* 25(8), pp. 774-780.

Mann, G., Lane, R. P. & Taylor, P. N., 2008. *A Feasibility study to asses the effect of Accelerometer Triggered Electrical Stimulation on Recovery of Upper Limb function in Chronic Stroke Patients.* Frieberg, International Functional Electrical Stimulation Society.

Mansfield, A. & Lyons, G. M., 2003. The use of accelerometry to detect heel contact events for use as a sensor in FES assisted walking. *Med. Eng. Phys.,* 25(10), pp. 879-885.

Marion, A., 1991. *An Introduction to Image Processing.* s.l.:Chapman and Hall.

McNeal, D. R., 1976. Analysis of a Model for Excitation of Myelinated Nerve. *IEEE Trans Biomed Eng,* 23(4), pp. 329-337.

Mendell, L. M., 2005. The size principle: a rule describing the recruitment of motorneurons. *J. Neurophysiol,* Volume 93, pp. 3024-3026.

Moe, J. H. & Post, H. W., 1962. Functional electrical stimulation for ambulation in hemiplegia. *J Lancet,* Volume 82, pp. 285-288.

Munih, M. & Ichie, M., 2001. Current Status and Future Prospects for Upper and Lower Extremity Motor System Neuroprostheses. *Neuromodulation,* 4(4), pp. 176-186.

Nahrstaedt, H. et al., 2008. Automatic Control of a Drop-Foot Stimulator Based on Angle Measurement Using Bioimpedance. *Artificial Organs,* 32(8), pp. 649-654.

Naito, A., 2004. Electrophysiological studies of muscles in the human upper limb: the biceps brachii. *Anatomical Science International,* Volume 79, pp. 11-20.

Nakamura, T., Yamamoto, Y., Yamamoto, T. & Tsuji, H., 1992. Fundmental characterististics of human limb electrical impedance for biodynamic analysis. *Med & Biol.Eng & Comput.,* Volume 30, pp. 465-472.

Nudo, R. J., 2006. Plasticity. *Journal of the American Society for Experimental Therapeutics,* Volume 3, pp. 420-427.

Ohta, M. et al., 2005. Study on the Application of the Bio-impedance Method for the Estimation of Tendon Elongation. *International Journal of Sport and Health Science,* Volume 3, pp. 296-303.

O'Keeffe, D. T. & Lyons, G. M., 2002. A versatile drop foot stimulator for research applications. *Med. Eng. Phys.,* 24(3), pp. 237-242.

Parker, P. A. & Scott, R. N., 1986. Myoelectric control of protheses. *Crit. Rev. biomed. Eng.,* Volume 13, pp. 293-310.

Popovic, M. B., 2003. Review - Control of neural protheses for reaching and grasping. *Med. Eng. Phys.,* 25(1), pp. 41-50.

Popovic, M. B. et al., 2002. Restitution of reaching and grasping promoted by functional electrical therapy. *Artif Organs,* 26(3), pp. 271-5.

Popovic, M. B., Popovic, D. B., Schwirtlich, L. & Sinkjaer, T., 2004. Functional Electrical Therapy (FET): Clinical Trial in Chronic Hemiplegic Subjects. *Neuromodulation,* 7(2), pp. 133-140.

Popovic, M. B., Popovic, D. B., Sinkjaer, T. & Stefanovic, A., 2002. Restitution of reaching and grasping promoted by functional electrical therapy. *Artif. Organs,* 26(3), pp. 271-275.

Popovic, M. B., Popovic, D. B. & Tomovic, R., 2002. Control of arm movement: reaching synergies for neuroprothesis with life-like control. *Journal of Automatic Control,* 12(1), pp. 9-15.

Popovic, M. R., Popovic, D. B. & Keller, T., 2002. Neuroprotheses for grasping. *Neurological Research,* 24(5), pp. 443-52.

Popovic, M. R. et al., 2005. Neuroprosthesis for Retraining Reaching and Grasping Functions in Severe Hemiplegic Patients. *Neuromodulation,* 8(1), pp. 58-72.

Porcari, J. P. et al., 2005. The Effect of Neuromuscular Electrical Stimulation training on Abdominal Strength, endurance, and sellected Anthropometric measures. *Journal of Sports Science and Medicine,* 4(1), pp. 66-75.

Preedy, V., 2012. *Handbook of Anthropometry: Physical Measures of Human Form in Health and Disease.* ISBN 144191788, 9781441917881 ed. s.l.:Springer Science & Business Media.

Prochazka, A., 1993. Comparison of natural and artificial control of movement. *IEEE Trans. Rehabil. Eng.,* 1(1), pp. 7-17.

Quintern, J., Riener, R. & Rupprecht, S., 1997. Comparison of simulation and experiments of different closed-loop strategies for functional electrical stimulation: experiments in paraplegics. *Artificial Organs,* 21(3), pp. 232-235.

Rakos, M. et al., 1999. Electromyogram-controlled functional electrical stimulation for treatment of paralysed upper extremity. *Artif. Organs,* 23(5), pp. 466-469.

Riener, R. & Quintern, J., 1997. A physiologically based model of muscle activation verified by electrical stimulation. *Bioelectrochemistry and Bioenergetics,* Volume 43, pp. 257-264.

Rushton, W. A. H., 1951. A theory of the effects of fibre size in medullated nerve. *J. Physiol.,* Volume 115, pp. 101-122.

Rutkove, S. B., Aaron, R. & Shiffman, C. A., 2002. Localised bio-impedance analysis in the evaluation of neuromuscular disease. *Muscle and Nerve,* 25(3), p. 390.397.

Rutkove, S. B., Fogerson, P. M., Garmirian, L. P. & Tarulli, A. W., 2008. Reference values for 50kHz electrical impedance myography. *Muscle Nerve,* Volume 38, pp. 1128-1132.

Saebo Inc., 2012. *EMG RETS feedback electrical stimulation system.* Charlette, NC: s.n.

Saxena, S., Nikolic, S. & Popovic, D., 1995. An EMG-controlled grasping system for tetraplegics. *Journal of Rehabilitation Research and Development,* 32(1), pp. 17-24.

Schuettler, M., Stieglitz, T. & Meyer, J., 1999. *A Multipolar Precision Hybrid Cuff Electrode for FES on Large Peripheral Nerves.* Atlanta, GA, USA, Proceedings of the First BMES/EMBS Conference Serving Humanity, Advancing Technology..

Seeberger, L. C., 2005. Cerebellar Tremor - Definition and Treatment. *CNI Review,* pp. 29-34.

Seward, B. & Rutkove, M., 2009. Electrical Impedance Myography: Background, Current State, and Future Directions. *Muscle Nerve,* 40(6), pp. 936-946.

Shiffman, C. A. et al., 1999. Resistivity and phase in localized BIA. *Phys. Med. Biol.,* Volume 44, pp. 2409-2429.

Shiffmann, C. A., Kashuri, H. & Aaron, R., 2008. Electrical impedance myography at frequencies up to 2 MHz. *Physiol. Meas.,* Volume 29, pp. 345-363.

Simcox, S. et al., 2005. Performance of orientation sensors for use with a functional electrical stimulation mobility system. *J. Biomech.,* 38(5), pp. 1185-1190.

Sinkjaer, T. et al., 2003. Biopotentials as command and feedback signals in functional electrical stimulation systems. *Med. Eng. Phys.,* 25(1), pp. 29-40.

So, C. F. C. K. S. W. T. K. S. C. J. W. Y., 2012. Recent Advances in Noninvasive Glucose Monitoring. *Medicla Devices: Evidence and Research,* Volume 5, pp. 45-52.

Song, C. G., Kim, S. C., Nam, K. & Kim, D. W., 2005. Optimum electrode configuration for detection of leg movement using bio-impedance. *Physiol Meas.,* pp. 59-68.

Song, T. et al., 2005. *Effects of pulse waveforms and muscle lengths on muscle force and fatigue resistance.* Montreal, 10th Annual Conference of the International FES Society.

Sweeney, P. C., Lyons, G. M. & Veltink, P. H., 2000. Finite state control of functional electrical stimulation for the rehabilitation of gait. *Med. Biol. Eng. Comput.,* 38(2), pp. 121-126.

Szlavik, R. B. & de Bruin, H., 1999. The effect of stimulus current pulse width on nerve fibre size recruitment patterns. *Med. Eng. Phys.,* Volume 21, pp. 507-515.

Tarulli, A. et al., 2005. Electrical impedance myography in the bedside assesment of inflammatory myopathy. *Neurology,* Volume 65, pp. 451-452.

Taylor, P. N. & Chappell, P. H., 2004. *Variations in system gain when using voluntary EMG to control electrical stimulation of the same muscle.* Bournemouth, UK, The 9th Annual Conference of the International FES Society (IFESS).

Thorsen, R., 1999. An artefact suppressing fast-recovery myoelectric amplifier. *IEEE Trans. Biomed. Eng,* 46(6), pp. 764-766.

Thorsen, R., Spadone, R. & Ferrarin, M., 2001. A pilot study of myoelectrically controlled FES of upper extremity. *IEEE Trans. Neural. Syst. Rehabil. Eng.,* 9(2), pp. 161-168.

Tong, K. Y., Mak, A. F. T. & Ip, W. Y., 2003. Command control for functional electrical stimulation hand grasp systems using miniture accelerometers and gyroscopes. *Med. Biol. Eng.,* 41(6), pp. 710-717.

Uhlir, J. P., Triolo, R. J., Davies, J. A. & Bieri, C., 2004. Performance of epimysial stimulating electrodes in the lower extremities of individuals with spinal cord injury.. *IEEE Trans Neural Syst Rehabil Eng.,* 2(12), pp. 279-87.

Vanhoest, A. & Donaldson, N., 2003. *Cross-talk in Nerve Root Stimulator Implants.* Bournemouth, UK., 9th Annual Conference of the Internatiional FES Society.

Veltink, P. H. et al., 2003. Three dimensional inertial sensing of foot movements for automatic tuning of a two-channel implantable drop-foot stimulator. *Med. Eng. Phys.,* 25(1), pp. 21-28.

Waters, R. L., 1984. The enigma of "carry-over". *Disability and Rehabilition,* 6(1), pp. 9-12.

Winter, D. A., 1990. *Biomechanics and Motor Control of Human Movement.* Second Edition ed. s.l.:Wiley.

Appendix A An introduction to neuromuscular electrical stimulation and its functional use as Functional Electrical Stimulation

For patients where the peripheral nervous system is intact, it is possible to produce movement in paralysed muscles by electrically stimulating the associated motor nerves, a process referred to as neuromuscular electrical stimulation (NMES). Paralysed muscle can be stimulated in this way to produce sequenced movement patterns. When done to produce patterns of movement that are functionally useful for the recipient, the technique becomes functional electrical stimulation (FES).

For a motor signal or action potential to reach a muscle from the brain both the central nervous system (CNS) and the peripheral nervous system (PNS) must be intact. Any break in the chain will result in the action potential failing to arrive and cause a muscle to remain flaccid. When this damage is confined to the CNS as is the case for stroke and spinal cord injuries (SCI) the action potentials can be artificially induced in the nerve bundles of the PNS (Figure 102) using electrical stimulation.

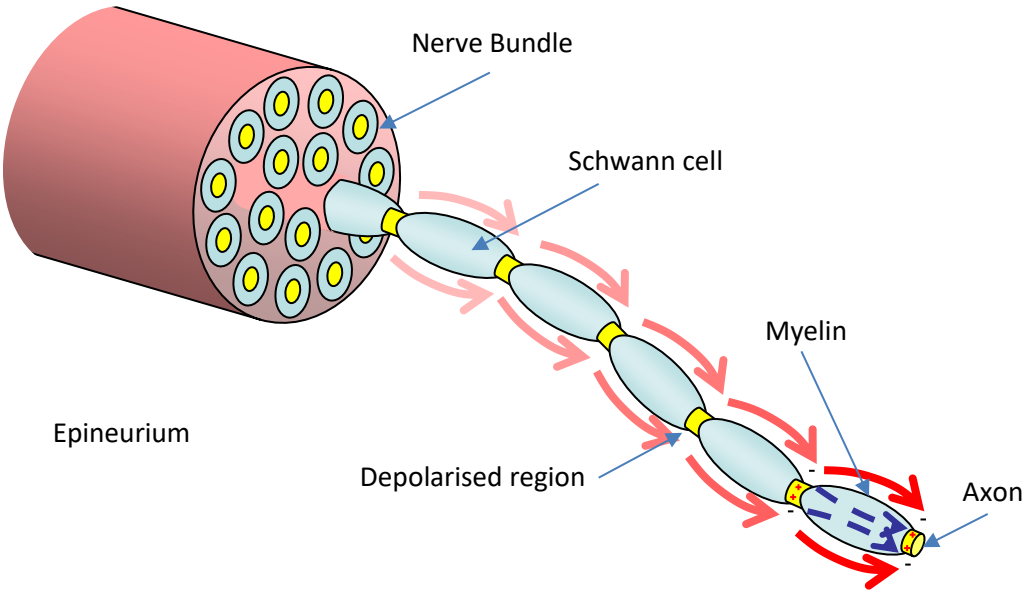

Figure 102 - Cross-section of a peripheral nervous system nerve bundle showing an individual nerve fibre. The red arrows are indicating how an action potential is propagated.

The electrical stimulation is created by rapidly switching a voltage on and off between two electrodes positioned adjacent to the nerve bundle. The effect is to rapidly change the electrical field around the nerve causing polarisation and depolarisation of the Swann cells which in turn evokes the action potentials (Figure 102). These invoked action potentials travel down the nerve fibre in the same way as the real action potentials and will produce similar muscle contractions.

By carefully selecting the nerve to stimulate it is possible to target the response to a particular muscle or muscle group. The effect of the stimulation can be controlled by changing the intensity or the frequency of the pulses.

There are two methods for positioning the stimulation electrodes adjacent to the nerve. The simplest and most widely used is to apply contact electrodes directly to the surface of the skin (Figure 103). The position of the electrodes is then adjusted until the desired result is achieved. A drawback with this method is the skill required to find the best electrode position. The electrical field has to propagate through the skin and subcutaneous layers to reach the required nerve. However it can often 'spill over' and effect adjacent nerves to cause undesired movements. Finding the best electrode position can be time consuming. It should be noted however that with sufficient practise most people can quickly become proficient at achieving the desired results.

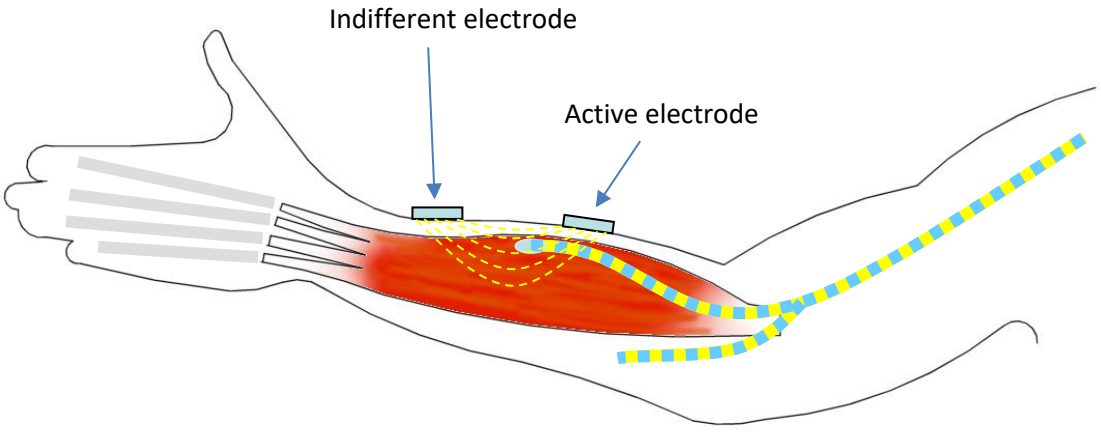

Figure 103 - Skin surface electrodes positioned to produce an electrical field around the nerve and motor-point of the main extensor muscle in the arm. Stimulating the posterior interosseous nerve will cause the hand to open.

The advantages of surface stimulation are;

- Simple to use
- Non-invasive
- Cost effective
- Flexible

The disadvantages are;

- Can be awkward to set up
- Poor cosmetic appearance because the electrodes and wires can be considered unsightly

The second technique is to place the electrodes directly onto the nerve bundle, inside the body. For clinical investigation work this can be done by using percutaneous or transcutaneous electrodes that penetrate the skin. A more permanent arrangement is to surgically implant the electrode and the stimulator into the patient (Figure 104).

This method of neuro muscular stimulation offers several advantages over the surface systems;

- Set-up time is not required for positioning electrodes
- The selectivity of the stimulation is much more precise as the electrical field is confined to the area of the nerve being stimulated,
- The electrodes can usually be positioned on the nerve bundle in such a way that less afferent nerves are recruited and 'pain' signals are not sent back to the brain. Unlike surface stimulation where the sensory receptors close to the skin surface are always inevitably excited.

The disadvantages of the technique are;

- Increased complexity of the stimulators required for implanting,
- Implants are costly,
- Patients have to submit to surgery.

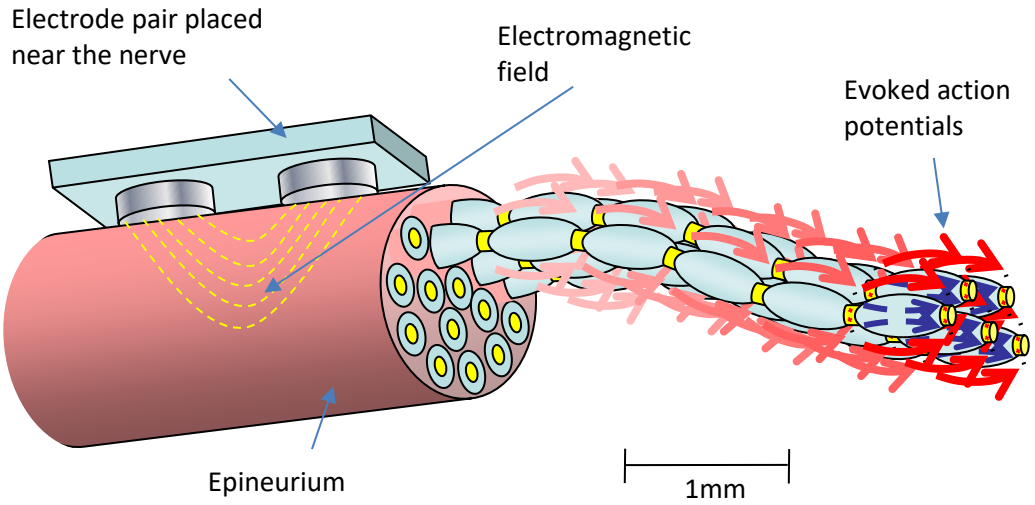

Figure 104 - Implanted electrode positioned in direct contact with the nerve bundle, the electrical field is confined to immediate area of the target nerve.

Typically the electrical stimulation provided is delivered as a stream of short duration pulses with a regular interval between them. Each of these individual bursts of energy causes polarisation of the nerve evoking an action potential that travels to the muscle. The characteristics of the stimulation can be altered by changing, the pulse width, level of the output current or the frequency of the stimulation pulses (Figure 105).

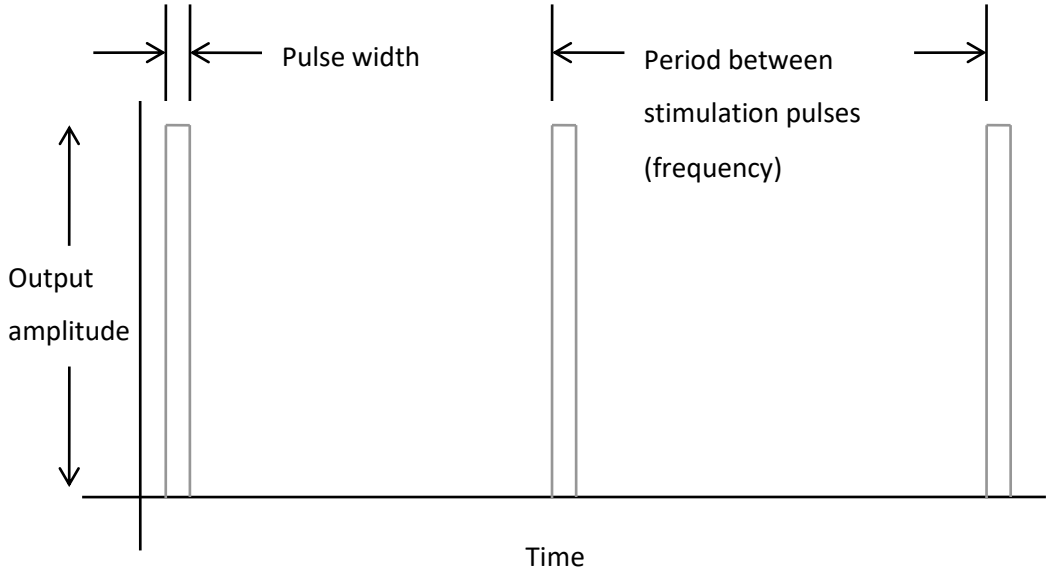

Figure 105 - Graphical portrayal of three successive stimulation pulses

It is desirable to avoid a sudden onset of stimulation at the start of a train of pulse as this can be uncomfortable, is sometimes alarming for the patient and can result in unhelpful reflex responses. A method for achieving a smooth commencement of stimulation is to ramp up the output over a short period by steadily increasing the pulse width (Figure 106).

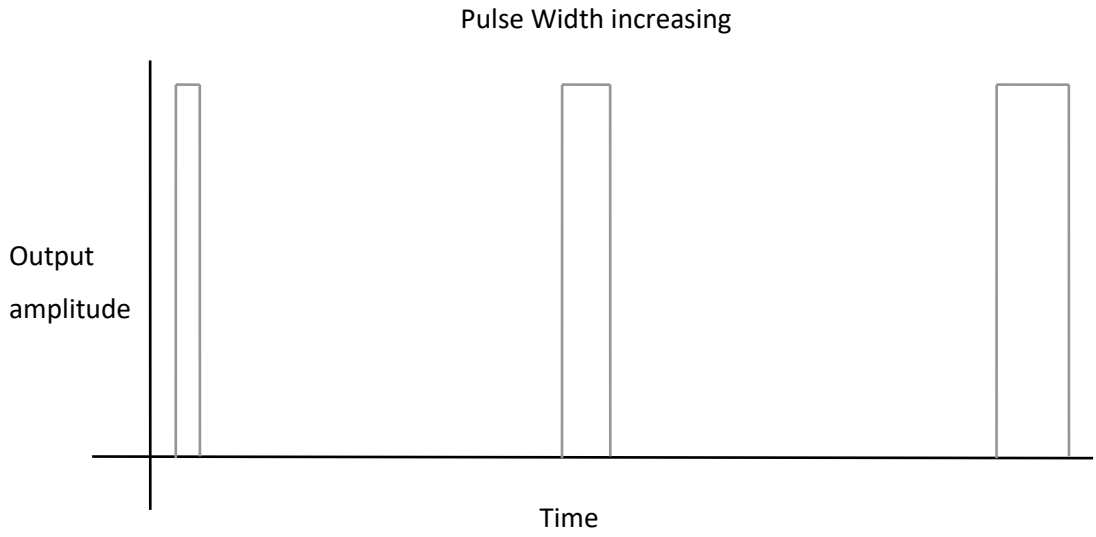

Figure 106 - To avoid a sudden onset of stimulation the pulse width increases over successive pulses to provide a controlled 'ramping' of the stimulation.

Another way to illustrate this technique is to put the pulse width on the vertical scale which then shows how the pulse width changes at the beginning and end of a stream of stimulation pulses (Figure 107).

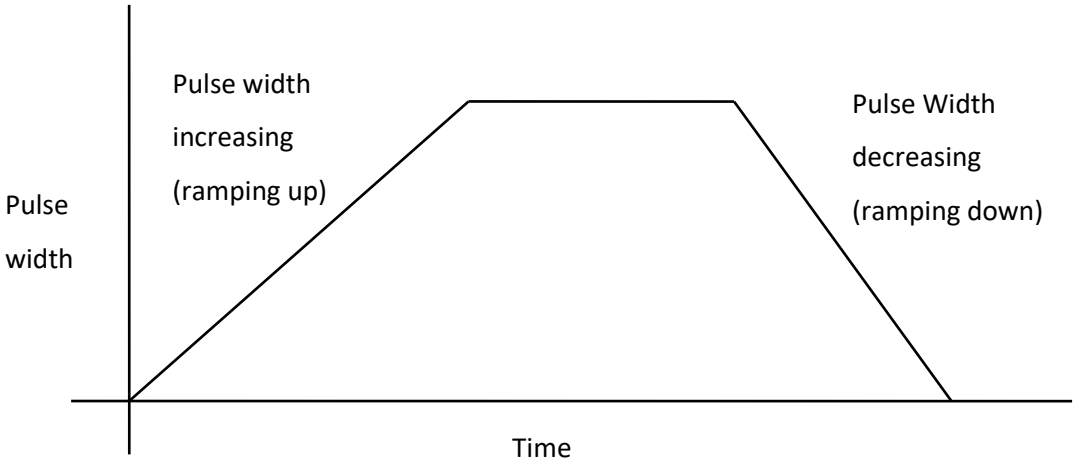

Figure 107 - An alternative way to depict the stimulation is to display the output envelope with the changes in pulse width shown on the y-axis.

The pulses are typically up to 350µs in duration and delivered at a frequency of up to 60Hz although 40Hz is normal (Figure 108). When skin surface electrodes are used these must be carefully positioned above the nerve to be excited.

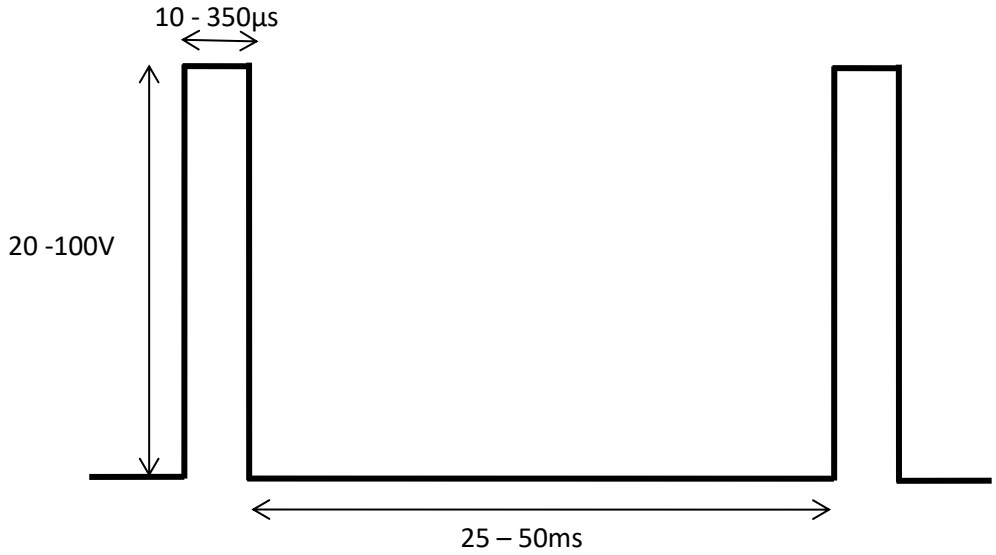

Figure 108 - Typical stimulation values used for skin surface electrode stimulation, for implanted systems the voltage will be in the 5 – 20V range.

Appendix B Integrated Bioimpedance and FES system Circuit diagram and Circuit layout

B.1 Circuit diagrams

B.1.1 AD5933 Impedance measurement circuit

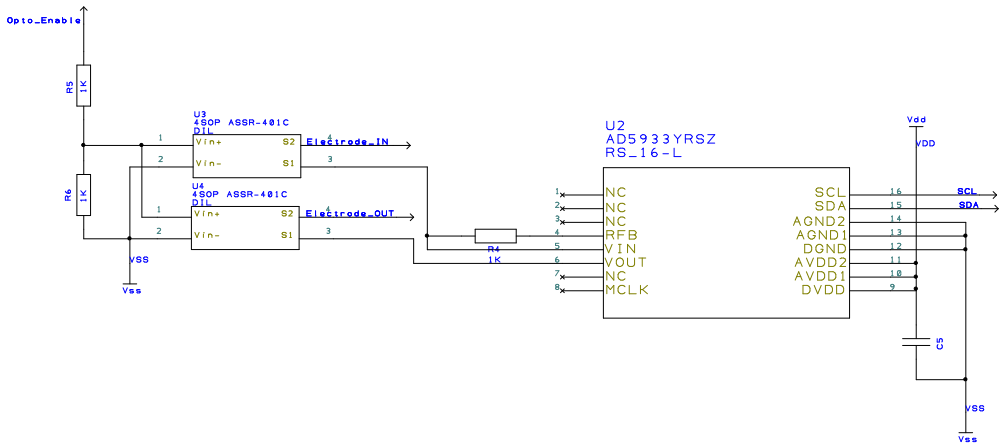

B.1.2 Boost regulator

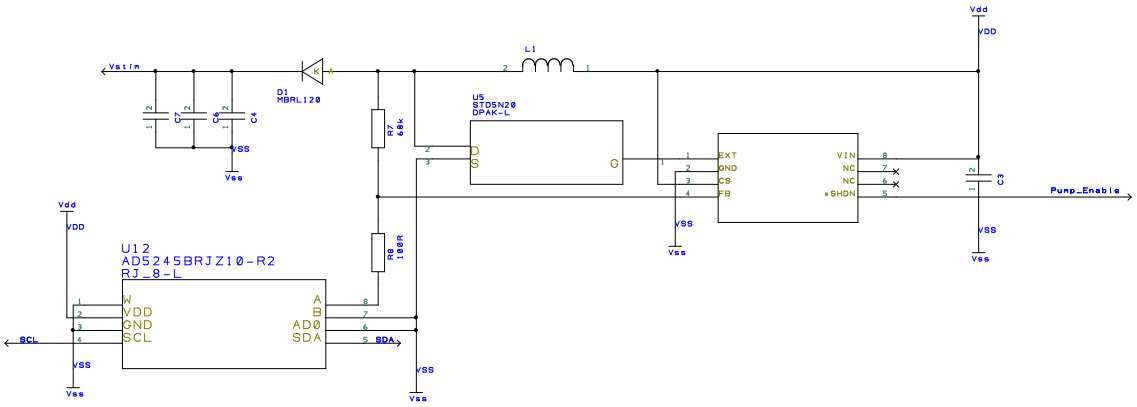

B.1.3 H-Bridge

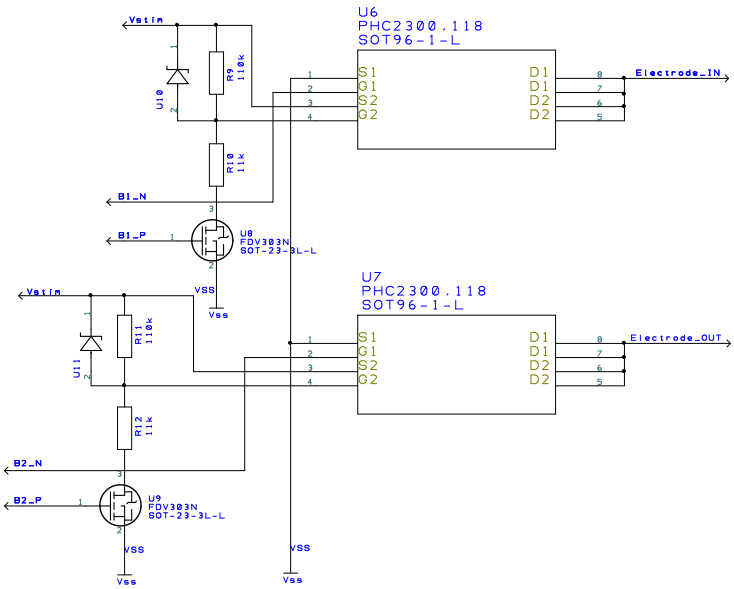

B.1.4 Microcontroller

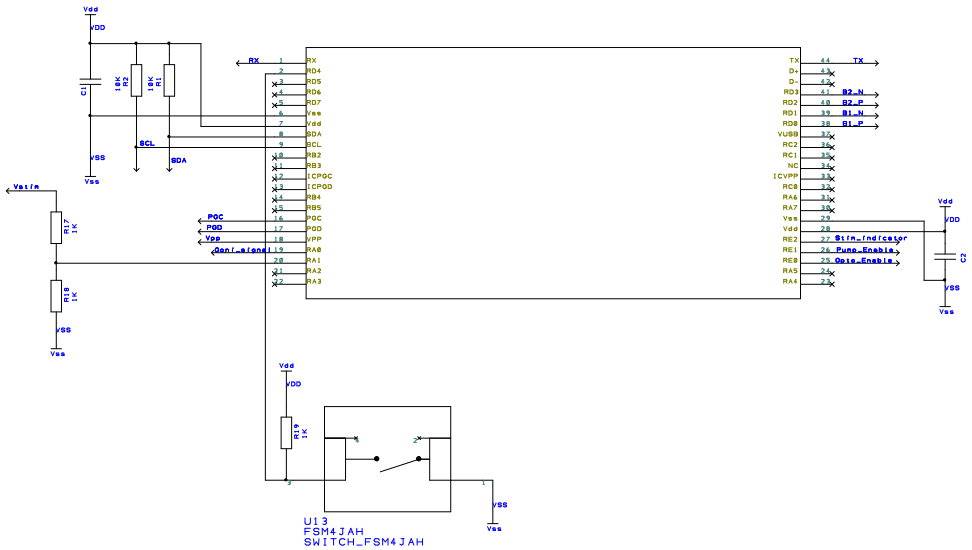

B.1.5 Headers and indicators

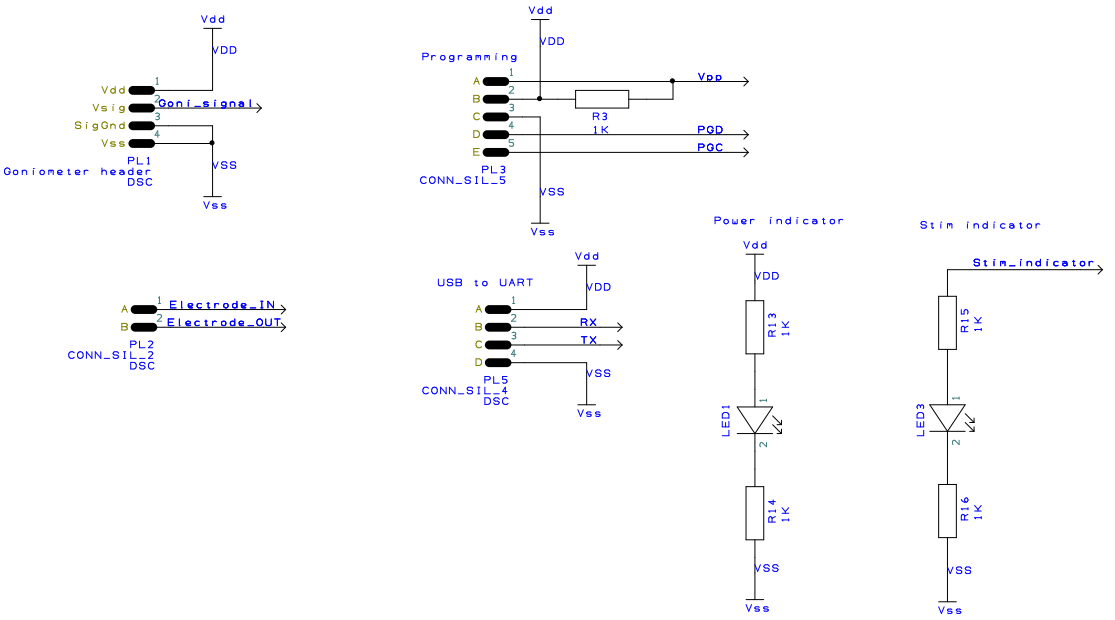

B.2 Circuit board layout

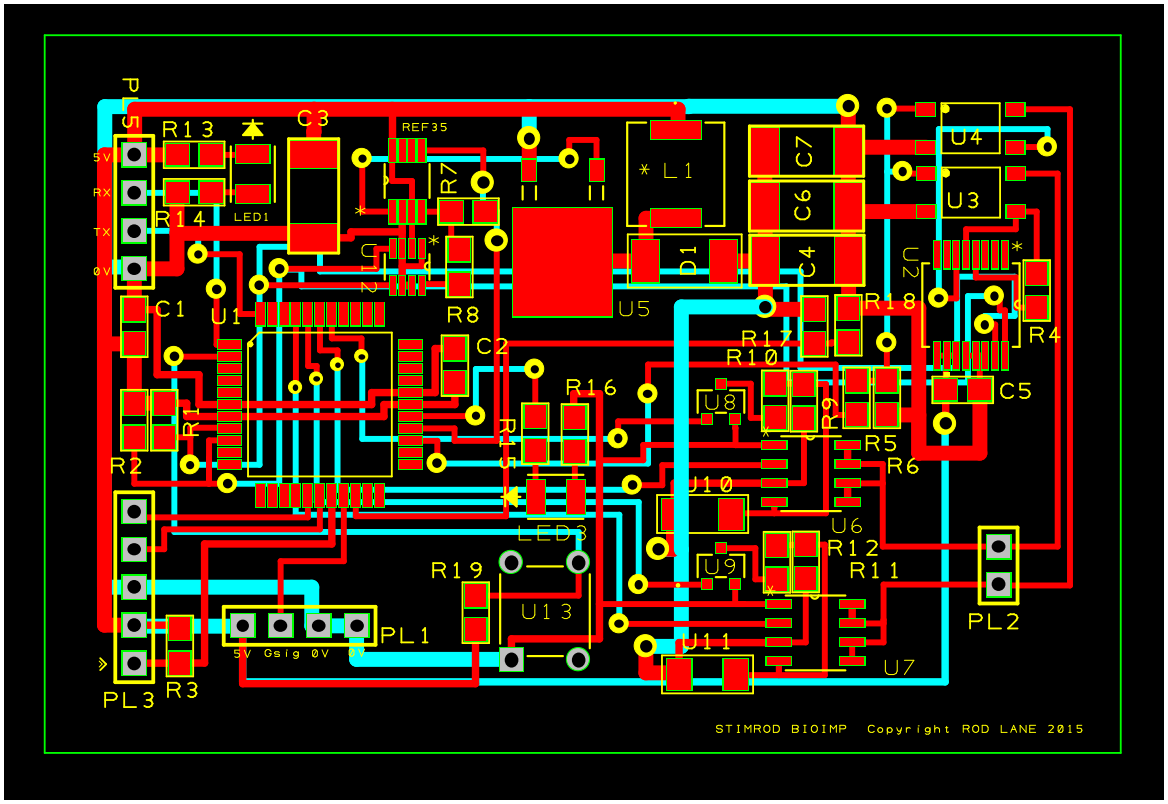

Appendix C Firmware code listing

```
*
 * File:   main.c
 * Author: r.lane
 *
 * Created on 05 May 2015, 11:10
 */

#define _XTAL_FREQ 8000000

#define Stim_LED          LATEbits.LATE2
#define Charge_pump       LATEbits.LATE1
#define Impedance         LATEbits.LATE0

#define on              1
#define off             0


#define HB_HS1          LATDbits.LATD0
#define HB_LS1          LATDbits.LATD1
#define HB_HS2          LATDbits.LATD2
#define HB_LS2          LATDbits.LATD3
#define off             0
#define forward         1
#define reverse         2
#define grounded        3

#define USE_OR_MASKS
#define USE_AND_MASKS


#include <xc.h>
#include <stdlib.h>
#include <stdio.h>
#include <math.h>
#include <time.h>
#include <string.h>
#include <plib/i2c.h>
#include <plib/usart.h>
#include <plib/adc.h>
#include <pic18f45k50.h>

// CONFIG1L
#pragma config PLLSEL = PLL4X   // PLL Selection (4x clock multiplier)
#pragma config CFGPLLEN = OFF   // PLL Enable Configuration bit (PLL Disabled (firmware controlled))
#pragma config CPUDIV = NOCLKDIV// CPU System Clock Postscaler (CPU uses system clock (no divide))
#pragma config LS48MHZ = SYS24X4// Low Speed USB mode with 48 MHz system clock (System clock at 24
MHz, USB clock divider is set to 4)
//#pragma config LS48MHZ = SYS48X8// Low Speed USB mode with 48 MHz system clock (System clock at
48 MHz, USB clock divider is set to 8)

// CONFIG1H
#pragma config FOSC = INTOSCIO  // Oscillator Selection (Internal oscillator)
#pragma config PCLKEN = ON      // Primary Oscillator Shutdown (Primary oscillator enabled)
#pragma config FCMEN = OFF      // Fail-Safe Clock Monitor (Fail-Safe Clock Monitor disabled)
```

```
#pragma config IESO = OFF       // Internal/External Oscillator Switchover (Oscillator Switchover mode
disabled)

// CONFIG2L
#pragma config nPWRTEN = OFF    // Power-up Timer Enable (Power up timer enabled)
#pragma config BOREN = SBORDIS  // Brown-out Reset Enable (BOR enabled in hardware (SBOREN is
ignored))
#pragma config BORV = 190       // Brown-out Reset Voltage (BOR set to 1.9V nominal)
#pragma config nLPBOR = OFF     // Low-Power Brown-out Reset (Low-Power Brown-out Reset disabled)

// CONFIG2H
//#pragma config WDTEN = SWON     // Watchdog Timer Enable bits (WDT controlled by firmware (SWDTEN
enabled))
#pragma config WDTEN = OFF      // Watchdog Timer Enable bits (WDT disabled in hardware (SWDTEN
ignored))
#pragma config WDTPS = 32768      // Watchdog Timer Postscaler (1:128)

// CONFIG3H
#pragma config CCP2MX = RC1     // CCP2 MUX bit (CCP2 input/output is multiplexed with RB3)
#pragma config PBADEN = ON     // PORTB A/D Enable bit (PORTB<5:0> pins are configured as digital I/O on
Reset)
#pragma config T3CMX = RC0      // Timer3 Clock Input MUX bit (T3CKI function is on RB5)
#pragma config SDOMX = RB3      // SDO Output MUX bit (SDO function is on RB3)
#pragma config MCLRE = ON       // Master Clear Reset Pin Enable (MCLR pin enabled; RE3 input disabled)

// CONFIG4L
#pragma config STVREN = ON      // Stack Full/Underflow Reset (Stack full/underflow will cause Reset)
#pragma config LVP = OFF        // Single-Supply ICSP Enable bit (Single-Supply ICSP disabled)
#pragma config ICPRT = OFF//ON      // Dedicated In-Circuit Debug/Programming Port Enable (ICPORT
disabled)
#pragma config XINST = OFF      // Extended Instruction Set Enable bit (Instruction set extension and Indexed
Addressing mode disabled)

// CONFIG5L
#pragma config CP0 = OFF        // Block 0 Code Protect (Block 0 is not code-protected)
#pragma config CP1 = OFF        // Block 1 Code Protect (Block 1 is not code-protected)
#pragma config CP2 = OFF        // Block 2 Code Protect (Block 2 is not code-protected)
#pragma config CP3 = OFF        // Block 3 Code Protect (Block 3 is not code-protected)

// CONFIG5H
#pragma config CPB = OFF        // Boot Block Code Protect (Boot block is not code-protected)
#pragma config CPD = OFF        // Data EEPROM Code Protect (Data EEPROM is not code-protected)

// CONFIG6L
#pragma config WRT0 = OFF       // Block 0 Write Protect (Block 0 (0800-1FFFh) is not write-protected)
#pragma config WRT1 = OFF       // Block 1 Write Protect (Block 1 (2000-3FFFh) is not write-protected)
#pragma config WRT2 = OFF       // Block 2 Write Protect (Block 2 (04000-5FFFh) is not write-protected)
#pragma config WRT3 = OFF       // Block 3 Write Protect (Block 3 (06000-7FFFh) is not write-protected)

// CONFIG6H
#pragma config WRTC = OFF       // Configuration Registers Write Protect (Configuration registers (300000-
3000FFh) are not write-protected)
#pragma config WRTB = OFF       // Boot Block Write Protect (Boot block (0000-7FFh) is not write-protected)
#pragma config WRTD = OFF       // Data EEPROM Write Protect (Data EEPROM is not write-protected)

// CONFIG7L
#pragma config EBTR0 = OFF      // Block 0 Table Read Protect (Block 0 is not protected from table reads
executed in other blocks)
```

```
#pragma config EBTR1 = OFF      // Block 1 Table Read Protect (Block 1 is not protected from table reads executed in other blocks)
#pragma config EBTR2 = OFF      // Block 2 Table Read Protect (Block 2 is not protected from table reads executed in other blocks)
#pragma config EBTR3 = OFF      // Block 3 Table Read Protect (Block 3 is not protected from table reads executed in other blocks)

// CONFIG7H
#pragma config EBTRB = OFF      // Boot Block Table Read Protect (Boot block is not protected from table reads executed in other blocks)

int i = 0;
unsigned char UART1Config = 0, baud = 0, baudconfig = 0;
unsigned char MsgFromPIC[] = "I'm here press button to start";
unsigned char MessageBuffer[200];
char rx;
int Goni, ADCValue = 0;
unsigned char ADCStringVal[4];
unsigned char DiPot_addr = 0x58;
unsigned char DiPot_inst = 0x01;
unsigned char DiPot_data = 0xFF;
unsigned char AD5933_addr = 0x1A;
unsigned char AD5933_status;
unsigned char tempReady = 0, valReady = 0 , sweepOver = 0;
unsigned char outputVoltage = 0x40; //2V gain = 5
unsigned char pulsewidth = 1, count, tally = 0;

unsigned char I2C_Send[25];
unsigned char I2C_Recv[10];
unsigned char sync_mode=0, slew=0;
unsigned char w, loop;

signed short realData, imagData;
float magnitude, phase, impedance, impTracker;
float  accumulator, realAcc, imagAcc;
float LPfiltered, phasefiltered;
float gain = 0.0000015;

int uTx(unsigned char byte);
void FloatToString(char * buf, float val);
int Bridge(unsigned char output_type);
void SetupClock(void);
void Delay1Second(void);
void communicate_DiPot(void);
void AD5933_write(unsigned char regAddr, unsigned char regVal);
void AD5933_single_write(void);
void AD5933_single_read(void);
void AD5933_status_report(void);
void AD5933_read_impVals(void);
void AD5933_addr_pointer(void);
void AD5933_block_write(void);
float LPf(float lastVal, double newVal, unsigned char responce);


void main()
{
```

```
  SetupClock();

  /*set up tri-states*/
  TRISA = 0b00000001;
  TRISB = 0b00000011;
  TRISC = 0b10000000;
  TRISD = 0b00010000;
  TRISE = 0b00000000;

  LATA = 0;
  LATB = 0;
  LATC = 0;
  LATD = 0;
  LATE = 0;

  ANSELA = 1;
  ANSELB = 0;
  ANSELC = 0;
  ANSELD = 0;
  ANSELE = 0;

  INTCONbits.GIE        = 0; //disable interrupts
  WDTCONbits.SWDTEN     = 0; //watchdog timer

  WPUB = 0b11110100; //PortB weak pull-ups set and enable
  INTCON2bits.nRBPU     = 0;

  /*UART*/
   UART1Config =     USART_TX_INT_OFF
             |  USART_RX_INT_ON
             |  USART_ASYNCH_MODE
             |  USART_EIGHT_BIT
             |  USART_CONT_RX
             |  USART_BRGH_HIGH ;
   baud = 8;                          //51; //9600
   Open1USART(UART1Config,baud);

   baudconfig =      BAUD_8_BIT_RATE
             |  BAUD_AUTO_OFF;
   baud1USART (baudconfig);

   /*ADC*/
   OpenADC( ADC_FOSC_2 & ADC_LEFT_JUST & ADC_20_TAD,  //config
         ADC_CH0 & ADC_INT_ON,                //config2
         ADC_REF_VDD_VDD & ADC_REF_VDD_VSS );     //config3

   ADC_INT_ENABLE(); //Easy ADC interrupt setup



/*I2C ---INITIALISE THE I2C MODULE FOR MASTER MODE WITH 100KHz --- */
  CloseI2C(); //close I2C module and reinitialise if already running
  sync_mode = MASTER;
  slew = SLEW_OFF;
  OpenI2C1(sync_mode,slew);
  SSPADD=39; //100kHz Baud clock(9) @8MHz
```

```
/* Stall after start up and wait for button press to proceed */

  do{
     LATEbits.LE2 = 1;
  }
  while(PORTDbits.RD4 == 1);
    LATEbits.LE2 = 0;

/* Proceed */

  while(1){

     puts1USART((char *)
          "\r\n\nMENU OPTIONS\r\n"
          " 1 -  Read register\r\n"
          " 2 -  Write register\r\n"
          " 3 -  Address pointer\r\n"
          " 4 -  Block write\r\n"
          " 5 -  Read results\r\n"
          " 6 -  DigiPot\r\n"
          " 7 -  Start impedance and angle measurements\r\n"
          " 8 -  Read Goniometer\r\n"
          " 9 -  H-Bridge\r\n"
          " 10 - Start charge-pump\r\n"
          " 11 - Stimulator\r\n"
          " 12 - Impedance sensing output voltage\r\n\n"

          );

     for(w=0;w<199;w++)
     MessageBuffer[w]=0;

     gets1USART((char *)MessageBuffer,1);

     switch(MessageBuffer[0]){
        case 1:
        {
         puts1USART((char *)"Enter register address\r\n");
         AD5933_single_read();
         break;
        }
        case 2:
        {
         puts1USART((char *)"Enter register address and data byte\r\n");
         AD5933_single_write();
         break;
        }
        case 3:
        {
         puts1USART((char *)"Enter register address\r\n");
         AD5933_addr_pointer();
         break;
        }
        case 4:
        {
         puts1USART((char *)"\r\n");
```

```
          AD5933_block_write();
          break;
        }
        case 5:
        {
          puts1USART((char *)"\r\n");
          AD5933_read_impVals();

          break;
        }
        case 6:
        {
          puts1USART((char *)"Enter instruction byte, integer value (0xFF = 0 Ohm)\r\n");
          communicate_DiPot();
          break;
        }
        case 7:
        {
           AD5933_write(0x80, 0xB3);              //place in standby
           AD5933_write(0x80, 0x13);              //initialise start frequency
           puts1USART((char *)"Press button to stop\r\n\n");
           AD5933_write(0x80, 0x23);              //commence sweep

           Impedance = 1;
           LPfiltered = 0;

           while(PORTDbits.RD4 == 1)
           {
              ei();  //enable master interrupt
              ConvertADC();
              di();
              Goni = LPf(Goni,ADCValue,4);
              puts1USART(utoa( ADCStringVal, Goni,10)); //convert to string
              puts1USART(",");

              realAcc = 0;
              imagAcc = 0;

//              /*single sample method*/
//              AD5933_write(0x80, outputVoltage);      //repeat frequency
//              AD5933_read_impVals();
//
//              realAcc += realData;
//              imagAcc += imagData;
//
//              magnitude = sqrt((realAcc * realAcc) + (imagAcc * imagAcc));
//              impedance = (1 / (magnitude * gain));
//              FloatToString(MessageBuffer, impedance);


              /*Averaged method*/
              for(loop = 0; loop < 5; loop ++ )
              {
                 AD5933_write(0x80, outputVoltage);      //repeat frequency
                 AD5933_read_impVals();
                 realAcc += realData;
                 imagAcc += imagData;
```

```
            }

             realAcc /= 5;
             imagAcc /= 5;

             magnitude = sqrt((realAcc * realAcc) + (imagAcc * imagAcc));
             impedance = (1 / (magnitude * gain));
//             FloatToString(MessageBuffer, impedance);


            /*Filtered method*/
//             AD5933_write(0x80, outputVoltage);      //repeat frequency
//             AD5933_read_impVals();
            LPfiltered = LPf(LPfiltered,impedance,25);
            FloatToString(MessageBuffer, LPfiltered);


            while(Busy1USART());
            puts1USART((char *)MessageBuffer);
            puts1USART("\r\n");

          }
          Impedance = 0;
          break;
        }
        case 8: //ADC read goniometer
        {
           ei();  //enable master interrupt
           ConvertADC();
           di();
           break;
        }
        case 9: //H-Bridge
        {
          puts1USART((char *)"Enter instruction; 0-off, 1-forward, 2-reverse, 3-grounded\r\n");
          gets1USART((char *)MessageBuffer,1);

           switch(MessageBuffer[0])
           {
              case 0:
              {
                 Bridge(off);
                 break;
              }
              case 1:
              {
                 Bridge(forward);
                 break;
              }
              case 2:
              {
                 Bridge(reverse);
                 break;
              }
              case 3:
              {
                 Bridge(grounded);
                 break;
```

```
      }
    }

}
case 10:
{
   Charge_pump = 1;
   break;
}
case 11:
{
   pulsewidth = 10;
   tally = 0;
   impedance = off;            //isolate impedance measuring circuit
   Goni = 0;                 //clear angle variable
   impTracker = 100;

   /*Initial read goniometer */
   ei();  //enable master interrupt
   ConvertADC();
   __delay_ms(50);
   Goni = ADCValue;
   di();

   AD5933_write(0x80, 0xB3);              //place in standby
   AD5933_write(0x80, 0x13);              //initialise start frequency

   puts1USART((char *)"Press button when ready\r\n");
   while(PORTDbits.RD4 == 1); //wait for user to press button

   AD5933_write(0x80, 0x25);              //commence sweep

   /*RAMP UP */
   while(PORTDbits.RD4 == 0)  //begin stim sequence
   {
      Stim_LED = on;
      /*Pulse duration*/
      Bridge(forward);       //connect charge pump potential
      for(count=0; count < pulsewidth; count++)
      {
         asm("nop");
      }
      Bridge(reverse);
      for(count=0; count < pulsewidth; count++)
      {
         asm("nop");
      }
      Bridge(grounded);          //disconnect from output
      __delay_us(100);

      Bridge(off);

      /*Ramp control*/
      if(tally < 5){tally += 1;}
      if(tally == 5)
      {
         if(pulsewidth < 12) {pulsewidth += 1;} // ramp to a set maximum
         tally = 0;
```

```
            }

            Impedance = on;
            __delay_us(100);

//            Stim_LED = off;
            /*Read goniometer */
            ei();  //enable master interrupt
            ConvertADC();
            di();
            Goni = LPf(Goni,ADCValue,5);
            puts1USART(utoa( ADCStringVal, Goni,10)); //convert to string
            puts1USART(",");

            /*Averaged method*/
            realAcc = 0;
            imagAcc = 0;

            for(loop = 0; loop < 5; loop ++ )
            {
              AD5933_write(0x80, outputVoltage);      //repeat frequency
              AD5933_read_impVals();
              realAcc += realData;
              imagAcc += imagData;
            }

            realAcc /= 5;
            imagAcc /= 5;

            magnitude = sqrt((realAcc * realAcc) + (imagAcc * imagAcc));
            impedance = (1 / (magnitude * gain));

            if(impedance < impTracker)
            {
               impTracker = impedance;
            }
            else if(impedance > (impTracker + 0.25))
            {
               pulsewidth = 5;
            }



//            /*Filtered method*/
//            AD5933_write(0x80, outputVoltage);      //repeat frequency
//            AD5933_read_impVals();
            LPfiltered = LPf(LPfiltered,impedance,5);
            FloatToString(MessageBuffer, LPfiltered);

//            AD5933_write(0x80, outputVoltage);       //repeat frequency
//            AD5933_read_impVals();

            Impedance = off;

//            FloatToString(MessageBuffer, impedance);
            while(Busy1USART());
            puts1USART((char *)MessageBuffer);
//            puts1USART(",");
```

```
//              phase = atan2(imagAcc, realAcc);
//              phasefiltered = LPf(phasefiltered,phase,5);
//              FloatToString(MessageBuffer, phasefiltered);
//              puts1USART((char *)MessageBuffer);
            puts1USART("\r\n");

          }
          break;

        }
        case 12:
        {
          puts1USART((char *)"-G1- 1 2V, 2 1V, 3 0.4V, 4 0.2V -G5- 5 2V 6 1V 7 0.4V 8 0.2V\r\n");
          gets1USART((char *)MessageBuffer,1);

          switch(MessageBuffer[0])
          {
            case 1: //2V gain=1
            {
              outputVoltage = 0x41;
              break;
            }
            case 2: //1V gain=1
            {
              outputVoltage = 0x47;
              break;
            }
            case 3: //0.4V gain=1
            {
              outputVoltage = 0x45;
              break;
            }
            case 4: //0.2V gain=1
            {
              outputVoltage = 0x43;
              break;
            }
            case 5: //2V gain=5
            {
              outputVoltage = 0x40;
              break;
            }
            case 6: //1V gain =5
            {
              outputVoltage = 0x46;
              break;
            }
            case 7: //0.4V gain=5
            {
              outputVoltage = 0x44;
              break;
            }
            case 8: //0.2V gain=5
            {
              outputVoltage = 0x42;
              break;
            }
          }
```

```
            break;
          }
        }


        LATEbits.LE2 = 1;
        __delay_ms(50);
        LATEbits.LE2 = 0;
        __delay_ms(50);
        LATEbits.LE2 = 1;
        __delay_ms(50);
        LATEbits.LE2 = 0;
        __delay_ms(50);


    }

}
/*******************************************************************************
 * NAME: Lowpass filter
 *******************************************************************************
 * FUNCTION
 * Low pass filter function with variable response
 * The function accepts a value and an argument
 * The value is a reading (ADC or Impedance measurement)
 * The argument determines the response speed
 * A fraction of the filtered value is removed and replaced with a similar
 * fraction of the new reading.
 * The fraction size is determined by the response variable
 * using bit shift variables ensures higher speed execution ie 2,4,8,16 etc
 * HOW TO USE
 * Call it with the value and argument
 *******************************************************************************/
float LPf(float lastVal, double newVal, unsigned char responce)
{
   float filteredVal;


   filteredVal = (lastVal - (lastVal / responce)) + (newVal / responce);

   return(filteredVal);

}

/*******************************************************************************
 * NAME: communicate_DiPot
 *******************************************************************************
 * FUNCTION
 * Accepts two part command over the UART, the first byte is the instruction
 * the second byte is the data
 * Valid instruction are:
 * 0x40 - Reset to midscale
 * 0x20 - Shutdown
 * 0x10 - Wake up or accept new settings in the following byte
 * The code is expecting two byte even for the reset and shutdown functions, for
 * these options send a null second byte.  When coming out of shutdown the second
 * byte is ignored and the last setting used.
 * These settings are relayed over I2C
```

```
 * The data register value is read back and returned over the UART to the
 * terminal programme for confirmation
 *
 * HOW TO USE
 * Call it
 ********************************************************************************/
void communicate_DiPot(void)
{
  signed char status;
  unsigned char data, w;

   gets1USART((char *)MessageBuffer,2);

   /*I2C */
      for(w=0;w<9;w++)
      I2C_Recv[w]=0;

      StartI2C1();
      data = SSP1BUF; //read any previous stored content in buffer to clear buffer full status
      I2C_Send[0] = MessageBuffer[0];  //initialise send array with instruction byte
      I2C_Send[1] = MessageBuffer[1];  // and data byte

      do
      {
      status = WriteI2C1( DiPot_addr | 0x00 ); //write the address of slave
         if(status == -1) //check if bus collision happened
         {
            data = SSP1BUF; //upon bus collision detection clear the buffer,
            SSPCON1bits.WCOL=0; // clear the bus collision status bit
         }

      }
      while(status!=0); //write untill successful communication

    //***WRITE THE THE DATA TO BE SENT FOR SLAVE***
      for(w=0;w<1;w++)
      putsI2C1(I2C_Send);
     // while(putsI2C1(I2C_Send)!=0); //write string of data to be transmitted to slave

      StopI2C1();

      LATEbits.LE2 = 1;
      __delay_ms(50);
      LATEbits.LE2 = 0;
      __delay_ms(50);

      RestartI2C1();

      data = SSP1BUF;

    //Read latched value from DigiPot
      do
      {
      status = WriteI2C1( DiPot_addr | 0x01 ); //write the address of slave
         if(status == -1) //check if bus collision happened
         {
            data = SSP1BUF; //upon bus collision detection clear the buffer,
            SSPCON1bits.WCOL=0; // clear the bus collision status bit
```

```
        }

    }
    while(status!=0); //write untill successful communication

    while( getsI2C1(I2C_Recv,1) );


    NotAckI2C();
    while (SSPCON2bits.ACKEN1!=0);
    //---TERMINATE COMMUNICATION FROM MASTER SIDE---
    StopI2C1();

    utoa(MessageBuffer, I2C_Recv[0], 10);
    while(Busy1USART());
    puts1USART((char *)MessageBuffer);

}

/*****************************************************************************
 * NAME: ADCInterrupt
 *****************************************************************************
 * FUNCTION
 * Reads ADC voltage coverts to string and outputs to terminal
 *
 * HOW TO USE
 * Call it
 *****************************************************************************/
void interrupt ADCInterrupt()
{

  //check if the interrupt is caused by ADC
  if(PIR1bits.ADIF == 1)
  {

    ReadADC();

    if(ADRESH < 180)
    {
      ADCValue = (ADRESH * 0.5167) + 19.652;
    }
    else
    {
      ADCValue = (ADRESH * 2.1452) - 277;
    }

    //Reset interrupt flag and start conversion again
    ADIF = 0;

  }
}



/*****************************************************************************
 * NAME: AD5933_single_write
 *****************************************************************************
```

```
 * FUNCTION
 * Accepts two part command over the UART, the first byte is the register
 * address the second byte is the data
 * These settings are relayed over I2C
 * The data register value is read back and returned over theUART to the
 * terminal programme for confirmation
 *
 * HOW TO USE
 * Call it
 ********************************************************************************/
void AD5933_single_write(void)
{
  signed char status;
  unsigned char data, w;

   gets1USART((char *)MessageBuffer,2);

   /*I2C */
      StartI2C1();

      do
      {
      status = WriteI2C1( AD5933_addr | 0x00 ); //write the address of slave
        if(status == -1) //check if bus collision happened
        {
          data = SSP1BUF; //upon bus collision detection clear the buffer,
          SSPCON1bits.WCOL=0; // clear the bus collision status bit
        }

      }
      while(status!=0); //write untill successful communication

    //***WRITE THE THE DATA TO BE SENT FOR SLAVE***
      WriteI2C1(MessageBuffer[0]);
      WriteI2C1(MessageBuffer[1]);

    //---TERMINATE COMMUNICATION FROM MASTER SIDE---

      StopI2C1();

      LATEbits.LE2 = 1;
      __delay_ms(50);
      LATEbits.LE2 = 0;
      __delay_ms(50);

}

/********************************************************************************
 * NAME: AD5933_single_read
 ********************************************************************************
 * FUNCTION
 * Accepts two part command over the UART, the first byte is the register
 * address the second byte is the data
 * These settings are relayed over I2C
 * The data register value is read back and returned over theUART to the
 * terminal programme for confirmation
 *
 * HOW TO USE
```

```
 * Call it
 ****************************************************************************/
void AD5933_single_read(void)
{
  signed char status;
  unsigned char data, w;

  gets1USART((char *)MessageBuffer,1);
//
/*I2C */
      StartI2C1();

      I2C_Send[0] = 0xB0;  // initialise send array with address
      I2C_Send[1] = MessageBuffer[0];  // and data byte

      do
      {
      status = WriteI2C1( AD5933_addr | 0x00 ); //write the address of slave
        if(status == -1) //check if bus collision happened
        {
          data = SSP1BUF; //upon bus collision detection clear the buffer,
          SSPCON1bits.WCOL=0; // clear the bus collision status bit
        }

      }
      while(status!=0); //write untill successful communication

//    ***WRITE THE THE DATA TO BE SENT FOR SLAVE***
      WriteI2C1(0xB0);
      WriteI2C1(MessageBuffer[0]);


//      while(putsI2C1(I2C_Send)!=0); //write string of data to be transmitted to slave

    //---TERMINATE COMMUNICATION FROM MASTER SIDE---

      StopI2C1();

//    //---Address Pointer set

      //***flush receive buffer
      for(w=0;w<9;w++)
      I2C_Recv[w]=0;

      StartI2C1();

      data = SSP1BUF;

    //Read latched value from AD5933 register

      do
      {
      status = WriteI2C1( AD5933_addr | 0x01 ); //write the address of slave
        if(status == -1) //check if bus collision happened
        {
          data = SSP1BUF; //upon bus collision detection clear the buffer,
          SSPCON1bits.WCOL=0; // clear the bus collision status bit
        }
```

```
    }
    while(status!=0); //write untill successful communication

    while( getsI2C1(I2C_Recv,1) );


    NotAckI2C1();
    while (SSPCON2bits.ACKEN1!=0);

    //---TERMINATE COMMUNICATION FROM MASTER SIDE---
    StopI2C1();


    utoa(MessageBuffer, I2C_Recv[0], 10);
    while(Busy1USART());
    puts1USART((char *)MessageBuffer);

}

/*****************************************************************************
 * NAME: AD5933_status_report
 *****************************************************************************
 * FUNCTION
 * Accepts two part command over the UART, the first byte is the register
 * address the second byte is the data
 * These settings are relayed over I2C
 * The data register value is read back and returned over theUART to the
 * terminal programme for confirmation
 *
 * HOW TO USE
 * Call it
 *****************************************************************************/
void AD5933_status_report(void)
{
  signed char status;
  unsigned char data, w;

  AD5933_status   = 0;
  tempReady       = 0;
  valReady        = 0;
  sweepOver       = 0;

/*Set address pointer to status register */
    StartI2C1();

    do
    {
    status = WriteI2C1( AD5933_addr | 0x00 ); //write the address of slave
      if(status == -1) //check if bus collision happened
      {
        data = SSP1BUF; //upon bus collision detection clear the buffer,
        SSPCON1bits.WCOL=0; // clear the bus collision status bit
      }

    }
    while(status!=0); //write untill successful communication
```

```
    WriteI2C1(0xB0);
    WriteI2C1(0x8F);

    StopI2C1();

    for(w=0;w<9;w++)
    I2C_Recv[w]=0;

    StartI2C1();

    data = SSP1BUF;

/* Read status register */
    do
    {
    status = WriteI2C1( AD5933_addr | 0x01 ); //write the address of slave
      if(status == -1) //check if bus collision happened
      {
        data = SSP1BUF; //upon bus collision detection clear the buffer,
        SSPCON1bits.WCOL=0; // clear the bus collision status bit
      }

    }
    while(status!=0); //write untill successful communication

    while(getsI2C1(I2C_Recv,1));

    NotAckI2C1();
    while (SSPCON2bits.ACKEN1!=0);

    StopI2C1();

    AD5933_status = I2C_Recv[0];
    if( AD5933_status & (0x01 << 0) )
    {
      tempReady = 1;
    }

    if( AD5933_status & (0x01 << 1) )
    {
      valReady = 1;
    }
    if( AD5933_status & (0x01 << 2) )
    {
      sweepOver = 1;
    }
}

/*****************************************************************************
 * NAME: AD5933_write
 *****************************************************************************
 * FUNCTION
 * Accepts two part command over the UART, the first byte is the register
 * address the second byte is the data
 * These settings are relayed over I2C
 * The data register value is read back and returned over theUART to the
 * terminal programme for confirmation
 *
```

```
 * HOW TO USE
 * Call it
 ********************************************************************************/
void AD5933_write(unsigned char regAddr, unsigned char regVal)
{
  signed char status;
  unsigned char data, w;

   StartI2C1();
   do
   {
   status = WriteI2C1( AD5933_addr | 0x00 ); //write the address of slave
      if(status == -1) //check if bus collision happened
      {
         data = SSP1BUF; //upon bus collision detection clear the buffer,
         SSPCON1bits.WCOL=0; // clear the bus collision status bit
      }

   }
   while(status!=0); //write untill successful communication
   WriteI2C1(regAddr);
   WriteI2C1(regVal);
   StopI2C1();

}

/********************************************************************************
 * NAME: AD5933_read_impVals
 ********************************************************************************
 * FUNCTION
 * Accepts two part command over the UART, the first byte is the register
 * address the second byte is the data
 * These settings are relayed over I2C
 * The data register value is read back and returned over theUART to the
 * terminal programme for confirmation
 *
 * HOW TO USE
 * Call it
 ********************************************************************************/
void AD5933_read_impVals(void)
{
  signed char status;
  unsigned char data, w;


  magnitude = 0;
  impedance = 0;
  realData  = 0;
  imagData  = 0;

  while(valReady != 1)    //wait for valid reading to be available
  {
     AD5933_status_report();
  }
  valReady == 0;         //reset flag

  /*Set address pointer */
      StartI2C1();
```

```
    data = SSP1BUF; //read any previous stored content in buffer to clear buffer full status
    do
    {
    status = WriteI2C1( AD5933_addr | 0x00 ); //write the address of slave
      if(status == -1) //check if bus collision happened
      {
        data = SSP1BUF; //upon bus collision detection clear the buffer,
        SSPCON1bits.WCOL=0; // clear the bus collision status bit
      }

    }
    while(status!=0); //write untill successful communication

  //***WRITE THE THE DATA TO BE SENT FOR SLAVE***
    WriteI2C1(0xB0);   //Address pointer instruction code
    WriteI2C1(0x94);   //Register address

  //---TERMINATE COMMUNICATION FROM MASTER SIDE---
    StopI2C1();

  /*Block read instruction */
    StartI2C1();

    do
    {
    status = WriteI2C1( AD5933_addr | 0x00 ); //write the address of slave
      if(status == -1) //check if bus collision happened
      {
        data = SSP1BUF; //upon bus collision detection clear the buffer,
        SSPCON1bits.WCOL=0; // clear the bus collision status bit
      }

    }
    while(status!=0); //write untill successful communication

//    ***WRITE THE THE DATA TO BE SENT FOR SLAVE***
    WriteI2C1(0xA1);   //Block read instruction code
    WriteI2C1(0x04);   //Number of bytes to be read

    IdleI2C1();
  //---Address Pointer set
    RestartI2C1();
    data = SSP1BUF;
  /*flush receive buffer */
    for(w=0;w<9;w++)
    I2C_Recv[w]=0;

  //Read latched value from AD5933 register
    do
    {
    status = WriteI2C1( AD5933_addr | 0x01 ); //write the address of slave
      if(status == -1) //check if bus collision happened
      {
        data = SSP1BUF; //upon bus collision detection clear the buffer,
        SSPCON1bits.WCOL=0; // clear the bus collision status bit
      }

    }
```

```
      while(status!=0); //write untill successful communication

      while( getsI2C1(I2C_Recv,4) );

      NotAckI2C1();
      while (SSPCON2bits.ACKEN1!=0);

      //---TERMINATE COMMUNICATION FROM MASTER SIDE---
      StopI2C1();

      realData += I2C_Recv[0];
      realData <<= 8;
      realData += I2C_Recv[1];

      imagData += I2C_Recv[2];
      imagData <<= 8;
      imagData += I2C_Recv[3];

//      magnitude = sqrt((realData * realData) + (imagData * imagData));
//      impedance = (1 / (magnitude * gain));

//      FloatToString(MessageBuffer, impedance);
//      while(Busy1USART());
//      puts1USART((char *)MessageBuffer);
//      puts1USART("\r\n");


 }
/*****************************************************************************
 * NAME: AD5933_addr_pointer
 *****************************************************************************
 * FUNCTION
 * Accepts two part command over the UART, the first byte is the pointer
 * command the second byte is the address
 * These settings are relayed over I2C
 *
 * HOW TO USE
 * Call it prior to a block write or block read
 *****************************************************************************/
void AD5933_addr_pointer(void)
{
  signed char status;
  unsigned char data, w;

   gets1USART((char *)MessageBuffer,1);

   /*I2C */
      StartI2C1();
      data = SSP1BUF; //read any previous stored content in buffer to clear buffer full status
      I2C_Send[0] = 0xB0;            //initialise send array with instruction byte
      I2C_Send[1] = MessageBuffer[0];  // and data byte

      do
      {
      status = WriteI2C1( AD5933_addr | 0x00 ); //write the address of slave
         if(status == -1) //check if bus collision happened
         {
            data = SSP1BUF; //upon bus collision detection clear the buffer,
```

```
            SSPCON1bits.WCOL=0; // clear the bus collision status bit
          }

      }
      while(status!=0); //write untill successful communication

    //***WRITE THE THE DATA TO BE SENT FOR SLAVE***
      for(w=0;w<1;w++)
      putsI2C1(I2C_Send);
      //while(putsI2C1(I2C_Send)!=0); //write string of data to be transmitted to slave

      LATEbits.LE2 = 1;
      __delay_ms(50);
      LATEbits.LE2 = 0;
      __delay_ms(50);

    //---TERMINATE COMMUNICATION FROM MASTER SIDE---
      StopI2C1();

}

/*******************************************************************************
 * NAME: AD5933_block_write
 *******************************************************************************
 * FUNCTION
 * //Accepts 12 bytes of settings data over the UART
 * //These settings are relayed over I2C
 *
 * HOW TO USE
 * First use AD5933_addr_pointer to determine where the first byte will be
 * writen
 *******************************************************************************/
void AD5933_block_write(void)
{
  signed char status;
  unsigned char data, w;

   /*I2C */
      StartI2C1();
      data = SSP1BUF; //read any previous stored content in buffer to clear buffer full status

      do
      {
      status = WriteI2C1( AD5933_addr | 0x00 ); //write the address of slave
        if(status == -1) //check if bus collision happened
        {
          data = SSP1BUF; //upon bus collision detection clear the buffer,
          SSPCON1bits.WCOL=0; // clear the bus collision status bit
        }

      }
      while(status!=0); //write untill successful communication

    //***WRITE THE THE DATA TO BE SENT FOR SLAVE***
      WriteI2C1(0xA0);  //Block write instruction
      WriteI2C1(0x0A);  //number of bytes

      WriteI2C1(0x14);  //Start frequency
```

```
      WriteI2C1(0x7A);
      WriteI2C1(0xE1);

      WriteI2C1(0x00);  //Frequency increment
      WriteI2C1(0x0D);
      WriteI2C1(0x1B);

      WriteI2C1(0x00);  //Number of increments
      WriteI2C1(0x0A);

      WriteI2C1(0x00); //Settling cycles
      WriteI2C1(0x0A);

    //---TERMINATE COMMUNICATION FROM MASTER SIDE---
      StopI2C1();

      LATEbits.LE2 = 1;
      __delay_ms(75);
      LATEbits.LE2 = 0;
      __delay_ms(75);
      LATEbits.LE2 = 1;
      __delay_ms(75);
      LATEbits.LE2 = 0;
      __delay_ms(75);

 }

/*****************************************************************************
 * NAME: SetupClock
 *****************************************************************************
 * FUNCTION
 * Initialises internal clocks
 *
 * HOW TO USE
 * Call it
 *****************************************************************************/
void SetupClock(void){
   OSCCONbits.IDLEN = 0; //sleep on SLEEP()

   OSCCONbits.IRCF0 = 0;
   OSCCONbits.IRCF1 = 1;
   OSCCONbits.IRCF2 = 1;
   OSCCONbits.OSTS = 0;
}
/*****************************************************************************
 * NAME: Delay1Second
 *****************************************************************************
 * FUNCTION
 * One second time delay
 *
 * HOW TO USE
 * Call it
 *****************************************************************************/
void Delay1Second() {
   for(i=0;i<100;i++)
   {
       __delay_ms(10);
   }
```

```
}
/*****************************************************************************
 * NAME: SerialRxPinInterrupt
 *****************************************************************************
 * FUNCTION
 * Reads and stores a string echoing back after CR
 *
 * HOW TO USE
 * talk to it
 *****************************************************************************/
void interrupt SerialRxPinInterrupt()
{
//   //check if the interrupt is caused by RX pin
//   if(PIR1bits.RCIF == 1)
//   {
  ////////////////////////////////////////////////////////////
       //check if the interrupt is caused by RX pin
   if(PIR1bits.RCIF == 1)
   {
      rx = Read1USART(); //read the byte from rx register
      puts1USART(MsgFromPIC);
      Write1USART(rx);
      PIR1bits.RCIF = 0; // clear rx flag
   }
  ////////////////////////////////////////////////////////////
//       if(i<200) //our buffer size
//       {
//          MessageBuffer[i] = Read1USART(); //read the byte from rx register
//          if(MessageBuffer[i] == 0x02) //check for return key
//          {
//             puts1USART(MessageBuffer);
//             for(;i>0;i--)
//                MessageBuffer[i] = 0x00; //clear the array
//             i=0; //for sanity
//             return;
//          }
//          i++;
//          PIR1bits.RCIF = 0; // clear rx flag
//       }
//       else
//       {
//           puts1USART(MessageBuffer);
//           for(;i>0;i--)
//                MessageBuffer[i] = 0x00; //clear the array
//           i=0; //for sanity
//           return;
//       }
//   }
}

/*****************************************************************************
 * NAME: uTx
 *****************************************************************************
 * FUNCTION:
 * Sends Byte of data over UART it checks that buffer is empty first
 *
 * HOW TO USE:
 * Call it with data to send as argument
```

```
 ***************************************************************************/
int uTx(unsigned char byte){
   while(TXSTA1bits.TRMT == 0){}
     TXREG1 = byte;
     return 0;
}

/***************************************************************************
 * NAME: FloatToString
 ***************************************************************************
 * FUNCTION
 * Converts a float value to a string with 3 digits of accuracy
 *
 * HOW TO USE
 * call it
 ***************************************************************************/
void FloatToString(char * buf, float val)
{
   long intPart     = 0;
   short fracPart    = 0;
   short charPos     = 0;
   char localBuf[10] = {0,0,0,0,0,0,0,0,0,0};
   short i =   sizeof(localBuf) - 1;

   intPart = (long)val;
   fracPart = (short)((val - intPart) * 1000 + 0.5);

   while(i > sizeof(localBuf) - 4)
   {
      localBuf[i] = (fracPart % 10) + 0x30;
      fracPart /= 10;
      i--;
   }
   localBuf[i] = '.';

   if(intPart == 0)
   {
      i--;
      localBuf[i] = '0';
   }

   while(intPart)
   {
      i--;
      localBuf[i] = (intPart % 10) + 0x30;
      intPart /= 10;
   }

   for(charPos = i; charPos < sizeof(localBuf); charPos ++)
   {
      *buf = localBuf[charPos];
      buf ++;
   }
   *buf = 0;
}

/***************************************************************************
 * NAME: Bridge
```

```
 * FUNCTION:
 * H-Bridge settings to;
 * - Source from output 1 and Sink to output 2
 * - Sink to output 1 and Source from output 2
 * - Sink both outputs
 *
 * HOW TO USE:
 * Call it with argument
 * ***************************************************************************/
int Bridge(unsigned char output_type){

   switch(output_type){
      case 0: //All off
      {
         //High-side
         HB_HS1  = 0;    //arm 1 high side
         HB_HS2  = 0;    //arm 2 high side
         //Low-side
         HB_LS1  = 0;    //arm 1 low side
         HB_LS2  = 0;    //arm 2 low side
         break;
      }
      case 1: //Forward
      {
         //High-side
         HB_HS1  = 1;    //arm 1 high side
         HB_HS2  = 0;    //arm 2 high side
         //Low-side
         HB_LS1  = 0;    //arm 1 low side
         HB_LS2  = 1;    //arm 2 low side
         break;
      }
      case 2: //Reverse
      {
         //High-side
         HB_HS1  = 0;    //arm 1 high side
         HB_HS2  = 1;    //arm 2 high side
         //Low-side
         HB_LS1  = 1;    //arm 1 low side
         HB_LS2  = 0;    //arm 2 low side
         break;
      }
      case 3: //Outputs grounded
      {
         //High-side
         HB_HS1  = 0;    //arm 1 high side
         HB_HS2  = 0;    //arm 2 high side
         //Low-side
         HB_LS1  = 1;    //arm 1 low side
         HB_LS2  = 1;    //arm 2 low side
         break;
      }
      default:    //Off
      {
         //High-side
         HB_HS1  = 0;    //arm 1 high side
         HB_HS2  = 0;    //arm 2 high side
         //Low-side
```

```
        HB_LS1  = 0;    //arm 1 low side
        HB_LS2  = 0;    //arm 2 low side
      }
    }
    return 0;
}
```